Durham E-Theses

Cross-coupling reactions in the development of new luminescent iridium bis-terpyridyl complexes

Leslie, Wendy

Cross-Coupling Reactions in the Development of New Luminescent Iridium Bis-Terpyridyl Complexes

2003

Wendy Leslie

Graduate Society

University of Durham

Supervisor:

Dr J.A. Gareth Williams

A thesis submitted to the University of Durham in partial fulfilment of the regulations for the degree of Doctor of Philosophy.

1 9 JAN 2004

Cross-Coupling Reactions in the Development of New Luminescent Iridium Bis-Terpyridyl Complexes

Wendy Leslie

Abstract

Luminescent complexes of 2nd and 3rd row transition metal ions with polypyridyl ligands are of growing interest as molecular luminescent sensors. The long luminescence lifetime of iridium (III) bis-terpyridine, $[Ir(tpy)_2]^{3+}$, makes it and its derivatives of particular interest, but the further development of such compounds requires improved synthetic routes as well as a greater understanding of their photophysical properties.

The palladium-catalysed Suzuki cross-coupling methodology has been investigated as a means for the preparation of 4'-aryl and biaryl substituted 2, 2': 6', 2"-terpyridines under mild conditions. Optimal yields were obtained through the coupling of 4'-bromoterpyridine or 4'-bromophenylterpyridine with aryl boronic acids or esters, to yield aryl or biaryl-substituted terpyridines respectively. A photophysical study has revealed that most of the terpyridines prepared in this way emit in the near-UV region, from a ligand-centred (π_{tpy}-π_{tpy}*) state, with lifetimes in the 1-5 ns range. However, those bearing a *para*-amino group in the pendent aryl or biaryl substituent display solvatochromic emission assigned to an intramolecular charge transfer (ICT) state (π_{Ph}-π_{tpy}*). The ICT state is stabilised upon binding of zinc ions to the terpyridyl moiety, leading to a large red-shift in emission, a response which is almost unique to this metal ion.

The utility of the cross-coupling strategy for the *in situ* elaboration of bromo-functionalised iridium bis-terpyridyl complexes has also been demonstrated. The complex $[Ir(tpy)(tpy-\phi-Br)]^{3+}$ reacts with aryl boronates to yield biaryl-substituted complexes directly. These complexes display yellow-orange emission in degassed solution, with luminescence lifetimes in excess of 100 μs, assigned to an excited state of primarily $^3\pi$-π* character.

Homoleptic iridium (III) complexes of *para*-amino-substituted 4'-aryl terpyridines have been prepared directly by complexation of the metal to the ligands. These complexes display weak, short-lived emission in the near infra-red region of the spectrum, assigned to a ^{1}ILCT state which is stabilised relative to the free ligand by the binding of the iridium (III) ion to the terpyridine unit.

Acknowledgements

Declaration

The work reported in this thesis has been carried out within the Department of Chemistry within the University of Durham between October 2000 and September 2003. This work has not been submitted for any other degree either in Durham or elsewhere and is the original work of the author except where otherwise stated.

Statement of Copyright

Financial Support

Glossary of Symbols and Abbreviations

- ## List of Chemical Abbreviations

DME - 1, 2-dimethoxyethane

THF - tetrahydrofuran

DCM - dichloromethane

DMF - dimethylformamide

DMSO - dimethyl sulphoxide

COD – 1,5-cyclooctadiene

COE - cyclooctene

B_2neo_2 – bis(neopentylglycolato)diboron

B_2Pin_2 - bis(pinacolato)diboron

py - pyridine

tpy - 2,2': 6', 2"-terpyridine (NB terpyridine = 2,2': 6', 2"-terpyridine unless stated otherwise).

ttpy - 4'-(4-tolyl)-2, 2': 6', 2"-terpyridine

bpy - 2,2'-bipyridine

ppy - 2-phenylpyridine

phen – 1,10-phenanthroline

- ## List of Photophysical Abbreviations

LC - ligand centred

CT – charge-transfer

PET – photoinduced electron transfer

MLCT – metal to ligand charge-transfer

LMCT – ligand to metal charge-transfer

ILCT – intraligand charge-transfer

TICT – twisted intramolecular charge-transfer

- ## List of Commonly Used Photophysical Symbols

λ - wavelength of emission

ε - extinction coefficient

ϕ - quantum yield of luminescence

τ - lifetime of luminescence

- **List of Abbreviations for Analytical Techniques**

TLC – thin layer chromatography

NMR – nuclear magnetic resonance
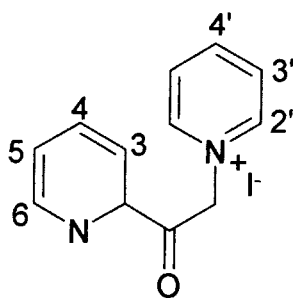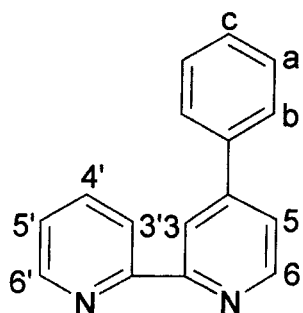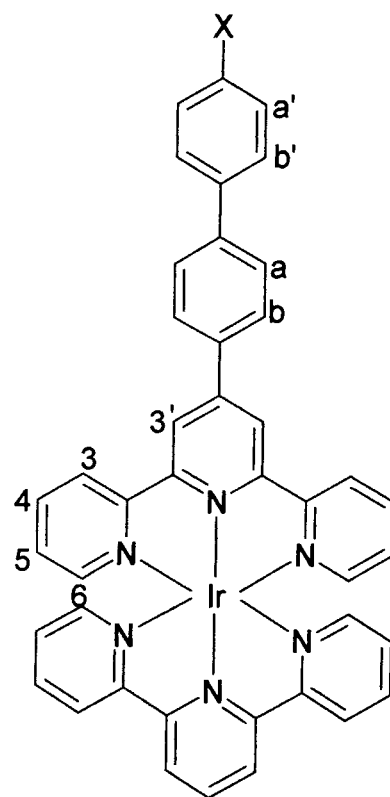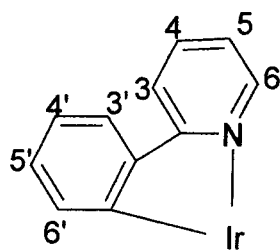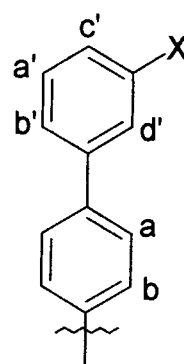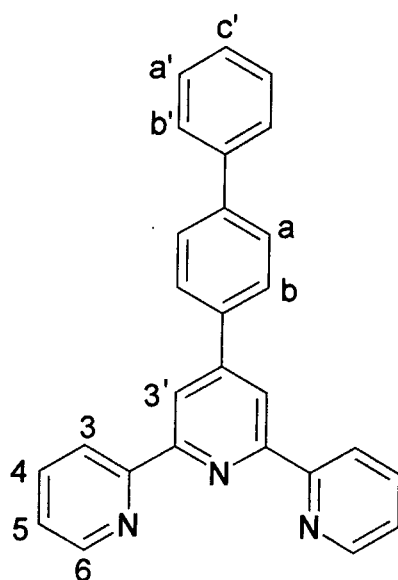
ESMS – electrospray mass spectrometry

EIMS – electron ionisation mass spectrometry

CIMS – chemical ionisation mass spectrometry

GCMS – gas chromatography mass spectrometry

General Schemes For NMR Assignments.

Contents

1. Introduction

1.1. Molecular Luminescent Sensors

The development of molecular luminescent sensors and switches that are able to signal the presence of molecules or ions in aqueous solution has long been a vibrant area of research.[1-5] Such luminescent sensors have important applications in the analysis of biological and environmental samples, potentially providing exciting new applications for many users, ranging from analytical chemists and environmental scientists, through to medical scientists and information technologists.

At present, there are many commercially available luminescent sensors, however most are based on organic systems and, therefore, are strictly fluorescent systems, in which the emission is characterised by short lifetimes. However, as discussed in several recent reviews on the application of metal complexes as luminescent sensors,[2-5] transition metal complexes have many potential advantages over purely organic systems as luminescent probes, including long excited state lifetimes, typically in the range 0.1-100μs (compared to lifetimes on a nanosecond timescale for organic fluorophores) and often high luminescence quantum yields.[6,7] Long lifetimes of emission are a desirable characteristic in luminescent sensors, as they allow discrimination from the ubiquitous shorter-lived background fluorescence found in biological/environmental samples. They also open up the possibility of using changes in lifetime as a probe of the presence and concentration of an analyte, as opposed to the more usual methods of intensity and wavelength-based sensing.[8]

A further advantage of transition metal complexes is that they often absorb strongly in the visible region, allowing excitation beyond the range of absorption of most biological molecules.[8] Moreover, the large spectral shifts between the absorption and emission bands minimise potential self-absorption, which is sometimes a problem for fluorescent molecules where the Stokes shifts are smaller.[5] These desirable characteristics are a result of the fact that the emissive state in such complexes is normally formed indirectly following absorption, often involving processes that are formally spin-forbidden.

1.1.1. Electronic Structure of Transition Metal Complexes

Figure 1.1 shows a schematic orbital diagram for a representative octahedral MX_6 d^6 low spin metal complex. The d^6 configuration is exemplified because of its central role in current research of transition metal complex luminescence including the systems described in this thesis. Since weak field systems are not favourable in luminescence, only the strong field case, where all six electrons pair and fill the t_2 orbitals is considered. This is, of course, almost always the case for complexes of the second and third row transition metals.

Orbitals   **Spectroscopic States**
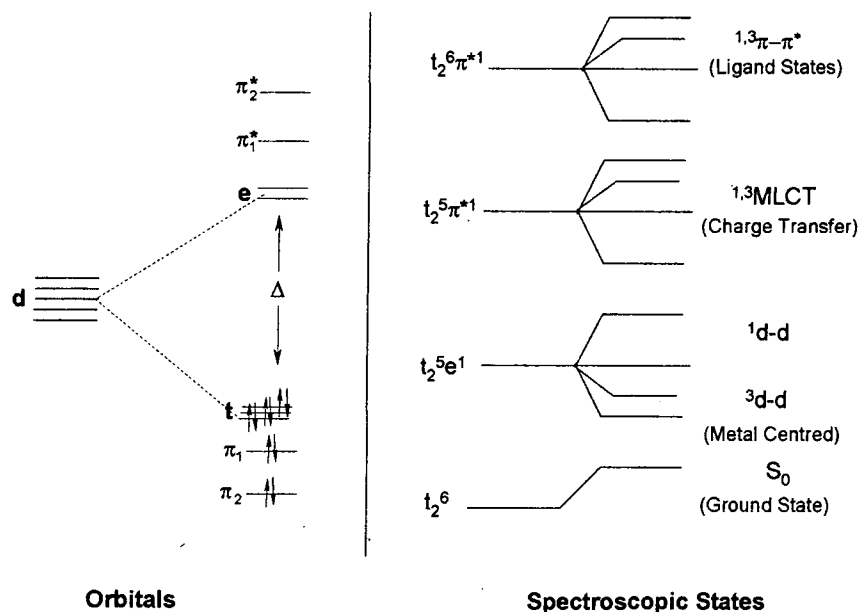
Figure 1.1 – *Simplified orbital and state diagram for a d^6 metal complex in an octahedral environment showing the d and π bonding and antibonding orbitals.* [5]

Three classes of excited states may occur in transition metal complexes: metal centred d-d states (d-d), ligand-centred π-π^* (LC), and charge transfer (CT). (Only the ligand π orbitals are spectroscopically important for visible and near uv absorptions and emissions, therefore the sigma orbitals are not considered).

Ligand centred π-π^* transitions are localised on the organic ligands and tend to be similar to those of the free ligand. Metal centred d-d transitions are Laporte forbidden and are therefore characterised by low extinction coefficients and long natural radiative lifetimes, but high susceptibility to non-radiative deactivation, so that most have very low luminescence yields. Additionally the t_2^6-$t_2^5e^1$ transition promotes an electron into an anti/non-bonding orbital and thus states with this configuration tend to be reactive to decomposition. Hence there are almost no d-d emitting d^6 molecules that are likely candidates for sensors or probes. Charge transfer transitions arise by promoting an

electron from a ligand orbital to a metal orbital (LMCT) or more commonly, and especially for α-diimine ligands of the type to be focused on for this discussion, which are easily reduced, from a metal orbital to a ligand orbital (MLCT). Since charge-transfer transitions are more strongly allowed, they have shorter radiative lifetimes, larger extinction coefficients and are less susceptible to intramolecular and environmental quenching.

1.1.2. Design of Transition Metal Complexes for Luminescent Sensors

Consideration of the electronic structure as given above is important, since the emissive properties of the transition metal complex depend on the ordering and occupancy of the orbitals.

Two principles dominate the design of transition metal complexes for luminescent sensors. Firstly, according to Kasha's Rule, emission should only occur from the lowest excited state energy level, since non-radiative decay from upper excited levels to the lowest excited level is normally extremely efficient.[9] So, in order to control the luminescent properties of transition metal complexes, the nature of the lowest excited state and the energies of the upper excited states are crucial. Secondly, for complexes of second and third row transition elements, the high spin-orbit coupling of the metal promotes intersystem crossing to the triplet manifold, so that emission normally involves spin forbidden triplet to singlet transitions.

The criteria that have to be met for the successful design of a molecular luminescent sensor[5] are:

- High quantum yield
- Long excited state lifetime
- Ability to bind selected analytes with high selectivity
- Easily excited at wavelengths > 350 nm
- Photochemically/chemically robust

With reference to the electronic structure of transition metal complexes discussed in the previous section, it can be seen that in order to achieve the criteria set out above, the lowest excited state must be either charge-transfer in nature, or ligand π-π*. As mentioned previously, d-d transitions usually lead only to unstable excited states, therefore to maximise luminescence and minimise decomposition, the energy gap

between the higher energy d-d state and the emitting state must be maximised in order to minimise mixing with the former. This is achieved by selecting a combination of ligands and metal that offers a large crystal field splitting parameter, Δ_o. This parameter is critical to the design of luminescent complexes, hence altering the ligand geometry or metal ion can have a profound effect on the luminescence properties. In general, crystal field strength increases in the order $Cl^- <$ pyridine (py) $\ll$ bpy, phen $< CN^- < CO$, and is larger for 2nd and 3rd row transition metals than for those of the first row.

As noted above, a further property of the heavier metals of the 2nd or 3rd transition series is their high spin-orbit coupling, which increases the "allowedness" of formally spin-forbidden emission, making radiative decay more competitive with non-radiative decay. Pure π-π^* phosphorescence is too slow for efficient emission at room temperature, as it cannot compete with other deactivation processes, hence either spin-orbit coupling or mixing with more allowed charge-transfer states must be exploited to increase the rate of this process and allow it to compete with other deactivation pathways.

Once all of these factors are taken into consideration, it becomes immediately obvious why most examples of transition metal complexes that have been designed as molecular luminescent sensors include 2nd and 3rd row transition metals, with almost no examples from the 1st transition series, and also why the most popular ligands are strong-field ligands such as α-diimines, cyano, phosphines and carbonyl ligands.

1.1.3. Examples of Transition Metal Complexes as Molecular Luminescent Sensors

Although investigations into the design of transition metal complexes as molecular luminescent sensors have led to many examples in the literature, the majority to date have been based around polypyridyl complexes of Ru (II).[10-14] The luminescence of $Ru(bpy)_3^{2+}$ from a ^3MLCT state is well-known, and has been investigated intensively. An example of a system of this type is shown in fig 1.2, in which the $Ru(bpy)_3^{2+}$ moiety is covalently linked to a p-tert-butylcalix[4]arene.[10]
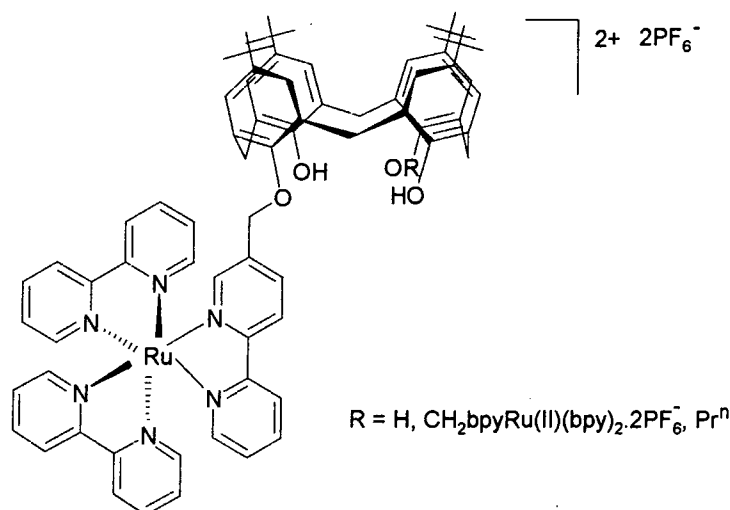
Figure 1.2 - *p-tert-butylcalix[4]arene-linked ruthenium (II) tris(bipyridyl) complex[10]*

These complexes display pH-sensitive luminescence. The trisbipyridyl ruthenium (II) moiety acts as a luminophore while the free phenolic units of the calix[4]arene act as the acid-base sites. Formation of the phenolate anion(s) causes photoinduced intramolecular electron transfer to take place from the phenoxide ion to the trisbipyridyl ruthenium (II) moiety, thus quenching the luminescence. Once the phenolate anions are protonated no such electron transfer may take place and hence the luminescence is restored. So, by monitoring the intensity of luminescence, one can effectively gain information about the pH of the solution.

More recently, complexes very closely related to $[Ru(bpy)_3]^{2+}$, but in which one of the bipyridine ligands bears a protonatable (pyridyl) or deprotonable (phenolic) substituent, have been investigated (the ligands are shown in figure 1.3). In this case, protonation or deprotonation of the pendent group can switch on or off the ^3MLCT emission of the $[Ru(bpy)_3]^{2+}$ core.[11]
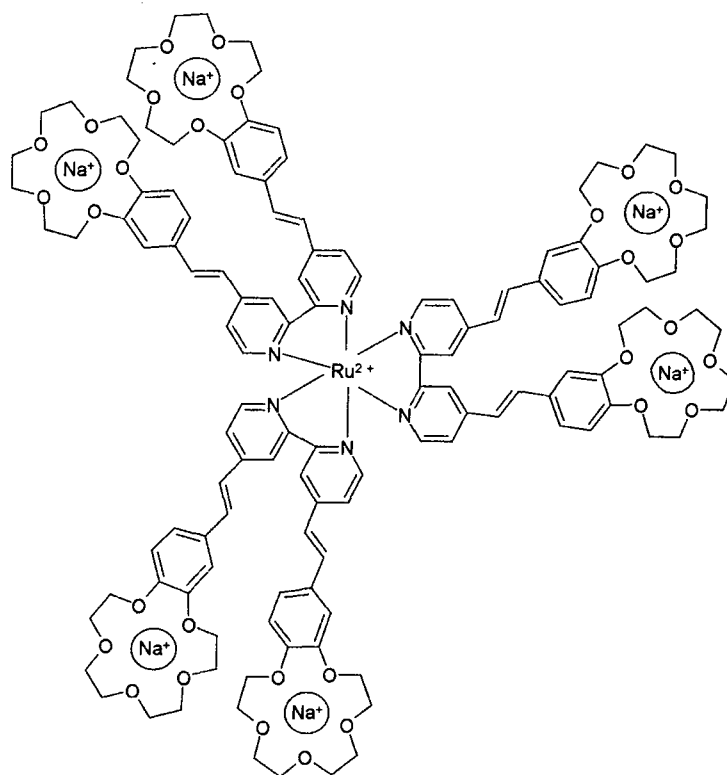
Figure 1.4 - *Specific metal ion sensor for group IA and IIA cations[15]*

This structure was designed for the recognition of group IA and IIA metal cations. The λ_{max} and ε values for both the low-energy ligand-based π-π* transition and the metal-to-ligand charge transfer band observed for the complexes are sensitive to the binding of sodium and magnesium cations.

A cyclam-bipyridine-containing Ru (II) complex has been prepared for use as a luminescent sensor for Ni^{2+}/Cu^{2+}.[14]

$M^{2+}=Cu^{2+}$ or Ni^{2+}
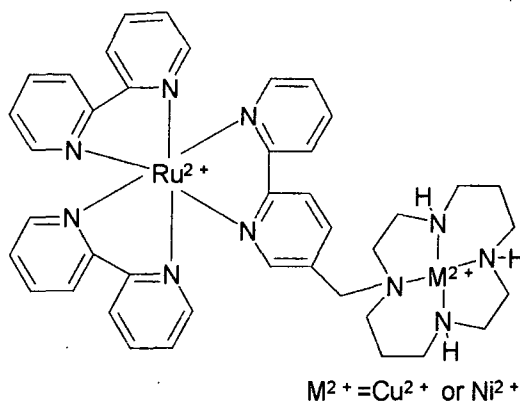
Figure 1.5 - *Metal ion sensor for Ni^{2+} and Cu^{2+}[14]*

Binding of Ni^{2+} or Cu^{2+} to the cyclam appears to totally quench the luminescence, but the cyclam ion complex may form too slowly and bind too strongly to permit its use as an analytical tool.

1.2. Photophysical Study of Iridium (III) bis(terpyridine) Complexes

The photophysics of Ir (III) polypyridine complexes is extremely diverse, since iridium is able to form a large range of complexes, including mono-, bis- and tris-cyclometallated systems, as well as those coordinated solely by nitrogen.[16] All these classes are potentially luminescent, with predominantly charge-transfer (MLCT) or ligand-centred emissive states, depending on the charge density donated from the ligands to the metal. For example, when some ligands are anionic (e.g. chloride, cyclometallating ligand), sufficient charge compensation for the metal-centred oxidation exists, hence the emitting states have MLCT character. On the other hand, the presence of neutral ligands, which donate less charge density, leads to ligand-centred emission, with no metal-based oxidation observed.

$Ir(bpy)_3^{3+}$, which falls into the latter category, is perhaps one of the most well understood iridium polypyridyl complexes in terms of its photophysical properties.[16] Emission from this complex is generally ligand-centred with a lifetime of ca 80 µs at 77K[17, 18] as a result of the increased positive charge of iridium making oxidation of the metal to create MLCT states much more difficult (metal-centred oxidation of $Ir(bpy)_3^{3+}$ occurs at a rather high potential of +2.17 V[17, 19]). However, it is noteworthy that at room temperature it exhibits a reasonably long lifetime of 2.4 µs, suggesting that emission has a small amount of MLCT character (less than 20-30%).[17, 18]

Replacement of two of the bipyridine ligands by two phenylpyridine ligands, leads to the formation of an *ortho*-metallated complex, reducing the overall charge of the complex, in this case to +1. The strong σ donating nature of the coordinating carbon leads to an increase of electron density at the metal centre, making it easier to oxidise the metal and hence more MLCT character is observed in the emission. Thus, $[Ir(ppy)_2(bpy)]^+$ is luminescent at room temperature with a lifetime of 0.34 µs in degassed acetonitrile.[20] The photophysical properties of $[Ir(ppy)_2(bpy)]^+$ were first reported by Watts and King in 1987,[21] and more recently this complex has been investigated extensively for integration into luminescent supramolecular arrays due to its desirable photophysical and redox properties.[22]

The charge-neutral tris-cyclometallated analogue, [Ir(ppy)₃] has also attracted much interest over the past four years for oLED technology,[23] however, in terms of the construction of supramolecular arrays, the replacement of bidentate pyridyl-based ligands by terdentate analogues offers several advantages from a structural viewpoint. This led to work by Mamo, Campagna *et al.* who investigated the combination of Ir (III) and cyclometallating terdentate ligands[24] in order to combine the advantages of terpyridine from a structural viewpoint, with the favourable redox and photophysical properties of cyclometallated complexes.
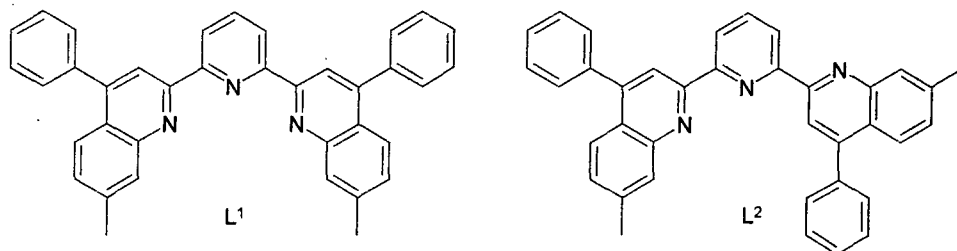
Figure 1.6 - *Cyclometallated terdentate bis(quinolyl)pyridine ligands*[24]

The complexes [Ir(L¹)(L²)]²⁺ and [Ir(L₂)₂]⁺ prepared from the ligands shown in figure 1.6 represent the first luminescent and redox-active Ir (III) cyclometallated bis(terdentate) compounds.[24] Both complexes exhibit intense luminescence at 77K, in a rigid matrix and at room temperature in deoxygenated acetonitrile solution. The emission was assigned to ³MLCT levels in all cases, on the basis of emission spectral shapes, energies and lifetimes.[24] The lifetime for the homoleptic complex in deoxygenated acetonitrile was 0.325 μs, and 20 μs in a rigid matrix at 77K; lifetimes for the heteroleptic complex were 2.3 μs and 9 μs in acetonitrile and a rigid matrix respectively. The oxidation pattern of the homoleptic complex showed a reversible one-electron process at +1.40 V vs SCE attributed to metal-centred oxidation. Four reversible one-electron reduction processes were also observed, assigned to the reduction of each ligand. Considering the heteroleptic complex, it is expected that metal-based oxidation would be shifted towards more positive potentials, because of the presence of the non-cyclometallating ligand. Indeed, no oxidation process was observed for this complex up to +2.00 V vs SCE. As for the homoleptic complex, four reversible one-electron reduction processes are observed for the reduction of the ligands.[24]

Only slow progress has been made in the field of N₆-coordinated iridium (III) polypyridine complexes, due to difficulties encountered in the synthesis and purification of complexes.[16] Indeed it was not until 1990 that Demas and co-workers reported the first synthesis of [Ir(tpy)₂]³⁺ following the initial stage of the procedure they had used in

1974 for the synthesis of $[Ir(bpy)_3]^{2+}$.[25] The luminescence properties of $[Ir(tpy)_2]^{3+}$ were reported in this work, the observed emission being assigned to a primarily ligand-centred excited state, reflecting the lower charge density donated from neutral terpyridine ligands, compared to cyclometallated ligands in the examples given above.

A further photophysical study of Ir(III) bis(terpyridine) complexes was published in 1999, with an investigation of the complexes shown in fig 1.7.[26] In this work too, the authors ascribed the luminescence from the complexes to a ligand-centred (LC) excited state, with possibly some metal to ligand charge transfer (MLCT) character facilitating the emission.
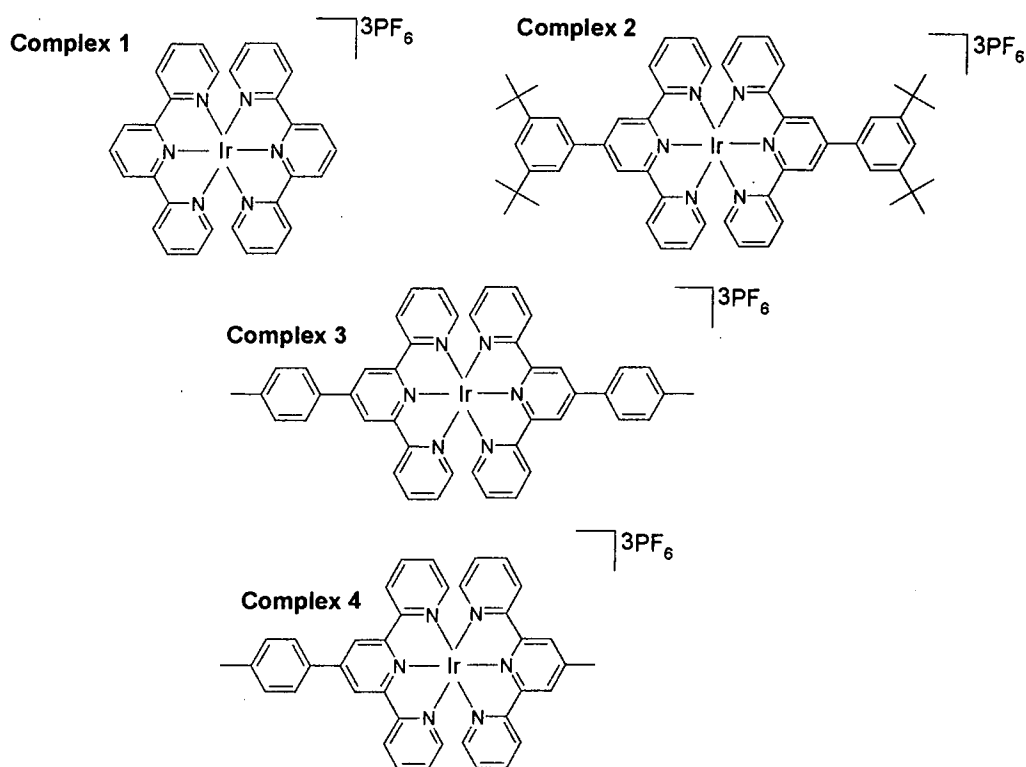
Figure 1.7 - *Ir (III) bis(terpyridine) complexes prepared by Collin et al[26].*

Assignment of the emission as predominantly ligand-centred was made on the basis of the vibrational resolution of the luminescence spectra. The profiles of complexes 2-4, which closely overlap each other, are less vibrationally resolved than the spectrum of complex 1, but this may be explained by considering the larger framework available for complexes 2-4.

However, the transitions in the latter may not be purely ligand-centred, as the less well resolved emission profiles of complexes 2-4 could be due to the presence of excited states of MLCT nature, that are known to exhibit unresolved luminescence bands. This

hypothesis was tested by comparing the luminescence profiles with those of $[Zn(tpy)_2]^{2+}$ and $[Zn(ttpy)_2]^{2+}$ at 77K, which are expected to conform to pure ligand-centred emissions from tpy and ttpy ligands.[25] It was found that the profile exhibited by complex 1 closely matched that from the corresponding zinc complex, however the profiles exhibited for complexes 2-4 were different, indicating that the luminescence of the complexes containing an aryl tpy ligand is not of pure ligand-centred nature and might involve excited states of MLCT nature. Further evidence to support the claim that the emission was not purely ligand-centred came from the measurement of the radiative lifetimes, which were found to be on a microsecond timescale. This is arguably too short to be pure ligand-centred emission, but much too long to be an MLCT state, suggesting that there is a dominant contribution from the π-π^* state, with possibly some mixing with the more allowed MLCT states.

Temperature dependent studies of the luminescence properties in the 95-298K range indicate that higher lying levels of these complexes are not efficient pathways for deactivation of the luminescent states, unlike the case of the ^{3}MLCT-^{3}MC coupling which occurs in Ru (II) polypyridine emitters.[27, 28]

Investigations have begun to exploit the long-lived emission of the iridium bis(terpyridine) core in sensing applications.[29-31] Derivatives that display long-lived pH-sensitive emission have been prepared, by incorporating pendent pyridyl or phenolic substituents (figure 1.8),[29] in a strategy similar to that described earlier based on $[Ru(bpy)_3^{2+}]$.[11]
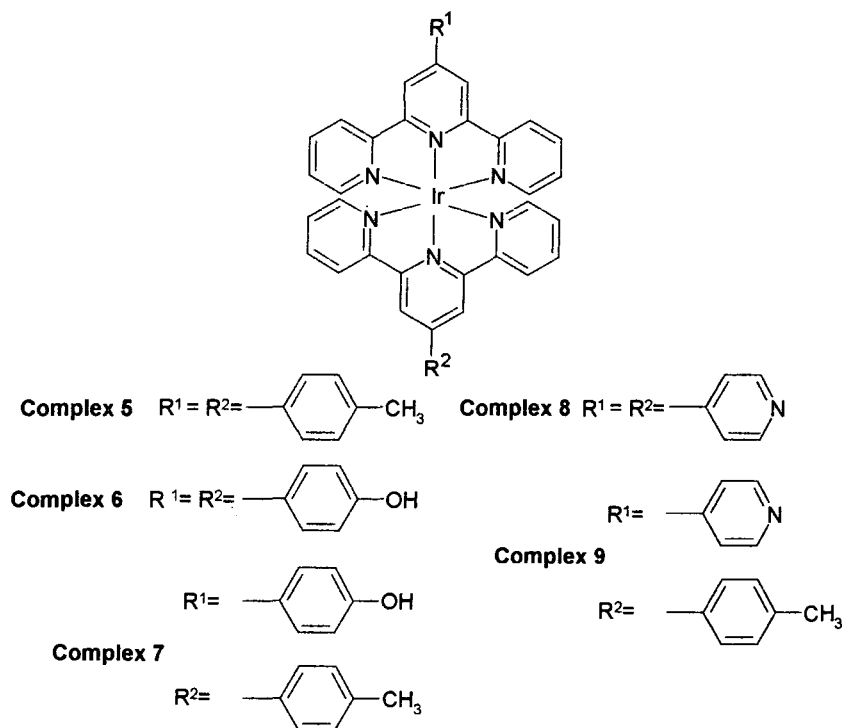
Figure 1.8 - *Ir(III) bis(terpyridine) complexes displaying pH sensitive emission*[29]

Of particular interest was complex 9, which displayed long-lived emission at pH 7 in air equilibrated aqueous solution, comparable to the parent bis-tolyl complex. Protonation of the pyridyl nitrogen on the pendent ring resulted in a reduction in the lifetime and emission intensity by a factor > 8, making it potentially amenable to applications as a pH sensor.

This effect was explained by considering that the mixing of shorter lived, higher lying d-π^* charge transfer excited states into emissive π-π^* ligand-centred states can promote deactivation and thereby shorten the observed lifetime. Although not energetically accessible in the neutral complex, protonation will lower the energy of such MLCT excited states, leading to increased mixing with the emissive LC state and hence to the shorter lifetimes and reduced intensities that are observed (figure 1.9)[29]

The energy is determined by:

1) The ease of oxidation of iridium
2) The ease of reduction of the ligand

Reduction of the ligand should be facilitated upon protonation
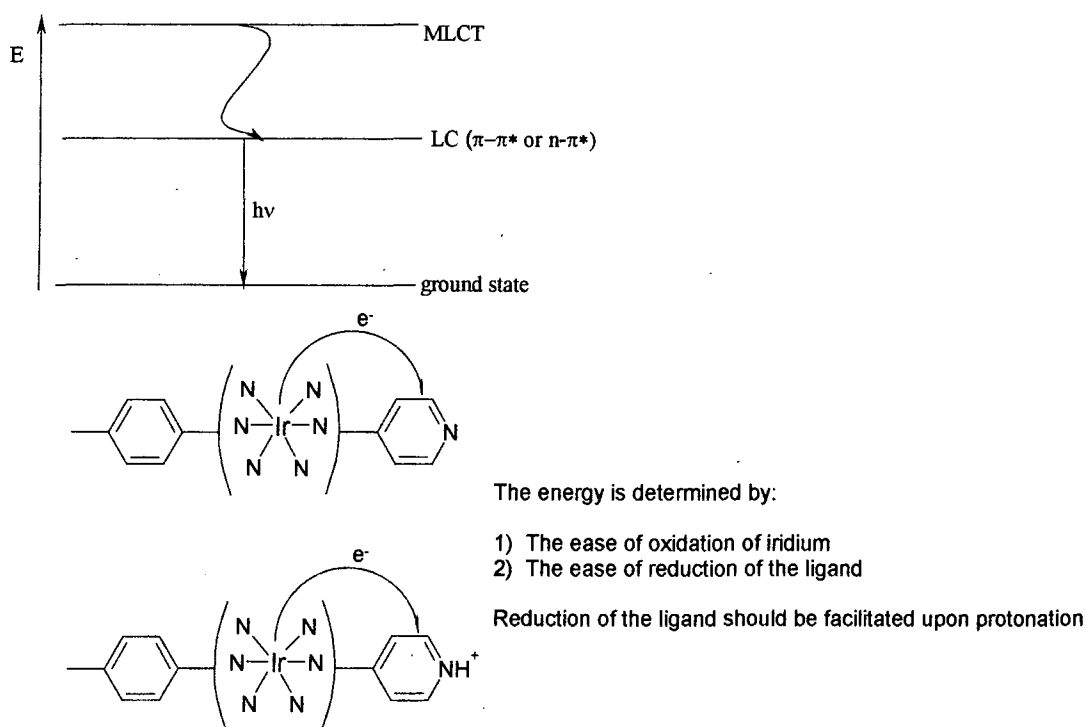
Figure 1.9 - *Mixing of the higher charge-transfer state with the lower ligand centred emissive state*

Subsequent studies using time-resolved spectroscopy revealed biexponential luminescence decay kinetics, attributed to simultaneous emission from the two terpyridines, which are not fully equilibrated at room temperature. The major and minor components had lifetimes of 4.6 ($\pm$0.2)μs and 1.0 ($\pm$0.2)μs, attributed to the tolyl-terpyridine and pyridyl-terpyridine ligands, respectively. This assignment was based on a comparison with the behaviour of the corresponding homoleptic complexes and the wavelength dependence of the relative weightings of the two components in the kinetic decay of the heteroleptic complex.[29]

In a study carried out by the author of this thesis, immediately prior to the work described here, the N-methylated analogue of complex 9 (complex 10) together with the corresponding *meta* complex (complex 11), were investigated as luminescent sensors for chloride ions.[30]

Complex 10   **Complex 11**
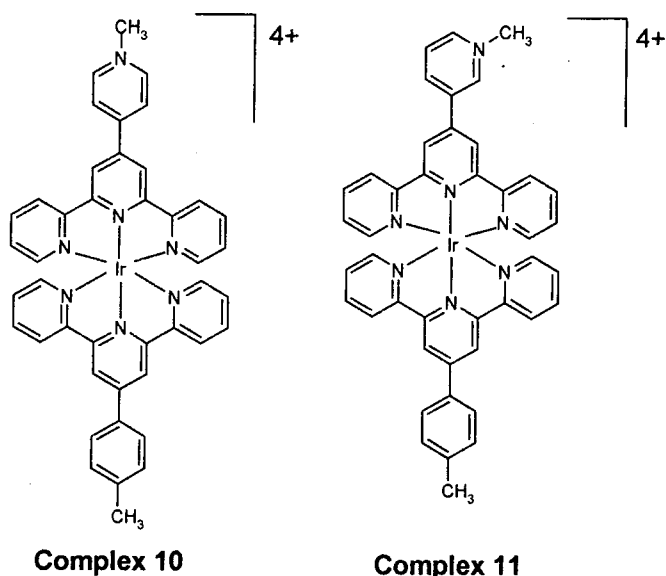
Figure 1.10 - *Ir(III) bis(terpyridine) complexes displaying chloride sensitive emission*[30]

Again, biexponential decay was observed. Complex 11 was much more strongly luminescent than 10, probably because the site of the N^+-Me positive charge is now not in direct conjugation with the terpyridine and hence will be less effective at lowering the energy of the higher lying MLCT state.

The addition of halide ions led to partial quenching of the emission of both complexes, in aqueous solution. The *meta* isomer displayed no change in the spectral profile on addition of chloride, and obeyed modified Stern-Volmer kinetics over the physiologically relevant range 0.01-0.1 mol dm^{-3}. The *para* isomer, on the other hand, displayed a much more sensitive response to chloride, and in this case quenching was accompanied by a marked change in the form of the spectrum, displaying a red shift in the emission maximum. A more complex temporal decay of emission was observed in the presence of chloride that could not be fitted to double exponential decay or to a Stern-Volmer plot.

Following these results, Lo *et al.* reported the synthesis, characterisation and photophysical properties of a series of luminescent iridium (III) terpyridine complexes functionalised with an isothiocyanate moiety.[31] The incorporation of the isothiocyanate group allows these complexes to react with primary amine groups of biological substrates to form bioconjugates with stable thiourea linkages, making them novel biological labelling reagents.
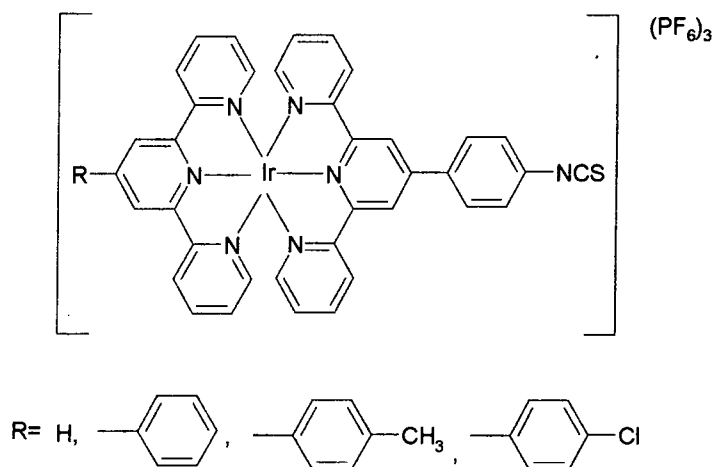
Figure 1.11 - *Iridium (III) bis(terpyridine) complex functionalised with an isothiocyanate moiety*[31]

The group carried out a photophysical study of the free complexes, drawing similar results and conclusions regarding the nature of the luminescence of the complexes as those discussed by Collin *et al.*[26] and Williams *et al.*[29, 30]

They then went on to label two proteins, HSA (human serum albumin) and BSA (bovine serum albumin), with the complex where R = H, purifying the bioconjugates by size-exclusion chromatography to remove the unreacted complex. The electronic absorption spectra of the conjugates displayed intense absorptions in the visible region, ascribed to the absorption properties of the Ir (III) chromophores of the labels. Upon photoexcitation, these conjugates exhibit intense and long-lived yellow emission, whose maxima are indistinguishable from that of the free complex, suggestive of a $^3LC/^3MLCT$ emissive state.

1.3. Synthesis of Terpyridine Ligands

Terpyridine was first isolated by Morgan and Burstall during the 1930's as a by-product of the oxidative coupling of pyridine by iron (III) chloride at elevated temperature and

pressure.[32, 33] The authors were attempting to synthesise bpy for the study of various coordination compounds when they isolated tpy as a by-product and observed that it *"forms a remarkable series of coordination compounds with metallic salts in which the base acts as a tridentate group".*[34] Further investigations into dehydrogenation reactions using a variety of metal chlorides were made, however all were found to be less successful than the iron (III) coupling.[35] Further work was carried out in an attempt to improve the synthesis of terpyridine, including investigations into the Ullman Coupling reaction[34], oxidative coupling using iodine[34] and dehydrogenative coupling of pyridine using Raney nickel,[36] but none gave yields of the desired terpyridine above 10%, and much of this work is now mainly of historical interest only.

Contemporary syntheses can be divided into one or other of two general methodologies.[37, 38] One approach involves the construction of the central pyridine ring or, more rarely, of the two terminal pyridine rings, whilst the second approach is to build up a terpyridine fragment through a series of cross-coupling reactions on pyridyl substrates in a controlled manner.

1.3.1. Condensation Methodology

A popular method of terpyridine synthesis involves the construction of the central pyridine ring *via* the condensation of two ketones with an aldehyde to give a 1,5-diketone. The diketone then undergoes ring closure upon treatment with, for example ammonium acetate,[39, 40] hydroxylamine,[41] formamide[39] or acetamide,[39] to form a terpyridine.

The earliest condensation methods developed were based on the Hantzsch[42] or Tschitschibabin[43] syntheses of pyridine. The Hantzsch synthesis involves the construction of a pyridine ring *via* the condensation of two equivalents of a 3-oxocarboxylate ester with an aldehyde, followed by cyclisation with ammonia to give a dihydropyridine ester. Oxidation of the dihydropyridine ester with nitric acid affords the pyridine ring. The desired 2,6-disubstituted pyridine˙ is obtained following saponification and then decarboxylation of this ester.[42]
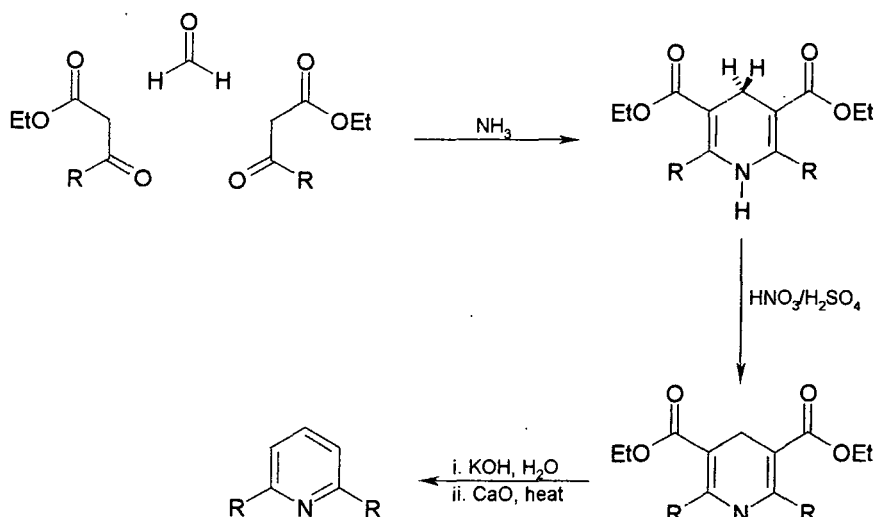
Figure 1.12 - *Representative Hantzsch synthesis of pyridines*

The Tschitschibabin pyridine synthesis involves the co-condensation of two ketones and an aldehyde in aqueous ammonia, with catalytic amounts of ammonium acetate at elevated temperature and pressure.[43]
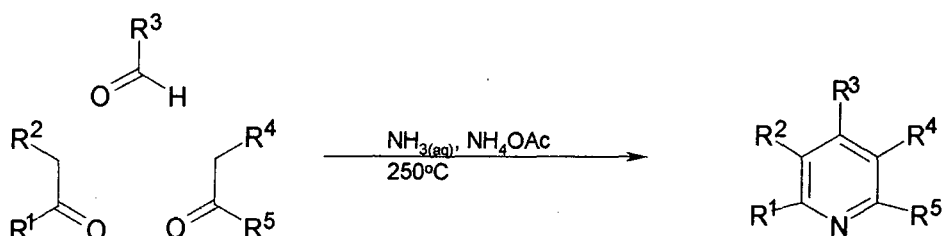
Figure 1.13 - *Representative Tschitschibabin synthesis of pyridines*

One of the earliest examples of terpyridine synthesis reported in 1956 by Case and Kasper[44] involved a modified Tschitschibabin reaction. Synthesis of the terpyridines shown in figure 1.14 was achieved through heating a stoichiometric mixture of the appropriate 2-substituted acetylpyridine or quinoline, benzaldehyde, ammonium acetate and ammonia in 28% aqueous solution in a sealed tube at 250°C for 5 hours.

R¹ = H   R² = H
R¹ = CH₃   R² = H
R¹ = C₂H₅   R² = H
R¹ = C₆H₅   R² = H
R¹ = H   R² = C₆H₅
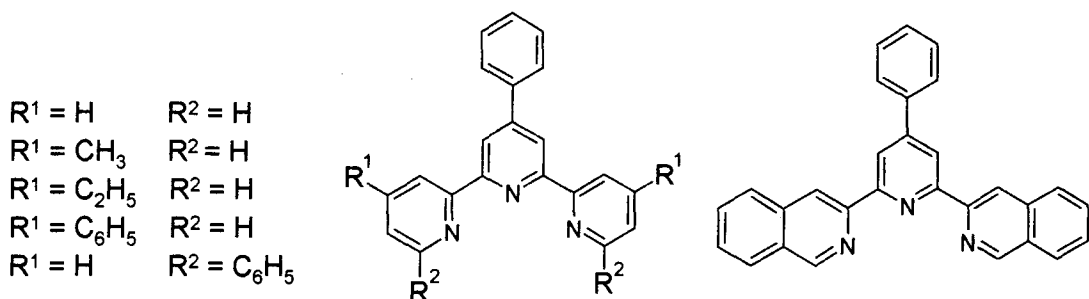
Figure 1.14 - *Terpyridines synthesised by Case and Kasper[44]*

Spahni and Calzaferri[45] synthesised the group of terpyridines shown in figure 1.15 using a similar procedure, but in this case by refluxing a mixture of the appropriate aldehyde and 2-acetyl pyridine in acetamide, in the presence of ammonium acetate.

R=CH₃-O, Cl, Br, CH₃, CH₂Br, HO
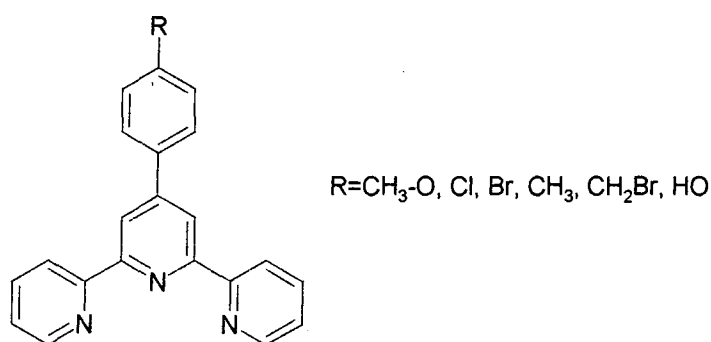
Figure 1.15 - *Terpyridines synthesised by Spahni and Calzaferri[45]*

Although a one-pot procedure, the synthesis almost certainly involves three distinct reactions. An aldol condensation between the aldehyde and the first equivalent of 2-acetyl pyridine leads to an α, β-unsaturated ketone, which then undergoes a Michael reaction, in which it is attacked by the enolate of the second equivalent of acetyl pyridine. Ring closure with ammonium acetate results in the formation of a dihydropyridine, which forms the terpyridine upon aerial oxidation.
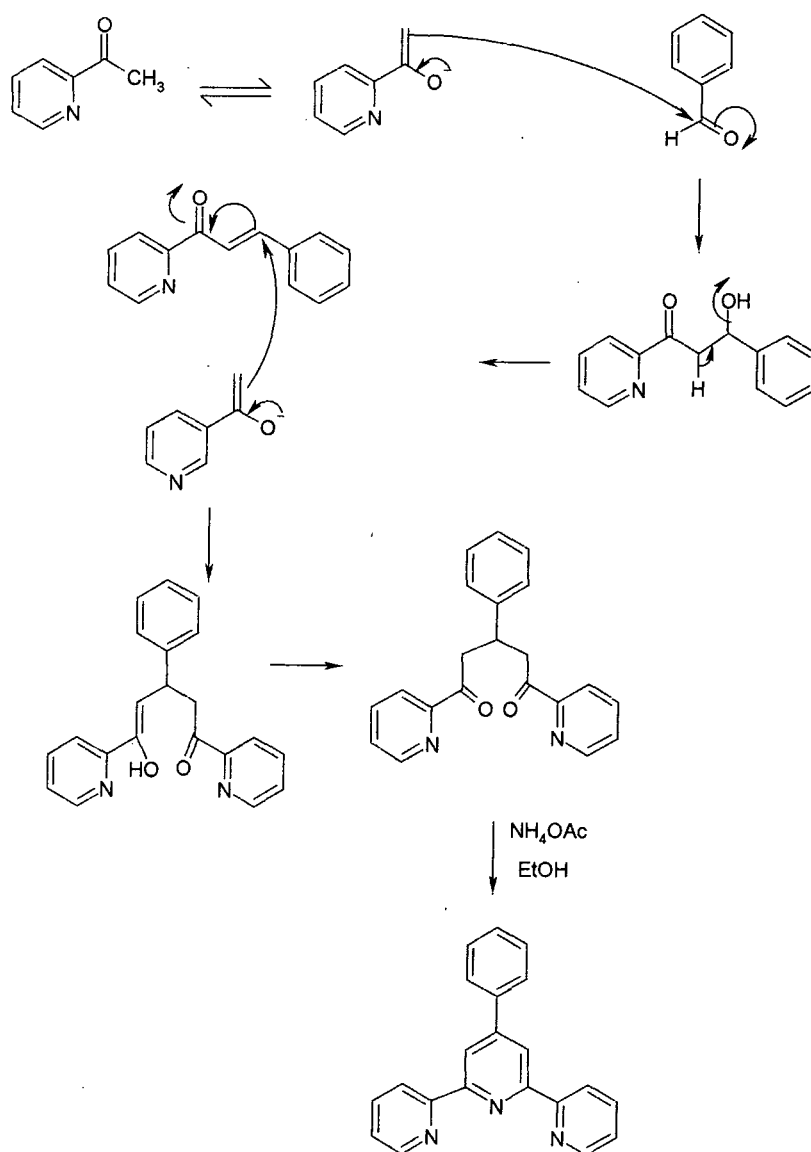
Figure 1.16 - *Multi-step synthesis of terpyridines via 2 condensation reactions*

The drawbacks of the Tschitschibabin synthesis are the relatively harsh reaction conditions required, the low yields eventually obtained from the extraction of the crude reaction mixture, and the amount of by-product formation. Work carried out in an effort to improve the yield and product specificity of the reaction has led to the use of multi-step variants on the above methodology, in which the formation of the α, β-unsaturated ketone and the ring closure are carried out in two distinct steps.[46, 47]

In the case of activated substrates, the reaction may proceed readily at room temperature or lower, for example, as reported by Persaud and Barbiero for the synthesis of 4'-pyridylterpyridine.[47] In this instance, the formation of the 1, 5-diketone occurs at

−10°C, and ring closure is then effected upon treatment with ammonium acetate in refluxing ethanol, without isolation of the intermediate. Constable has also used this procedure at room temperature with the intermediate dione being isolated, prior to the reaction with NH₄OAc.[46]

Recently, Cave and Raston published a solvent-free variant, in which the initial Aldol condensation and Michael addition reactions were carried out in the absence of a solvent.[48] Acetylpyridine, the appropriate aldehyde and sodium hydroxide pellets were crushed together until the diketone was formed as a pale yellow powder. A solvent is still required, however, in the subsequent reaction of the diketone with ammonium acetate, which was carried out in acetic acid.

Earlier, Krönhke had developed a variation on this multistep strategy towards terpyridine synthesis using pyridinium salts as the synthetic equivalent of an enolate.[39, 49]
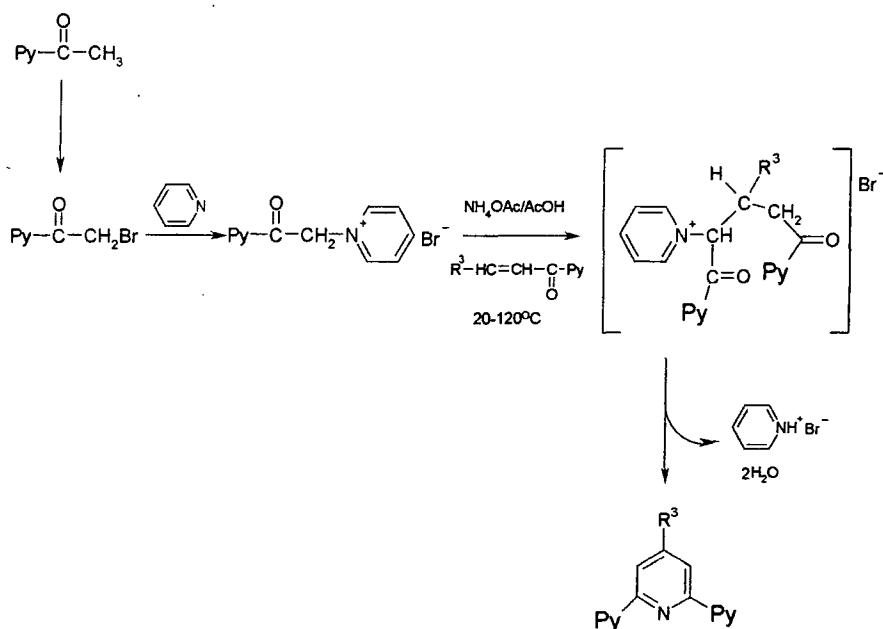
Figure 1.17 - *Krönhke synthesis of terpyridines[39]*

One of the main advantages of this methodology is the high reactivity of the N-methylene hydrogen atoms in many pyridinium salts, which exceeds that of the methyl hydrogen atoms in methyl ketones. A further advantage provided by the use of N-acylpyridinium salts is that the pyridinium group acts as an internal oxidant, effecting the dehydrogenation step required to aromatise the dihydropyridine obtained from the ring closure.

Krönhke published a comprehensive review of the methodology, in which the mechanism is discussed in detail prior to a consideration of its application to the synthesis of bipyridines, terpyridines, quaterpyridines, quinqepyridines and septipyridines.[39]

In a variant on this methodology, Potts reported a high yield synthesis of the substitutionally versatile ligand 4'-methylthio-2, 2': 6', 2"-terpyridine, which features an α-oxoketene dithioacetal as the synthetic intermediate in place of the α, β-unsaturated ketone. Apart from its utility in the synthesis of thiol-substituted oligopyridines, the procedure offers an interesting route to terpyridine itself, through removal of the thiomethyl group.[50-53]
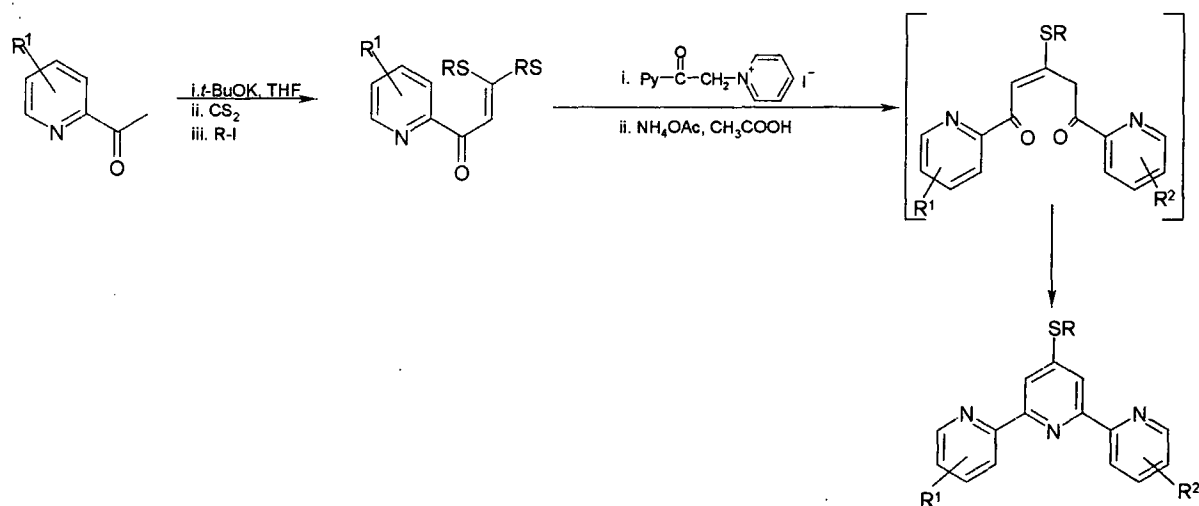
Figure 1.18 - *Synthesis of terpyridines via the Potts methodology*

A more direct route to terpyridine has subsequently been developed, offering multi-gramme quantities in a straightforward 2-step process, with an overall yield of 47%.[54]
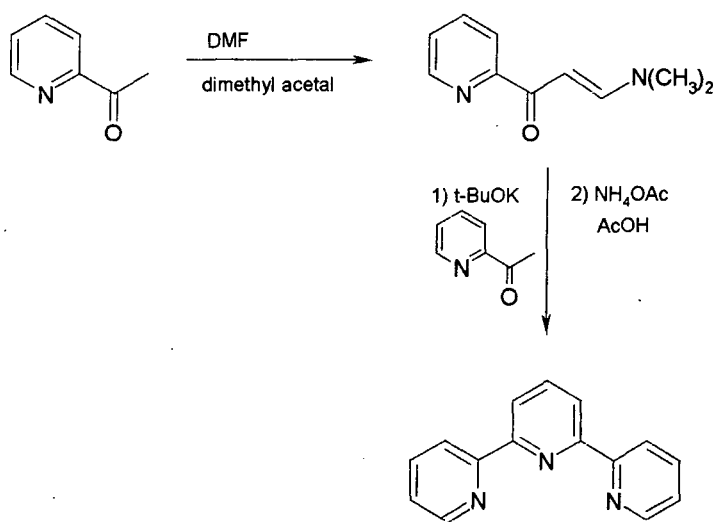
Figure 1.19 - *Synthesis of terpyridine using an enaminone intermediate[54]*

In this case, the key synthetic intermediate is an enaminone, which is prepared in high yield upon treatment of 2-acetylpyridine with N, N-dimethylformamide dimethyl acetal.

Many of the condensation methodologies discussed above have also been applied to the assembly of the two terminal pyridine rings of the 2, 2': 6', 2"-terpyridine in a variety of 6, 6"-diaryl-2, 2': 6', 2"-terpyridines. Indeed, these reactions form the basis of the synthesis of 2, 2': 6', 2": 6", 2'": 6'", 2""-quinquepyridines.[39, 50]

1.3.2. Coupling Methodologies

As noted previously, early syntheses of terpyridine were based on coupling reactions mediated by simple metal salts, but gave low yields and complex mixtures.[37, 38] More recently, a number of examples of nickel-catalysed dimerisation reactions have been reported, involving homo-coupling of halo-aryl substrates and leading to "back-to-back" polypyridyl ligands and complexes.[55-58] For example, the quaterpyridine in fig.1.20 was prepared in this way from 4'-chloroterpyridine, using [Ni(PPh₃)₂Cl₂]/Zn/PPh₃ as the catalyst precursors.[59]
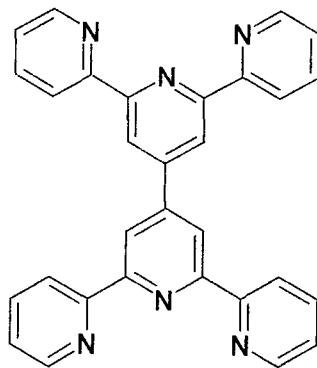
Figure 1.20-*6', 6"-bis (2-pyridyl)-2, 2': 4', 4": 2", 2"'-quaterpyridine*[59]

Far more powerful, versatile and attractive however, is the use of controlled *cross-coupling* reactions, especially those catalysed by Pd (0).

1.3.2.1. Introduction to Palladium-Mediated Coupling Reactions

Many organometallic reagents have proven to be highly useful as nucleophiles for palladium catalysed cross-coupling reactions e.g. organolithium,[60] organosilicon,[61] organostannanes[62-64] and organoboranes.[65]

e.g. X=OTf, Br, I, Cl   Y= -Li, -SiR$_3$, -SnR$_3$, -B(OR)$_2$
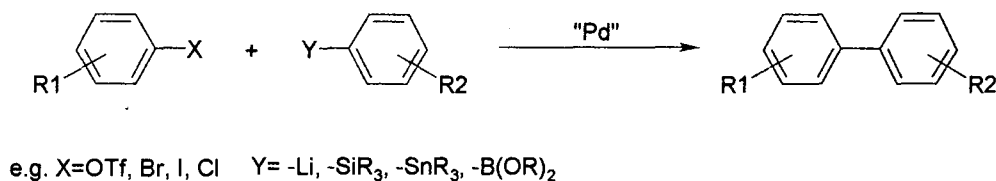
Figure 1.21 - *Cross-Coupling reactions mediated by palladium*

The palladium-catalysed cross-coupling of organostannanes with organohalides, was reported by Stille,[64] and the cross-coupling of organoboranes with organohalides and organotriflates by Suzuki.[66] The Stille methodology using pyridine substrates has now become established as an efficient method of terpyridine synthesis.[38, 67] Prior to the work described in this thesis, however, the Suzuki cross-coupling reaction had scarcely been considered for the synthesis of terpyridines.[68]

Both the Suzuki and the Stille cross-coupling reactions, and indeed the majority of cross-coupling reactions catalysed by Ni (0),[69, 70] Pd (0)[71] and Fe (III),[72] may be rationalised in terms of a common catalytic cycle, whose mechanistic detail is discussed in a comprehensive review by Suzuki and Miyaura.[65] The cycle involves an oxidative addition-transmetallation-reductive elimination sequence.
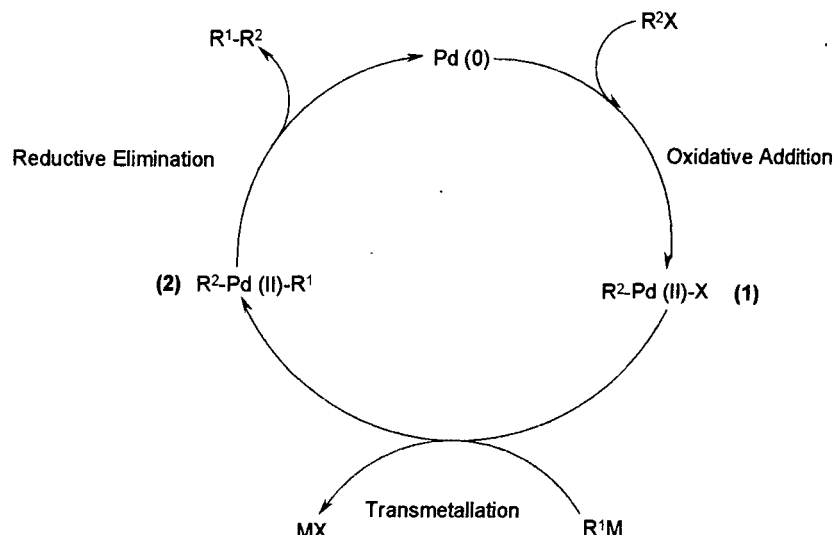
Figure 1.22 - *Catalytic cycle of palladium catalysed coupling reactions*

In both cases, central to the cycle is the Pd (0) catalyst and its precursors, of which there are a very wide range that are effective for the cross-coupling reaction.[65] $Pd(PPh_3)_4$ is the most commonly used, but $PdCl_2(PPh_3)_2$ and $Pd(OAc)_2$ plus PPh_3 or other phosphine ligands are also efficient since they are stable to air and readily reduced to the active Pd (0) complexes. Palladium complexes that contain fewer than four phosphine ligands, or bulky phosphines such as tris(2,4,6-trimethoxyphenyl)phosphine, are, in general, highly reactive for the first step of the cycle (the oxidative addition) because of the ready formation of coordinatively unsaturated palladium species.[73]

The oxidative addition is often the rate determining step of the catalytic cycle with the relative reactivity decreasing in the order of I > OTf > Br >> Cl. However, aryl and 1-alkenyl halides activated by the proximity of an electron withdrawing group are more reactive to the oxidative addition than those containing donating groups, thus allowing the use of chlorides in some cases.[65] The oxidative addition of, for example 1-alkenylhalide or aryl halide to a Pd (0) complex affords a stable trans-σ-palladium (II) complex. The reaction proceeds with complete retention of stereochemistry for alkenyl

halides, however an inversion of stereochemistry is observed for allylic and benzylic halides.[65]

The third step of the cycle, reductive elimination of organic partners from (2), regenerates the Pd (0) complex. The reaction takes place directly when (2) is in the *cis* configuration, and the *trans* complex only reacts after its isomerisation to the corresponding *cis* complex. The order of reactivity is diaryl>(alkyl) aryl>dipropyl>diethyl>dimethyl palladium (II), suggesting participation by the π-orbital of the aryl group during the bond formation.[74]
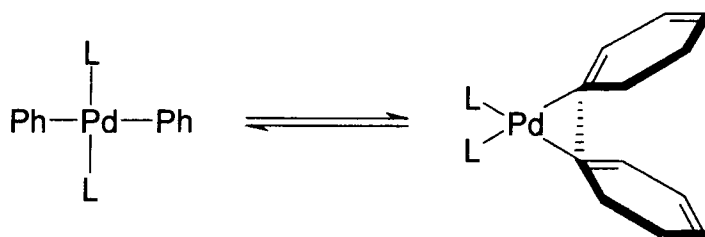
Figure 1.23 - *Participation of π orbitals during reductive elimination*

The mechanisms of oxidative addition and reductive elimination sequences are reasonably well understood and are presumably fundamentally common processes for all cross-coupling reactions of organometallics, but less is known about the transmetallation step because the mechanism is highly dependent on organometallics or reaction conditions used for the couplings. A more detailed discussion of the transmetallation step is given later in the chapter when the catalytic cycle is discussed in further detail for the coupling of aryl boronic acids to aryl triflates and aryl bromides.

1.3.2.2. Stille Cross-Coupling Reaction

The Stille cross-coupling reaction was first reported as a method of synthesising terpyridines in 1996 by Cárdenas and Sauvage.[67] The 2,6-oligopyridines shown in figure 1.24 were prepared from the starting materials 1 and 3, which were obtained from the bromo derivatives 2 and 5 respectively *via* lithiation followed by stannylation with Me_3SnCl. The reaction of the appropriate stannane and electrophile in DMF in the presence of $Pd(PPh_3)_2Cl_2$ for 15 h at 90°C led to the formation of the terpyridine products, which were purified and obtained in good yield after column chromatography.

Electrophile	Stannane	Product	Yield (%)
4	1		67
5	3		46
4	3		67
6	1		68
6	3		82
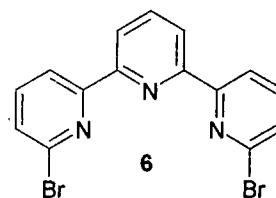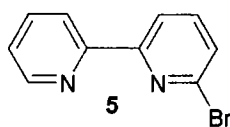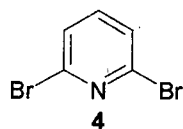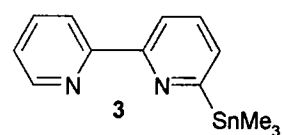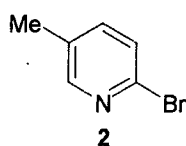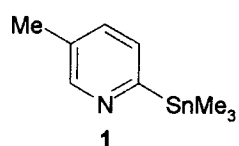
Figure 1.24 - *2, 6-oligopyridines prepared by Cárdenas and Sauvage*[67]

27

Since this original paper, Fallahpour has reported extensively on the application of the Stille cross-coupling reaction for the synthesis of oligopyridines,[38] including a series of 4-nitro-6-bromo-2, 2'-bipyridines and symmetrical and unsymmetrical 4'-nitro-2, 2': 6', 2"-terpyridines, from which the corresponding 4'-amino derivatives could be prepared by reduction.[75]
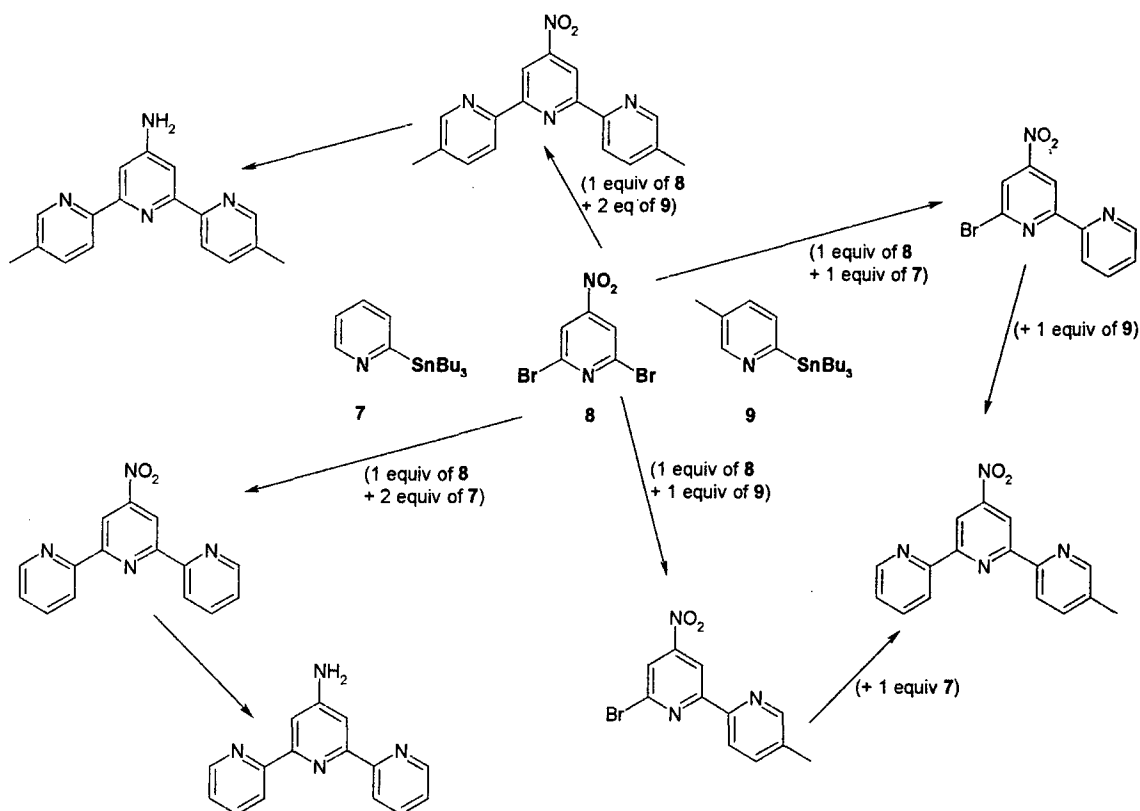
Figure 1.25 - *Terpyridines and bipyridines prepared by Fallahpour*[75]

The conversions were achieved by dissolving the appropriate stannyl and bromo compounds together in toluene, and refluxing in the presence of Pd(PPh₃)₄ as the catalyst.

Sauer *et al.* showed that it is possible to synthesise 4-tributylstannyl-2,6-terpyridine by means of an inverse electron demand Diels-Alder cycloaddition reaction of a dipyridyl triazine with ethynyl tin. This compound was subsequently used as a synthon in Stille coupling reactions to introduce a pendent ring, or to couple terpyridine fragments together to synthesise branching oligopyridines.[76]
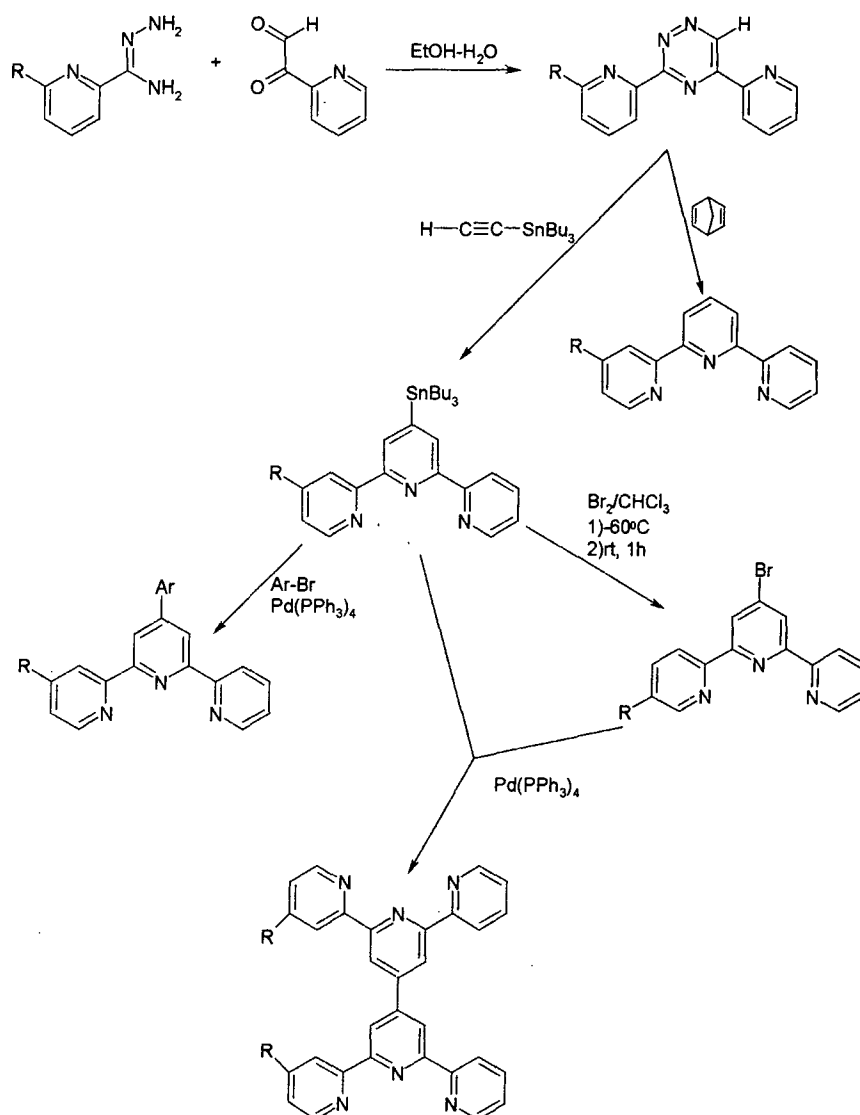
Figure 1.26 - *Synthesis of terpyridines using the Sauer methodology*[76]

29

1.3.2.3.   Suzuki and Miyaura Cross-Coupling Reactions - A mechanistic overview.

The work described in subsequent chapters of this thesis has made use of aryl boronic acids in Suzuki-type cross-couplings, as opposed to the Stille reactions of the previous section.   The "classical" synthesis of aryl boronic acids involves lithiation of haloaromatics or Grignard formation, followed by reaction with $B(OMe)_3$ or $B(O^iPr)_3$ and hydrolysis.[77]   However, an alternative approach, reported by Miyaura in 1995, involves a milder palladium-catalysed cross-coupling of an aryl halide with an alkoxyboron, such as bis(pinacolato)diboron.[78]   The reaction has now become one of the most convenient methods for the synthesis of aryl boronic esters, especially as it allows compounds with functionality sensitive to BuLi to be derivatised.

The mechanistic cycle of this reaction, henceforth referred to as the Miyaura reaction, is very closely related to that of the Suzuki cross-coupling reaction.   In this section, the results of mechanistic studies will be outlined, with reference to the observation that, whilst the Suzuki reaction requires a strong base to be present, the Miyaura reaction has been found to proceed most efficiently in the presence of KOAc.[78, 79]

The catalytic cycle for the Miyaura reaction is shown in fig 1.27 and involves the oxidative addition of a haloarene to a Pd (0) complex to give a ArPd(II)X adduct, the transmetallation between (1) and ArPd(II)X to provide a ArPd(II)B(OR)$_2$ intermediate, and the reductive elimination of the product 3 to regenerate the Pd(0) complex.
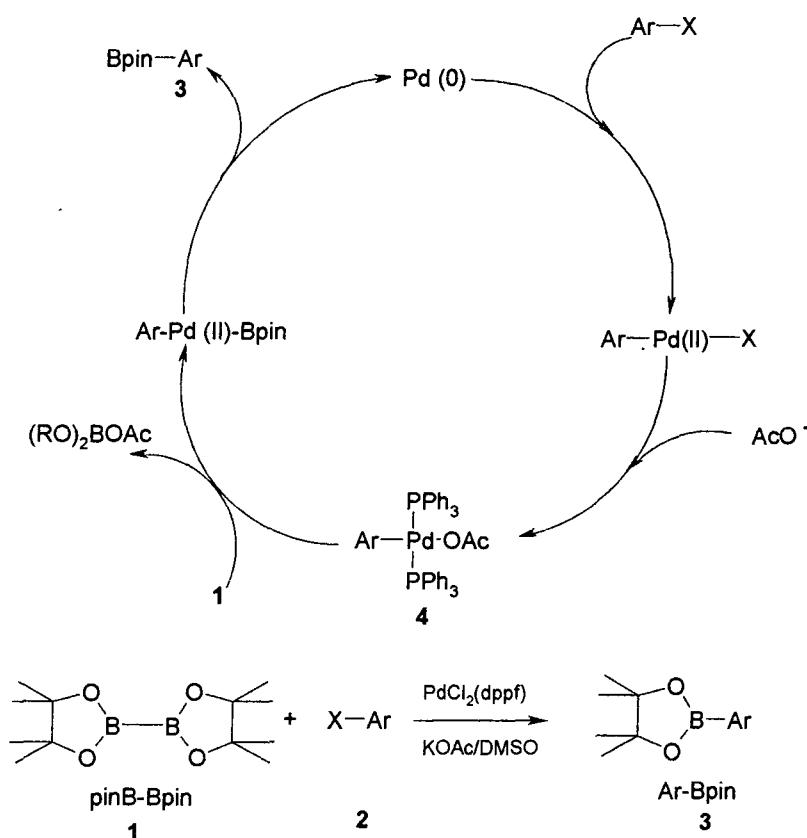
Figure 1.27 – *Catalytic cycle for the Miyaura cross-coupling reaction*[78]

In his original paper,[78] Miyaura discusses in detail the optimum reaction conditions: 80°C is accepted as the optimum temperature, and the reaction was observed to be accelerated in polar solvents: e.g. DMSO≥DMF>dioxane>toluene. The catalyst $PdCl_2$(dppf) gave the best results for haloarenes having either electron withdrawing groups or electron donating groups. The $Pd(PPh_3)_4$ catalysed reactions gave by-products arising from coupling with a phenyl group on PPh_3. The group also experimented with $Ni(PPh_3)_4$, $Pt(PPh_3)_4$ and $RhCl(PPh_3)_3$, but found no catalytic activity at all. Haloarenes having electron-donating groups, such as NMe_2 or OMe, were less reactive than those with electron-withdrawing substituents, which enhanced the rate of reaction. Notably, functional groups such as CO_2Me, COMe and CN, that would have required protection under the conditions of the Grignard or lithium reactions, tolerated the reaction conditions. Also, sterically hindered halides, such as iodomesitylene and heteroaromatic halides, were able to form the corresponding arylboronates in high yields.

The cycle for the Suzuki reaction is similar, with the aryl boronic acid in place of (1) and usually a stronger base in place of AcO[.65] The role of the base during the transmetallation step in both the Miyaura and Suzuki cross-coupling reactions is not fully understood, however a remarkable accelerating effect on the transmetallation between R-Pd-X and trialkylborates or organoboronic acids is certainly observed upon the addition of a base. Two different mechanisms are proposed to explain this effect.[79]
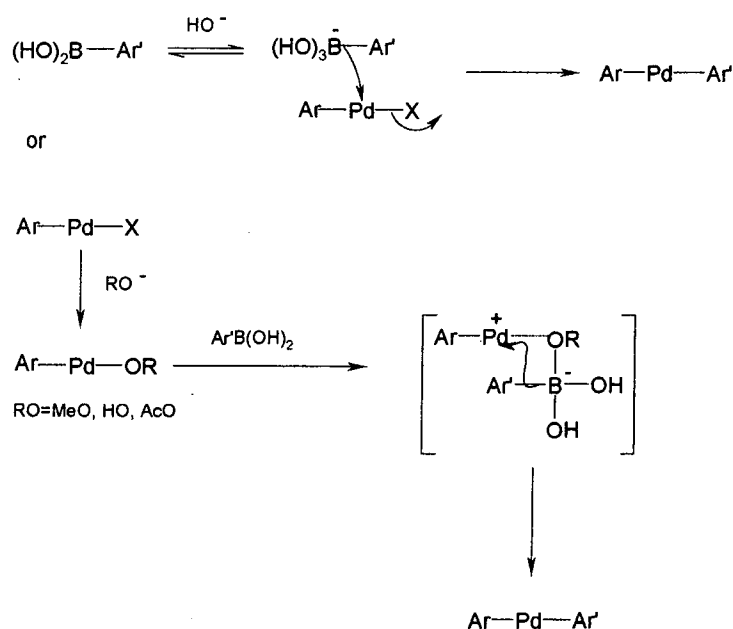
Figure 1.28 - *Role of the base during transmetallation*[79]

The first mechanism suggests that quarternization of the boron atom with a negatively charged base enhances the nucleophilicity of the organic group on the boron atom for alkylation of R-Pd-X. However, there is no direct evidence of hydroxyboronate anions, $ArB(OH)_3^-$.[79] By the second mechanism, the base first displaces the halide from the Ar-Pd-X species to give an alkoxo-, hydroxo- or acetoxopalladium (II) species in solution; these species are known to transmetallate with organoboron compounds under neutral conditions. Evidence for this mechanism was produced in a series of experiments detailed in Miyaura's original paper.[78, 79]

Whilst the Suzuki reaction requires a stronger base, e.g. Na_2CO_3, to accelerate the reaction, weak bases are favoured for the Miyaura reaction, with KOAc reported to offer the best yields and highest selectivity. Strong bases promote further reaction of (3) with the aryl halide resulting in substantial contamination (30-60% yields) of biphenyls.[78]

Another reason why KOAc is particularly effective for the Miyaura reaction is suggested in a proposed model for the role of acetate *via* mechanism 2, where acetate may be seen to act as a nucleophile rather than a base.[80]
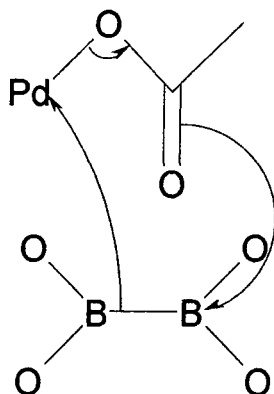
Figure 1.29 - *The role of acetate as a nucleophile rather than a base*[80]

The Suzuki cross-coupling pre-dates the Miyaura reaction by about 20 years.[66] The first coupling of aryl boron derivatives was the synthesis of the biaryls shown in figure 1.30.[81]
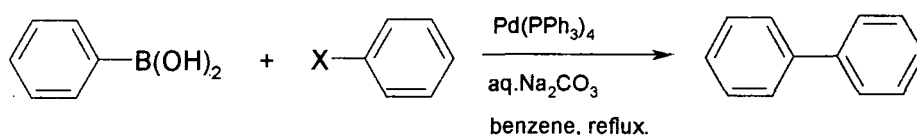
Figure 1.30 - *Synthesis of biaryls via the Suzuki reaction*[81]

Since this discovery many modifications have been made, however a combination of $Pd(PPh_3)_4$ or $PdCl_2(PPh_3)_2$ and aqueous Na_2CO_3 in DME appears to work well in most cases.[82, 83] The reaction is successful for aryl triflates and iodo- and bromoarenes; however, chlorobenzene derivatives are generally quite inert to the oxidative addition, although recent reports indicate that they can react with high-activity catalysts.[84]

As for the Stille coupling reaction, the Pd (0) catalyst is central to the catalytic cycle. Phosphine-based palladium catalysts are generally used since they are stable on prolonged heating; however, on occasions extremely high coupling reaction rates have been achieved by using palladium catalysts without a phosphine ligand such as $Pd(OAc)_2$, $[\eta^3-(C_3H_5)PdCl_2]$ and $Pd_2(dba)_3C_6H_6$.[85, 86]

It should be noted that the Stille reaction does not require the presence of a base; however, in the case of organoboron compounds, the nucleophilicity of the boron must be enhanced by quaternisation with a negatively charged base for the organoboron to act as an efficient nucleophile, as discussed above. In most cases, aqueous Na_2CO_3 in DME appears to work well,[82, 83] however other bases have also been employed e.g. Et_3N,[87] $NaHCO_3$,[82] Cs_2CO_3[88] Tl_2CO_3[89] and K_3PO_4.[90]

The reaction proceeds more rapidly in homogeneous conditions (aqueous base in DME), but reasonable yields have also been obtained under heterogeneous conditions. For example, for base or water sensitive reactions, K_2CO_3 suspended in toluene works well.[91] Couplings may also be carried out in aqueous media by using water soluble phosphine ligands (m-$NaO_3SC_6H_4PPh_2$).[65] This method, in conjunction with extremely mild conditions using CsF or Bu_4NF, allows the synthesis of various functionalised biaryls; however, the reaction under aqueous conditions can yield undesirable by-products due to competitive hydrolytic deboronation.

Steric hindrance of aryl halides is not a major factor for the formation of substituted biaryls, however low yields are obtained when using *ortho* substituted arylboronic acids due to steric hindrance during the transmetallation to Pd (II) halide. However, the addition of stronger bases e.g. aqueous NaOH or $Ba(OH)_2$, both in benzene and DME, induces a remarkable acceleration of the coupling rate,[65, 92] despite the fact that weaker bases give better results for less hindered boronic acids.

Electron-donating substituents are known to promote aryl-aryl exchange between the palladium centre and the phosphine ligand in Pd (II) complexes (figure 1.31).[93, 94] This side reaction results in contamination of the biaryl-coupling product with the aryl group on the phosphine ligand. Tris (2-methoxyphenyl) phosphine is effective in reducing the formation of such by-products while maintaining a high yield of the desired product.[95]
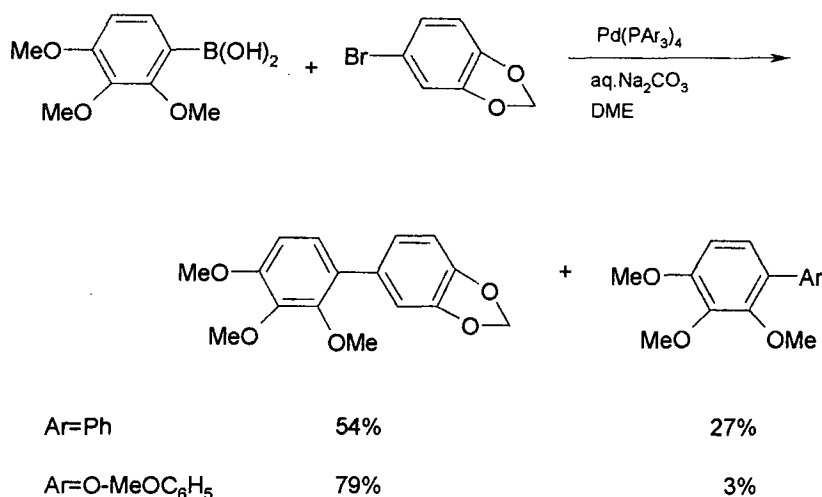
Figure 1.31 - *Aryl-aryl exchange between the palladium centre and the phosphine ligand in Pd (II) complexes*[65]

1.3.2.4.   Suzuki and Miyaura Cross-Coupling Reactions - Applications to terpyridine synthesis

In the context of metal-mediated catalytic cross-couplings, the Suzuki reaction has proved to be a useful synthetic strategy to biaryl and biheteroaryl systems, finding application in e.g. pharmaceutical/agrochemical industries.[96] However, despite its versatility and extensive application, at the outset of this work there were still only very few examples in the literature of Suzuki cross-coupling reactions involving pyridyl boronic acids/pyridyl boronic esters.[68, 96]

In 2001, Williams and Aspley described the use of the Miyaura reaction in the first reported synthesis of boronic acid-substituted terpyridines (fig 1.32), together with their ruthenium complexes [68] (fig 1.33).
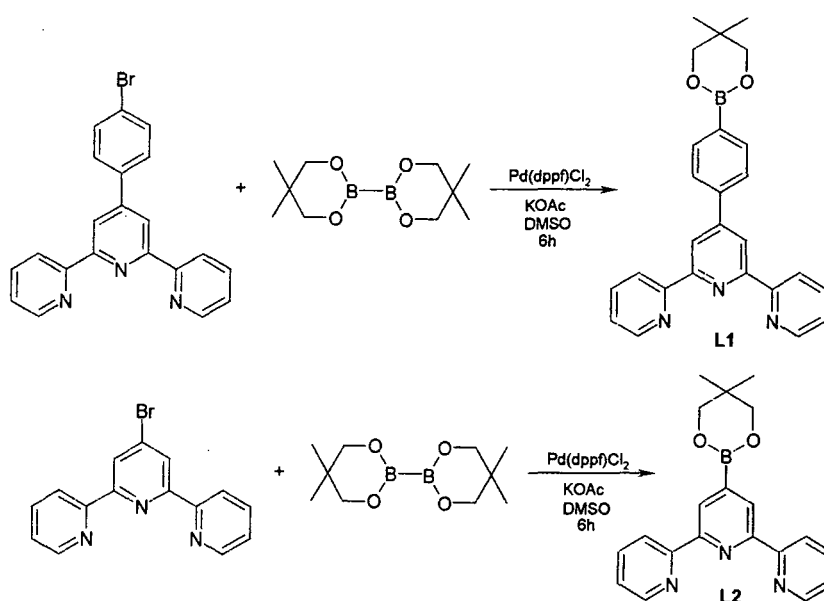
Figure 1.32 - *Synthesis of boronate ester substituted terpyridine ligands*[68]
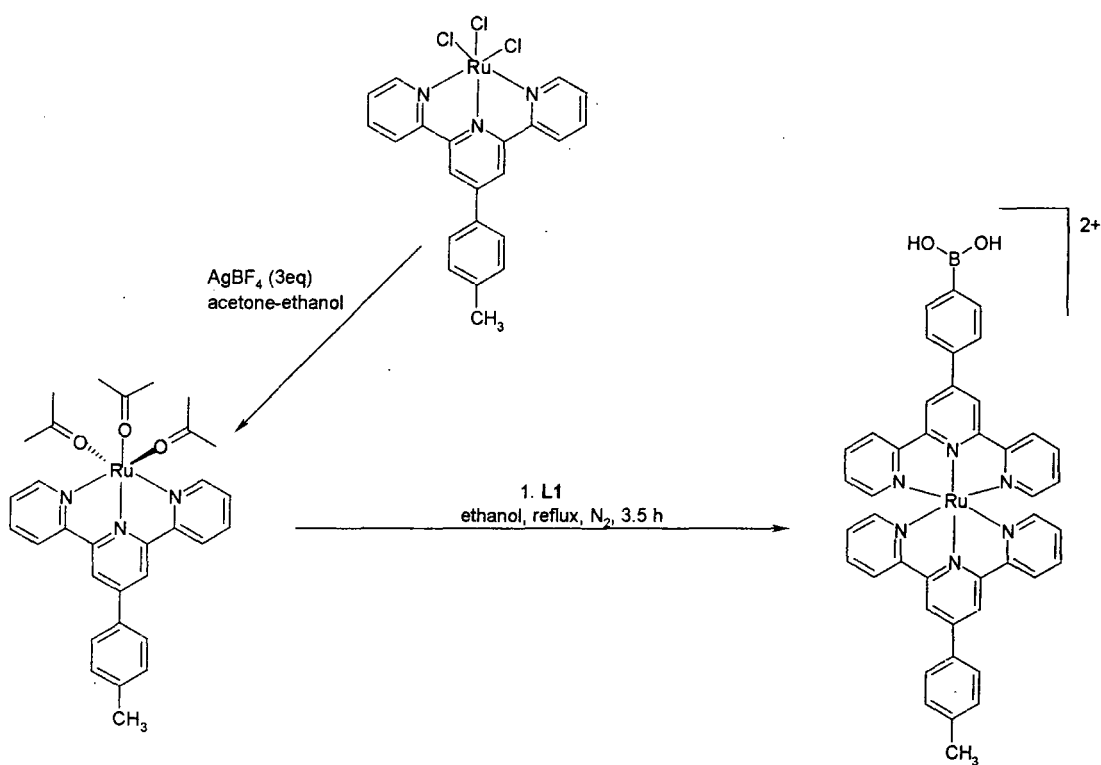
Figure 1.33 - *Preparation of ruthenium (II) complexes of boronate-substituted terpyridine ligands*[68]

The boronate-substituted complex could also be prepared directly from the bromo complex, by the Miyaura reaction, although the route was much less satisfactory.

Unfortunately, all attempts to prepare the structurally related complex, [(ttpy)Ru(L^2)] (PF$_6$)$_2$, either directly from the free ligand or by cross-coupling from [(ttpy)Ru(tpyBr)] (PF$_6$)$_2$ met with failure, possibly due to an effect of the metal ion in increasing the lability of the C-B bond. The cross-coupling reaction between [(ttpy)Ru(tpyBr)](PF$_6$)$_2$ and B$_2$neo$_2$ led only to the isolation of [(ttpy)Ru(tpy-OH)](PF$_6$)$_2$ and [(ttpy)Ru(tpy)](PF$_6$)$_2$

Investigations into palladium catalysed Suzuki cross-coupling reactions of bromo- or boronic acid substituted complexes, with aryl boronates or aryl halides respectively, were very successful. The complex [(ttpy)Ru(L1)](PF$_6$)$_2$ reacted with haloaromatics under standard palladium catalysed Suzuki-Miyaura cross-coupling conditions to generate more elaborate 4'-aryl-substituted terpyridyl complexes.
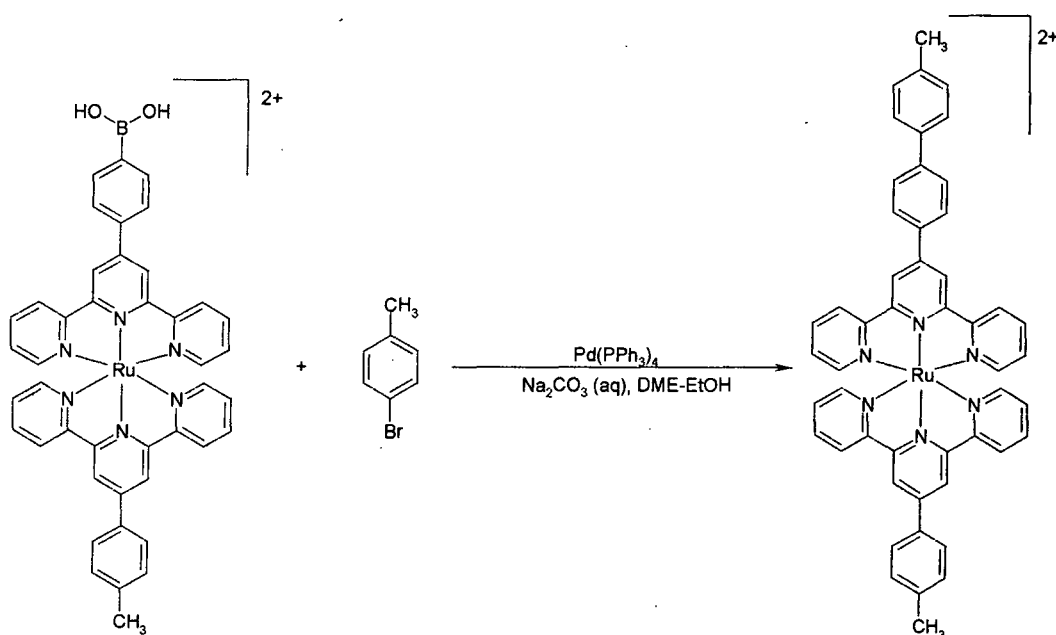
Figure 1.34-*Application of the Suzuki reaction to Ru (II) complexes of boronate substituted terpyridines*[68]

The reverse scenario of coupling [(ttpy)Ru(tpy-φ-Br)] (PF₆)₂ with an arylboronic acid under similar conditions was also successful, for example as shown in figure 1.35
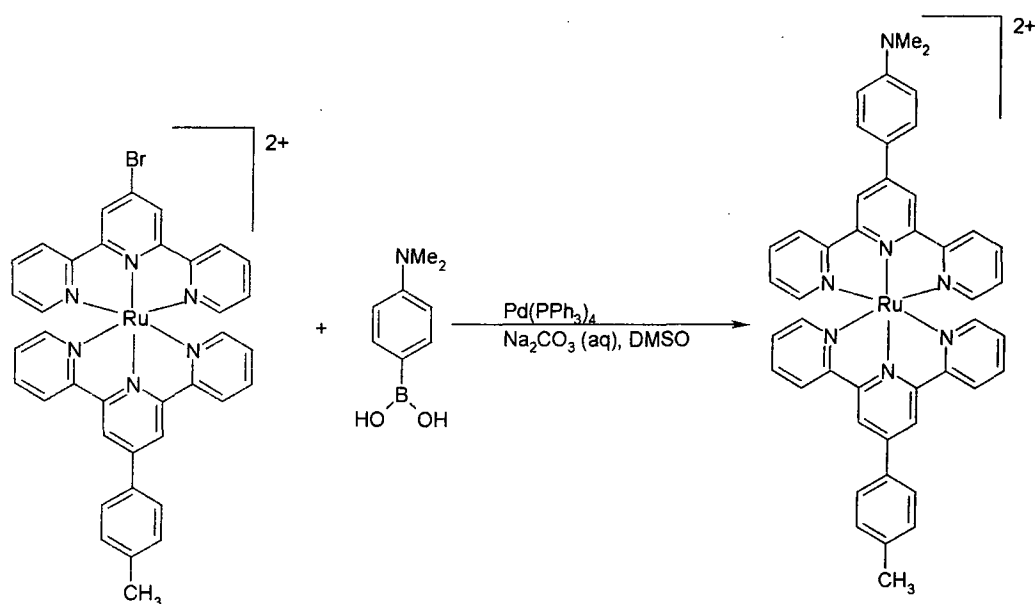
Figure 1.35 - *Application of the Suzuki reaction to Ru (II) complexes of bromo substituted terpyridines*[68]

1.4. Preparation of Iridium (III) bis(terpyridine) complexes

As a third row transition metal with a low-spin d^6 configuration, the complexation chemistry of iridium (III) is characterised by the inert nature of its coordination sphere with respect to ligand substitution reactions, with harsh reaction conditions often being required to substitute the chloride ligands of the usual iridium precursors (e.g. $IrCl_3.3H_2O$).[16]

The synthesis of $[Ir(tpy)_2^{3+}]$ was first described in 1990 by Demas *et al.* following a procedure based on one they had published previously in 1974 for the synthesis of $[Ir(bpy)_3^{3+}]$.[25] The first stage involved the preparation of iridium sulphate, prepared *in situ* from K_3IrCl_6. The reason for the preparation of iridium sulphate was that the authors had speculated while preparing $[Ir(bpy)_3]^{3+}$ that *"an iridium (a "soft" metal) compound containing only "hard" ligands would react more readily with "softer" 2, 2'-bipyridine to give [Ir(bpy)₃]³⁺ than do chloride (a "soft" ligand) containing species."* The iridium sulphate went on to react with tpy in refluxing ethylene glycol for a few minutes and then at 150°C for 6 h. The desired complex was isolated after what is reported to be a tedious work-up and purification.

In more recent work,[26] the possibility of using more labile iridium (I) complexes was investigated, followed by oxidation to the +3 state after introduction of the ligands into the coordination sphere. Such a strategy is commonplace in, for example, Co and Cr chemistry.[97, 98] However, although the use of ((Ir (COD) Cl$_2$)$_2$ or [Ir$_2$(μ-Cl)$_2$-(COE)$_4$]) led to the desired complexes, the yields were poor.

A simpler and preferable procedure was found to be the sequential reaction of the two terpyridines with IrCl$_3$ in alcoholic solvents.[26] Ir(tpy)Cl$_3$ is first prepared by heating IrCl$_3$.3H$_2$O in the presence of the ligand. (It should be noted that Ir(tpy)Cl$_3$ was first reported by Morgan and Burstall in an historic paper in 1937, prepared by the reaction of Na$_3$IrCl$_6$ and tpy in water[33]). This reaction proceeds readily in ethanol solution at reflux for aryl-substituted terpyridines, whilst ethylene glycol at 160°C is required in the case of terpyridine itself. The introduction of the second ligand is a lot harder than the coordination of the first, as it requires the dechlorination of the Ir(tpy)Cl$_3$ precursor. Procedures commonly used in ruthenium chemistry, in which dechlorination is assisted by addition of AgBF$_4$ in acetone, favouring the reaction by precipitation of AgCl and subsequent co-ordination of acetone as a readily-displaced ligand, were unsuccessful.[26] However, the desired complexes (fig 1.7, section 1.2) could be obtained by reacting Ir(L)Cl$_3$ with the second ligand in ethylene glycol, at reaction temperatures between 140°C-196°C for 15 mins - 2.5 h, depending on the complex.[26]

Unfortunately, the high reaction temperatures required to break the Ir-Cl bond may also cause the Ir-L bond to break, resulting in the formation of scrambled products. Also, the higher the temperature and the longer the reaction time, the higher the probability of obtaining orthometallated complexes.

The same procedure has been used to synthesise the iridium bis(terpyridine) complexes discussed earlier that display luminescence sensitive to pH[29] (fig 1.8, section 1.2) and to halide ions[30] (fig 1.36). The photophysical properties of these complexes are reviewed in section 1.5.
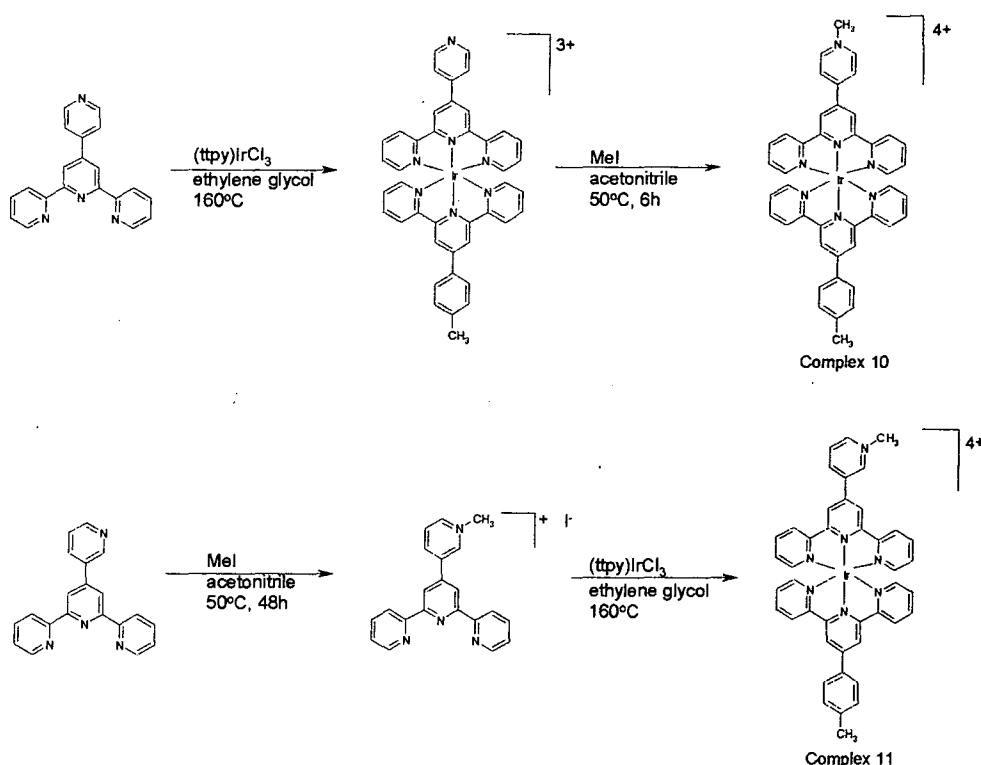
Figure 1.36 - *Ir (III) bis(terpyridine) complexes that display Cl⁻ sensitive emission*[30]

Recently, Lo *et al.* attempted to overcome this problem through preparing the new intermediate [Ir(tpy-R)(CF₃SO₃)₃](R=C₆H₅, C₆H₄-CH₃-*p*, C₆H₄-Cl-*p*) from the reaction of [Ir(tpy-R)Cl₃](R=C₆H₅, C₆H₄-CH₃-*p*, C₆H₄-Cl-*p*) and trifluoromethanesulphonic acid in refluxing 1, 2-dichlorobenzene.[31] This approach was based on earlier work by Meyer, in which [Ir(bpy)₃]²⁺, *cis*-[Ir(bpy)₂(PPh₃)H]²⁺ and cis[Ir(bpy)₂H₂]⁺ could be conveniently synthesised from the precursor complex *cis*-[Ir(bpy)(CF₃SO₃)₂](CF₃SO₃).[99] Using this new series of intermediate complexes, four bis(terpyridyl) complexes were prepared (fig 1.11, Section 1.2).

1.5. Concluding Remarks

This short review of the literature has attempted to highlight the important features concerning the design of molecular luminescent sensors, and to summarise the luminescent properties of Ir (III) bis(terpyridine) complexes that make them interesting for further study into this application. A summary of the experimental procedures developed for the synthesis of terpyridine ligands and their Ir (III) complexes has also been presented, including details of their application for the synthesis of complexes, which have potential as pH/Cl⁻ ion sensors by the author of this thesis.

In an effort to obtain a route to more elaborate terpyridine ligands derivatised with functional groups capable of binding a greater range of analytes, thereby increasing the scope of these ligands and their Ir (III) complexes to act as molecular luminescent sensors, investigation into a new methodology for the synthesis of terpyridine ligands derivatised on the 4'-pendent ring has been carried out. Chapters 2 and 4 discuss the results of investigations made during this work into the utilisation of the Suzuki cross-coupling methodology for the functionalisation of terpyridine ligands at the 4'-position of the pendent ring on the free terpyridine ligand, and whilst bound to an Ir (III) metal centre, respectively. Chapters 3 and 5 continue with a discussion of the photophysical properties of the ligands and complexes prepared through the cross-coupling methodology. Finally, chapter 6 discusses the outcome of attempts to couple two iridium complexes *via* the Suzuki methodology.

1.6. References

[1]   'Handbook of Fluorescent Probes and Research Chemicals', R. P. Haughland, Eugene, Oregon, 6th ed., 1996.

[2]   A. P. De Silva, H. Q. N. Gunaratne, T. Gunnlaugsson, A. J. M. Huxley, C. P. McCoy, J. T. Rademacher, and T. R. Rice, *Chem. Rev.*, 1997, **97**, 1515.

[3]   A. P. De Silva, D. B. Fox, A. J. M. Huxley, and T. S. Moody, *Coord. Chem. Rev*, 2000, **205**, 41.

[4]   R. A. Bissell, A. P. De Silva, H. Q. N. Gunaratne, P. L. M. Lynch, G. E. M. Maguire, and K. R. A. S. Sandanayake, *Chemical Society Reviews*, 1992, 187.

[5]   J. N. Demas and B. A. De Graff, *Coord. Chem. Rev*, 2001, **211**, 317.

[6]   J. N. Demas and B. A. De Graff, *Anal. Chem*, 1991, **63**, 829A.

[7]   L. Sacksteder, M. M. Lee, J. N. Demas, and B. A. Degraff, *J. Am. Chem. Soc*, 1993, **115**, 8230.

[8]   *Principles of Fluorescence Spectroscopy*, J. R. Lakowicz, Kluwer Academic/Plenum, New York, 2nd edn, 1999

[9]   *Modern Molecular Photochemistry*, N. J. Turro, University Science Books, Mill Valley, California, 1991

[10]   R. Grigg, J. M. Holmes, S. K. Jones, and W. D. J. A. Norbert, *J. Chem. Soc., Chem. Commun*, 1994, 185.

[11]   A. M. W. Cargill Thompson, M. C. C. Smailes, J. C. Jeffery, and M. D. Ward, *J. Chem. Soc., Dalton Trans*, 1997, 737.

[12]   J. R. Bacon and J. N. Demas, *Anal. Chem*, 1987, **59**, 2780.

13   E. R. Carraway, J. N. Demas, B. A. Degraff, and J. R. Bacon, *Anal. Chem*, 1991, **63**, 337.

14   C. S. Rawles, P. Moore, and N. W. Alcock, *J. Chem. Soc., Chem. Commun*, 1992, 684.

15   P. D. Beer, O. Kocian, R. J. Mortimer, and C. Ridgway, *J. Chem. Soc., Dalton Trans.*, 1993, 2629.

16   I. M. Dixon, J.-P. Collin, J.-P. Sauvage, L. Flamigni, S. Encinas, and F. Barigelletti, *Chem. Soc. Rev.*, 2000, **29**, 385.

17   R. J. Watts, *Comments Inorg. Chem*, 1991, **11**, 303.

18   J. N. Demas, E. W. Harris, C. M. Flynn, Jr., and D. Diemente, *J. Am. Chem. Soc*, 1975, **97**, 3838.

19   J. l. Kahl, K. W. Hanck, and M. K. De Armond, *J. Phys. Chem*, 1978, **82**, 540.

20   F. O. Garces, K. A. King, and R. J. Watts, *Inorg. Chem.*, 1988, **27**, 3464.

21   K. A. King and R. J. Watts, *J. Am. Chem. Soc*, 1987, **109**, 1589.

22   E. A. Plummer, J. W. Hofstraat, and L. De Cola, *J. Chem. Soc. Dalton Trans.*, 2003, 2080.

23   M. A. Baldo, M. E. Thompson, and S. R. Forrest, *Nature*, 2000, **403**, 750.

24   A. Mamo, I. Stefio, M. F. Parisi, A. Credi, M. Venturi, C. Di Pietro, and S. Campagna, *Inorg. Chem.*, 1997, **36**, 5947.

25   N. P. Ayala, C. M. Flynn, Jr., L. Sacksteder, J. N. Demas, and B. A. Degraff, *J. Am. Chem. Soc*, 1990, **112**, 3837.

26   J.-P. Collin, I. M. Dixon, J.-P. Sauvage, J. A. G. Williams, F. Barigelletti, and L. Flamigni, *J. Am. Chem. Soc*, 1999, **121**, 5009.

27   V. Balzani, A. Juris, M. Venturi, S. Campagna, and S. Serroni, *Chem. Rev.*, 1996, **96**, 759.

28   F. Scandola, M. T. Indelli, C. Chiorboli, and C. A. Bignozzi, *Top. Curr. Chem*, 1990, **158**, 63.

29   M. Licini and J. A. G. Williams, *J. Chem. Soc., Chem. Commun*, 1999, 1943.

30   W. Goodall and J. A. G. Williams, *J. Chem. Soc., Dalton Trans.*, 2000, 2893.

31   K. K.-W. Lo, C.-K. Chung, D. C.-M. Ng, and Zhu.N, *New J. Chem*, 2002, **26(1)**, 81.

32   G. T. Morgan and F. H. Burstall, *J. Chem.Soc*, 1932, 20.

33   G. T. Morgan and F. H. Burstall, *J.Chem.Soc.*, 1937, 1649.

34   F. H. Burstall, *J. Chem. Soc.*, 1938, 1662.

35   G. T. Morgan and F. H. Burstall, *J. Ind. Chem. Soc*, 1933, 1.

36   G. M. Badger and W. H. F. Sasse, *J. Chem. Soc.*, 1956, 616.

37   A. M. W. Cargill Thompson, *Coord. Chem. Rev*, 1997, **160**, 1.

38   R.-A. Fallahpour, *Synthesis*, 2003, **No.2**, 155.

39   F. Krohnke, *Synthesis*, 1976, 1.

40   M. Weiss, *J. Am. Chem. Soc*, 1952, **74**, 200.

41   R. L. Frank and E. F. Riener, *J. Am. Chem. Soc*, 1950, **72**, 4182.

42   C. Hollins, 'Synthesis of Nitrogen Ring Compounds', Van Nostrand, London, 1924.

43   A. E. Tschitschibabin, *J. Prakt. Chem*, 1924, **107**, 123.

44   H. Case and T. J. Kasper, *J. Am. Chem. Soc*, 1956, **78**, 5842.

45   W. Spahni and G. Calzaferri, *Helv. Chim. Acta*, 1984, **67**, 450.

46   E. C. Constable and A. M. W. Cargill Thompson, *J. Chem. Soc., Dalton Trans*, 1992, 2947.

47   L. Persaud and G. Barbiero, *Can. J. Chem*, 1991, **69**, 315.

48   G. W. V. Cave and C. L. Raston, *J. Chem. Soc., Chem. Commun*, 2000, 2199.

49   F. Krohnke and W. Zecher, *Angew. Chem. internat. Edit.*, 1962, **1**, 626.

50   K. T. Potts, M. J. Cipullo, P. Ralli, and G. Theodoridis, *J. Org. Chem*, 1982, **47**, 3027.

51   K. T. Potts, M. J. Cipullo, P. Ralli, G. Theodoridis, and P. Winslow, *Org. Synth*, 1986, **64**, 189.

52   K. T. Potts, M. J. Cipullo, P. Ralli, and G. Theodoridis, *J. Am. Chem. Soc*, 1981, **103**, 3585.

53   K. T. Potts, D. A. Usifer, A. Guadalupe, and H. D. Abruna, *J. Am. Chem. Soc*, 1987, **109**, 3961.

54   D. L. Jameson and L. E. Guise, *Tetrahedron. Lett*, 1991, **32**, 1999.

55   E. C. Constable and M. D. Ward, *J. Chem. Soc., Dalton Trans.*, 1990, 1405.

56   P. M. Griffiths, F. Loiseau, F. Puntoriero, S. Serroni, and S. Campagna, *J. Chem. Soc., Chem. Commun*, 2000, 2297.

57   S. Fanni, C. Di Pietro, S. Serroni, S. Campagna, and J. G. Vos, *Inorg. Chem. Commun*, 2000, **3**, 42.

58   K. O. Johansson, J. A. Lotoski, C. C. Tong, and G. S. Hanan, *J. Chem. Soc., Chem. Commun*, 2000, 819.

59   E. C. Constable and M. D. Ward, *J. Chem. Soc., Dalton Trans.*, 1990, 1405.

60   S. Murahashi, M. Yamamura, K. Yanagisawa, N. Mita, and K. Kondo, *J. Org. Chem*, 1979, **44**, 2408.

61   Y. Hatanaka and T. Hiyama, *J. Org. Chem*, 1988, **53**, 918.

62   M. Kosugi, I. Hagiwara, and T. Migita, *Chem. Lett*, 1983, 839.

63   M. Kosugi, Y. Simizu, and T. Migita, *Chem. Lett*, 1977, 1423.

64   D. Milstein and J. K. Stille, *J. Am. Chem. Soc*, 1979, **101**, 4992.

65   N. Miyaura and A. Suzuki, *Chem. Rev.*, 1995, **95**, 2457.

66   N. Miyaura, K. Yamada, and A. Suzuki, *Tetrahedron. Lett*, 1979, **36**, 3437.

67   D. J. Cardenas and J.-P. Sauvage, *Synlett*, 1996, 916.

68   C. J. Aspley and J. A. G. Williams, *New J. Chem*, 2001, **25**, 1136.

69   K. Tamao, K. Sumitani, and M. Kumada, *J. Am. Chem. Soc*, 1972, **94**, 4374.

70   R. J. P. Corriu and J. P. Masse, *J. Chem. Soc., Chem. Commun*, 1972, 144.

71   M. Yamamura, I. Moritani, and S. Murahashi, *J. Organomet. Chem*, 1975, **91**, C39.

72   M. Tamura and J. K. Kochi, *J. Am. Chem. Soc*, 1971, **93**, 1487.

73   V. Farina and B. Krishnan, *J. Am. Chem. Soc*, 1991, **113**, 9585.

74   F. Ozawa and A. Yamamoto, *Bull. Chem. Soc. Jpn*, 1987, 773.

75   R. Fallahpour, M. Neuburger, and M. Zehnder, *New J. Chem.*, 1999, **23**, 53.

76   G. R. Pabst and J. Sauer, *Tetrahedron*, 1999, **55**, 5067.

77   D. S. Matteson, 'The Chemistry of the Metal-Carbon Bond', ed. F. R. Hartley and S. Patai, Wiley, New York, 1987.

78   T. Ishiyama, M. Murata, and N. Miyaura, *J. Org. Chem.*, 1995, **60**, 7508.

79   N. Miyaura, *J. Organomet. Chem*, 2002, **653**, 54.

80   T. B. Marder, *Personal Communication*, 2003

81   N. Miyaura, T. Yanagi, and A. Suzuki, *Synth. Commun*, 1981, **11**, 513.

82   S. Gronowitz, V. Bobosik, and K. Lawitz, *Chem. Scr*, 1984, **23**, 120.

83   B. I. Alo, A. Kandil, P. A. Patil, M. J. Sharp, M. A. Siddiqui, and V. J. Snieckus, *J. Org. Chem*, 1991, **56**, 3763.

84   S. Achab, M. Guyot, and P. Potier, *Tetrahedron. Lett*, 1993, **34**, 2127.

85   T. I. Wallow and B. M. Novak, *J. Org. Chem.*, 1994, **59**, 5034.

86   G. M. Alois, A. Villiger, and R. Buchecker, *Tetrahedron. Lett*, 1994, **35**, 3277.

87   W. Muller, D. A. Lowe, H. Neijt, S. Urwyler, P. Herrling, D. Blaser, and D. Seebach, *Helv. Chim. Acta*, 1992, **75**, 855.

88   H. E. Katz, *J. Org. Chem*, 1987, **52**, 3932.

89   Y. Hoshino, N. Miyaura, and A. Suzuki, *Bull. Chem. Soc. Jpn*, 1988, **61**, 3008.

90   R. S. Coleman and E. B. Grant, *Tetrahedron. Lett*, 1993, **34**, 2225.

91   W.-C. Shieh and J. A. Carlson, *J. Org. Chem*, 1992, **57**, 379.

44

[92]   T. Watanabe, N. Miyaura, and A. Suzuki, *Synlett*, 1992, 207.

[93]   B. E. Segelstein, T. W. Butler, and B. L. Chenard, *J. Org. Chem*, 1995, **60**, 12.

[94]   K.-C. Kong and C.-H. Cheng, *J. Am. Chem. Soc*, 1991, **113**, 6313.

[95]   D. F. O'Keefe, M. C. Dannock, and S. M. Marcuccio, *Tetrahedron Lett*, 1992, **33**, 6679.

[96]   P. R. Parry, W. Changsheng, A. S. Batsanov, M. R. Bryce, and B. Tarbit, *J. Org. Chem*, 2002, **67**, 7541.

[97]   L. Monsted, O. Monsted, G. Nord, and K. Simonsen, *Acta Chem. Scand.*, 1993, **47**, 439.

[98]   T. Suzuki, M. Rude, K. Simonsen, M. Morooka, H. Tanaka, S. Ohba, F. Galsbol, and J. Fujita, *Bull. Chem. Soc. Jpn.*, 1994, **67**, 1013.

[99]   B. P. Sullivan and T. J. Meyer, *J. Chem. Soc., Chem. Commun*, 1984, 403.

2. Synthesis of Terpyridine

Ligands

2.1. Introduction

Since Morgan and Burstall first reported the synthesis of tpy almost 70 years ago,[1, 2] the chemistry of this tridentate ligand and its substituted derivatives has attracted much attention from many different areas of chemistry.

One such area is catalysis, where terpyridine complexes of transition metals have been studied for their activity in the catalysis of, for example, the oxidation of alcohols[3, 4] and the catalysis of hydroformylation reactions.[5] Applications of terpyridine ligands have also been reported in materials chemistry, with the polymerisation of tpy,[6] and the anchoring of functionalised terpyridine ligands to TiO_2 surfaces,[7] gold surfaces[8] or to silica-titanium to build semi-conductors.[8] Small metal clusters incorporating terpyridines have been prepared, for example the dicobalt cluster-functionalised terpyridine ligands reported by Constable *et al.* (fig 2.1).[9]
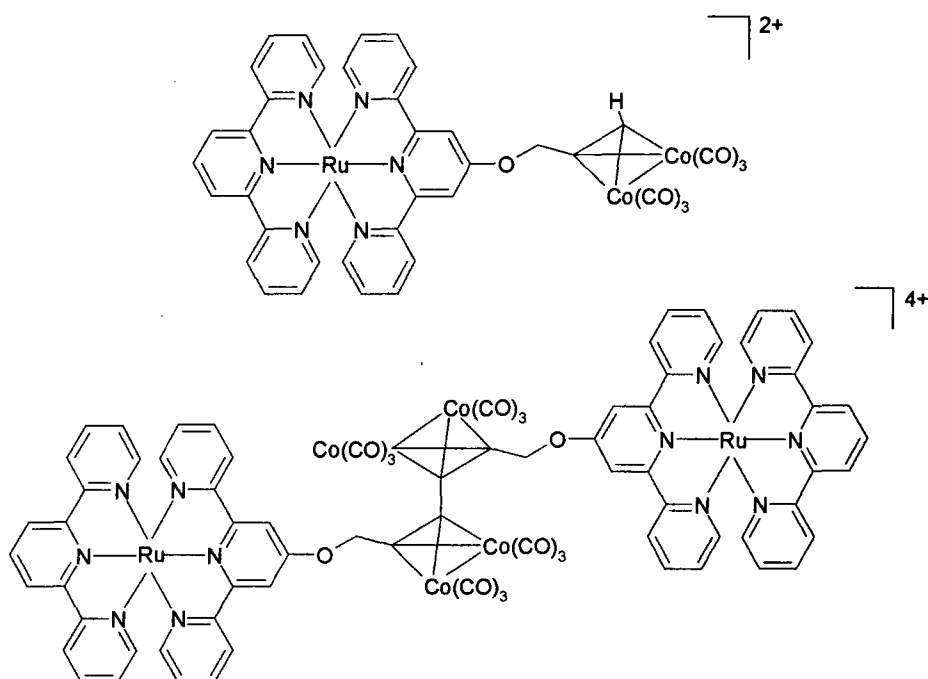
Figure 2.1 - *Dicobalt cluster-functionalised 2, 2': 6', 2"-terpyridines and their ruthenium complexes*

Platinum,[10] gold[8] and ruthenium complexes[10] of terpyridine derivatives have been applied to biological systems; for example, redox pathways in DNA oxidation have been probed through the kinetic studies of guanine and sugar oxidation by *para*-substituted terpyridine derivatives of oxoruthenium (IV), $[Ru(tpy)(bpy)O]^{2+}$.[10]

However, it is perhaps in the field of supramolecular chemistry that examples of the application of terpyridine ligands have been most widely investigated. An area of particular interest in this field is the study of metal bonded derivatives of terpyridine ligands functionalised with spacers at the 4'-position for use as photoactive centres for energy/electron transfer in linearly arranged multicomponent arrays.[11-15]
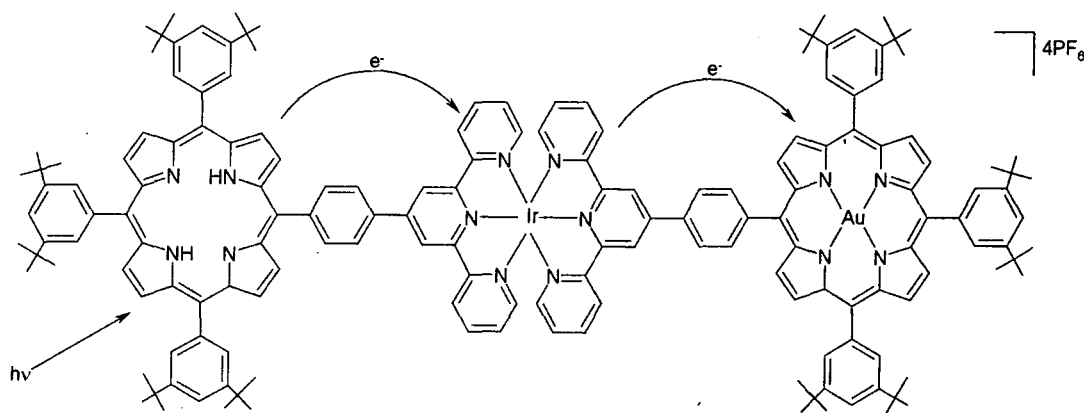
Figure 2.2 – *Terpyridine complexes as photoactive centres in multicomponent arrays*[13]

Functionalisation of terpyridines at the 4'-position is of particular importance in this role, as it provides a means of directionality and linear electronic communication along the coordination axis. Also, the insertion of a single substituent in the 4'-position of the terpyridine ligand results in no change to the centrosymmetric nature, and no problems associated with the formation of enantiomers.

The introduction of aryl substituents onto the 4'-position of terpyridine ligands bound to a metal centre has also been used to tune the luminescent properties of the terpyridine complexes.[16, 17] Recently, iridium bound terpyridine ligands bearing pendent groups capable of binding/responding to biologically interesting analytes have been utilised as molecular luminescent sensors.[16, 17] As discussed previously (chapter 1, section 1.2), the systems shown in figure 2.3 possess long-lived emission in aqueous solution under ambient conditions, which is perturbed by a change in pH or the presence of chloride ions.
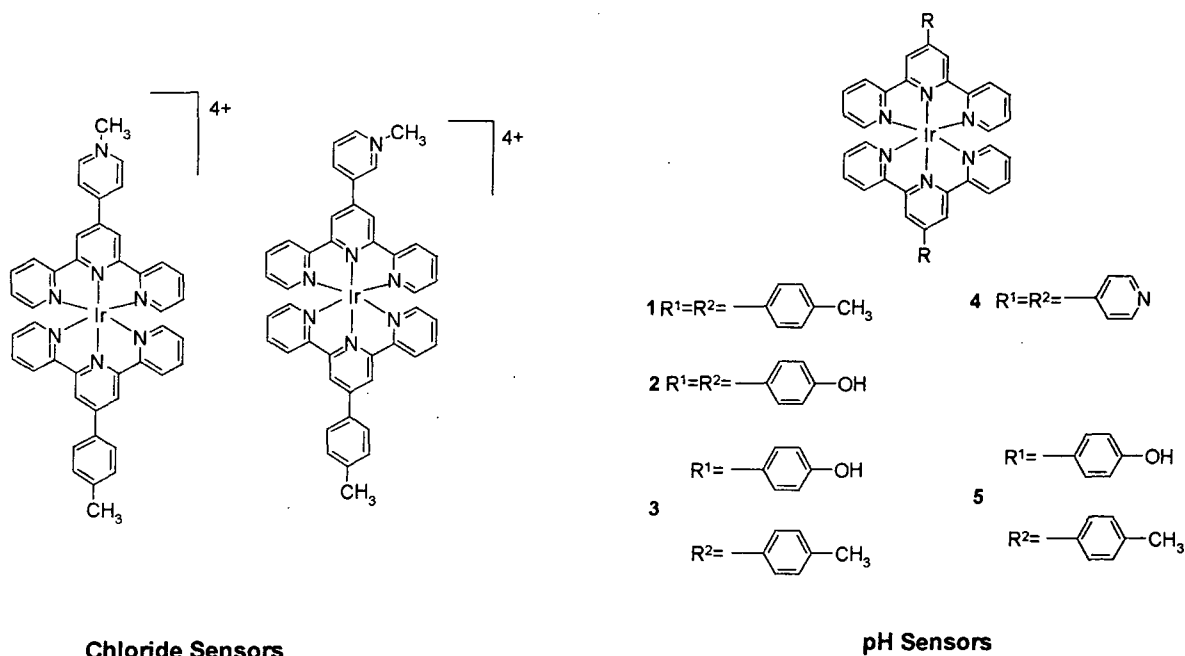
Figure 2.3 - *Ir (III) bis(terpyridine) complexes as pH/chloride sensors*

Clearly, in order to widen the range of target analytes for such systems, the synthesis of terpyridine ligands bearing pendent groups capable of binding/responding to biologically interesting analytes is a central issue. Unfortunately, the existing routes to 4'-aryl terpyridines (discussed in chapter 1) represent a limitation to the scope of the functional groups that can be substituted onto the pendent aryl ring, especially as these methodologies often rely on the availability of the appropriate aryl aldehyde, and are not compatible with base sensitive functionalities.[18]

In view of this situation, a versatile synthetic methodology for the functionalisation of the terpyridine core at the 4'-position was desirable. Given the widespread utility and versatility of the Suzuki palladium-catalysed cross-coupling reaction in the formation of biphenyl linkages,[19] the application of this coupling procedure for the elaboration of the 4'-position of terpyridine with aryl substituents has been investigated. The key results of these investigations are described in this chapter.

2.2.   Synthesis of Terpyridine Ligands by the Suzuki Cross-Coupling Reaction

Recall the catalytic cycle that governs the Suzuki reaction[19] as discussed previously in chapter 1, and the key steps of which are reproduced in figure 2.4.
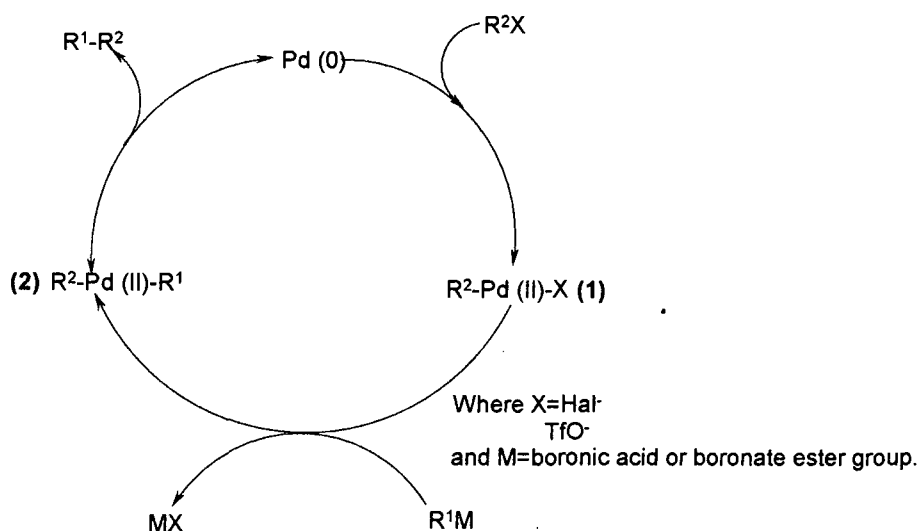
Figure 2.4 - *Suzuki cross-coupling catalytic cycle*

It is noteworthy that, although the effects of the substituents on Suzuki cross-coupling reactions have been widely investigated for aryl-aryl coupling reactions, there are very few systematic studies involving pyridyl (or other N-heterocyclic) boronic acids.[20]

In principle, for any cross-coupled product R^1-R^2, there are two possible pairs of starting materials, namely R^1M and R^2X, or R^1X and R^2M, assuming that all four compounds are accessible. In those instances where N-heterocycles have been used, the heterocycle almost invariably incorporates the X substituent (rather than the boronic acid) with the boronic acid usually in the carbocyclic ring.

In order to explore the utility of the Suzuki cross-coupling reaction for the elaboration of terpyridines at the 4'-position, it was of interest to establish which pair of reagents is more appropriate: use of an aryl boronic acid in combination with a bromo or triflate terpyridine (I), or the alternative strategy of an aryl bromide with a boronic ester substituted terpyridine (II) (figure 2.5). Other relevant factors to be considered were the identity of the leaving group (Br⁻, I⁻, OTf⁻), the catalyst and the effect of the solvent.
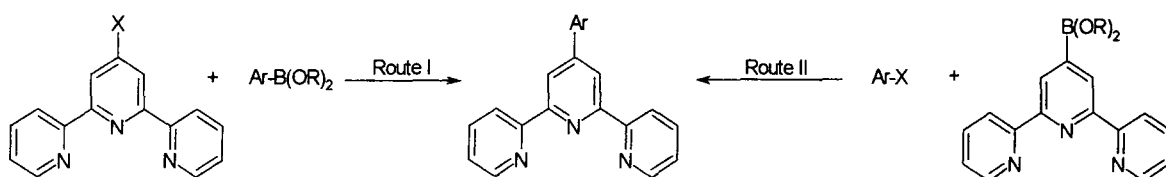
Figure 2.5 - *Routes I and II for the synthesis of terpyridines via the Suzuki cross-coupling reaction*

The experiments carried out in an attempt to address these issues are discussed in subsequent sections, and summarised in table 2.1 and figure 2.6, which also show the structures of the terpyridines prepared in this way.[21]
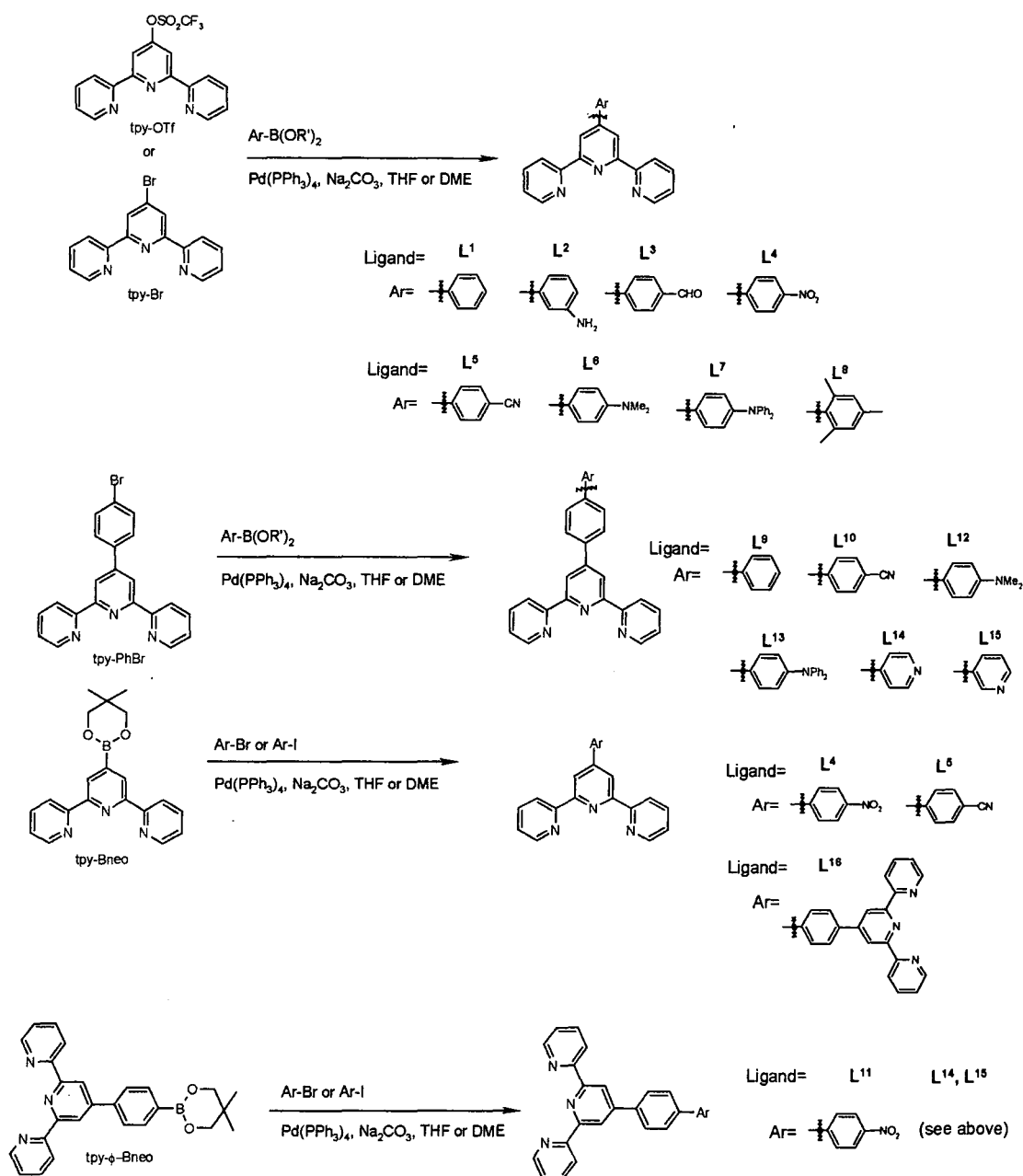
Figure 2.6 - *Summary of terpyridines synthesised via the Suzuki cross-coupling reaction*
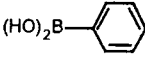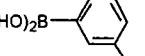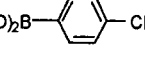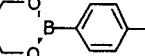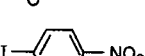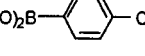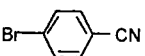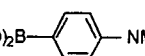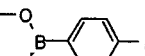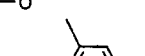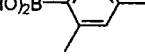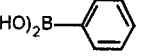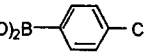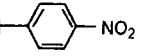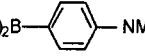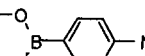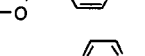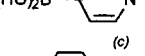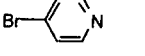
Ligand	Starting Terpyridine	Reacting Aryl Partner	Solvent	Isolated Yield (%)
L^1	tpy—OTf	(HO)$_2$B—⟨phenyl⟩	thf	10
	tpy—Br		dme	80
L^2	tpy—Br	(HO)$_2$B—⟨phenyl⟩—NH$_2$	thf	80
	tpy—OTf		thf	14
L^3	tpy—OTf	(HO)$_2$B—⟨phenyl⟩—CHO	thf	13
L^4	tpy—Br	neopentyl-B—⟨phenyl⟩—NO$_2$	dme	75
	tpy—OTf		thf	9 [b]
	tpy—Br	I—⟨phenyl⟩—NO$_2$	dme	30
	tpy—Bneo		thf	64
L^5	tpy—Br	(HO)$_2$B—⟨phenyl⟩—CN	thf	80
	tpy—Bneo	Br—⟨phenyl⟩—CN	thf	34
L^6	tpy—OTf	(HO)$_2$B—⟨phenyl⟩—NMe$_2$	thf	65
L^7	tpy—Br	neopentyl-B—⟨phenyl⟩—NPh$_2$	dme	59
$L^{8\ (d)}$	tpy—Br	(HO)$_2$B—⟨trimethylphenyl⟩	dme	61
L^9	tpy-φ-Br	(HO)$_2$B—⟨phenyl⟩	dme	60
$L^{10\ (d)}$	tpy-φ-Br	(HO)$_2$B—⟨phenyl⟩—CN	dme	57
$L^{11\ (d)}$	tpy-φ-Bneo	I—⟨phenyl⟩—NO$_2$	dme	28
$L^{12\ (d)}$	tpy-φ-Br	(HO)$_2$B—⟨phenyl⟩—NMe$_2$	dme	43
L^{13}	tpy-φ-Br	neopentyl-B—⟨phenyl⟩—NPh$_2$	dme	60
$L^{14\ (d)}$	tpy-φ-Br	(HO)$_2$B—⟨pyridyl⟩	dme	36
	tpy-φ-Bneo	Br—⟨pyridyl⟩ (c)	dme	4
$L^{15\ (d)}$	tpy-φ-Br	(HO)$_2$B—⟨pyridyl⟩	dme	67
	tpy-φ-Bneo	Br—⟨pyridyl⟩	dme	46
L^{16}	tpy-Bneo	tpy-φ-Br	dme	69

Table 2.1-*routes to terpyridines L^1-L^{16}: coupling partners, solvent and isolated yields*[a]

[a]*Solvent employed was tetrahydrofuran (for the coupling involving triflates) or dimethoxyethane (for most reactions employing aryl bromides or iodides). The catalyst was Pd(PPh$_3$)$_4$, and sodium carbonate was used as the base in each case, except for L^8 where barium hydroxide was employed.* [b]*Traces of PPh$_3$ (<5%) remained in the product, despite repeated recrystallisations.* [c]*The hydrochloride salt was used; immediate conversion into the free pyridine is expected under the basic conditions employed.* [d]*Ligands prepared by Kathryn J Arm and Kirstin Wild.*

Typically, the cross-couplings were carried out by dissolving the boronic acid and triflate/bromo compound in THF or DME, and degassing the solution *via* three freeze-pump–thaw cycles. This was followed by the addition of the palladium catalyst and Na_2CO_3 solubilised in a minimum volume of water.[22] The resulting mixture was normally stirred vigorously under nitrogen for 1 h at room temperature, before heating to 85°C, with the progress of the reaction monitored by TLC or GCMS where possible. Although a number of highly-active Pd catalysts have been reported recently employing bulky phosphines,[23] the widely used compound $Pd(PPh_3)_4$ was used here, being cheap and readily available.

2.2.1. Coupling Reactions using 4'-triflate terpyridine

Initial investigations focused on the coupling of 4'-triflate terpyridine with aryl boronic acids/esters. This was in part owing to the ease of access of the former from 2, 6-bis(2-pyridyl)-4(1H)-pyridone upon treatment with trifluoromethane sulfonic anhydride in ~70 % yield.[24] The required pyridone is itself accessible in large quantities by the base catalysed condensation of ethyl 2-pyridine carboxylate with acetone and subsequent ring closure with ammonium acetate,[25] figure 2.7. There also exists a great deal of literature detailing the successful employment of aryl triflates, in place of aryl halides, in Suzuki cross-coupling reactions.[19] In most cases involving triflates, THF has been found to be the solvent that offers optimal conversion, and minimises competitive hydrolysis of the triflate group.[22]
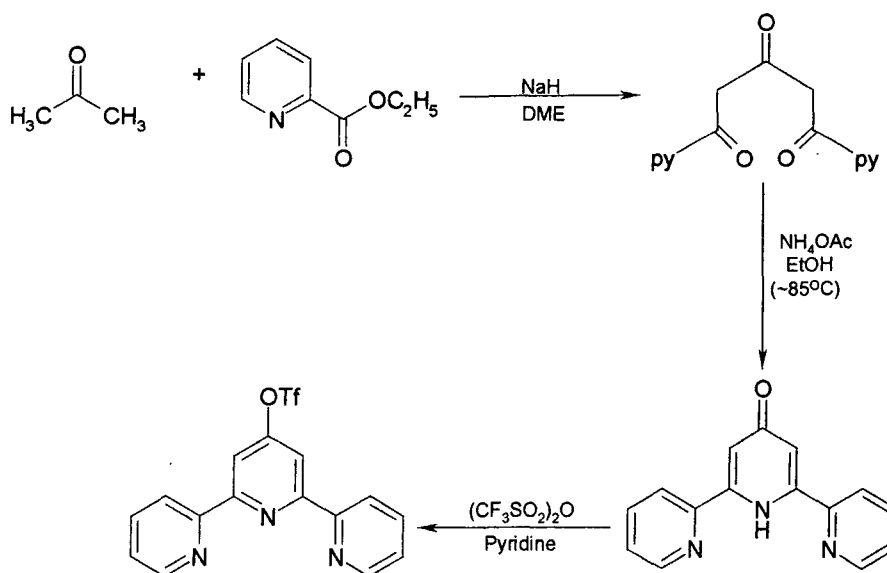
Figure 2.7 - *Synthesis of 4'-triflate terpyridine*

Ligands L^1-L^4 and L^6 were successfully prepared through coupling 4'-triflate terpyridine with aryl boronates under the conditions described above (THF, Pd(PPh₃)₄ as catalyst, Na_2CO_3 (aq, sat) as the base[22]). However, the crude yields were disappointing. Other drawbacks included long reaction times for complete consumption of starting material (25-72 h), and tedious purification caused by significant amounts of triphenylphosphine and probably mixtures of tetraarylphosphonium salts[19, 26, 27] that were difficult to separate from the terpyridine product both by recrystallisation and by chromatography.

The result was disappointingly low isolated yields. On the other hand, poor yields obtained from triflate coupling reactions are not unprecedented. Previous literature has attributed the phenomenon to decomposition of the catalyst, leading to precipitation of palladium black at an early stage of the reaction.[19, 26, 27] The liberated triarylphosphine then reacts irreversibly with the triflate substrate leading to formation of phosphonium salts (figure 2.8). However, the addition of one equivalent of lithium or potassium bromide has been reported to be effective in preventing such decomposition of the catalyst, which is known to convert the labile cationic palladium (II) species to organopalladium (II) bromide.[19, 26, 27]

$$\text{ROTf} \xrightarrow{\text{Pd(0).L}_4} \text{[R-Pd(I)][TfO]}^-.\text{L}_n \xrightarrow{\text{LiBr}} \text{R-Pd-Br.L}_2$$

$$\downarrow \text{Ph}_3\text{P}$$

$$\text{[Ph}_3\text{PR]}^+\text{[TfO]}^- + \text{Pd(0)}$$
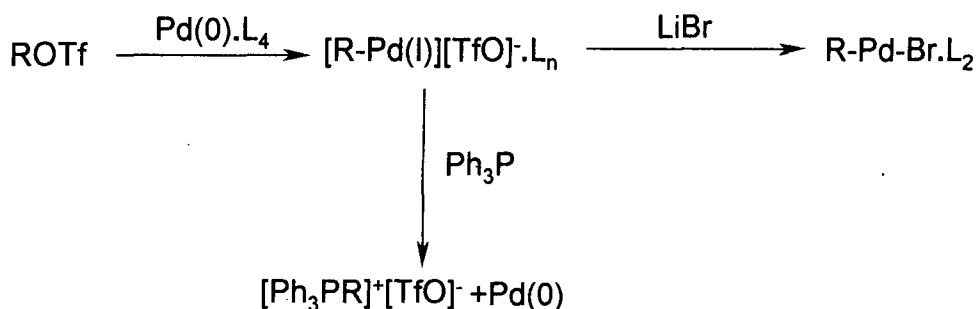
Figure 2.8 - *Decomposition of palladium catalysts during triflate cross-coupling reactions[19]*

In view of the difficulties encountered with catalytic decomposition during triflate coupling reactions, investigations into the use of phosphine-free catalysts were made. Pd(PPh₃)₄, a slightly air sensitive yellow crystalline solid, had originally been chosen, as this is the most commonly reported catalyst, appearing to give satisfactory results in most cases. It is generally stable on prolonged heating and is relatively straightforward to make by reduction of $PdCl_2$ with hydrazine hydrate in DMSO in the presence of PPh₃.[28]

However, it has been suggested that the activity of Pd(PPh$_3$)$_4$ is reduced due to inhibition by the four equivalents of phosphine per palladium, and the use of Pd(OAc)$_2$ in the absence of phosphine has been reported to give greatly enhanced reactivity.[29] Unfortunately, the use of Pd(OAc)$_2$ as an alternative phosphine free catalyst for the synthesis of ligands L^4 and L^6 met with complete failure, resulting only in recovery of starting material. The Pd(OAc)$_2$ showed no catalytic activity whatsoever in this reaction, neither at the very low concentrations previously reported, nor when larger amounts were added.

In the case of L^2 and L^6, purification was achieved more readily since acidification led to a water-soluble compound, probably the trication, in which the pendent amino group is protonated, as well as two of the three pyridyl nitrogens. The impurities could then be removed by washing the acidic aqueous solution with DCM, and the terpyridine subsequently isolated by basicification and back-extraction into dichloromethane.

It is clear from table 2.1 that only for the *para*-dimethylamino-substituted ligand L^6 was a satisfactory yield obtained using triflate terpyridine as the precursor. It is likely that the yield of this reaction is high in comparison to L^1-L^4, because the nucleophilicity of the boron is increased by the electron donating –NMe$_2$ group which is in direct conjugation with it, which will result in an increase in the rate of transmetallation, making it more competitive with the side reactions discussed previously. Notably, there was no evidence of aryl-aryl exchange between the palladium centre and the triphenylphosphine ligand to give 4-(dimethylamino)biphenyl, despite precedence suggesting that such competing reactions become significant in the presence of electron-donating substituents in the aryl boronic acid.[19, 30, 31]

2.2.2. Coupling Reactions with 4'-bromoterpyridine

In the light of the poor results obtained from the triflate coupling reactions, attention was turned to the use of 4'-bromoterpyridine in its place. Bromoaromatics are generally regarded as more reactive and robust than their triflate analogues, however 4'-bromoterpyridine had seen little previous exploitation in the literature, probably owing to the rather difficult preparation of this starting material. At the outset of this work, the only reported route involved the reaction of 2, 6-dipyridyl pyridone with $POBr_3$.[32] Unfortunately, this method requires large quantities of the molten brominating agent, proceeds with long reaction times, and rarely gives a yield of more than 50% (significantly lower on scaling-up). Given the reliability of the preparation of triflate-terpyridine from the same starting material[24] (which requires only stoichiometric amounts of triflic anhydride), the conversion of this compound to the bromo analogue was investigated. Treatment with a concentrated solution of HBr in AcOH (47%) at 110°C for 4-6 h was found to give almost quantitative yields of the 4'-bromoterpyridine, and this procedure was therefore used preferentially. Even more attractive would be the direct conversion of the pyridone to the bromide. However, this did not prove possible using HBr/AcOH (figure 2.9). Clearly, the pyridone oxygen must first be converted to a good leaving group prior to displacement by Br⁻, and simple protonation is apparently not sufficient.
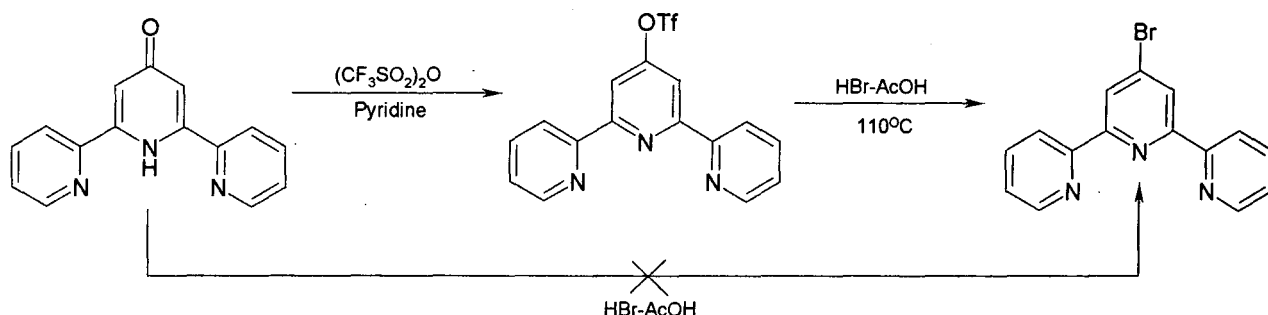
Figure 2.9 - *Synthesis of 4'-bromo terpyridine*

There is a wide consensus in the literature that dimethoxyethane provides optimal conversions in Suzuki couplings of bromoaromatic substrates.[19] This solvent was therefore employed here. However, for L^2, THF was used, in order to provide an example that allows a direct comparison between the triflate and the bromide. Consultation of table 2.1 confirms that coupling of 4'-bromoterpyridine offers a much better synthetic route to the 4'-aryl-substituted terpyridines than use of the triflate. In the case of 4'-(3-aminophenyl)-terpyridine, an approximate 6-fold increase in the isolated yield was obtained when using 4'-bromoterpyridine rather than 4'-triflate-

terpyridine. For both 4'-phenyl-terpyridine and 4'-(4-nitrophenyl)-terpyridine an approximate 8-fold increase in the isolated yield was obtained. In summary, it may be concluded that the coupling reactions of 4'-bromoterpyridine gave better yields, and fewer side-products (thereby facilitating purification) than the corresponding coupling reactions of the 4'-triflate terpyridine in THF, with $Pd(PPh_3)_4$ employed as the catalyst throughout.

The cross-coupling of 4'-(4-bromophenyl)-terpyridine with boronic acids, carried out in the same manner as the analogous coupling reactions of 4'-bromo terpyridine, led to the isolation of ligands L^9 to L^{16}. In this instance, the synthesis of 4'-(4-bromophenyl)-terpyridine was achieved through the one-pot condensation reaction of *para*-bromobenzaldehyde with 2-acetylpyridine in the presence of NH_4OAc via the methodology of Spahni and Calzaferri.[33]

2.2.3. Access to aryl boronic acids or boronate esters

Most of the aryl boronic acids used in this work are available commercially, normally having been prepared *via* treatment of the corresponding aryl lithiate with $B(OMe)_3$ or $B(O^iPr)_3$. However, *p*-nitrobenzene boronic acid was not available, and could not be prepared by such a procedure, owing to the incompatibility of the $-NO_2$ group with BuLi. The preparation of this compound was therefore carried out using a Miyaura-type cross-coupling reaction,[34, 35] the background to which was discussed in chapter 1.
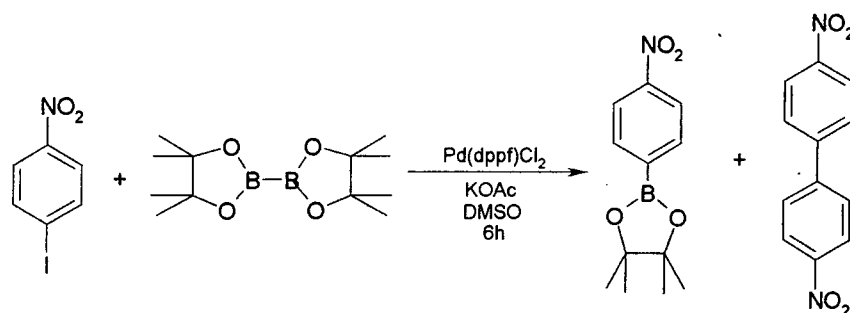
Figure 2.10 -*Preparation of para-nitrobenzene boronic acid*

The catalyst $Pd(dppf)Cl_2$ was used as it is widely acknowledged as the most efficient catalyst for the coupling of haloarenes possessing either electron-withdrawing groups or electron donating groups.[34] It also avoids the problems of by-product formation arising from coupling of the phenyl groups of PPh_3 when $Pd(PPh_3)_4$ is used as the catalyst, and seems to disfavour the potentially competitive cross-coupling of the product with the starting material in a Suzuki-type reaction. The synthesis of $Pd(dppf)Cl_2$ was achieved

by dissolving $PdCl_2$ in dry acetonitrile to form $PdCl_2(CH_3CN)_2$, followed by treatment of this intermediate with a solution of dppf in anhydrous toluene, under an atmosphere of nitrogen.[36] The desired coupling was then attempted, using *para*-nitroiodobenzene, and bis(pinacolato)diboron, in the presence of the catalyst and potassium acetate, using DMSO as the solvent.[34] Unfortunately, the product was found to be contaminated with a substantial amount (34%) of 4,4'-dinitrobiphenyl. However, purification could be achieved through dissolution of the crude material in DCM, followed by selective extraction of the desired product into aqueous base. Acidification of the aqueous layer led to precipitation of the desired product, which back-extracted into DCM. [The reversible formation of the water-soluble boronate anion was exploited on a number of occasions during the course of this work in order to purify boronate esters, and is discussed in more detail in section 2.2.4.] It is now increasingly well established that the presence of strongly electron-withdrawing groups (of which $-NO_2$ is a prime example) favours competitive homocoupling of the starting bromoaromatic to generate biphenyl side-products during the Miyaura reaction. Although this side-product could have been formed by Suzuki cross-coupling of the boronic ester product with the starting material at a rate competitive with the rate of its formation, it is likely that the palladium catalyst acts in some way to catalyse the homo-coupling of the starting aryl bromide. There is indeed precedent for this in the case of 4-nitroiodobenzene which, in the presence of $Pd(OAc)_2$ and PPh_3, has been reported to give 4, 4'-dinitrobiphenyl.

Surprisingly, the problem was resolved by the replacement of the pinacol ester (B_2pin_2) by the neopentyl ester (B_2neo_2). Under identical reaction conditions, this reaction was found to proceed cleanly to the desired product (64% yield) with no significant formation of the biphenyl. The *para*-nitrobenzeneboronate was then employed in a Suzuki cross-coupling with 4'-triflate terpyridine in THF. However, only a poor conversion was achieved, and separation of the product from PPh_3 derived from the catalyst proved troublesome. Indeed the problems encountered previously with the triflate coupling reactions seemed to be exacerbated by the presence of the electron-withdrawing group on the boronic ester.

For the synthesis of L^7 and L^{13}, a boronic acid derivative of triphenylamine was required. Clearly, 4-bromo-N,N-diphenylaniline is a starting point. Initially, the preparation of this compound was attempted through the selective bromination of triphenylamine with NBS, which had been reported to offer selective monobromination,

of just one of the three rings, and selectively in the *para* position.[37] However, attempting the reaction in both benzene[38] and DMF,[37] and varying the concentration and rate of addition of NBS failed, in our hands, to provide the selectivity for mono-substitution reported in the literature.[37, 38] Mixtures of the mono-, di- and tri-brominated products were obtained and, on one occasion, in benzene, although a very high proportion of mono-substituted compound was observed, this was found by GCMS to be a mixture of the *ortho-*, *meta-* and *para*-substituted compounds.

The synthesis was eventually achieved using a very different strategy starting from diphenylamine in place of triphenylamine. Thus the desired compound was obtained in reasonable yield (41%) by a copper (I) catalysed Ullmann coupling of diphenylamine with 4-bromo-iodobenzene in the presence of 1,10-phenanthroline.[39] Under these conditions, substitution occurs specifically at the iodine atom, since the presence of 1, 10-phenanthroline accelerates the reaction, allowing it to proceed at lower temperatures, at which the bromo group in 4-bromoiodobenzene is no longer active, whilst the iodine can still act as an effective leaving group. The rate acceleration observed through the addition of phenanthroline to the reaction is difficult to rationalise, since the exact structure of the catalytically active species is not known with certitude other than the fact that only copper (I) states actively participate as catalysts.[39]

4-(Neopentylglycolato)-N, N-diphenylaniline was subsequently prepared by a Miyaura coupling of 4-bromo-N,N-diphenylaniline with bis(neopentylglycolato)diboron. In this case, the reaction proceeded readily, with no competitive dimerisation of the starting material, and indeed the desired boronic ester was obtained in quantitative yield. In this case, the subsequent reaction of this boronate ester with 4'-bromoterpyridine or 4'-(4-bromophenyl)terpyridine was carried out, and this reaction was found to proceed very satisfactorily, giving the desired product terpyridine in 51% isolated yield. As noted for L[6], it is likely that the electron-donating nature of the *para*-amino substituent favours the reaction by increasing the nucleophilicity of the boron at the transmetallation stage.
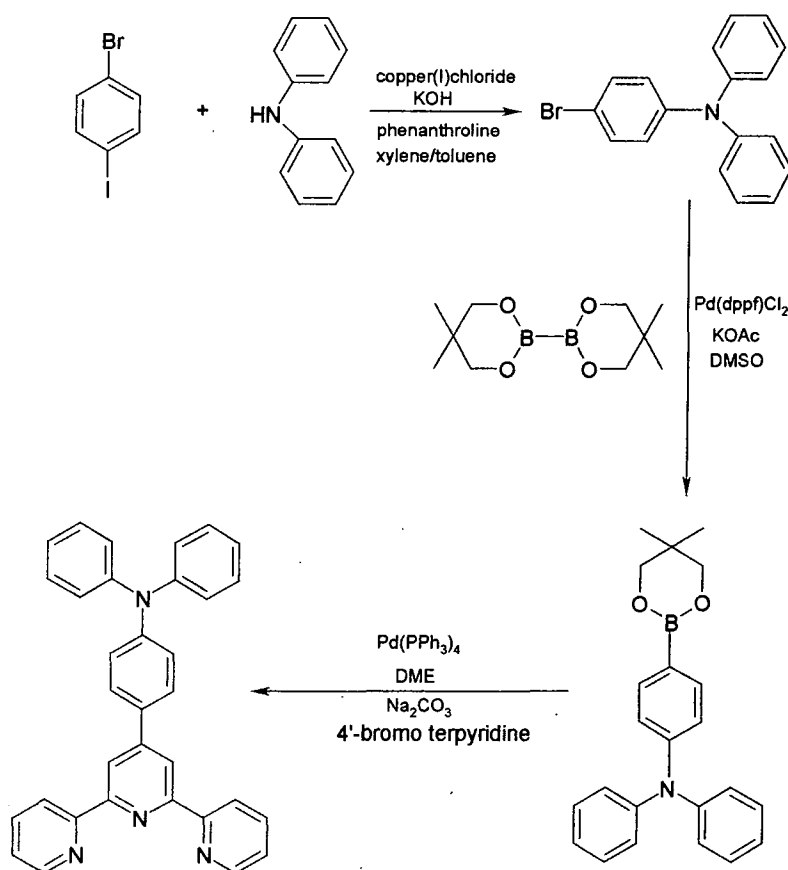
Figure 2.11 - *Synthesis of L^7 via sequential Ullman, Miyaura and Suzuki cross-coupling reactions*

2.2.4. Coupling Reactions using Terpyridine Boronate Esters

As noted in the introduction to this section, it was of interest to consider the "reverse" coupling strategy, namely reaction of terpyridine-4'-boronate with a bromoaromatic. This could be particularly useful where the first coupling sense gives poor results, or where the boronic acid is difficult to access, for example in the *para*-nitrobenzene boronate. The synthesis of 4'-(4-neopentylglycolatoboron)terpyridine (tpy-Bneo), and its analogue with an interposed phenyl group, through the Miyaura coupling of B$_2$neo$_2$ with· 4-bromoterpyridine or 4'-(4-bromophenyl)terpyridine respectively, under the conditions set out earlier for the nitrophenyl boronic ester, had been reported in this laboratory[40] immediately prior to this work. However, these investigations revealed that the formation of 4'-(4-neopentylglycolatoboron)terpyridine may frequently be accompanied by a small amount of the homocoupled "back-to-back" bis(terpyridine), occasionally up to 10 mol%. Once again, it is suggested that this is due to the inductively electron-withdrawing nature of the pyridine ring, as found for the

nitrobenzene compound. However, during this work, it has been found that separation of the contaminating bis(terpyridine) can be readily achieved using the procedure described previously for the nitro system (section 2.2.3). The fully reversible formation of the water-soluble boronate anion upon addition of aqueous base provides a means of separation of the by-products, formed as a result of homocoupling during the Miyaura reaction, by selective extraction of the homocoupled products into DCM, while the boronate anion of the desired product remains in solution in the aqueous layer, so long as it is basic. Acidification of the aqueous layer leads to precipitation of the desired product, which is finally isolated through back-extraction into DCM (figure 2.12). To our knowledge, this procedure has not been previously reported as a method of purifying boronate esters from homocoupled by-products, possibly because hydrolysis of the boronate ester would normally be expected under such conditions. However, purification of the systems described here using this methodology resulted in isolation of the desired product as the boronate ester, with no evidence of significant hydrolysis.
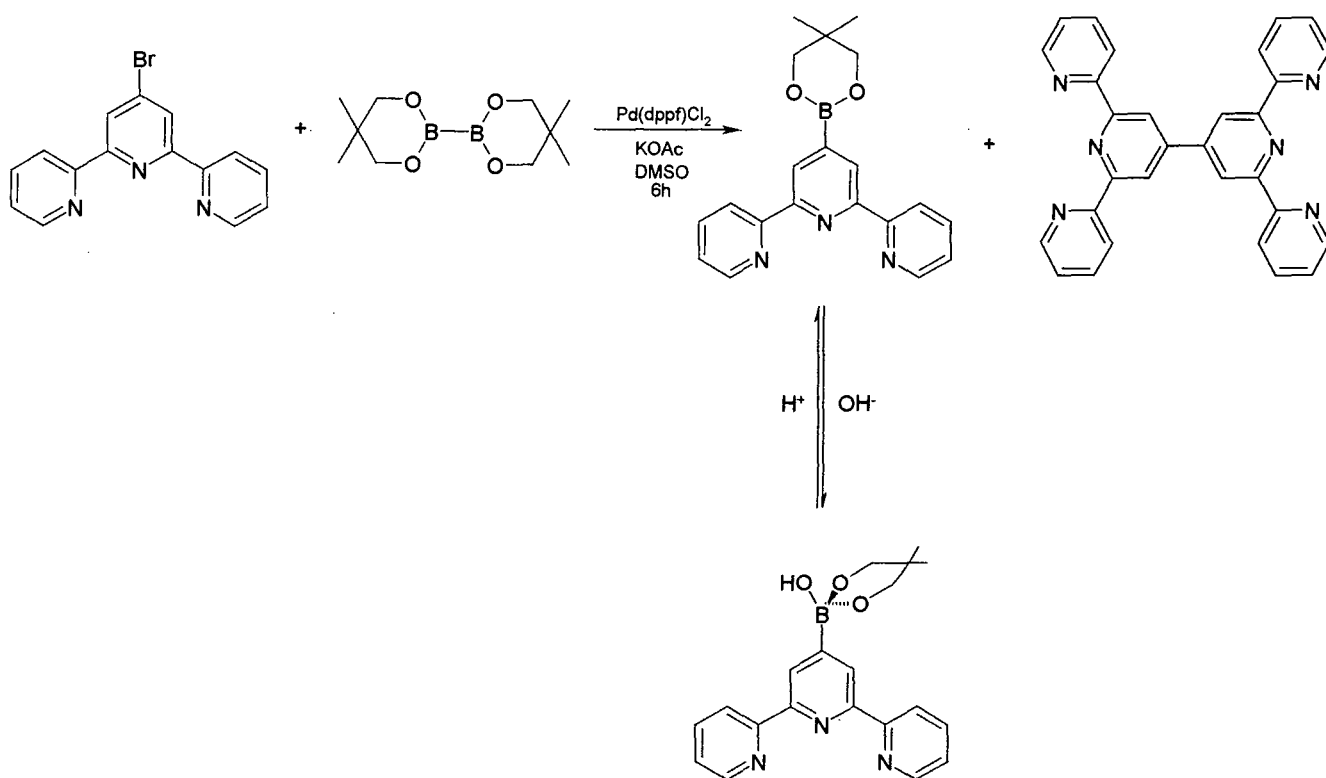
Figure 2.12 - *Purification of 4'-(4-neopentylglycolatoboron)terpyridine through formation of the water-soluble boronate anion*

61

In an attempt to promote the cross-coupling and minimise the competitive homo-coupling of the 4'-bromoterpyridine, some alternative reaction conditions were investigated.

- The replacement of DMSO by dioxane was investigated. Although dioxane is generally found to be a less active solvent for cross-coupling reactions, it has been used successfully in the reaction of aryl triflates with bis(pinacolato)diboron.[35] Unfortunately, in the present instance, no reaction was observed at reflux (101°C), whilst an increase in the reaction temperature to 150°C under pressure in an autoclave led to a mixture of the desired product, the homo-coupled terpyridine and unsubstituted terpyridine. It is suggested that the forcing reaction conditions led to the formation of the latter by hydro-dehalogenation of the starting material.

- Replacement of the Pd(dppf)Cl$_2$ catalyst by a mixture of Pd(CH$_3$CN)$_2$Cl$_2$ and tri-o-tolylphosphine, to produce a catalytic species *in situ*, once again led to contamination of the desired product by the homo-coupled terpyridine. Indeed Pd(CH$_3$CN)$_2$Cl$_2$-tri-o-tolylphosphine proved to be inferior to Pd(dppf)Cl$_2$ in that only partial conversion of the starting material was achieved after 24 h.

- Reaction in methanol in the presence of lithium methoxide (in place of KOAc) and Pd(dppf)Cl$_2$ was investigated. At room temperature, these conditions have been reported to suppress the homo-coupling of aryl halides containing electron-withdrawing substituents, whilst allowing the cross-coupling with tetraalkoxodiboron to proceed.[41] However, in our hands, no reaction between 4-bromoterpyridine and B$_2$neo$_2$ was observed under these conditions after 24 h. Increasing the temperature to 55°C (18 h) led to a complex mixture of the starting 4'-bromoterpyridine, the desired product, the homo-coupled terpyridine, methoxyterpyridine, and unsubstituted terpyridine.

As a result of these investigations, it was concluded that the original conditions put forward by Miyaura[34] as offering optimal conversions were indeed the most successful, for the synthesis of terpyridine boronates, with high conversions and shorter reaction times (typically 5-6 h).

The subsequent cross-coupling reactions of terpyridine boronates with aryl halides were moderately successful. Indeed, in the case of the elusive L^4, a higher yield was obtained than with the opposite coupling sense. However, this appears to be an isolated case, as

in general this strategy does not appear to offer improvements in terms of yields or reaction times, as can be seen in the case of L^5 (Table 2.1).

Consideration of these results, together with the problems in synthesising the terpyridine boronates, and their tendency to pick up iron from the dppf catalyst during their formation, leads to the conclusion that couplings with 4'-bromo and 4'-bromophenyl terpyridines are clearly more attractive in general.

2.3. Crystal Structure of 4'-(4-N,N-dimethylaminophenyl)-terpyridine and 4'-mesityl-terpyridine

The X-ray crystal structures of the ligands 4'-mesityl-terpyridine (top) and 4'-(4-N,N-dimethylaminophenyl)-terpyridine (bottom) are shown below in figure 2.13.
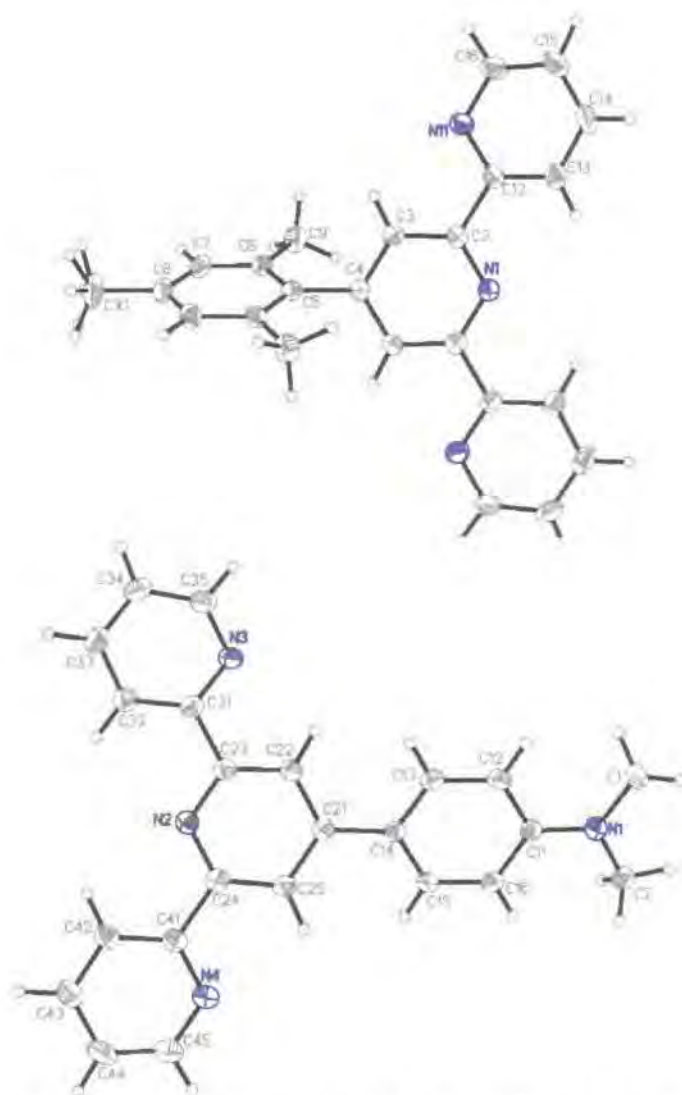
Figure 2.13 - *Crystal structures of 4'-mesityl-terpyridine, L^8 (top) and 4'-(4-N,N-dimethylaminophenyl)-terpyridine, L^6 (bottom)*

The structures confirm that the three pyridine rings exhibit transoid configurations about the interannular C-C bonds, thereby minimising electrostatic interactions between the nitrogen lone pairs, and also the Van der Waals interactions between H^3 and $H^{3'}$.[42] Observation of this configuration is consistent with those reported previously in the literature for 4'-phenyl-terpyridine,[43, 44] 6, 6"-dibromo-4'-phenyl-terpyridine[44] and 2, 2': 6', 2': 6", 2'''-quaterpyridine.[44]

The interannular C-C bonds (between the pyridine rings) for L^6 (C(24)-C(41) and C(23)-C(31)) are 1.495(19) and 1.496(18) Å respectively, and for L^8 (C(2)-C(12)) 1.494(18) Å. These values are within the typical range reported for free oligopyridines (1.482-1.497 Å).[42, 43, 45] For both ligands, the three pyridine rings do not lie exactly coplanar, and in the case of L^8, the two terminal rings each make a least squares plane angle of 9.3° with the central ring. These small deviations from planarity are typical and compare with those observed in 4'-phenyl-terpyridine (5.7°),[43] 6, 6"-dibromo-4'-phenyl-terpyridine (10.9°) and 2, 2': 6', 2': 6", 2'''-quaterpyridine (0.4° and 5.6°).[45] The lack of a mirror plane in L^6 means that calculation of the least squares plane angle is not possible in this case.

The N(1)-C(11) distance in L^6 of 1.375(17) Å is considerably shorter than the N(1)-C(1) or N(1)-C(2) distances of 1.444(18) Å and 1.441(18) Å respectively, and is typical of a conjugated aromatic amine. Similar values were reported in the literature by Constable et al. for 4'-(N,N-dimethylamino)-2, 2': 6', 2"-terpyridine, where the N(3)-C(8) distance of 1.366 Å is shorter than the N(3)-C(9) distance of 1.448 Å.[44]
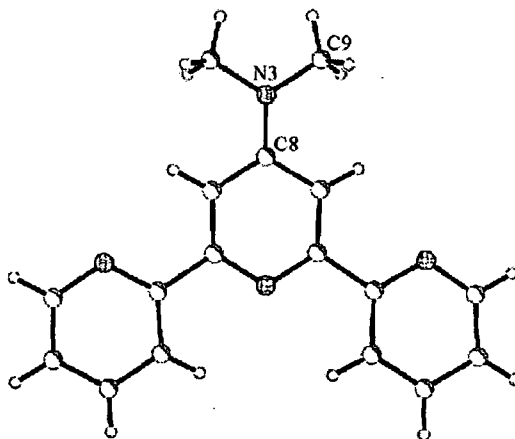
Figure 2.14 – The crystal structure of Me_2Ntpy

The bond lengths from the pendent ring to the central pyridine ring i.e. C(14)-C(21) for L^6 and C(4)-C(5) for L^8 are 1.481 Å and 1.502 Å respectively. These values are very close to the literature value of 1.492 Å measured for the bond length between the pendent phenyl ring and the central terpyridine ring in 4'-phenyl-2, 2'; 6', 2"-terpyridine.[43]

The extent of twisting induced by the *ortho* methyl substituents of the pendent mesityl group, however, is evident from the solid state structure of L^8. The torsion angle between the pendent aryl ring and the central pyridine ring in this case is revealed to be 67.5°, compared to 32.7° in the case of L^6; typical values of about 30° are found in most biphenyl structures omitting *ortho* substituents.[43]
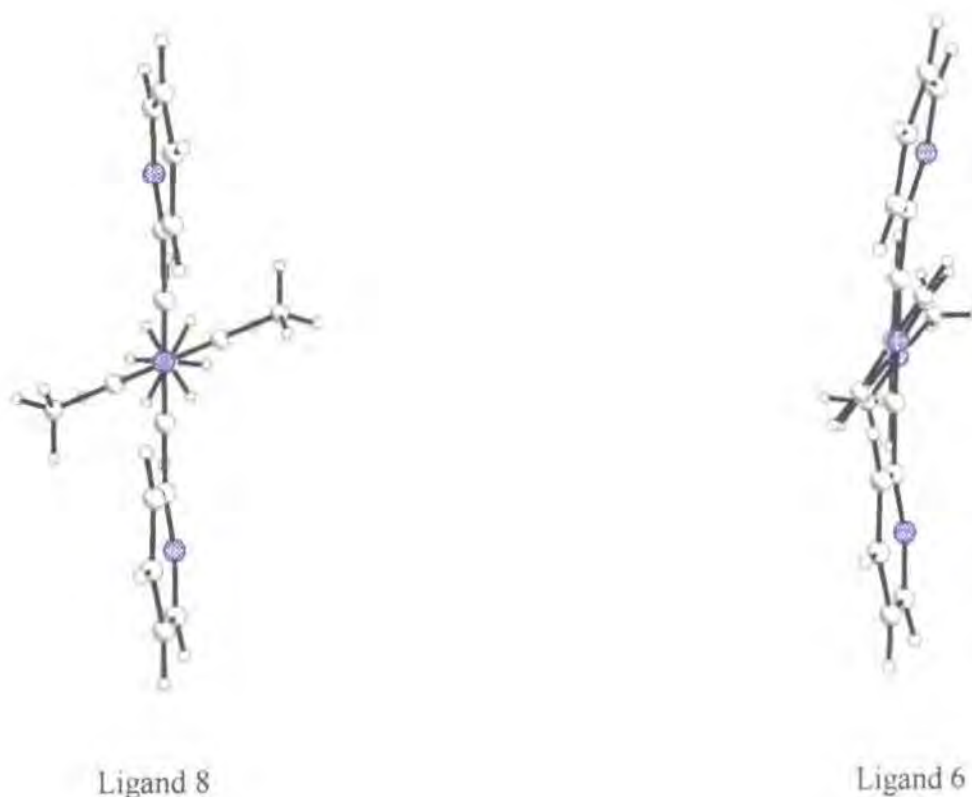
Ligand 8   Ligand 6

Figure 2.15 – *Degree of distortion as revealed by the torsion angle between the pendent aryl ring and the central pyridine ring of ligands 6 and 8*

2.4. NMR Characteristics of the Terpyridine Products

^{1}H NMR data (acquired at 500 MHz) for the ligands synthesised via the Suzuki cross-coupling reaction are collated in tables 2.2 and 2.3, and the numbering scheme employed is shown in figure 2.16

Ligand	H^3	H^4	H^5	H^6	H$^{3'}$	H^a	H^b	H^c	Other		
L^1	8.68 d 8.0	7.90 t 7.5	7.37 dd 7.5, 5.0	8.74 d 6.5	8.76 s --	7.52 t 7.5	7.92 d 7.0	7.46 t 7.0	--		
L^2	8.67 d 10.0	7.87 td 9.5, 1.5	7.34 dd 9.5, 6.0	8.73 d 6.0	8.70 s --	7.28 *(b)* 1H, m *(b)*	7.29 *(b)* 1H, m *(b)*	6.77 1H, dt 9.0, 2.5	7.22 1H, br s H$^{d'}$		
L^3	8.69 d 8.1	7.90 td 7.5, 2.0	7.37 ddd 7.5, 5.0, 1.5	8.73 d 4.5	8.77 s --	8.06 *(b)* d 8.0	8.02 *(b)* d 8.0	--	10.05 (1H) s (CHO)		
L^4	8.67 d 7.5	7.90 td 7.5, 2.0	7.32 ddd 7.5, 4.5, 1.0	8.73 d 4.5	8.74 s --	8.36 d 8.0	8.04 d 8.0	--	--		
L^5	8.69 d 8.0	7.90 td 7.5, 2.0	7.32 ddd 6.0, 5.0, 1.5	8.73 d 5.0	8.74 s --	7.82 d 10.0	8.00 d 8.5	--	--		
L^6	8.68 d 8.0	7.88 td *(c)*	7.36 ddd 7.5, 5.0, 1.0	8.75 d 5.0	8.74 s --	6.83 d 9.0	7.90 d *(c)*	--	3.05 (6H) s (CH$_3$)		
L^7	8.67 d 7.5	7.87 td 8.0, 2.0	7.35 ddd 7.5, 5.0, 1.0	8.72 d 4.0	8.71 s --	7.17 d *(c)*	7.79 d 8.5	--	7.30 (4H) t(*m*-Ph) 7.5	7.17 (4H) d (*o*-Ph) *(c)*	7.07 (2H) t(*p*-Ph) 7.5
L$^{8(d)}$	8.64 d 7.5	7.83 td 7.5, 1.5	7.28 dd 7.0, 5.5	8.62 d 4.5	8.26 s --	6.90 s --	--	--	2.29 (3H) s (*p*-CH$_3$) --	2.03 (6H) s (*o*-CH$_3$) --	

Table 2.2- ^{1}*H NMR data for the phenyl-substituted ligands* L^1-L^8

Spectral details as in footnote (a) to table 2.3
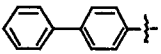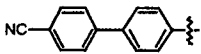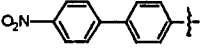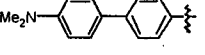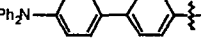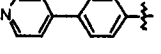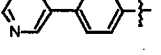
Ligand	H³	H⁴	H⁵	H⁶	H³'	Hᵃ	Hᵇ	Hᵃ'	Hᵇ'	Hᶜ'	other
L⁹	8.69 d 7.9	7.89 td 7.6, 1.7	7.37 dd 6.4, 4.5	8.74 d 4.0	8.80 s --	7.75 d 8.3	8.01 d 8.4	7.49 t 7.5	7.68 t 7.5	7.39 t, 1H 7.5	--
L¹⁰ (d)	8.68 d 8.0	7.89 t 7.5	7.37 dd 7.0, 5.0	8.74 d 4.5	8.77 s --	7.72 d 8.5	8.01 d 8.5	7.74 s (4H) --		--	--
L¹¹ (d)	8.69 d 7.9	7.92 td 7.8, 1.8	7.38 ddd 7.4, 4.9, 1.1	8.75 d 4.7	8.79 s --	7.77 d 8.4	8.04 d 8.6	8.33 d 8.8	7.82 d 6.8	--	--
L¹² (d)	8.68 d 7.9	7.89 t 7.4	7.36 dd 6.8, 5.0	8.75 d 4.5	8.79 s --	7.71 d 8.2	7.97 d 8.2	6.84 d 8.5	7.60 d 8.7	--	3.02 (CH₃) s (6H) --
L¹³	8.69 d 8.0	7.89 td 8.0, 2.0	7.36 ddd 7.5, 5.0, 1.0	8.74 d 4.0	8.79 s --	7.72 d 8.5	7.99 d 8.0	7.17 d 7.5(c)	7.56 d 8.5	--	7.17, 4H, d 7.0(c), o-Ph 7.29, 4H, t 8.5, m-Ph 7.05, t 7.0, p-Ph
L¹⁴ (d)	8.70 d 8.0(c)	7.90 td 7.5, 1.5	7.38 dd 7.5, 4.5	8.75 d 4.5	8.79 s --	7.80 d 8.0	8.05 d 8.0	8.71 d 5.5 (c)	7.60 d 4.5	--	--
L¹⁵ (d)	8.70 d 7.8	7.90 td 7.8, 1.5	7.38 ddd 7.5, 4.8, 1.2	8.75 ddd 4.8, 1.8	8.80 s --	7.75 d 8.7	8.05 d 8.4	7.42 dd (1H) 8.1, 4.5	7.97 dd (1H) 7.8, 2.4, 1.8	8.64 dd, 1H 4.8, 1.5	8.94 (Hᵈ') d (1H) 2.4

Table 2.3-^{1}*H NMR data for the biphenyl-substituted ligands L⁹-L¹⁵ (a)*

(a)*All spectra acquired in CDCl₃ at 500MHz and assigned using* ^{1}*H-*^{1}*H NOESY.* δ *in ppm relative to residual CHCl₃ at 7.26 ppm; J in Hertz. All signals integrate to two protons except where stated otherwise.* ᵇ*Signals too close to allow unambiguous assignment and, for L², determination of coupling constant.* ᶜ*Overlap of resonances prohibits reliable determination of coupling constants.* ᵈ*Ligands prepared by Kathryn J Arm and Kerstin Wild.*
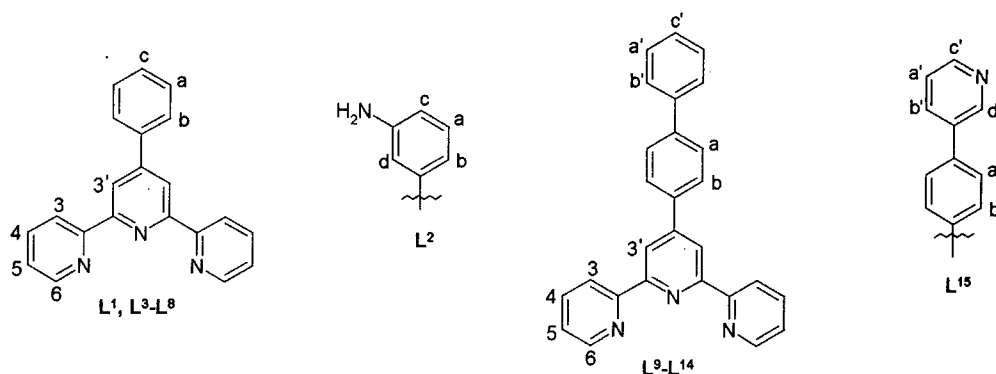
Figure 2.16 - *Key to NMR assignments in terpyridine ligands*

Ligands L^1-L^4, L^6 and L^9 have been prepared previously by conventional methodology,[46] and partial NMR data are reported in the literature, with which the data presented here are consistent. However, our data are at higher field strength, offering greater resolution, and allowing unambiguous assignment, and is included here for comparative purposes.

Full assignment of the spectra was made through consultation of the splitting patterns, coupling constants, ^{1}H-^{1}H COSY and ^{1}H-^{1}H-NOESY spectra. However, the assignment was greatly simplified by the occurrence of repeating patterns in the chemical shift values, splitting patterns and coupling constants in the resonances of the lateral pyridine rings (H^2, H^3, H^4, H^5) and the central pyridine ring ($H^{3'}$) throughout the series of terpyridine ligands obtained.

For example, with only one exception, the three highest chemical shift values in each case were H^6, $H^{3'}$, and H^3. The resonance of $H^{3'}$ was easily distinguished as a singlet, while the resonances of H^6 and H^3 were split into doublets, with H^6 at a higher chemical shift value than H^3, and displaying a smaller coupling constant. In the majority of cases $H^{3'}$ is at a higher chemical shift than H^6. However, the chemical shift values of $H^{3'}$ and H^6 are very similar, and in ligands L^2, L^6 and L^7, where an electron withdrawing group is substituted onto the pendent ring directly bound to the terpyridine moiety, the doublet of H^6 is higher than the singlet of $H^{3'}$.

With respect to the remaining protons on the lateral pyridine rings, H^4 couples equally to H^3 and H^5, and then to H^6, making it recognisable as a triplet of doublets, always centred around 7.9 ppm. H^5 displays the lowest chemical shift value from the protons

68

situated on the lateral pyridine rings, and a more complicated coupling pattern giving it a characteristic ddd pattern.

NOESY proved to be a particularly powerful tool for providing unambiguous assignment of the resonances of the pendent rings, owing to noe between the singlet of $H^{3'}$ and H^b (but not H^a). The absence of noe between H^6 and $H^{3'}$ is consistent with a predominately transoid arrangement of the pyridine rings about the interannular C-C bonds, which was observed in the crystal structures of ligands L^6 and L^8, and discussed previously in section 2.3.

Once the assignment of the resonance due to H^b had been confirmed in this way from the NOESY spectrum, elucidation of the remaining resonances of the pendent ring of ligands L^1-L^8 through consultation of the ^1H-^1H COSY was straightforward. In the case of ligands L^9-L^{15}, where H^b was a proton on the phenyl spacer ring, assignment of H^a could be made by consultation of the coupling constants and the ^1H-^1H COSY spectrum as before. The NOE between H^a and $H^{b'}$ could then be used to identify the resonance of $H^{b'}$, after which the elucidation of the resonances of the distal ring could be made by utilising the ^1H-^1H-COSY spectra as for ligands L^1-L^8.

The only ligand whose NMR spectrum deviated significantly from this pattern was L^8. The ^1H-^1H NOESY spectrum allowed the two equally intense singlets in this compound, namely those due to $H^{3'}$ and H^a, to be distinguished; $H^{3'}$ displayed a single cross-peak to the *ortho* methyl groups only (2.03 ppm, 6H), whilst H^a showed coupling to both the *ortho* and *para* methyl groups.

2.4.1. Effect of Substitution of the Pendent Ring on Proton Resonances

Changes in the substitution pattern in the 4'-aryl pendent group scarcely affect the resonances of the lateral pyridine rings (H^2, H^3, H^4, H^5) and the central pyridine ring ($H^{3'}$). The exception is the 4'-mesityl compound, L^8, for which there is a large shift in the $H^{3'}$ resonance of about 0.5 ppm to low frequency. This may be rationalised in terms of the usual deshielding effect of the π cloud of the 4'-pendent ring being reduced as the mean torsion angle between the pendent aryl ring and the central pyridine ring increases due to the presence of the *ortho* methyl substituents on the pendent ring, as discussed previously in section 2.3. The effect is transmitted to some extent to H^6 and H^5, which

appear at slightly lower frequency than in other compounds; indeed, it is only in this compound that H^6 appears to lower frequency than H^3.

The relative shifts of the protons in the pendent aryl group are governed by the aryl substituent. The more strongly electron-withdrawing nature of the terpyridine unit compared to a phenyl group is evident for the unsubstituted phenyl ligand L^1 and all the biaryl systems L^9-L^{15}, where the proton *ortho* to the terpyridine (H^b) appears to high frequency of the *meta* proton (H^a) as a consequence of this effect. The difference is amplified in the cases of L^6 and L^7 by the presence of electron-donating substituents at the *para* position. In contrast, the situation is reversed for the *p*-nitro substituted compound, indicating that the electron-withdrawing influence of the terpyridine is weaker than that of the nitro group. In the formyl-substituted compound L^3, the substituent and terpyridyl effects are almost balanced, hence the chemical shifts are approximately coincident.

The distal ring of the biaryl substituted compounds exhibits a similar trend, with $H^{b'}$ at higher frequency in all cases, except for the electron withdrawing 4-nitro and 4-pyridyl systems, L^{11} and L^{14}. The balance between the electron withdrawal by the substituent and the 4'-phenylterpyridine fragment is attained in this case in the cyano system (L^{10}).

A strikingly similar homology was revealed in the resonances of the pyridyl carbons when the ^{13}C NMR spectra were assigned with the aid of ^1H-^{13}C correlation spectroscopy (tables 2.4 and 2.5). Once again the most significant deviation was found in the mesityl system, L^8, in which the $C^{3'}$ resonance displayed a modest shift of 4 ppm to high frequency compared with other compounds.
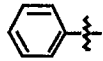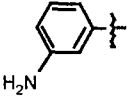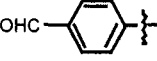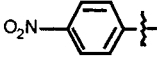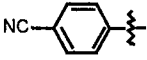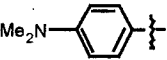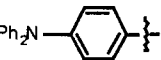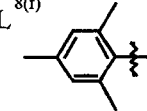
Ligand	C^3	C^4	C^5	C^6	$C^{3'}$	C^a	C^b	C^c (b)	Quaternaries	Other
L^1	121.4	137.0	123.9	149.0	119.0	128.9	127.4	129.0	156.1, 155.8, 150.4, 138.4	--
L^2	121.4	136.9	123.7	149.1	118.9	117.7(c)	129.8(c)	115.7	156.3, 155.8, 150.5, 146.9, 139.5	113.8 $(C^{d'})$
L^3	121.4	137.0	124.0	149.1	119.0	128.0(c)	130.3(c)	--	156.2, 155.8, 148.9, 144.4, 136.4	192.0 (CHO)
L^4	121.4	137.0	124.2	149.2	118.9	124.2	128.3	--	156.3, 155.6, 147.8, 144.9, 148.1	
L^5	121.3	137.0	124.1	148.3	118.6	132.7	128.0	--	156.3, 155.7, 143.1, 118.7(d)	112.6 CN
L^6	121.5	137.2	123.7	150.1	117.7	112.4	128.1	--	156.3, 155.3, 151.1, 148.8, 125.0	40.4 (CH$_3$)
L^7	121.4	136.8	123.8	148.7	118.3	129.4	128.0	--	156.3, 155.8, 149.7, 149.2, 147.4, 131.8	124.8, m-Ph 123.3, o-Ph 123.1, p-Ph
$L^{8(f)}$	121.1	136.7	123.6	149.1	121.9	128.0	--	--	156.2, 155.5, 151.6, 137.0, 136.6, 134.9	20.9 (p-CH$_3$) 20.6 (o-CH$_3$)

Table 2.4-^{13}C NMR data for ligands L^1-$L^{8\,(a)}$

$^{(a)}$Spectra recorded in $CDCl_3$ at 125.7 MHz; assigned using ^1H-^{13}C COSY, observing ^1H at 499.8 MHz and decoupling ^{13}C at 125.7 MHz. δ in ppm relative to $CDCl_3$ at 77.0 ppm. $^bC^c$ assigned only for L^1 and L^2 (Table 2.4) and $C^{c'}$ only for L^9 and L^{15} (Table 2.5), where these are secondary carbon atoms. $^cC^a$ and C^b (table 2.4) and $C^{a'}$ and $C^{b'}$ (table2.5) not assignable unambiguously, due to coincidence or near-coincidence of corresponding protons in the ^1H spectrum. ^{d}ipso C-CN not detected. ^{e}Overlap of ^1H resonances of ortho-Ph and $H^{a'}$ prohibits unambiguous assignment of these resonances by ^1H-^{13}C correlation spectroscopy. ^{f}Ligands synthesised by Kathryn J Arm and Kerstin Wild.

71
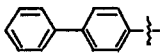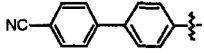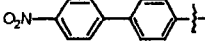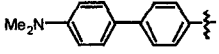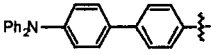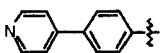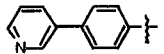
Ligand	C^3	C^4	C^5	C^6	C$^{3'}$	C^a	C^b	C$^{a'}$	C$^{b'}$	C$^{c'}$	Quaternaries	Other
L^9	121.4	136.9	123.9	149.2	118.7	127.6	127.7	128.9	127.2	127.6	156.3, 156.0, 149.8, 141.9, 140.5, 137.3	--
L$^{10\,(f)}$ NC–	121.4	136.9	123.9	149.1	118.7	127.7	128.0	132.6 (c)	127.6 (c)	--	156.1, 156.0, 149.2, 144.8, 139.6, 138.7 (d)	111.2 (-CN)
L$^{11\,(f)}$ O$_2$N–	121.4	137.0	123.9	149.2	118.7	127.9	128.1	124.2	127.9	--	156.1, 156.0, 149.1, 147.2, 146.8, 139.2, 139.0	--
L$^{12\,(f)}$ Me$_2$N–	121.3	136.8	123.8	149.1	118.5	126.5	127.6	112.7	128.2	--	156.3, 155.9, 150.2, 149.9, 141.9, 135.7, 127.7	40.5 (CH$_3$)
L^{13} Ph$_2$N–	121.4	136.9	123.8	149.1	118.6	127.0	127.5	124.5 (e)	126.7	--	156.3, 155.9, 149.8, 147.5, 141.3, 136.9, 136.7, 134.1	129.3, m-Ph 123.8, o-Ph (e) 123.0, p-Ph
L$^{14\,(f)}$	121.6	137.0	124.0	149.2	118.7	127.5	128.1	121.6	121.4	--	156.1, 150.3, 149.4, 147.6, 139.3, 138.6	--
L$^{15\,(f)}$	121.4	136.9	124.0	149.4	118.6	127.5	128.0	123.6	134.3	149.1	156.1, 156.0, 148.8, 138.5, 138.2, 135.9	148.2 (C$^{d'}$)

Table 2.5-^{13}C *NMR data for the biphenyl-substituted ligands L^9-L^{15}*

Spectral details as in footnote to table 2.4

2.5. References

[1] G. T. Morgan and F. H. Burstall, *J. Chem. Soc.*, 1932, 20.

[2] F. H. Burstall, *J. Chem. Soc.*, 1938, 1662.

[3] Z. Travnicek, R. Pastorek, Z. Sindelar, and J. Marek, *J. Coord. Chem*, 1998, **44**, 208.

[4] E. L. Lebeau and T. J. Meyer, *Inorg. Chem.*, 1999, **38**, 2174.

[5] L. Alvila, T. A. Pakanen, and O. Krause, *J. Mol. Catal*, 1993, **84**, 1145.

[6] S. Kelch and M. Rebhahn, *J. Chem. Soc., Chem. Commun*, 1999, 1123.

[7] M. K. Nazeeruddin, S. M. Zakeeruddin, R. Humphry-Baker, T. A. Kaden, and M. Gratzel, *Inorg. Chem.*, 2000, **39**, 4542.

[8] M. C. DeRosa, F. Al-Mutlaq, and R. J. Crutchley, *Inorg. Chem.*, 2001, **40**, 1406.

[9] E. C. Constable, C. E. Housecroft, and L.-A. Johnston, *Inorg. Chem. Commun*, 1998, **1**, 68.

[10] B. T. Farrer and H. H. Thorp, *Inorg. Chem.*, 2000, **39**, 44.

[11] L. Flamigni, F. Barigelletti, N. Armaroli, J.-P. Collin, J.-P. Sauvage, and J. A. G. Williams, *Chem. Eur. J*, 1998, **4**, 1744.

[12] L. Flamigni, F. Barigelletti, N. Armaroli, B. Venturi, J.-P. Collin, J.-P. Sauvage, and J. A. G. Williams, *Inorg. Chem.*, 1999, **38**, 661.

[13] L. Flamigni, F. Barigelletti, N. Armaroli, J.-P. Collin, I. M. Dixon, J.-P. Sauvage, and J. A. G. Williams, *Coord. Chem. Rev*, 1999, **190-192**, 671.

[14] J.-P. Collin, S. Guillerez, J.-P. Sauvage, F. Barigelletti, L. De Cola, L. Flamigni, and V. Balzani, *Inorg. Chem.*, 1991, **30**, 4230.

[15] J.-P. Collin, S. Guillerez, J.-P. Sauvage, F. Barigelletti, L. De Cola, L. Flamigni, and V. Balzani, *Inorg. Chem.*, 1992, **31**, 4112.

[16] M. Licini and J. A. G. Williams, *Chem. Commun*, 1999, 1943.

[17] W. Goodall and J. A. G. Williams, *J. Chem. Soc., Dalton Trans.*, 2000, 2893.

[18] R.-A. Fallahpour, *Synthesis*, 2003, **No.2**, 155.

[19] N. Miyaura and A. Suzuki, *Chem. Rev.*, 1995, **95**, 2457.

[20] P. R. Parry, W. Changsheng, A. S. Batsanov, M. R. Bryce, and B. Tarbit, *J. Org. Chem*, 2002, **67**, 7541.

[21] J. A. G. Williams, W. Goodall, K. Wild, and K. J. Arm, *J. Chem. Soc., Perkin Trans. 2*, 2002, 1669.

[22] J. Cossy and D. Belotti, *Tetrahedron*, 1999, **55**, 5145.

[23] D. F. O'Keefe, M. C. Dannock, and S. M. Marcuccio, *Tetrahedron Lett*, 1992, **33**, 6679.

[24] K. T. Potts and D. Konwar, *J. Org. Chem.*, 1991, **56**, 4815.

[25] E. C. Constable and M. D. Ward, *J. Chem. Soc., Dalton Trans.*, 1990, 1405.

[26] T. Oh-e, N. Miyaura, and A. Suzuki, *Synlett*, 1990, 221.

[27] T. Oh-e, N. Miyaura, and A. Suzuki, *J. Org. Chem*, 1993, **58**, 2201.

[28] D. R. Coulson, *Inorg. Synth.*, 1972, **13**, 121.

[29] T. I. Wallow and B. M. Novak, *J. Org. Chem.*, 1994, **59**, 5034.

[30] B. E. Segelstein, T. W. Butler, and B. L. Chenard, *J. Org. Chem*, 1995, **60**, 12.

[31] K.-C. Kong and C.-H. Cheng, *J. Am. Chem. Soc*, 1991, **113**, 6313.

[32] P. Pechy, F. P. Rotzinger, M. K. Nazeeruddin, O. Kohle, S. M. Zakeeruddin, R. Humphry-Baker, and M. Gratzel, *J. Chem. Soc., Chem. Commun*, 1995, 65.

[33] W. Spahni and G. Calzaferri, *Helv. Chim. Acta*, 1984, **67**, 450.

[34] T. Ishiyama, M. Murata, and N. Miyaura, *J. Org. Chem.*, 1995, **60**, 7508.

[35] T. Ishiyama, Y. Itoh, T. Kitano, and N. Miyaura, *Tetrahedron Lett*, 1997, **38**, 3447.

[36] T. Hayashi, M. Konishi, and M. Kumada, *Tetrahedron. Lett*, 1979, 1871.

[37] S. C. Suh, M. C. Suh, and S. C. Shim, *Macromol.Chem.Phys*, 1999, **200**, 1991.

[38] M. Nicolas, *Electroanal. Chem*, 2000, **482**, 211.

[39] H. B. Goodbrand and N.-X. Hu, *J. Org. Chem*, 1999, **64**, 670.

[40] C. J. Aspley and J. A. G. Williams, *New J. Chem*, 2001, **25**, 1136.

[41] S. M. Marcuccio and H. Weigold, *Int. Pat. Appl.*, PCT/AU00/01246

[42] E. C. Constable, S. M. Elder, J. V. Walker, P. D. Wood, and D. A. Tocher, *J. Chem. Soc., Chem. Commun*, 1992, 229.

[43] E. C. Constable, J. Lewis, M. C. Liptrot, and P. R. Raithby, *Inorg. Chim. Acta*, 1990, **178**, 47.

[44] E. C. Constable, A. M. W. Cargill Thompson, D. A. Tocher, and M. A. M. Daniels, *New J. Chem*, 1992, **16**, 855.

[45] E. C. Constable, S. M. Elder, J. A. Healy, and D. A. Tocher, *J. Chem. Soc., Dalton Trans.*, 1990, 1669.

[46] A. M. W. Cargill Thompson, *Coord. Chem. Rev*, 1997, **160**, 1.

3. Photophysical Properties of

Terpyridine Ligands

3.1.   Photophysical Properties of 4'-aryl-substituted 2, 2': 6', 2"-terpyridines

3.1.1.   Photophysical Properties of tpy, tpyH$^+$ and tpyH$_2$$^{2+}$

The first comprehensive investigation of the photophysical properties of 2, 2': 6', 2"-terpyridine itself was carried out by Maestri *et al.* in 1998.[1] The group reported that tpy displayed only weak emission with λ_{max}=338 nm, before going on to investigate the photophysical properties of the protonated species, tpyH$^+$ and tpyH$_2$$^{2+}$, which are summarised in table 3.1.   As well as changes associated with the two successive protonation processes in aqueous solution with pK_a=4.73 and 3.34, it was observed that the addition of more than two equivalents of acid does not cause additional spectral change compared to the stoichiometric addition of exactly two equivalents of acid, clearly indicating that only the monoprotonated (tpyH$^+$) and diprotonated (tpyH$_2$$^{2+}$) species are formed.

Investigation into the emission properties of the protonated species concluded that the addition of the first equivalent of acid results in the replacement of the very weak emission band with λ_{max}=338 nm by a strong band with λ_{max}=410 nm, which is in turn replaced by an even stronger band with λ_{max}=360 nm upon the addition of the second equivalent of acid.[1, 2] Although the spectral changes brought about by the protonation were complicated, they were fully reproducible.

	$\lambda_{max, em}$ (nm)	ϕ_{em}	τ (ns)
tpy	338	3×10^{-3}	-
tpyH$^+$	410	0.17	3.0
tpyH$_2$$^{2+}$	360	0.71	2.7

Table 3.1-*photophysical properties of terpyridine and its protonated species*[1]

3.1.2. Effect of the 4'-aryl substituent

The work carried out by Maestri et al.[1] revealed 2, 2': 6', 2"-terpyridine itself was only very weakly emissive. However, 4'-phenyl substitution of terpyridine ligands bound to Ru (II) has been reported to improve the efficiency of luminescence exhibited by these complexes compared to the corresponding tpy complex at room temperature,[3] suggesting that 4'-phenyl substitution might give improved photophysical properties to tpy itself.

To this end, investigations into the effect of the 4'-aryl substituent on the photophysical properties of terpyridine ligands are now presented. The results of experiments carried out include the effect of the substituent on the intensity and the lifetime of emission from the terpyridine, and the effect of protonation of 4'-aryl substituted terpyridines. A summary of the absorption and emission properties of the terpyridines prepared for this work are collated in table 3.2. During the course of this study, Araki et al. published a related report into the fluorescence tuning of terpyridine ligands through substitution,[4] and parallels with their data are also drawn in the following discussion. Overall, it can be concluded that 4'-aryl substituted terpyridines almost always display more intense and longer wavelength emission than those of the unsubstituted terpyridine, and that their fluorescence is tuneable, in some cases profoundly so, by the introduction of substituents having different electron affinity into the *para*-position of the pendent phenyl ring.

Ligand	Absorption λmax/nm, (log₁₀ε (mol⁻¹ dm³ cm⁻¹))	Emission λmax / nm	I / I Phtpy (b)	τ/ ns (c)
L¹	282 (4.57)	339, 351	1.00	1.2
L²	280 (4.52) 308(sh) (4.12)	348	0.03	(d)
L³	283 (4.56)	339, 352	0.10	(d)
L⁴	289 (4.49)	368	<0.01	(d)
L⁵	277 (4.62) 320(sh) (3.98)	365	1.59	3.0
L⁶	291 (4.56) 348 (4.48)	531(e)	0.11(e)	2.6(e)
L⁷	290 (4.59) 360 (4.41)	513(e)	3.12(e)	2.5(e)
L 8 (f)	284 (4.74)	339	0.05	(d)
L⁹	289 (4.80)	374	2.92	1.5
L 10 (f)	294 (4.93)	346(sh) 359	2.16	1.9
L 11 (f)	288 (4.80) 318 (4.61)	367 382(sh)	0.20	0.80
L 12 (f)	287 (4.81) 344 (4.28)	567(e)	0.24(e)	(d)
L 13	284 (4.50) 347 (4.32)	545(e)	1.88(e)	1.5(e)
L 14 (f)	287 (4.53)	346(sh) 358	2.40	2.8
L 15 (f)	287 (4.59)	346 (sh) 358	1.90	2.0

Table 3.2-*photophysical data for the ligands L¹-L¹⁵ (a)*

(a)In solution in ethanol at 293±3K. (b)Integrated emission intensity relative to L¹, upon excitation at 285 nm for isoabsorbant solutions, except for those marked (e), which were excited at 350 nm. Spectra were aquired using excitation and emission band-passes of 2.5 nm in each case, and were corrected for the wavelength dependence of the photomultiplier tube. The quantum yield of L¹ was measured to be 0.08±0.02, using 2-aminopyridine in 0.05 M H₂SO₄ (aq) as standard, for which φ=0.6±0.05 for excitation at 285nm.⁵ (c)Estimated uncertainty ±0.2 ns. (d)Emission too weak to allow measurement of the fluorescence lifetime using available instrumentation. (e)For excitation at 350 nm. (f)Ligands prepared by Kathryn J Arm and Kirsten Wild.

The fluorescence quantum yield of 4'-phenyl-terpyridine L^1 was measured (using 2-aminopyridine in 0.05 M H_2SO_4 (aq) as the standard) and found to have a value of 0.08 ± 0.02, clearly much higher than that of tpy itself. This compound was used as a secondary standard, against which all the terpyridines were compared.

Ligands L^2, L^3, L^4 and L^8 are less emissive than L^1. Most significantly, substitution of the strongly electron-withdrawing nitro group into the *para*-position of the pendent ring reduces the quantum yield dramatically compared to phenyl terpy, a result also observed by Araki et.al.[4] However, this result is not surprising as organic compounds containing nitro groups are rarely emissive. A more interesting case however, is comparison of L^1 and the mesityl analogue L^8, which reveals that the emission of L^8 is less intense than L^1 by a factor of 20. It is suggested that this effect is a result of the increased torsion angle between the pendent aryl ring and the central pyridine due to the presence of the *ortho*-methyl substituents, as discussed in section 2.3. The resulting twist now inherent in the structure means that the coplanar conformation of the excited state, which favours fluorescence, cannot be attained, resulting in a decrease in the emission intensity.

The introduction of the *meta*-amino (L^2) substituent leads to a reduction in the intensity of the emission relative to 4'-phenyl terpyridine by a factor of 33. It is possible that in this instance, the reduction in the observed quantum efficiency is a result of photoinduced electron transfer (PET) from the lone pair electrons on the *meta*- amino functionality, to the terpyridine moiety, fig 3.1.[6] Luminescence and electron transfer are often competing pathways of deactivation of excited states, with the electron transfer rate being much faster than the luminescence rate when PET is thermodynamically allowed. Indeed, de Silva *et al.* have calculated the feasibility of PET within a similar system, combining an amine with a common fluorophore, anthracene, linked *via* a methylene spacer.[6] In this case, the Gibbs free energy of the PET process in polar media was found to be favourable, and the process expected to be rapid compared to fluorescence, based on the radiative rate constant of 9-methylanthracene. This effect has been exploited in a variety of sensory systems, as the PET process is inhibited upon protonation of the nitrogen or coordination to a metal ion.[7] The relative ease of reduction of pyridyl-based ligands, including tpy, will favour such a PET process in the presence of a potential electron donor, such as the *meta*-amino phenyl substituent in this system.
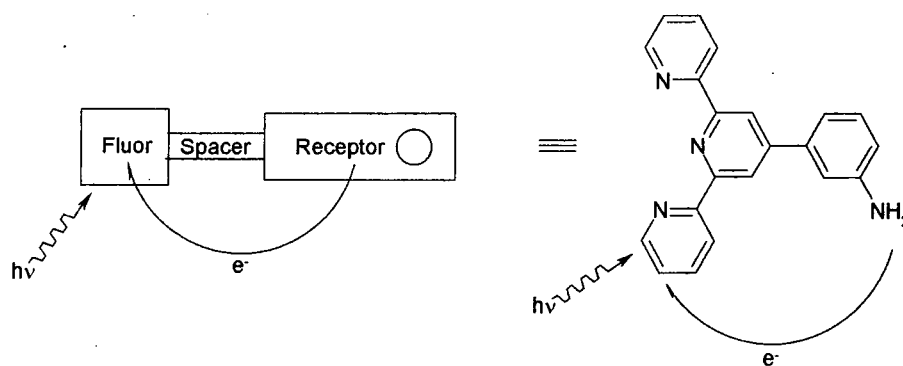
Figure 3.1 - *Schematic representation of a photoinduced electron transfer process*

Since a formyl group is unlikely to act in this way, the explanation for the low fluorescence quantum yield of L^3 must lie elsewhere. In this case, it is possible that competing acetal formation (in ethanol) opens up other competitive deactivation processes, including photochemical side-reactions.

The introduction of the *para*-cyano substituent (L^5) gives rise to a small red-shift in absorption and emission spectra, and an increase in the emission intensity of the ligand, compared to phenyl tpy (L^1). However, the effect of the substituent in changing the photophysical properties of the ligand compared to those of L^1 is very small in this case. The results of Araki *et al.* also show that substitution of relatively weak electron donating or electron withdrawing groups, such as bromo-, chloro-, methyl- and methoxy- onto the pendent phenyl ring lead to only a very small effect on the fluorescence maxima and quantum yield compared to phenyl tpy.[4] Discussion of the very different photophysical properties of the amino-functionalised systems L^6, L^7, L^{12}, L^{13} is deferred until section 3.1.4.

3.1.3. Effect of the phenyl spacer ring

Interest in the photophysics of the biphenyl substituted terpyridine L^9 and its metal complexes has been awakened following the recognition of different possible π-stacking interactions in the solid state, leading to distinct effects on the excited states.[8, 9] For example, Hannon and Pikramenou *et al.* added biphenyl units to the periphery of bis(terpyridine) metal complexes and used the π stacking interactions between these tails as an alternative means of controlling the aggregation of the photoactive metal centres into polymetallic arrays.[9] X-ray analysis of these arrays suggested different types of stacking, some of which are illustrated in the figure below.
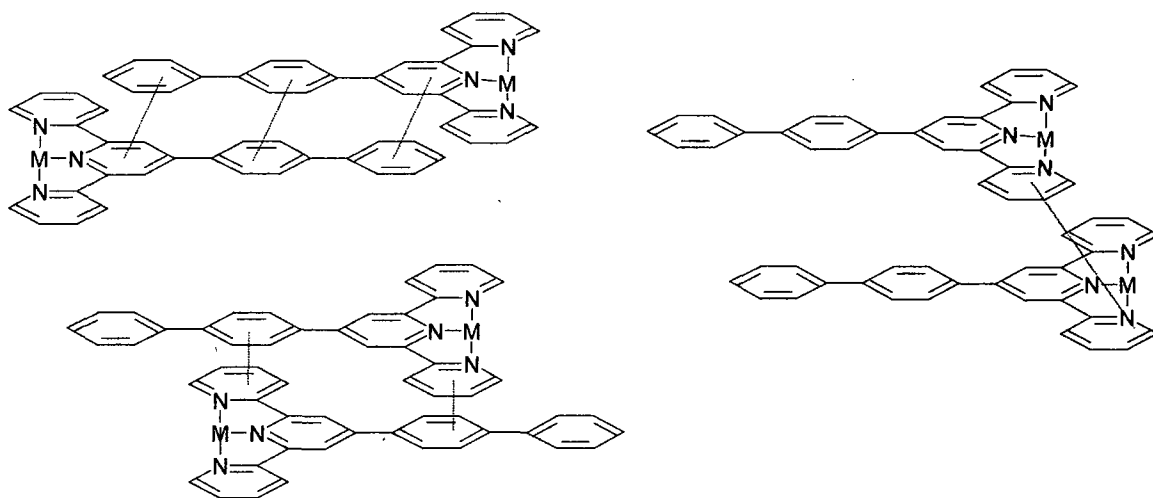
Figure 3.2 - *Stacking motifs observed in biphenyl-appended terpyridine complexes (M=Co(II), Ru(II), Ni(II), Cu(II), Zn(II), Cd(II)).*[9]

Comparison of L^1 and L^9 reveals that in this instance the additional phenyl ring leads to a small red-shift in the emission, and a significant enhancement in the intensity. This is not surprising, as it is well known that increasing conjugation in hydrocarbons shifts the first (π-π^*) absorption maximum towards longer wavelength, i.e. lower energy, as a consequence of higher aromatic stabilisation energy due to increased delocalisation. It is also established that a high ring density of the π electrons seems to be important for high quantum yields.

Once again, the *para*-nitro substituent has a deleterious effect on emission (L^{11}), although to a lesser extent than in L^4. The *para*-cyanophenyl and 4- and 3- pyridyl substituted analogues (L^{10}, L^{14}, L^{15}) reveal a small blue shift in the emission maximum and somewhat longer lifetimes.

The measured fluorescence lifetimes are typical of conjugated aromatic molecules, being in the range of 1-5 ns; It should be noted that almost no lifetime data have previously been published for terpyridine ligands (as opposed to complexes), with the exception of the study by Maestri above.[1] In this instance, measurement of the lifetimes was made *via* two different methods, namely time correlated single photon counting and frequency modulation. Further details are provided in the experimental section (chapter 7).

3.1.4. Effect of protonation

As discussed previously in section 3.1.1, it is well established that terpyridine itself undergoes two successive protonation processes upon acidification in solution, with the mono- and di-protonated species characterised by red-shifted and more intense emission compared to the free base.[1,2] However, no systematic study of the effect of protonation on the photophysical properties of 4'-aryl substituted terpyridines appears to have been carried out. Hence it was pertinent to consider the effect of protonation on the ligands prepared here.

In the case of the 4'-monoaryl-substituted compounds (L^1-L^5) a small red-shift in the emission upon the addition of triflouroacetic acid (>2 equiv), similar to that observed previously in the parent unsubstituted terpyridine, was recorded.[1,2] However, the effects on the intensity of emission upon protonation were variable and very small, with an initial increase at low concentrations of acid pronounced only for ligands L^2 and L^3. Under highly acidic conditions however, all compounds displayed a reduction in intensity. It is suggested that the initial increase in emission intensity observed for ligand L^2 at low concentrations of acid is a response to the switching off of the PET process (discussed in section 3.1.2) that competes with luminescence as a mechanism of deactivation of the excited state of these ligands. In general, protonation of an amine moiety raises its oxidation potential, increasing the value of the free energy of the PET process to a proximate fluorophore, so that it is no longer favourable. Hence PET becomes strongly inhibited, resulting in a revival of fluorescence (figure 3.3).[6]
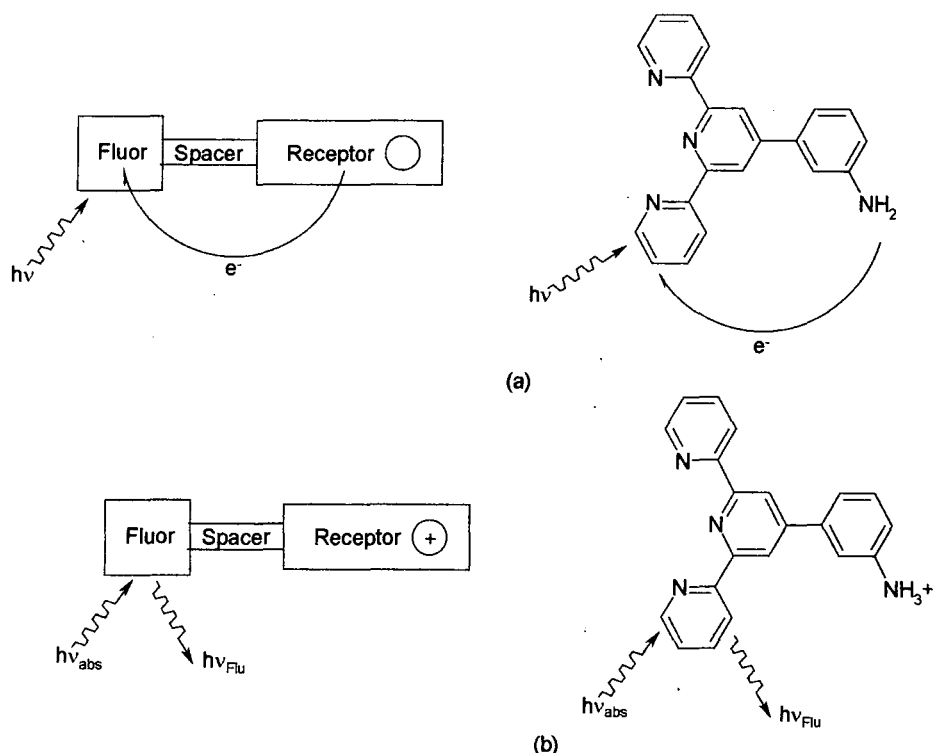
Figure 3.3 - *Schematic representation of photoinduced processes in a system (a) when non-protonated and (b) when protonated on the pendent amino group.*

The 4'-biaryl compounds L^9, L^{11}, L^{14} and L^{15} display a more pronounced red-shift upon protonation than their monoaryl analogues, with maxima shifted to 410-440 nm, and an accompanying increase in intensity, leading to strong, visible blue emission. This observation corresponds to the effect of coordination of Lewis acidic metal ions to L^9, reported recently by Hannon and Pikramenou.[9] In that case, coordination of zinc or cadmium red-shifted the emission from 390 nm in methanol for the free ligand, into the visible blue region of the spectrum as observed for our own work, and increased the quantum yield from 0.55 for the free ligand to 0.80 for the zinc complex, and 0.71 for the cadmium complex. It is suggested that the red-shift in the emission upon protonation may be ascribed to an increased involvement of charge transfer excited states, discussed in more detail below, over the intra-ligand π-π^* transitions which dominate the nature of the emission from the free, unprotonated ligand.

3.1.5. Para-amino-functionalised Ligands

Investigations into the photophysical properties of ligands L^6 and L^7 in ethanol revealed that the lowest energy π-π^* absorption band in each case was shifted by 50-80 nm to longer wavelength compared to L^1. A similar trend was observed in the emission spectrum, with fluorescence observed at λ_{max}=531 and 513 nm for ligands L^6 and L^7 respectively, compared to λ_{max}=345 nm for L^1. A similar result was reported at the same time by Araki et al. for 4'-(4-aminophenyl)-2, 2': 6', 2"-terpyridine.[4]

Further investigations revealed a solvent dependency for the λ_{max} of the emission as well as the lifetimes and quantum yields.[10] In particular, the solvent dependence of the fluorescence maximum, which appeared at more than 130 nm longer wavelength in ethanol compared to cyclohexane (figures 3.4 and 3.5), suggested that an Intramolecular Charge Transfer (ICT) process was involved in the excited state of these two ligands. It is well known that ICT emission is solvent-dependent, with polar solvents stabilising the charge-separated excited states, leading to large red-shifts in the emission.[11] On the other hand, the ICT state is not normally formed directly upon absorption of light, but indirectly from a "locally excited" state in which there is little charge separation. Hence the absorption spectrum shows little solvent dependence.
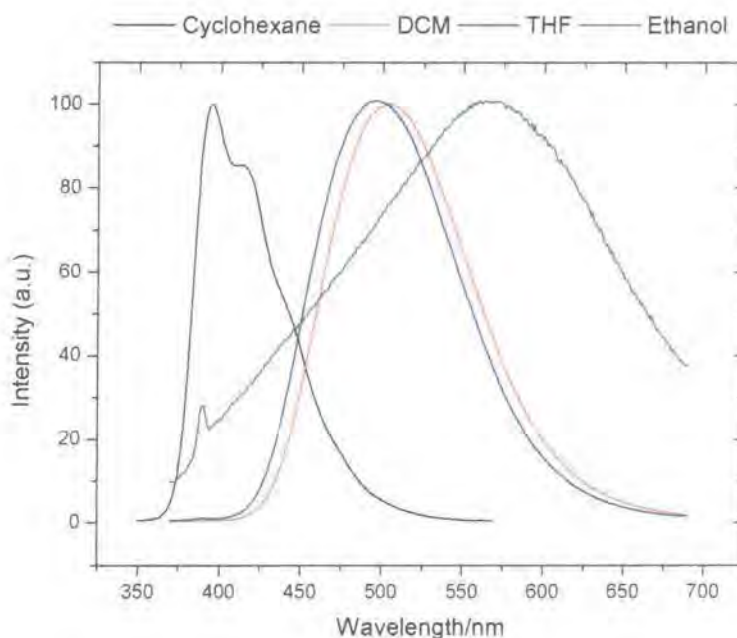
Figure 3.4 –Normalised emission spectrum of L^6 in cyclohexane, THF, DCM and ethanol, λ_{ex}=350nm.(Corresponding quantum yields are given in table 3.3; note that the compound is much less emissive in ethanol than in the other solvents).
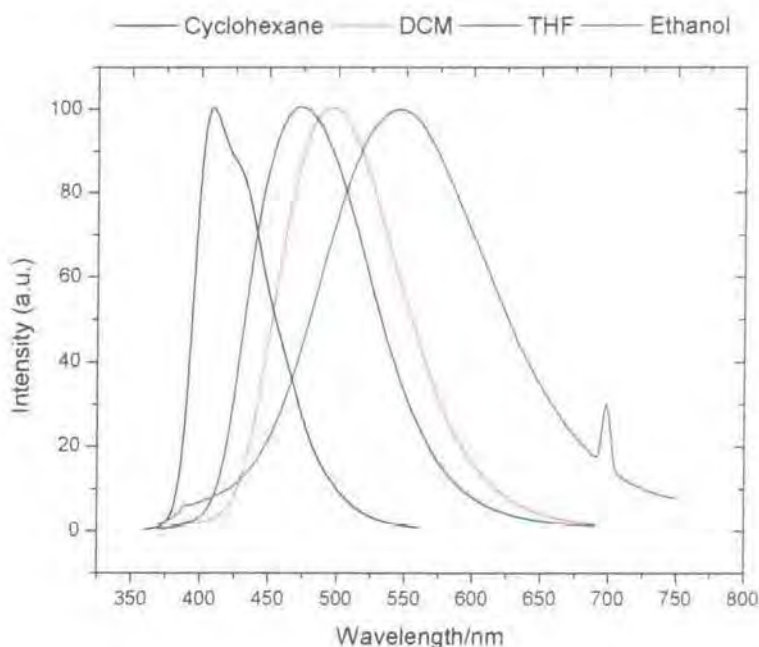
Figure 3.5 – *Normalised emission spectrum of L⁷ in cyclohexane, THF, DCM and ethanol, λ_{ex} 350nm.*

It was suggested that substitution of the electron donating amino groups onto the *para*-position of the aryl ring had raised the energy of the π_{Ph} to a higher level than that of the π_{tpy}. As a result the π_{Ph} becomes the HOMO, as opposed to the π_{tpy}, shifting the lowest energy excited state from the locally excited transition ($\pi_{tpy}.\pi_{tpy}*$) to the ICT transition ($\pi_{Ph}.\pi_{tpy}*$). This hypothesis has been confirmed by Araki for the NH_2 analogue of L6, through semi-empirical molecular orbital calculations for L⁶.[4]

The ICT nature of the emissive state may also account for the anomalously low quantum yields observed for the $-NMe_2$ substituted compounds L⁶ and L¹² in ethanol, compared to the other three compounds investigated.
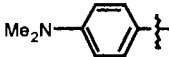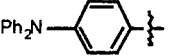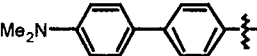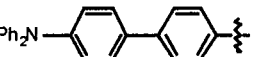
		Cyclohexane	THF	DCM	EtOH
Me_2N—⟨⟩—} **L**[6]	λ_{max} / nm (abs)[a]	337	346	348	348
	λ_{max} / nm (em)[b]	369, 385(sh)	469	470	531
	τ_f/ ns[c]	1.7	5.2	5.2	2.6
	ϕ_f[d]	0.31[e]	0.22	0.27	0.01
Ph_2N—⟨⟩—} **L**[7]	λ_{max} / nm (abs)[a]	356	360	361	362
	λ_{max} / nm (em)[b]	392, 414(sh)	453	472	513
	τ_f/ ns[c]	1.2	3.4	4.0	2.5
	ϕ_f[d]	0.36	0.51	0.58	0.25
Me_2N—⟨⟩—⟨⟩—} **L**[12 (g)]	λ_{max} / nm (abs)[a]	335	350	350	348
	λ_{max} / nm (em)[b]	395, 413(sh)	496	504	567
	τ_f/ ns[c]	1.2	2.5	2.7	(f)
	ϕ_f[d]	0.60[e]	0.52	0.64	0.02
Ph_2N—⟨⟩—⟨⟩—} **L**[13]	λ_{max} / nm (abs)[a]	354	352	353	347
	λ_{max} / nm (em)[b]	404, 425(sh)	472	494	545
	τ_f/ ns[c]	1.2	2.3	2.9	1.5
	ϕ_f[d]	0.60	0.40	0.43	0.15

Table 3.3-The effect of solvent on the photophysical properties of the amino-functionalised ligands L^6, L^7, L^{12}, L^{13}

[a]Position of longest wavelength absorption band. [b]Wavelength of maximum emission upon excitation into the lowest energy absorption band, obtained after correction for the wavelength dependence of the photomultiplier tube. [c]Estimated uncertainty ±0.2 ns. [d]Fluorescence quantum yields were measured using an excitation wavelength of 350 nm and excitation and emission band-passes set to 2.5 nm in each case; quinine sulphate was used as the standard (ϕ=0.546 in 1M H_2SO_4);[12] estimated uncertainty ±25%. [e]Measured using an excitation wavelength of 340 nm: a steeply decreasing absorbance profile at 350 nm in cyclohexane prohibits the reliable use of this wavelength. [f]Emission too weak to allow reliable determination of lifetime. [g]Ligand prepared by Kirstin Wild.

This difference is clear when comparing the fluorescence quantum yields of the diphenylamino and dimethylamino compounds in ethanol: 0.009 for the dimethyl-compound L^6, compared with 0.25 for the diphenyl-compound, L^7. Since the fluorescence lifetimes of the two compounds in this solvent are the same within experimental error, the smaller quantum yield of L^6, is likely to be due to a reduction in the efficiency of formation of the emissive ICT state, following excitation to the

initially populated excited state, rather than to enhanced non-radiative deactivation. This observation may be explained by considering that it is known in systems of the "push-pull" type (e.g. the classic compound dimethylamino-benzonitrile), of which the amino-substituted aromatics L^6 and L^7 are examples, that ICT emission requires a dynamic relaxation of the initially populated state through twisting of the dialkylamino group, coupled with electron transfer from the amino nitrogen to the remote π^* orbital of the acceptor moiety. This twisting process may be partially inhibited in the case of L^6 in alcohol solutions, since the solvent may hydrogen-bond to the N atom of the donor, which will provide a thermodynamic barrier for the twisting process to occur.[13] Given the basicity of dimethylaniline compared to non-basic triphenylamine (pK_a values of the conjugate acids are 5.15 and ca. –5 respectively), such H-bonding is to be expected in L^6 but may well be absent (or only very weak) in L^7.

3.1.5.1.   Effect of the Phenyl Spacer Ring

Ligands L^{12} and L^{13} incorporate both a terpyridine unit and an amino-substituted phenyl group in the same fashion as L^6 and L^7, but with an interposed phenyl ring. As revealed in table 3.2, the two new systems behave in a manner similar to that of the earlier analogues. Once again, the absorbance maxima are almost independent of solvent, whilst the fluorescence maxima undergo large shifts to longer wavelength as the polarity increases. Larger overall effects are observed for the dimethylamino substituted compound compared to the diphenylamino substituted compound. Such behaviour is once again strongly indicative of intramolecular charge-transfer character in the emissive excited states of these compounds. However, in a given solvent, the emission of both L^{12} and L^{13} occurs at rather longer wavelength than the corresponding analogue L^6 or L^7 respectively in the same solvent, indicative of stabilisation of the excited state (of the order of 1000 cm^{-1}) as a result of the additional phenyl ring. Significantly, the intensity of emission of the dimethylamino-substituted compound L^{12}, just like its analogue L^6, is greatly reduced in ethanol compared to other solvents, whilst the diphenylamino compound is affected to a much lesser extent, reinforcing the theory based on the capacity of the nitrogen to act as a H-bond acceptor given earlier.[13]

For L^6, L^7, L^{12} and L^{13} the trend in lifetimes of emission is similar, increasing from cyclohexane through THF to DCM and then decreasing in ethanol.

3.1.5.2. *Effect of protonation*

Upon protonation, the behaviour of the amino-functionalised systems was once again very different from that of other 4'-aryl-substituted terpyridines.[10, 14] For example, a solution of L^7 in ethanol changed from colourless to yellow upon acidification, undergoing a substantial hypochromic shift in the longest wavelength absorption band to 430 nm (figure 3.6).
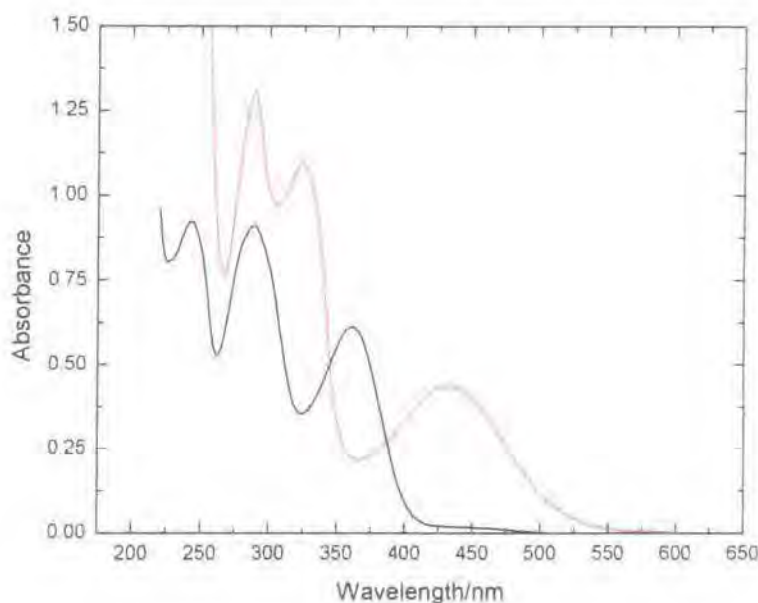
Figure 3.6 - *Absorption spectrum of L^7 in ethanol in the absence of acid (black), and in the presence of trifluoroacetic acid (red)*

A comparable red-shift was observed in the fluorescence emission band (from 513 to 642 nm), however the integrated emission intensity was enormously decreased, by a factor of >200 when excited at the isosbestic point (387 nm) (figure 3.7). Monitoring of the emission intensity at 513 nm in the presence of increasing concentrations of trifluoroacetic acid led to a pH profile with a single inflection point at 3.5, probably associated with diprotonation of the terpyridine (figure 3.8).
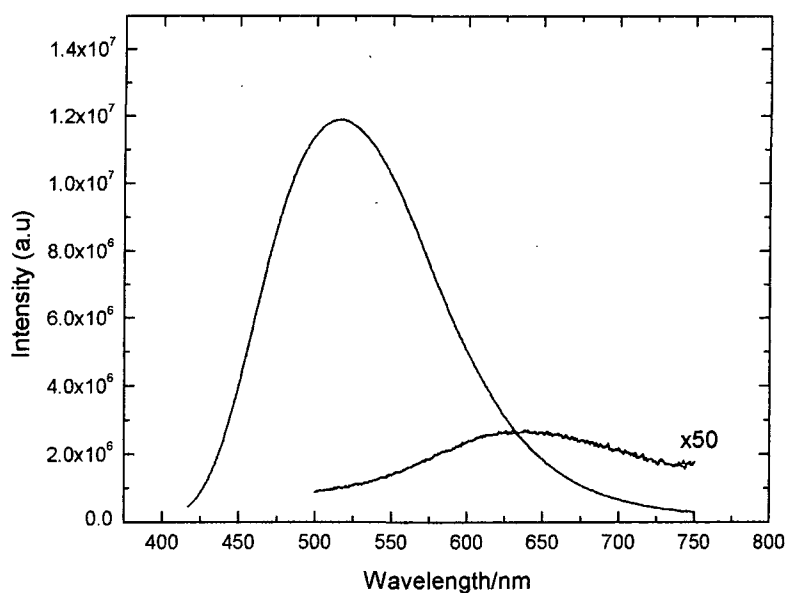
Figure 3.7 - *Corrected fluorescence emission spectra of L^7 in ethanol in the absence of acid (black) and in the presence of acid (red), upon excitation at the isosbestic point (387 nm)*
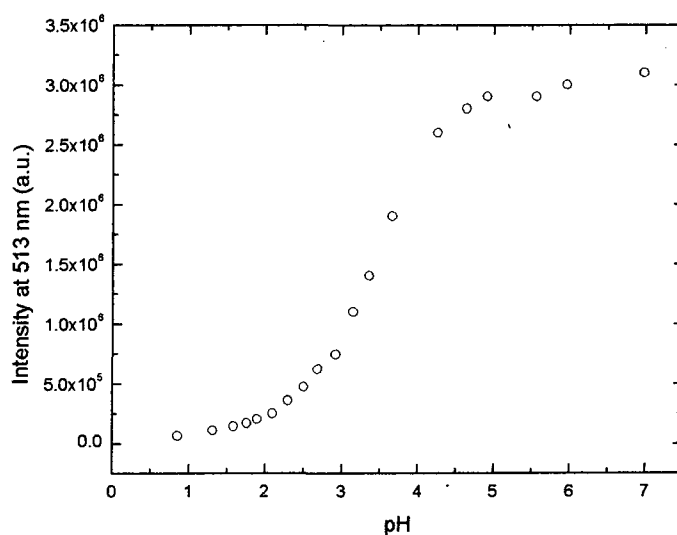
Figure 3.8 - *pH profile showing a single inflection point at 3.5, obtained when monitoring emission of L^7 in ethanol at 513 nm, whilst titrating with trifluoroacetic acid.*

The red-shift in emission is observed since protonation of the terpyridine moiety leads to an enhancement in its electron acceptor properties, thereby stabilising the charge-transfer state (figure 3.9).
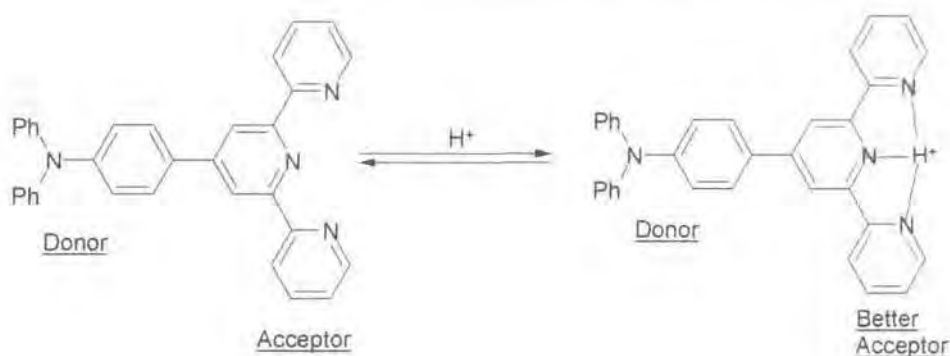
Figure 3.9 - *Stabilisation of the charge-transfer state through protonation*

Similar behaviour was noted for the dimethylamino analogue (figures 3.10 and 3.11), but with a smaller change in intensity (however, it should be noted that the starting non-protonated intensity in ethanol is much lower in this case, as discussed earlier), and a subtle displacement of the profile to higher pH, the inflection point being at 4.2 in this instance, compared to a value of 3.5 for L^7 (figure 3.12). The displacement of the profile of L^6 to higher pH is indicative of the more strongly electron-donating nature of the NMe$_2$ group, compared to NPh$_2$.
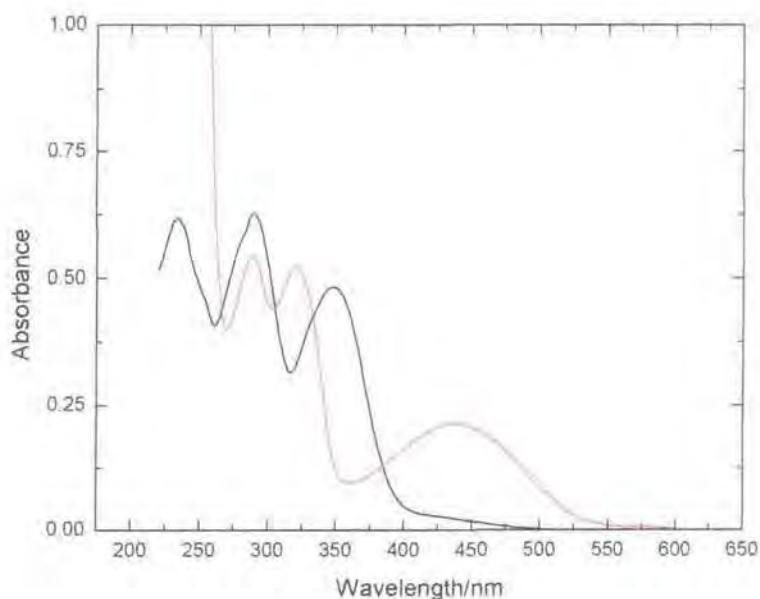
Figure 3.10 - *Absorption spectrum of L^6 in ethanol in the absence of acid (black), and in the presence of trifluoroacetic acid (red)*
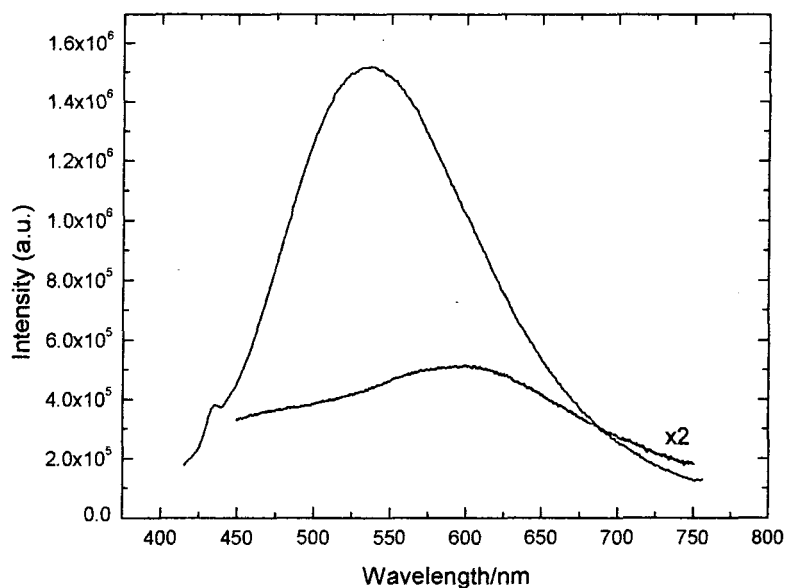
Figure 3.11 - *Corrected fluorescence emission spectra of L^6 in ethanol in the absence of acid (black) and in the presence of acid (red), upon excitation at the isosbestic point (382 nm)*
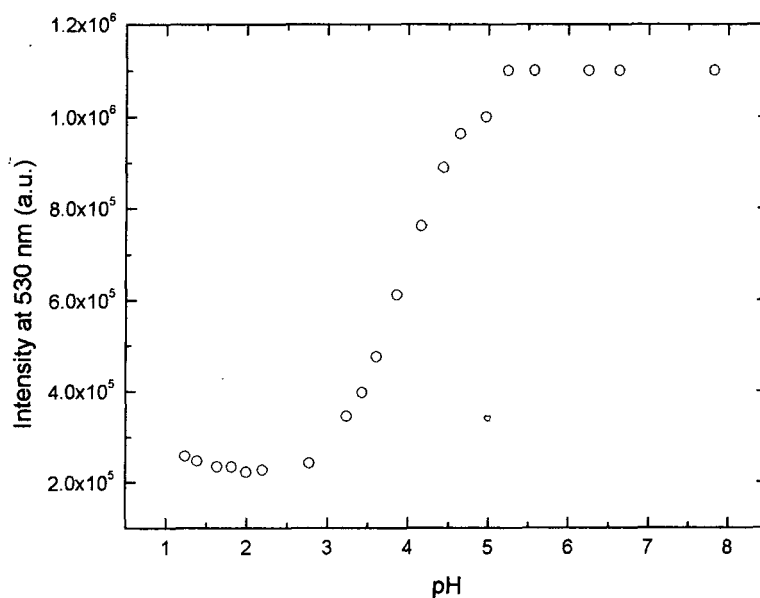
Figure 3.12 - *pH profile showing a single inflection point at 4.2, obtained when monitoring emission of L^6 in ethanol at 531 nm, whilst titrating with trifluoroacetic acid.*

Whereas protonation of L^6 and L^7 led to the appearance of a new long wavelength band (430nm) in the absorption spectrum, acidification of L^{12} and L^{13}, containing an extra phenyl spacer ring, led to a long tail in the absorption spectrum, extending to about 500 nm, rather than a well-defined new band (figures 3.13 and 3.14).
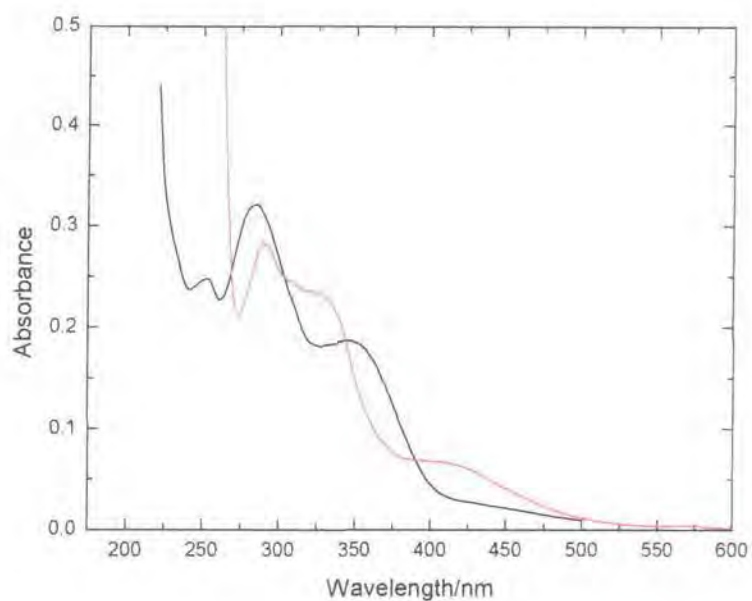
Figure 3.13 - *Absorption spectrum of L¹³ in ethanol in the absence of acid (black), and in the presence of trifluoroacetic acid (red)*
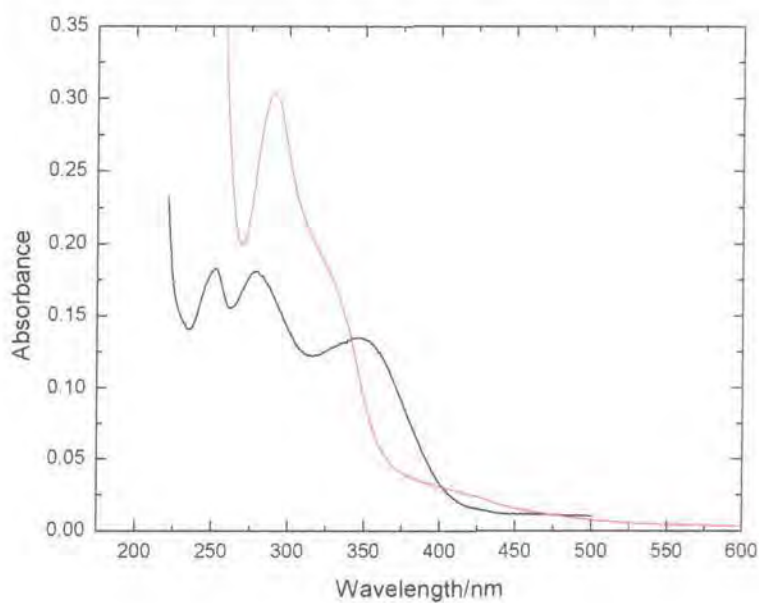
Figure 3.14 - *Absorption spectrum of L¹² in ethanol in the absence of acid (black), and in the presence of trifluoroacetic acid (red)*

Once again the emission is red-shifted, however the intensity is greatly reduced in this instance, with a scarcely detectable signal centred around 700 nm. Presumably, non-radiative deactivation of the ICT state is more efficient in the biaryl systems as a consequence of the additional rotations and vibrations that are possible.

3.1.6. Effect of Zinc Ions on the Amino-Functionalised Terpyridines: Towards a New Class of Zinc Sensor?

3.1.6.1. Biological role of zinc

The detection of zinc is desirable as it is recognised as biologically one of the most important metals, implicated in a huge number of processes, and apparently necessary to all forms of life. The body of an adult human contains about two grammes of zinc, mostly present as zinc enzymes.[15] However, as these enzymes are present in most body cells, its concentration is very low, and as a consequence of this, realisation of its importance was delayed. However, two zinc enzymes that have received much attention are Carboxypeptidase A and Carbonic anhydrase.[16] Carbonic anhydrase was the first zinc metalloenzyme to be discovered (1940) and is widely distributed in plants and animals. In animals it is found in mammalian erythrocytes (red blood cells) where it reversibly catalyses the reaction

$$H_2O + CO_2 \rightleftharpoons HCO_3^- + H^+$$
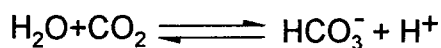
At the pH of blood, most of the CO_2 is present as HCO_3^-. The second important zinc enzyme is the pancreatic enzyme carboxypeptidase A, which catalyses the hydrolysis of the terminal peptide bond in proteins during the process of digestion. As well as a catalytic role in enzymes, zinc also plays a structural role in an important kind of DNA binding protein known as zinc fingers, which make contact with and identify DNA sequences. There are now many known zinc finger proteins and the crystal structures of some of their DNA complexes have been studied.[17]

Zinc is also present in the brain at concentrations ~0.1-0.5 mM, and the central nervous system (CNS), throughout which the concentration of zinc varies widely.[18] Within the CNS, zinc ions have the ability to modulate a variety of ion channels,[19] may play a role in neuronal death during seizures,[20] are involved in neurodegenerative disorders,[21] and may be vital to neurotransmission.[22] Because of its diverse functions, zinc continues to be an interesting subject of research in neurobiology, prompting much research into the development of zinc sensors.[23-29]

3.1.6.2. Existing zinc sensors

To this end, several strategies have been devised to detect Zn^{2+} via fluorescence, however the most widely used probes for detecting intracellular Zn^{2+} are the aryl sulfonamide derivatives of 8-aminoquinoline (figure 3.15).[24-27]
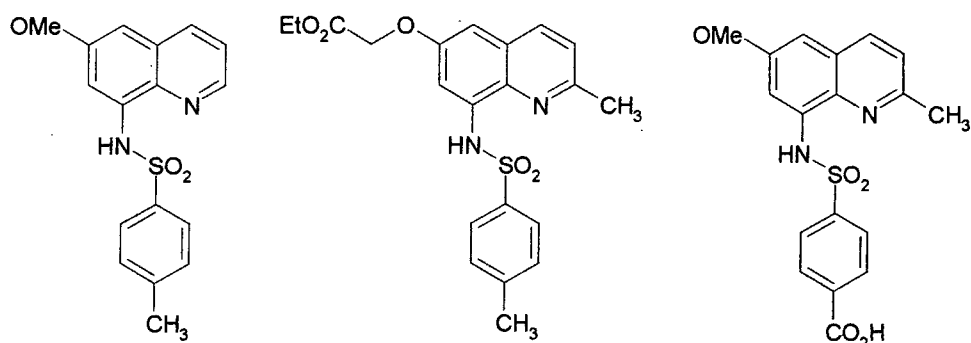
Figure 3.15 - Fluorescent sensors for Zn^{2+} based on aryl sulfonamide derivatives of 8-aminoquinoline

The intensity of fluorescence of these probes increases by 100 fold upon the addition of excess Zn^{2+}. Unfortunately, the quinoline probes can form mixed complexes with partially coordinated Zn^{2+}, generating uncertainty in measurements of free Zn^{2+}. They also possess relatively low quantum yields and extinction coefficients, and a wavelength of excitation that is somewhat shorter than desirable for intracellular study.

In a different approach, macrocyclic amines were applied to prepare dansylamidoethylcyclen for the detection of Zn^{2+} at sub-nanomolar concentrations (figure 3.16).[28]
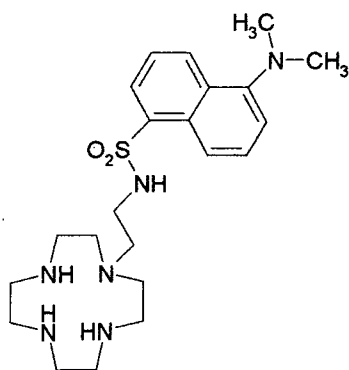
Figure 3.16 -Fluorescent sensor for Zn^{2+} based on dansylamidoethylcyclen

Like quinoline sulfonamides, the sensor shown in figure 3.16 has an excellent sensitivity for Zn^{2+} over Mg^{2+} and Ca^{2+}, which are often competing divalent cations present in biological systems. Unfortunately, it exhibits only a 5-fold enhancement in fluorescence intensity upon binding to Zn^{2+} and, as for compounds shown in fig 3.15,

has a low quantum yield in aqueous solution (0.11), and an excitation wavelength lower than what would be considered desirable for intracellular work.

The two sensors shown in fig 3.17 on the other hand have excitation and emission wavelengths $\lambda_{ex}/\lambda_{em}$=495/515 and 505/525 where x=H and Cl respectively, ideal for intracellular studies.[29]
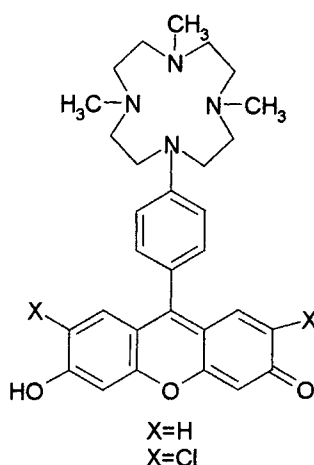
Figure 3.17 - *Xanthene-based fluorescent sensor for Zn^{2+} that employs a cyclen macrocycle as the metal ion binding moiety*

The fluorescence intensity, when X=H, increases 14-fold upon saturation of Zn^{2+}, and increases 26-fold when X=Cl. However, despite their exceptional optical properties, these compounds have a fairly low affinity for Zn^{2+}, and require an intricate multi-step synthesis with poor overall yields, 1.9% when X=H and 0.11% for X=Cl.

Recently, Lippard *et al.* have prepared Zn^{2+} sensors utilising fluoroscein as a chromophore (figure 3.18).[23]
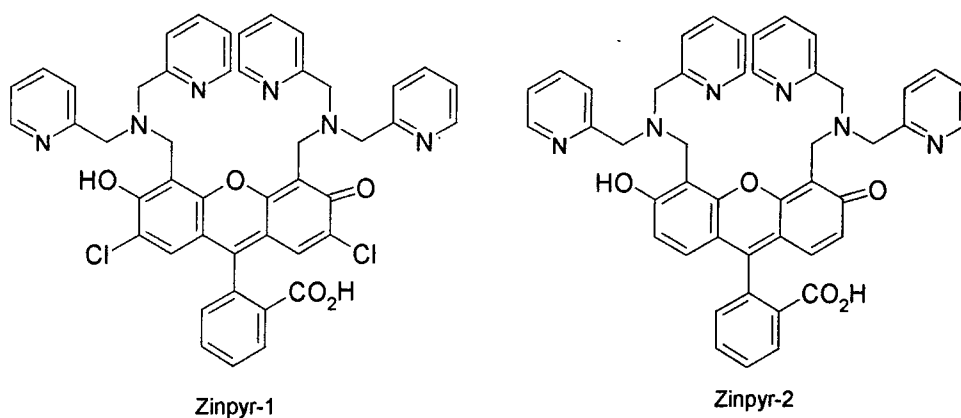
Zinpyr-1   Zinpyr-2

Figure 3.18 - *Fluoroscein based Zn^{2+} sensors*

Zinpyr-1 has an excitation maximum at 515 nm and a quantum yield of 0.39 in the absence of Zn^{2+}. Addition of excess $ZnCl_2$ induces a slight blue shift in the excitation maximum (507 nm) and an increase in the quantum yield to 0.87. The emission maximum also shifts slightly upon Zn^{2+} addition, from 525 nm to 529 nm. Similarly Zinpyr-2 has an excitation maximum at 498 nm, with a quantum yield of 0.25, which shifts to 490 nm accompanied by an increase in the quantum yield to 0.92 upon addition of excess $ZnCl_2$. The emission maximum of free Zinpyr-2 is 518 nm and that of the zinc complex, 513 nm.

3.1.6.3. *The photophysical properties of L^7 and its application as a zinc sensor*

Having discussed the wide range of activities of Zn^{2+} in biological systems, and the range of probes that are currently available for its detection, it is clear that there is a need for improved sensors for the detection of intracellular Zn^{2+}. A discussion of the photophysical properties of zinc complexes of terpyridine now follows, with respect to the potential application of L^7 as a zinc sensor.[10]

Terpyridines are known to possess quite a high affinity for Zn^{2+}, although the 2:1 complexes are kinetically more labile than those of transition metal ions with partially filled d sub-shells such as Fe^{2+}. The luminescence properties of $[Zn(tpy)_2]^{2+}$ were first investigated by Maestri *et al.*(chapter 1, section 1.2) with the complex generated *in situ* by adding an excess of solid $Zn(CH_3COO)_2$ to an acetonitrile or dichloromethane solution of the ligand.[1] In the present instance, addition of Zn^{2+} ions (in the form of zinc triflate) to a solution of L^7 in ethanol-water (9-1) led to the immediate formation of the zinc complex, causing similar effects in the absorbance and emission maxima as the addition of acid, namely a large red-shift (figures 3.19 and 3.20). However, although an accompanying decrease in the fluorescence intensity was observed, the reduction in intensity was to a much lesser extent than that which occurred upon protonation.

Figure 3.19 - *Absorption spectrum of L⁷ in ethanol (black); and L⁷ in the presence of Zn²⁺ (5 equivalents of zinc triflate) (red)*
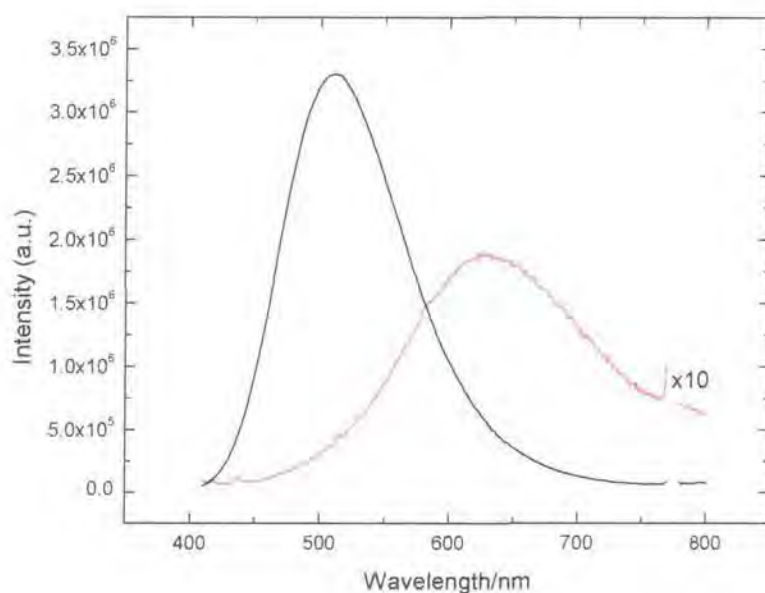
Figure 3.20 - *Corrected fluorescence emission spectra of L⁷ in ethanol (black); and L⁷ in the presence of Zn²⁺ (red) (x10) when excited at the isosbestic point (387 nm)*

That a red-shift is observed for the emission maximum is not surprising, since the positive charge on the metal ion will promote the ICT process from the pendent amine to the terpyridine in an analogous fashion to protonation (figure 3.21). However, the markedly higher emission intensity of the zinc complex is intriguing. It is suggested that this observation is due to the reduction in the efficiency with which the C-C stretching vibrations are able to act as energy accepting modes for deactivation of the

97

excited state, due to the greater rigidity of the zinc complex compared to the diprotonated terpyridine.[30] Upon binding to zinc, there is also less scope for interaction with the solvent, since the nitrogen lone pair electrons are no longer available.
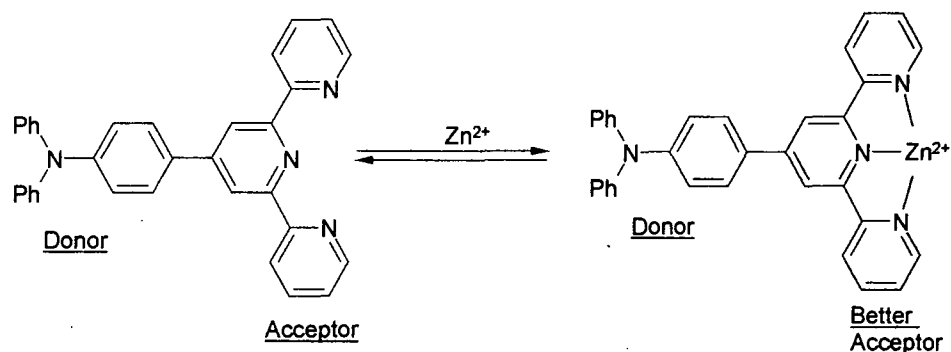
Figure 3.21 - *Stabilisation of the charge-transfer state upon complexation to Zn^{2+}*

The fluorescence was found to respond sensitively to zinc ions with estimates indicating an apparent 2:1 (ligand: Zn^{2+}) association constant of $(4.3\pm0.6) \times 10^9$ dm^6 mol^{-2}. This constant was calculated by measuring the increase in fluorescence intensity at 620 nm for ligand L^1 in ethanol, as a function of added zinc triflate at 293K with λ_{ex}=415 nm. The data obtained was analysed by non-linear least squares fitting to the equation shown in equation 3.1.

$$K_{ass} = \frac{\left(\dfrac{\Delta f}{\Delta f_{max}}\right)}{\left[[Zn^{2+}]_{tot} - \dfrac{\Delta f}{\Delta f_{max}}[L]_0\right]\left(1 - \dfrac{\Delta f}{\Delta f_{max}}\right)^2 [L_0]}$$

Equation 3-1

Δf is the observed change in fluorescence intensity at a given concentration, $[Zn^{2+}]_{tot,}$ of added zinc, Δf_{max} is the hypothetical Δf that would be observed if the ligand were fully complexed, and $[L]_0$ is the concentration of ligand employed.

Experiments carried out to test the effect of other metal ions (at concentrations equal to that required to bring about the maximum response to Zn^{2+}) found that with the single exception of Cd^{2+}, the response to zinc is unique among the metal ions investigated. Cd^{2+} induced similar changes to that of Zn^{2+}, binding significantly more strongly. The addition of calcium and magnesium ions (competing ions when zinc sensors are used in

physiological studies[23]) gave no change in the fluorescence, probably owing to the low affinity of these metal ions for terpyridines. Paramagnetic transition metal ions such as Fe^{2+}, Ni^{2+} and Cu^{2+} led to a quenching of the fluorescence, as did the heavy metal ion Pb^{2+}. However, the quenching response observed for these metal ions was very different to the red-shifting effect observed for Zn^{2+}.

As can be seen in figure 3.20, when monitoring the response of L^7 to Zn^{2+}, although there is a dramatic change in the emission profile, excitation at the isosbestic point actually leads to a net decrease in the intensity at the new maximum (630 nm), owing to the higher emissivity of the ligand and the broadness of its fluorescence band. Fluorescent sensors that respond with decreases in fluorescence intensity are undesirable. On the other hand, the changes in the absorption spectra that accompany formation of the zinc complex are synergistic, such that excitation at 415 nm (close to the absorbance maximum of the zinc complex) allows a 5-fold *increase* in the emission intensity at 630 nm to be achieved. The *ratio* of the emission intensity at 630 nm to that at 513 nm increases by a factor of 12 under these conditions. A wavelength change is preferable to a change in intensity in luminescent sensors, particularly as other metals may quench the emission, since the emergence of a new band at longer wavelength will be diagnostic. The nature of the response to zinc allows the ratio of signals at two emission or excitation wavelengths to be monitored (as opposed to the response to transition metal ions/heavy metal ions, which result in quenching of both bands) a procedure termed ratiometric fluorimetry. This practice is highly desirable in practical sensors, in order to cancel out variations in intensity arising from background changes in the analytical environment.[5]

Similar changes were observed in the absorption/emission spectra of L^6 upon binding to zinc as those observed for L^7 (figures 3.22 and 3.23), however the magnitude of the red-shift was much smaller in this instance. This response, combined with the lower inherent emissivity of L^7, renders this ligand less appropriate for further study as a potential zinc sensor.
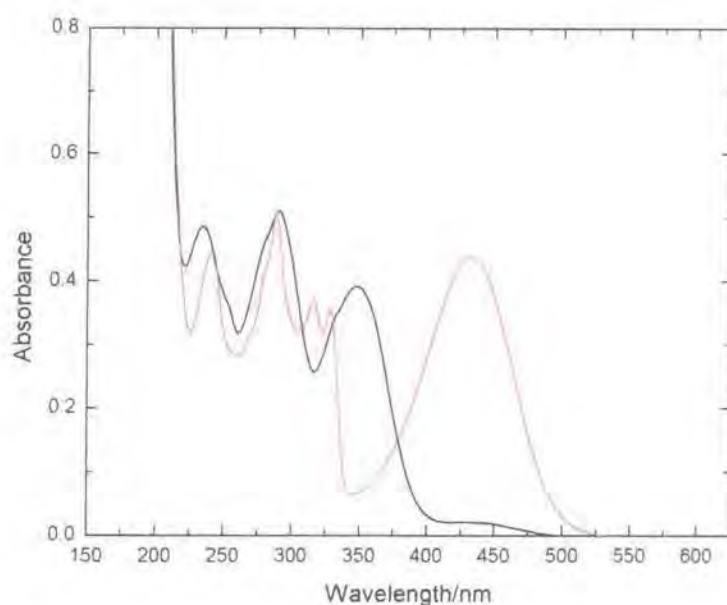
Figure 3.22 - *Absorption spectrum of L^6 in ethanol (black); and L^6 in the presence of Zn^{2+} (5 equivalents of zinc triflate) (red)*
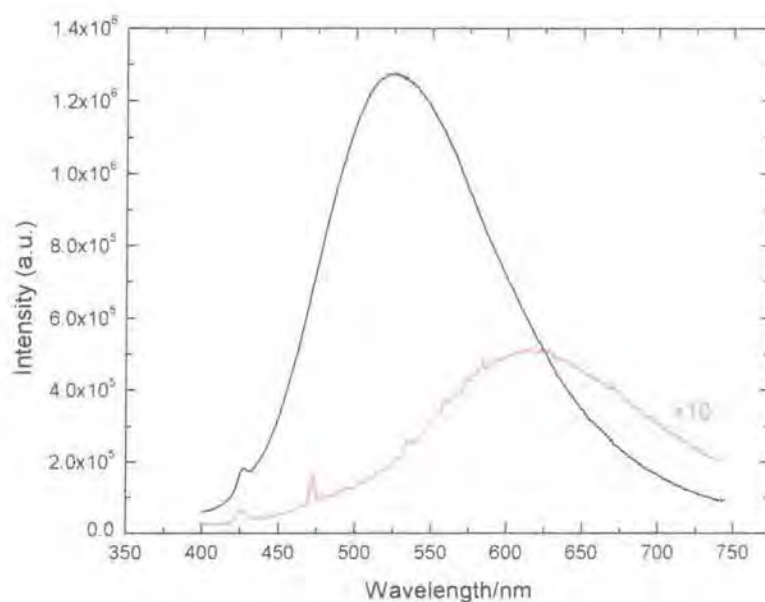
Figure 3.23 - *Corrected fluorescence emission spectra of L^6 in ethanol (black); and L^6 in the presence of Zn^{2+} (red) (x10) when excited at the isosbestic point (378 nm)*

Binding of Zn^{2+} to L^{12} and L^{13} leads to the formation of a new, distinct long wavelength band in the absorption spectrum as opposed to a long tail as was observed upon protonation of these ligands (figures 3.24 and 3.25). However, the emission intensity is

greatly reduced upon binding to Zn^{2+}, as it was upon protonation, giving a weak signal centred around 700 nm.
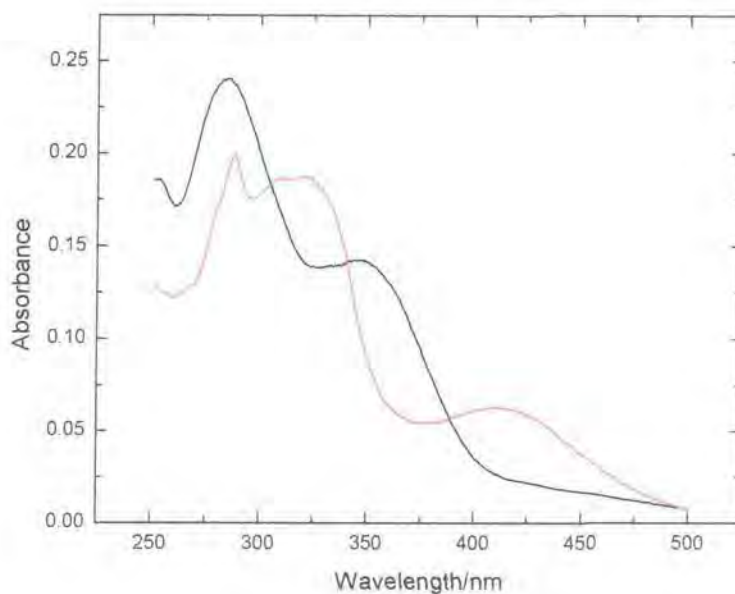
Figure 3.24 - *Absorption spectrum of L^{13} in ethanol (black); and L^{13} in the presence of Zn^{2+} (5 equivalents of zinc triflate) (red)*
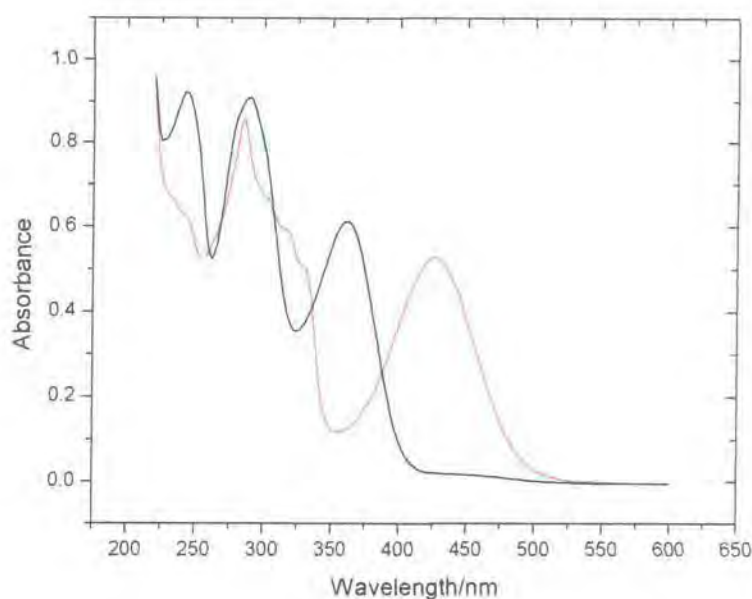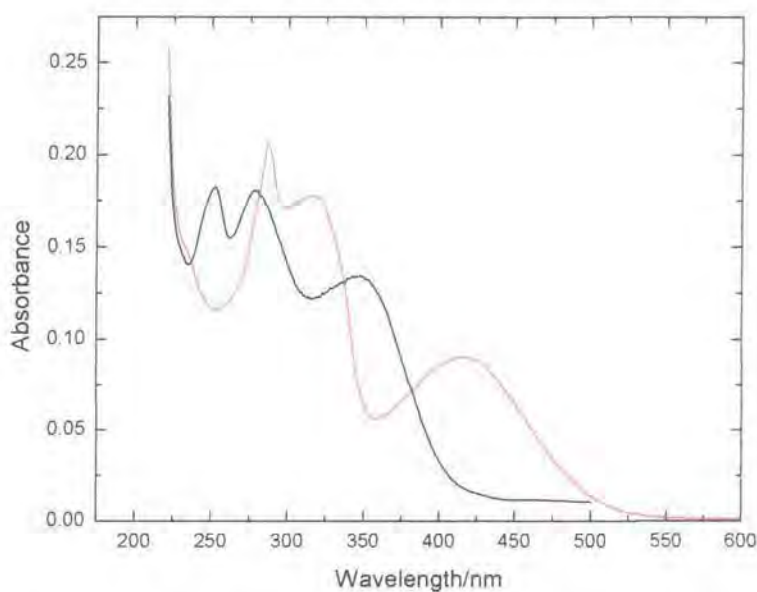

Figure 3.25 - *Absorption spectrum of L^{12} in ethanol (black); and L^{12} in the presence of Zn^{2+} (5 equivalents of zinc triflate) (red)*

Thus, in terms of applications as potential sensory systems for Zn^{2+}, the amino-functionalised ligands L^{12} and L^{13}, incorporating the additional phenyl ring, appear less attractive than L^7.

It is clear that L^7 has several advantages over established zinc sensors described previously, for example a high quantum yield, and excitation and emission wavelengths that are well into the optimal working region for intracellular studies. The luminescent response of this sensor is also completely selective towards Zn^{2+}, with the single exception of Cd^{2+}, with no perturbation in the emission caused by the presence of Mg^{2+} or Ca^{2+}, and a completely different distinguishable response demonstrated in the presence of other transition metals or heavy metals. Crucially, the response of this sensor to the presence of Zn^{2+} differs from those examples discussed previously, as it involves a shift in the maximum wavelength of emission by approximately 130 nm, rather than simply quenching the emission, as well as a large shift in the excitation maximum, allowing the detection of Zn^{2+} through the technique of ratiometric fluorimetry. It should also be noted that although fluorophores with ICT excited states have been considered previously for pH and metal ion sensing,[31] the system described here is very unusual in that the proton or metal ion binds to the moiety that acts as the acceptor (rather than the donor) in the charge transfer process.

The downside, of course, is that a water-soluble analogue would be required in order to allow use in physiological studies. One strategy to achieve this could be the substitution of poly(ethylene glycol) (PEG) chains onto the pendent phenyl rings. PEG offers the advantages of being inert to most chemical reactions as well as enhancing solubility in aqueous solution. In addition, PEG is also acceptable for *in vivo* administration due to its low toxicity.[32] Alternatively, substitution of sodium dodecyl sulphate (SDS) chains could possibly be used to the same effect.

3.2. References

1   G. Albano, V. Balzani, E. C. Constable, M. Maestri, and D. R. Smith, *Inorg. Chim. Acta*, 1998, **277**, 225.

2   A. Sarkar and S. Chakravorti, *J. Lumin*, 1995, **63**, 143.

3   M. Maestri, N. Armaroli, V. Balzani, E. C. Constable, and A. M. W. C. Thompson, *Inorg. Chem.*, 1995, **34**, 2759.

4   K. Araki, T. Mutai, J.-D. Cheon, and S. Arita, *J. Chem. Soc., Perkin Trans.2*, 2001, 1045.

5   *Principles of Fluorescence Spectroscopy*, J. R. Lakowicz, Kluwer Academic/Plenum, New York, 2nd edn, 1999

6   R. A. Bissell, A. P. De Silva, H. Q. N. Gunaratne, P. L. M. Lynch, G. E. M. Maguire, and K. R. A. S. Sandanayake, *Chemical Society Reviews*, 1992, 187.

7   A. J. Bryan, A. P. De Silva, S. A. De Silva, R. A. D. D. Rupasinghe, and K. R. A. S. Sandanayake, *Biosensors*, 1989, **4**, 169.

8   E. Ishow, A. Gourdon, and J.-P. Launay, *J. Chem. Soc., Chem. Commun*, 1998, 1909.

9   N. W. Alcock, P. R. Barker, J. M. Haider, M. J. Hannon, C. L. Painting, Z. Pikramenou, E. A. Plummer, K. Rissanan, and P. Saarenketo, *J. Chem. Soc., Dalton Trans.*, 2000, 1447.

10   W. Goodall and J. A. G. Williams, *J. Chem. Soc., Chem. Commun*, 2001, 2514.

11   *Modern Molecular Photochemistry*, N. J. Turro, University Science Books, Mill Valley, California, 1991

12   S. R. Meech and D. Phillips, *J. Photochem*, 1983, **23**, 193.

13   A. M. Brun, A. Harriman, Y. Tsuboi, T. Okada, and N. Mataga, *J. Chem. Soc. Faraday Trans*, 1995, **91**, 4047.

14   W. Goodall, K. Wild, K. J. Arm, and J. A. G. Williams, *J. Chem. Soc., Perkin Trans. 2*, 2002, 1669.

15   N. N. Greenwood and A. Earnshaw, 'Chemistry of the Elements', Pergamon Press plc, London, 1984.

16   R. H. Prince, *Adv. Inorg. Chem. Radiochem*, 1979, **22**, 349.

17   C. K. Mathews and K. E. Van Holde, 'Biochemistry', Benjamin/Cummings Publishing Company, California, 1996.

18   A. I. Bush, *Curr. Opin. Chem. Biol*, 2000, **4**, 184.

19   N. L. Harrison and S. J. Gibbons, *Neuropharmacology*, 1994, **33**, 935.

20   D. W. Choi and J. Y. Koh, *Ann. Rev. Neurosci*, 1998, **21**, 347.

21   M. P. Cuajungco and G. J. Lees, *Neurobiol. Dis*, 1997, **4**, 137.

22   B. L. Vallee and K. H. Falchuk, *Physiol. Rev*, 1993, **73**, 79.

23   S. C. Burdette and S. J. Lippard, *Coord. Chem. Rev*, 2001, **216-217**, 333.

24   C. J. Frederickson, E. J. Kasarskis, D. Ringo, and R. E. Frederickson, *J. Neurosci. Methods*, 1987, **20**, 91.

25   P. D. Zalewski, I. J. Forbes, and W. H. Betts, *Biochem. J*, 1993, **296**, 403.

26   I. B. Mahadevan, M. C. Kimber, S. F. Lincoln, E. R. T. Tiekink, A. D. Ward, W. H. Betts, I. J. Forbes, and P. D. Zalewski, *Aust. J. Chem*, 1996, **49**, 561.

27   T. Budde, A. Minta, J. A. White, and A. R. Kay, *Neuroscience*, 1997, **79**, 347.

28   T. Koike, T. Watanabe, S. Aoki, E. Kimura, and M. Shiro, *J. Am. Chem. Soc*, 1996, **118**, 12696.

29   T. Hirano, K. Kikuchi, Y. Urano, T. Higuchi, and T. Nagano, *Angew. Chem. Int. Ed. Engl*, 2000, **39**.

30   Y. Sato, M. Morimoto, H. Segawa, and T. Shimidzu, *J. Phys. Chem*, 1995, **99**, 35.

31   J. F. Letard, R. Lapouyade, and W. Rettig, *Pure Appl. Chem*, 1993, **65**, 1705.

32   N. Tirelli, M. P. Lutolf, A. Napoli, and J. A. Hubbell, *Reviews in Molecular Biotechnology*, 2002, **90**, 3.

4. Synthesis of Ir (III)

Bis(terpyridine) Complexes

4.1. Introduction

As discussed in chapter 1, the synthesis of $[Ir(tpy)_2]^{3+}$ was first reported in 1990 by Demas *et al.* following a procedure based on one they had previously published in 1974 for the synthesis of $[Ir(bpy)_3]^{3+}$.[1] Functionalised analogues have since been considered as potential molecular luminescent sensors,[2, 3] and as labels for biological molecules,[4] as discussed in the introduction. The suitability of the $[Ir(tpy)_2]^{3+}$ core to play the role of a photoactive centre, or to act as an electron relay, in linearly arranged multicomponent arrays, has also been investigated, for example as in the porphyrin assembly shown (figure 4.1).[5]
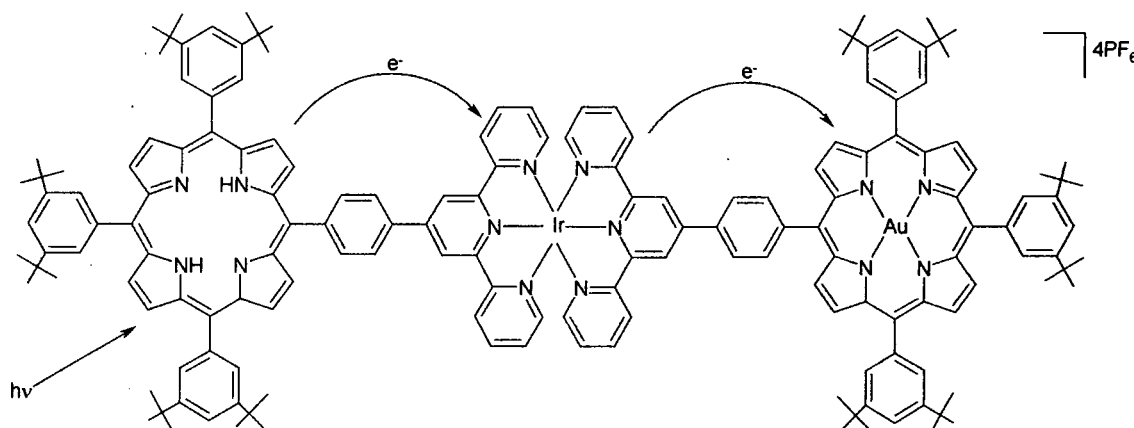
Figure 4.1 – *Structure of Ir (III) based triads*[5]

4.2. Preparation of Bis(terpyridyl) Iridium (III) Complexes using Conventional Methodology

With the exception of Demas' synthesis of $[Ir(tpy)_2]^{3+}$, which was carried out in the melt,[1] bis(terpyridyl) iridium complexes have hitherto been prepared by the sequential reaction of the two terpyridine ligands with $IrCl_3\cdot3H_2O$ in alcoholic solvents.[6] However, there are problems associated with this route, since as a third row transition metal with a low-spin d^6 configuration, the complexation chemistry of Ir (III) is characterised by the inert nature of its coordination sphere with respect to ligand substitution reactions. Although the coordination of the first terpyridine ligand, to form $[Ir(L')Cl_3]$, is relatively straightforward, proceeding in ethanol at reflux for aryl-substituted terpyridines, (and in ethylene glycol at 160°C in the case of tpy itself), the introduction of the second ligand to form $[Ir(L')(L'')]^{3+}$ is more difficult, usually requiring $[Ir(L')Cl_3]$ to be heated with the second ligand in ethylene glycol at reflux.[6]

The high temperatures required to break the Ir-Cl bond also result in cleavage of the Ir-L' bonds, resulting in the formation of "scrambled" homoleptic complexes, $[Ir(L')_2]^{3+}$ and $[Ir(L'')_2]^{3+}$, as side products.

In previous work, it has proved possible to separate the three complexes by column chromatography on silica under highly polar conditions, although the purification can be arduous. In the present study, the synthesis of the heteroleptic complexes shown in figure 4.2 was attempted through reacting the intermediate [Ir(ttpy)Cl₃] with 4'-(4-benzonitrile)-terpyridine or 4'-(4-N,N-dimethylaminophenyl)-terpyridine in ethylene glycol at reflux to form complexes 1 and 2 respectively. Unfortunately, complete separation of the desired heteroleptic complexes from the homoleptic complexes formed as side-products, by column chromatography did not prove possible , neither on silica or alumina. In an attempt to circumvent this scrambling problem, the use of the alternative intermediate, [Ir(ttpy)(CF₃SO₃)₃], in place of [Ir(ttpy)Cl₃], was investigated.[4]
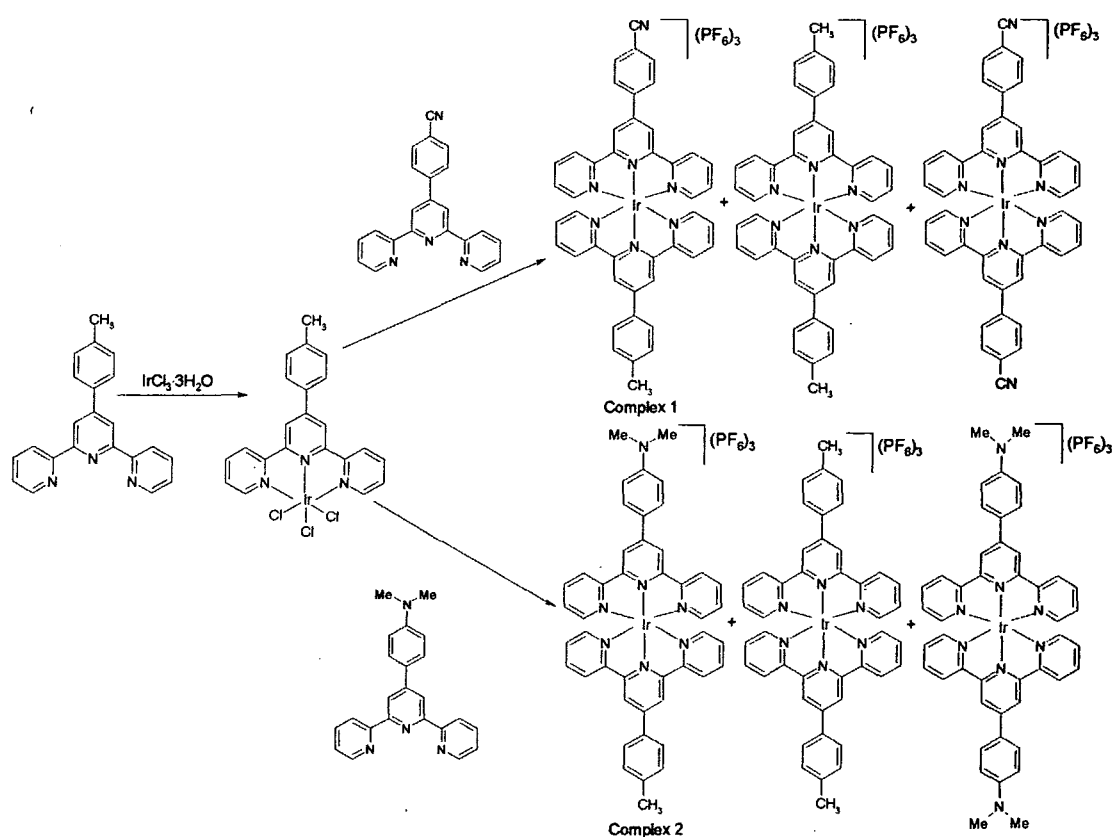
Figure 4.2 – *Synthesis of Ir (III) complexes via conventional methodology*

Lo *et al.* had recently reported higher yields of heteroleptic iridium (III) bis(terpyridine) complexes from the triflate precursor, which may be obtained from [Ir(ttpy)Cl₃] by reaction with trifluoromethanesulphonic acid in refluxing 1,2-dichlorobenzene.[4] It was

anticipated that the complexation of the second terpyridine would take place at lower temperature using the triflate analogue, since the Ir-OTf bond is more labile than the Ir-Cl bond. Unfortunately however, high temperatures were once again required for the complexation reaction, sufficient to cause the formation of significant quantities of the two homoleptic side products, which could not subsequently be separated by column chromatography.

On the other hand, scrambling is clearly not a problem if homoleptic products are sought, since only one ligand is present. The homoleptic complexes 3, 4, 5, and 6 shown in figure 4.3 were all prepared in one step by heating one equivalent of $IrCl_3 \cdot 3H_2O$ with two equivalents of the relevant terpyridine ligand in ethylene glycol at 200°C. Other coloured and often fluorescent side-products were also formed, the identity of which was unclear, but these could be removed by chromatography using a combination of silica and alumina sequentially. Only for complex 3 was purification straightforward, as this complex could be recrystallised from a mixture of acetone and toluene. The photophysical properties of the complexes shown in figure 4.3 are discussed in chapter 5.
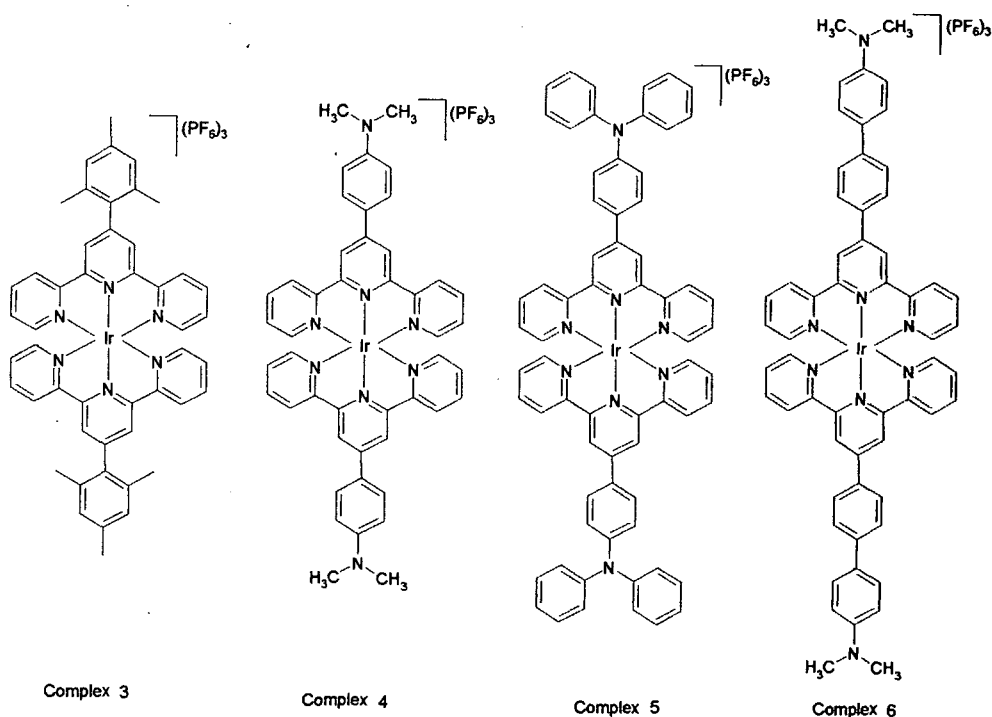
Figure 4.3 – *Homoleptic complexes 3-6 prepared via the conventional route*

4.3. Application of the Suzuki Cross-Coupling Reaction for the Elaboration of Terpyridine Ligands bound to Ir(III)

The difficulties encountered in the formation of Ir (III) bis(terpyridine) complexes through the conventional methodology[6] provided an incentive to investigate new synthetic routes. Motivated by the success of the Suzuki cross-coupling reaction in the preparation of terpyridine ligands, it was anticipated that such cross-coupling reactions could be utilised to couple aryl boronic acids to terpyridine ligands that were already bound to an iridium centre, allowing the formation of more elaborate Ir (III) bis(terpyridine) complexes *in situ*, and under much milder conditions than those required for the initial complexation.

Although cross-coupling reactions have been applied to the elaboration of terpyridine ligands,[7-11] almost no work has apparently been carried out on their application to pre-formed transition metal *complexes*. However, prior work in this laboratory had shown that the Suzuki reaction was successful in allowing an aryl boronic acid to be coupled to a ruthenium complex bearing a bromo-substituted terpyridine ligand (figure 4.4, Route 1).[12]
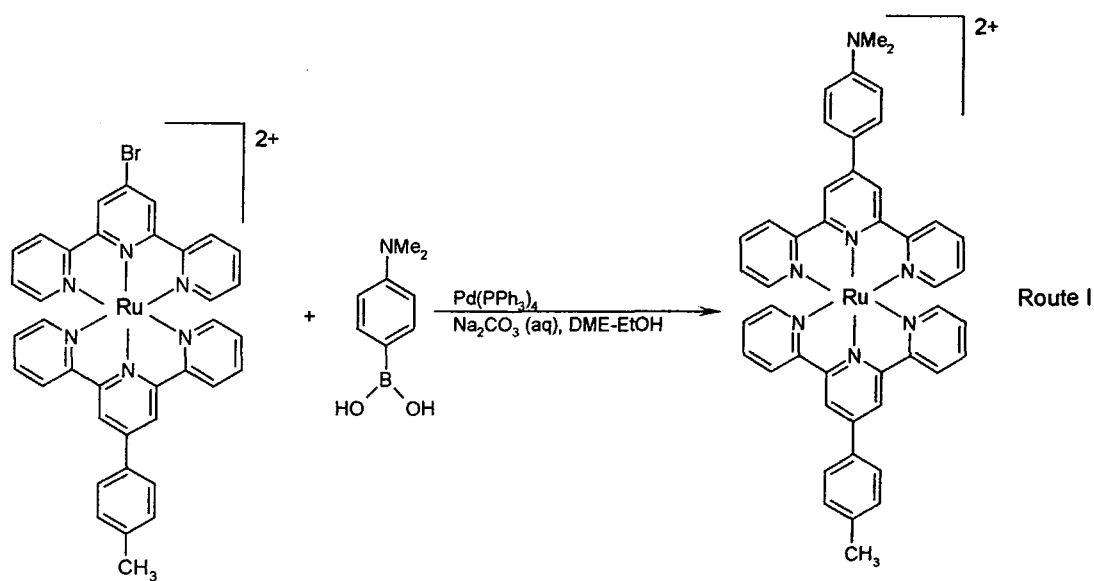
Figure 4.4 – *Palladium catalysed cross-coupling of a ruthenium complex with an aryl boronic acid*[12]

The reverse strategy of coupling an aryl bromide to a ruthenium complex bearing a boronic acid substituted terpyridine ligand was also successful (figure 4.5, Route 2). However, the second route is less attractive as it involves an extra step for the synthesis of the starting ruthenium complex bearing a boronic acid substituted terpyridine, as well as the formation of significant amounts of deboronated material, including $[Ru(ttpy)(tpyPh)]^{2+}$, during the cross-coupling reaction.[12]
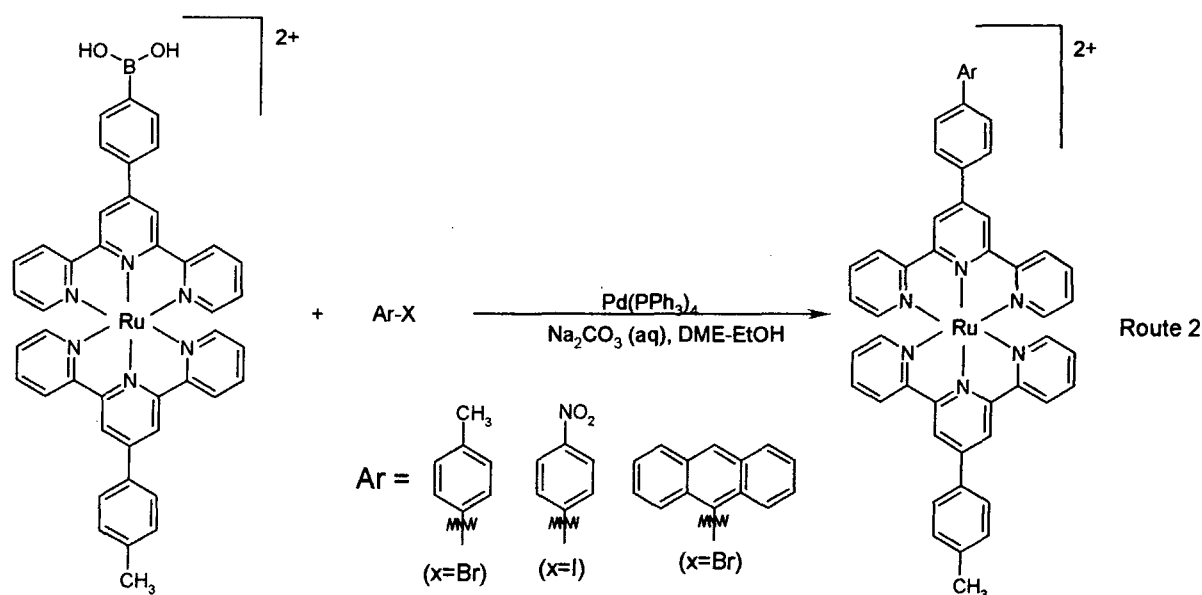
Figure 4.5 – *Palladium catalysed cross-coupling of a ruthenium complex with an arylhalide[12]*

It was the objective of this work to develop the Suzuki cross-coupling reaction for Ir(III) bis(terpyridine) complexes and, as a consequence of the observations made for the ruthenium systems discussed above,[12] it was anticipated that route 1 would be preferable, that is, using the complex shown in figure 4.6 as the metallo-synthon, bearing a bromo-substituted terpyridine ligand to couple to an aryl boronic acid, rather than the second strategy (route 2). The synthesis of this complex was attempted using the conventional methodology discussed in section 4.2.
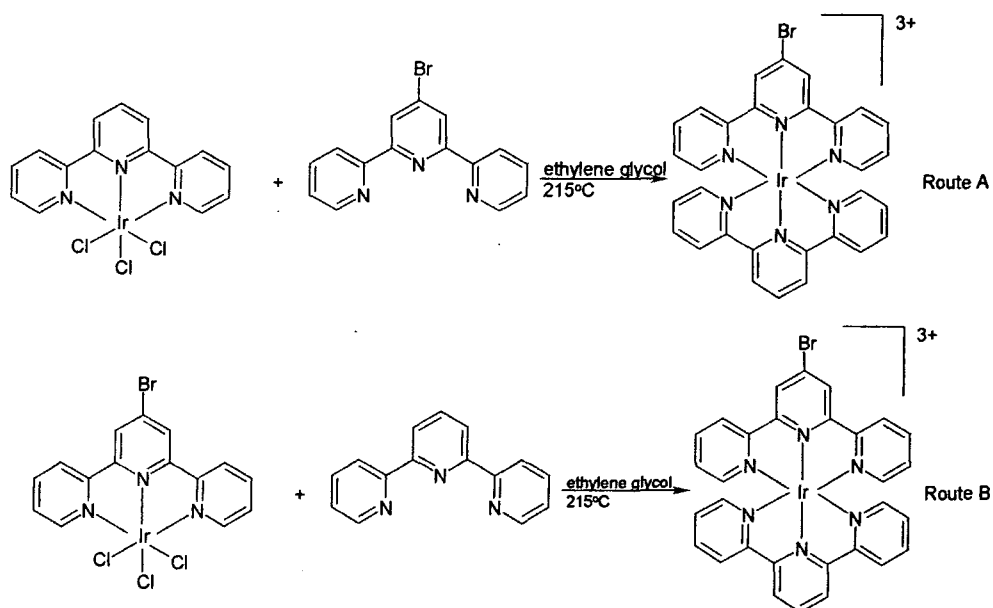
Figure 4.6 – *Synthesis of a bromo-substituted Ir (III) bis(terpyridine) complex to act as a central synthon in the Suzuki cross-coupling reaction*

110

Both intermediates shown in figure 4.6 were prepared using the procedure of Collin *et al.*[6] In each case the appropriate ligand was heated in the presence of IrCl$_3$.3H$_2$O either at 85°C in ethanol, or at 160°C in ethylene glycol for [Ir(tpyBr)Cl$_3$] and [Ir(tpy)Cl$_3$] respectively. In both instances the product precipitated as a red solid during the course of the reaction, and was collected and washed sequentially with toluene, ethanol and finally diethyl ether. Unfortunately, however, reaction of the intermediates through heating in the presence of the appropriate ligand at 215°C in ethylene glycol failed in each case to result in the isolation of the complex. In the case of Route A, ion-exchange of the solution after reaction, upon treatment with KPF$_6$ (aq), resulted in a precipitate which NMR and ESMS analysis revealed did not contain any product. The same procedure for Route B led to a precipitate that was shown, by electrospray mass spectrometry, to contain at least some of the desired product; however, attempted purification using column chromatography failed to allow the isolation of a pure sample.

Following the lack of success achieved through routes A and B, it was concluded that this complex was not a viable central synthon on which to elaborate the bromo-substituted terpyridine ligand by the Suzuki cross-coupling reaction, and investigations into the synthesis of complex 7 as an alternative synthon were made (figure 4.7).
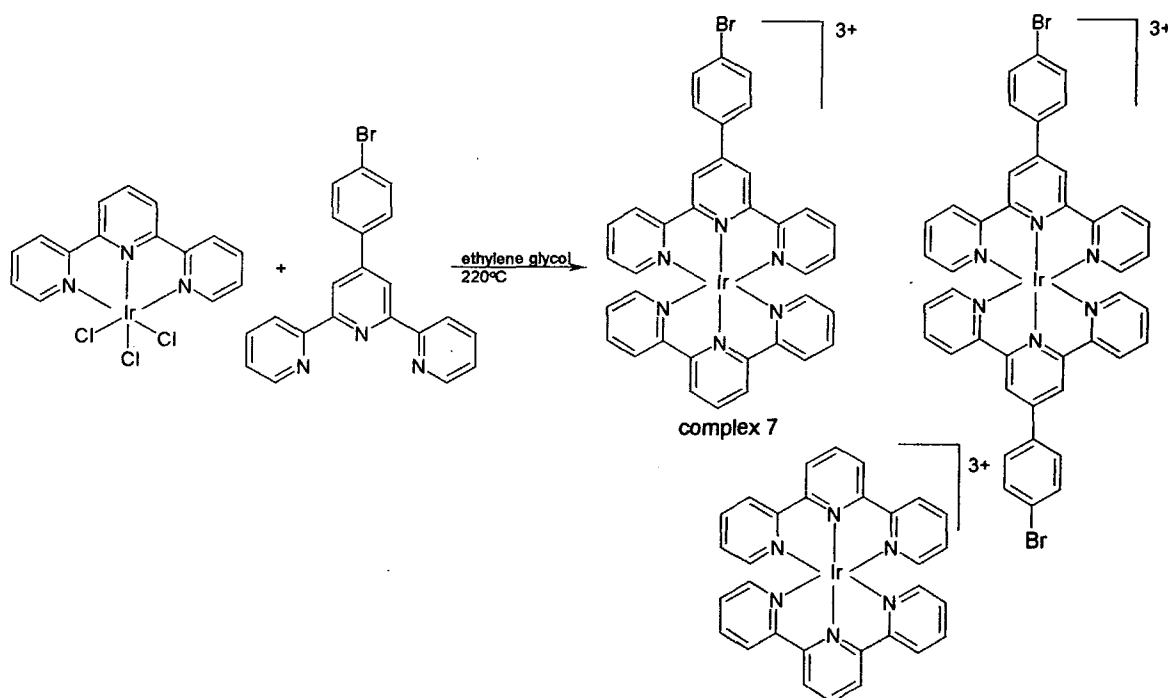
Figure 4.7 – *Synthesis of complex 7 to act as a central synthon for the Suzuki cross-coupling reaction*

The intermediate [Ir (tpy)Cl$_3$] was isolated as discussed previously, and reaction with 4'-(4-bromophenyl)-terpyridine in ethylene glycol at reflux, followed by ion-exchange with KPF$_6$ (aq), led to the crude product as the hexafluorophosphate salt, albeit contaminated with the two homoleptic complexes shown in figure 4.7. However, for this combination of two terpyridine ligands, one containing an aryl pendent ring, and the other being terpyridine itself, the R$_f$ values of the three complexes were significantly different to allow separation to be achieved using column chromatography on silica. [Ir(tpy-φ-Br)$_2$]$^{3+}$ eluted most readily from the column, with significantly more polar conditions being required to elute the desired complex. [Ir(tpy)$_2$]$^{3+}$ did not move from the top of the column under these conditions. Complex 7 was isolated in 60% yield.

Having isolated complex 7, the cross-coupling of this bromo-substituted complex with a range of aryl boronic acids was investigated. Typically, the cross-coupling reactions were carried out by dissolving the boronic acid and the bromo-substituted complex in DMSO (this solvent had been found to give the most satisfactory results in the work carried out on the ruthenium complexes discussed previously,[12] probably since it favours the dissolution of all the reactants), followed by the addition of aqueous Na$_2$CO$_3$ as the base. The solution was then degassed via three freeze-pump-thaw cycles, and the palladium catalyst, Pd(PPh$_3$)$_4$ was added under a positive pressure of nitrogen. The reactions were then heated under an inert atmosphere for 2-12 h as shown in figure 4.8, during which time the progress of the reactions was monitored by TLC. Two different factors may account for the increased rate of reaction observed for the cross-couplings carried out on the complexes, compared to the ligands themselves. Firstly, when the cross-coupling reaction is carried out on a complex, the terpyridine ligand is bound to an Ir (III) ion and therefore will not chelate the palladium from the catalyst. However, during cross-coupling reactions carried out on free ligands, the terpyridine moiety may bind to the palladium catalyst, rendering it inactive. Secondly, the iridium terpyridine moiety bound to the bromophenyl terpyridine ligand acts an electron-withdrawing group, which may accelerate the rate of oxidative addition the Suzuki reaction.[13]
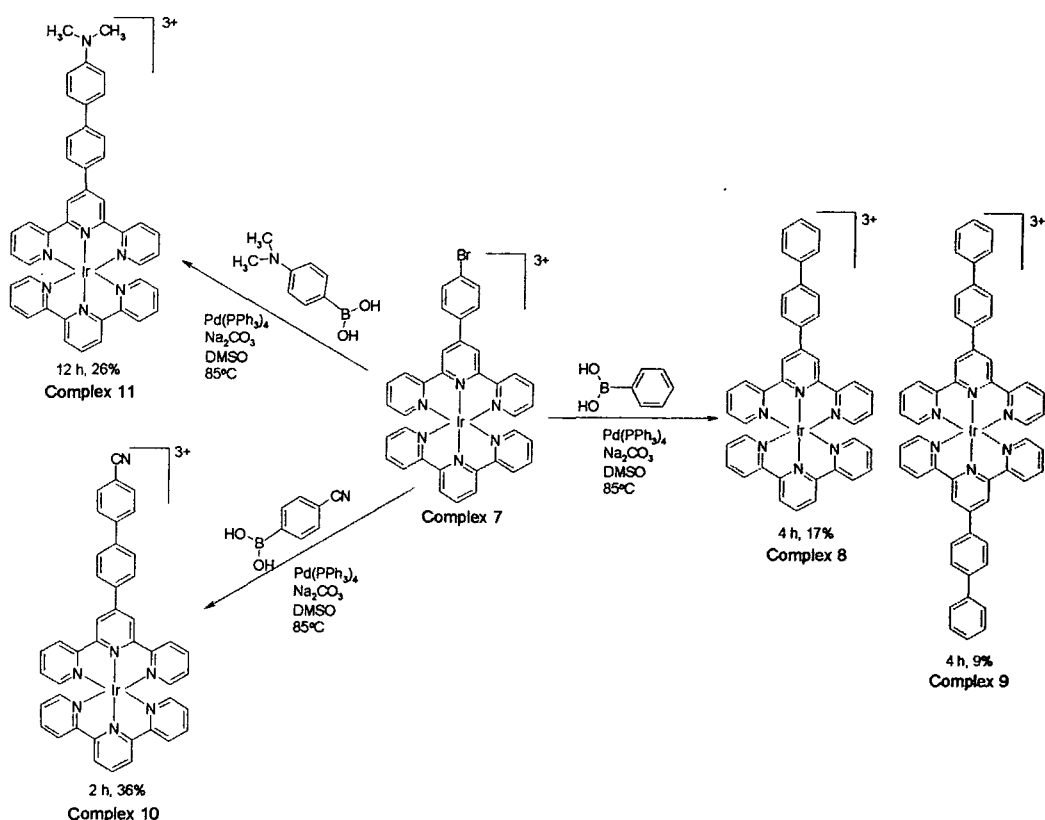
Figure 4.8 – *Suzuki cross-coupling reactions of Ir (III) bis(terpyridine) complexes with aryl boronic acids*

Purification of the complexes following the cross-coupling reaction proved to be straightforward, starting with precipitation of the crude product by dropwise addition of the DMSO reaction mixture into KPF_6 (aq, sat). ^{1}H NMR analysis revealed that the bulk of the crude product was the desired heteroleptic complex, with only trace amounts of the two homoleptic complexes, (for the amino and cyano systems). This is in contrast to the conventional methodology, for which the crude precipitate appeared to consist of much larger proportions of the "scrambled products", as well as the unreacted [Ir(L')Cl₃] starting material, making purification extremely difficult. No doubt facilitated by the greater purity of the crude product following the Suzuki cross-coupling, complexes 8-11 were successfully isolated by column chromatography. In the case of the simple, diphenyl substituted system, the proportion of the homoleptic complex 9 was a little higher and sufficient to allow its isolation from the column.

The formation of the homoleptic side products is remarkable, since isolation of these complexes indicates cleavage of the Ir-N bond, which is surprising given the mild conditions of the Suzuki reaction, which proceeds at 85°C, rather than the high

temperatures around 200°C, that are normally required. It is also worth considering that the complexes showed signs of decomposition if the reactions were left to continue for longer than necessary; such instability is not observed when the complexes are prepared *via* the more harsh reaction conditions of the conventional methodology.[6] The reasons are not certain, but it is possible that under the mildly reducing conditions associated with Pd (0) in the presence of PPh₃, there is some transient reduction of Ir (III) to Ir (I), (possibly favoured by the π^* acceptor nature of the terpyridyl ligands), in which case the rate of ligand substitution reactions will be promoted. The observation that the Ir-N bond is labilised under the conditions of the Suzuki reaction, implies that the Ir-Cl bond may also be more reactive under these conditions, which would allow the formation of complexes from the [Ir(L')Cl₃] intermediate at lower temperatures. To test this hypothesis, the synthesis of [Ir(ttpy)₂]³⁺ was attempted from [Ir(ttpy)Cl₃] and ttpy under the conditions of the Suzuki cross-coupling reaction; i.e. using DMSO as the solvent, aqueous Na₂CO₃ as the base and in the presence of Pd(PPh₃)₄ as the catalyst. The system was degassed before heating at 85°C under nitrogen for five days. However, TLC analysis of the reaction mixture throughout this time revealed the presence of large quantities of starting material, and only a very small amount of a fluorescent product, indicating that the Ir-Cl bond is not affected in the same way as the Ir-N bond under cross-coupling conditions.

In order to allow a direct comparison of the coupling methodology with the conventional route, the synthesis of complex 10 was attempted *via* the latter, by heating a mixture of [Ir(tpy)Cl₃] with 4'-(4'-cyanobiphen-4-yl) phenyl-terpyridine in ethylene glycol at 215°C for 20 minutes. Once again, the crude product contained a mixture of the desired product, the two homoleptic complexes, and a small amount of unreacted [Ir(tpy)Cl₃] starting material. Purification was considerably more difficult than in the preparation of the same complex made *via* the Suzuki reaction, due to the lower degree of purity of the crude product; however, it was isolated in 43% yield after column chromatography.

In conclusion, although the isolated yield of complex 10 obtained *via* the normal methodology was comparable to that obtained *via* the Suzuki methodology, the smaller proportion of side-products, and hence ease of purification of the product, following the Suzuki cross-coupling reaction suggests that it can provide a potentially useful improved methodology for the synthesis of Ir(III) bis(terpyridine) complexes under mild conditions.

4.4. ¹H NMR Characteristics of Ir (III) Bis(terpyridine) Complexes

Complex	H³'	H⁴'	H³	H⁴	H⁵	H⁶	Hᵇ	Hᵃ	Hᵇ'	Hᵃ'	Other
3	9.16 s	-	9.02 d 8.0	8.39 td 8.0	7.66 ddd 8.0	8.21 d 4.0	-	7.19 s	-	-	2.36, s CH₃ 2.42, s CH₃
4	9.42 s	-	9.14 d 7.5	8.37 td 5.0, 1.5	7.63 td 5.0, 1.5	8.31 d 9.5	8.28 d 5.0	7.05 d 10.0	-	-	-
5	9.42 s	-	9.10 d 8.0	8.33 td 5.0, 1.0	7.60 td 5.0	8.21 d 6.0	8.24 d, 9.0 7.45 m	8.24 d, 9.0 7.45 m	-	-	7.45 m p-Ph 7.26 m o-/m-ph
6	9.22 s	-	8.85 d 8.0	8.34 td 7.5	7.60 t 7.0	7.81 d	8.15 d 8.0	8.38 d 8.0	7.87 d 8.0	7.02 d 8.5	-
7	9.05 s (Br-φ-tpy) 8.86, d 8.5 (tpy)	8.77 t 8.5	8.70,d 8.0 (Br-φ-tpy) 8.59, d 8.0 (tpy)	8.21 td (both ligands)	7.48 m (both ligands)	7.68, d 5.5 (tpy or Br-φ-tpy) 7.59, d 5.5 (tpy or Br-φ-tpy)	8.12 d 8.5	7.98 d 8.5	-	-	-
8	9.13,s (Ph₂tpy) 8.86, d 8.0 (tpy)	8.78 t 8.0	8.73,d 8.0 (Ph₂tpy) 8.59, d 8.0 (tpy)	8.22 td (both ligands)	7.49 m (both ligands)	7.70,d 5.5 (Ph₂tpy) 7.59,m (tpy)	8.33 d 8.0	8.10 d 8.5	7.87 d 7.5	7.59 m	7.49 m p-Ph
9	9.14 s	-	8.75 d 8.0	8.25 td 8.0	7.51 m	7.73 d 5.0	8.34 d 8.5	8.10 d 8.0	7.87 d 7.0	7.59 t 7.5	7.51, m p-Ph
10	9.13 s (CNPh₂tpy) 8.86,d 8.0 (tpy)	8.78 t 7	8.73, d 8.0 (CNPh₂tpy) 8.59, d 8.0 (tpy)	8.23 td (both ligands)	7.49 m (both ligands)	7.69, d 6.0 (CNPh₂tpy or tpy) 7.59, d 4.5 (CNPh₂tpy or tpy)	8.35 d 8.5	8.14 d 8.5	8.02 d 8.5	7.95 d 8.5	-
11	9.11 s (Me₂Ntpy) 8.86, d 8.0 tpy	8.77 t 7.5	8.73, d 8.0 (Me₂Ntpy) 8.59, d 8.0 (tpy)	8.21 td (both ligands)	7.48 m (both ligands)	7.70, d 5.5 (tpy or Me₂NPh2tpy) 7.59, d 5.5 (tpy or Me₂NPh2tpy)	8.27 d 8.5	8.04 d 8.5	7.76 d 8.5	6.91 d 8.5	3.06 s CH₃

Table 4.1 – *¹H NMR data for complexes 3-11. All spectra acquired in CD₃CN at 500 MHz δ in ppm relative to residual CD₃CN at 1.95 ppm; J in Hertz.*

^{1}H NMR data for complexes 3-11 are presented in table 4.1. Full assignment of the spectra was made through consultation of the splitting patterns, coupling constants, ^{1}H-^{1}H COSY and ^{1}H-^{1}H NOESY spectra. As for the ligands, the assignment was aided by the occurrence of repeating patterns in the chemical shift values, splitting patterns and coupling constants in the resonances of the lateral pyridine rings (H^2, H^3, H^4, H^5) and the central pyridine ring ($H^{3'}$) throughout the series of Ir (III) bis(terpyridine) complexes. The effect of the conformational and electronic changes, which occur upon coordination of the ligand, on the ^{1}H chemical shifts, was aided by comparison with results obtained with Ru (II) complexes of 4'-substituted terpyridines, in a study carried out by Constable and Cargill-Thompson.[14]

Consultation of the data collected for the unsymmetrical complexes 7-11 reveals that the chemical shifts of the resonances assigned to a particular ligand are almost completely independent of the nature of the other ligand. For example, in complexes 7, 8, 9, 10 and 11 the chemical shift values of $H^{3'}$, H^3 and H^6 for the tpy ligand are the same, apparently completely unaffected by the substitution of different ligands on the other side of the complex. This is an intriguing observation, since it implies that the 4'-substituents in the terpyridine ligands have little effect on the electron density at the metal. A similar independence of the two ligands in NMR has been observed in heteroleptic ruthenium (II) complexes.[14]

Figures 4.9 and 4.10 display the changes inherent in the NMR spectra upon complexation of the free ligand to iridium, exemplified by complex 4. It is notable that without exception, the resonances of the central and lateral pyridine rings follow the same pattern throughout the range of complexes i.e. $H^{3'}$ has the highest chemical shift value, followed by H^3, H^4, H^6 and finally H^5, a trend also found in the ruthenium systems.[14]
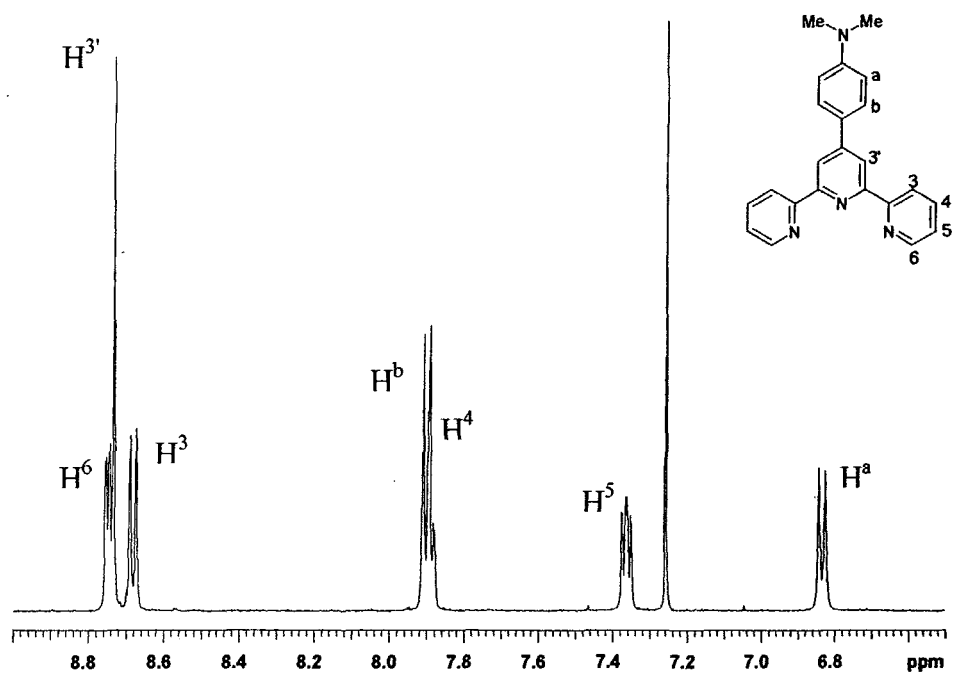
Figure 4.9 – *NMR spectrum of Me₂Nphtpy ligand before complexation to form complex 4*
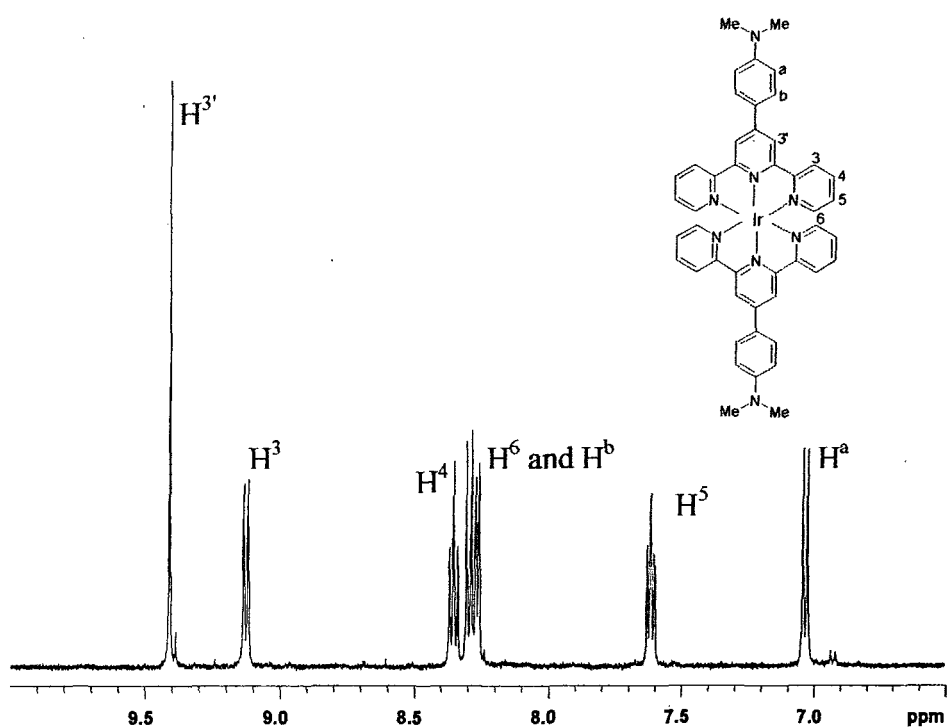
Figure 4.10 –*NMR spectrum of complex 4*

Figures 4.9 and 4.10 reveal that upon complexation, a downfield shift is observed for all signals (except H^6) in response to the effect of the positively charged metal ion in the complex. However, it is noteworthy that the downfield shift experienced by H^3 upon coordination may also be attributed to deshielding by $H^{3'}$, and is a direct consequence of the change from a transoid to a cisoid configuration about the interannular C-C bonds upon coordination, as well as the influence of the positively-charged metal ion in the complex. However, in both the iridium systems observed for this work, and the ruthenium systems, a similar shift is associated with H^4 upon coordination. It has been suggested that this is a consequence of induced charge and π cloud perturbation experienced by the ligand upon coordination,[14] an effect that may also explain the smaller downfield shift experienced by H^5. The change in the chemical shift value of H^6, in the opposite direction to H^3, is explained by the fact that the former is positioned in space in the shielding region associated with the central pyridine ring of the *other* ligand. The most notable downfield coordination shifts are associated with $H^{3'}$, located on the central pyridine ring. It is likely that it is the interaction with the metal, which is greater at the central ring than the terminal rings, that is the origin of this. (Unfortunately, no structural data exists for the complexes discussed in this work, however, X-ray structural data obtained for $[Ir(tpy)_2]^{3+}$ reports the Ir-N average bond lengths are 1.980 Å for the central pyridine ring and 2.056 Å for the peripheral cycles[6]). The resonance of $H^{3'}$ is also the most variable, being affected to a larger extent by the nature of the substituent on the terpyridine ligands. Finally, it is noteworthy that only H^6 experiences an upfield coordination shift. Once again this was observed in the ruthenium systems, and probably represents the fact that the expected downfield shifts resulting from the positive charge building up on coordination are more than outweighed by the shielding of the proton as it lies over the nearby pyridine ring.

4.5. References

[1] N. P. Ayala, C. M. Flynn, Jr., L. Sacksteder, J. N. Demas, and B. A. Degraff, *J. Am. Chem. Soc*, 1990, **112**, 3837.

[2] M. Licini and J. A. G. Williams, *J. Chem. Soc., Chem. Commun*, 1999, 1943.

[3] W. Goodall and J. A. G. Williams, *J. Chem. Soc., Dalton Trans.*, 2000, 2893.

[4] K. K.-W. Lo, C.-K. Chung, D. C.-M. Ng, and Zhu.N, *New J. Chem*, 2002, **26(1)**, 81.

[5] L. Flamigni, F. Barigelletti, N. Armaroli, J.-P. Collin, I. M. Dixon, J.-P. Sauvage, and J. A. G. Williams, *Coord. Chem. Rev*, 1999, **190-192**, 671.

[6] J.-P. Collin, I. M. Dixon, J.-P. Sauvage, J. A. G. Williams, F. Barigelletti, and L. Flamigni, *J. Am. Chem. Soc*, 1999, **121**, 5009.

[7] I. M. Dixon, J.-P. Collin, J.-P. Sauvage, F. Barigelletti, and L. Flamigni, *Angew. Chem. Int. Ed.*, 2000, **39**, 1292.

[8] J.-C. Chambron, C. Coudret, and J.-P. Sauvage, *New J. Chem*, 1992, **16**, 361.

[9] K. T. Potts and D. Konwar, *J. Org. Chem.*, 1991, **56**, 4815.

[10] A. Harriman, M. Hissler, A. Khatyr, and R. Ziessel, *J. Chem. Soc., Chem. Commun*, 1999, 735.

[11] W. Goodall, K. Wild, K. J. Arm, and J. A. G. Williams, *J. Chem. Soc., Perkin Trans. 2*, 2002, 1669.

[12] C. J. Aspley and J. A. G. Williams, *New J. Chem*, 2001, **25**, 1136.

[13] N. Miyaura and A. Suzuki, *Chem. Rev.*, 1995, **95**, 2457.

[14] E. C. Constable, A. M. W. Cargill Thompson, D. A. Tocher, and M. A. M. Daniels, *New J. Chem*, 1992, **16**, 855.

5. Photophysical Properties of

Ir(III) Bis(terpyridine) Complexes

5.1. Introduction

As discussed in chapter 1, $[Ir(tpy)_2]^{3+}$ is luminescent, as are analogues with simple aryl substituents at the 4'-position. Studies to date have assigned their relatively intense and long-lived emission to predominantly ligand centred, $(^3\pi\pi^*)$ states, with possibly some small admixture of MLCT character.[1-4]

This chapter discusses the photophysical properties of the new Ir (III) bis(terpyridine) complexes prepared as described in the preceding chapter, and summarised in figure 5.1.
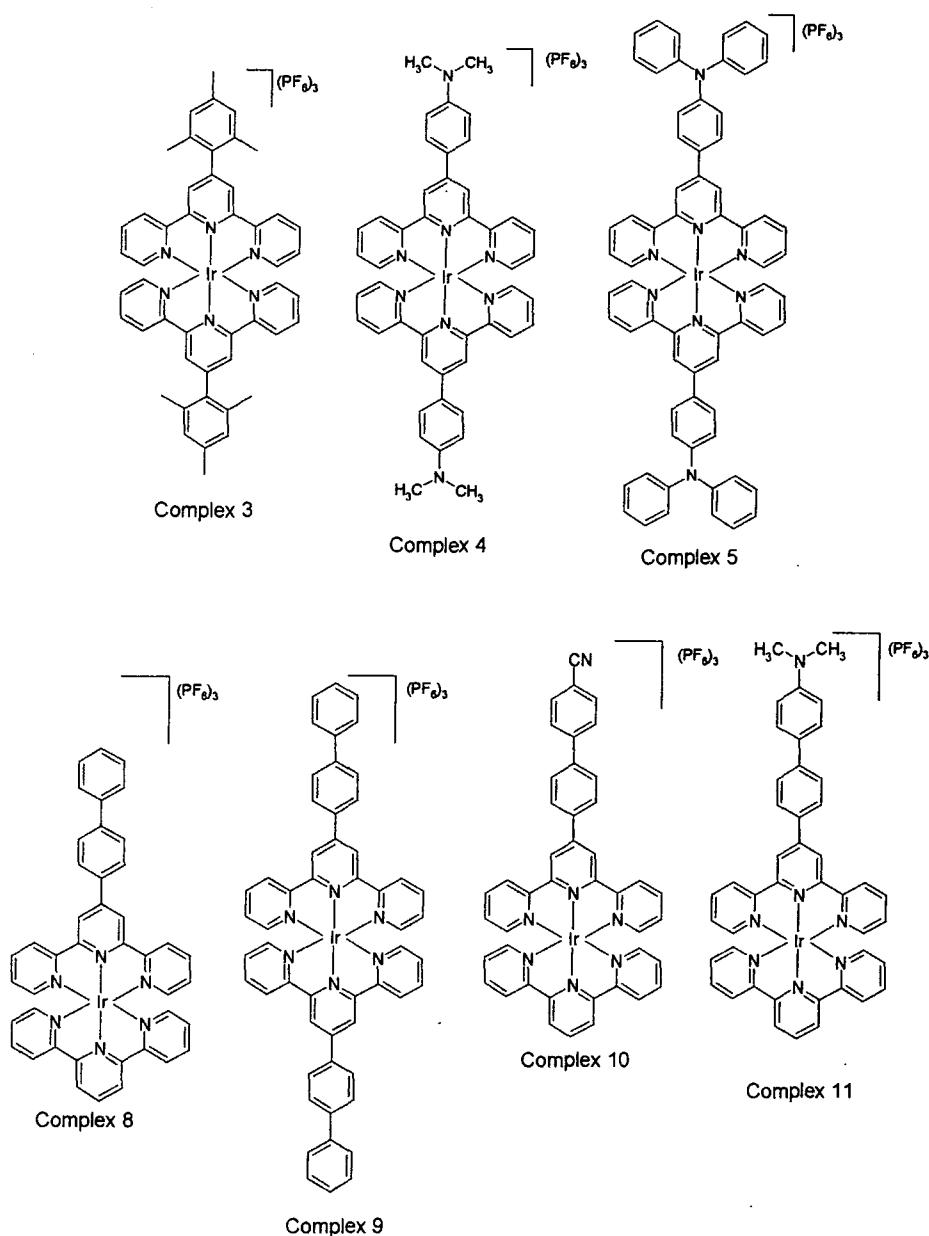
Figure 5.1 – *Ir (III) bis(terpyridine) complexes discussed in this chapter*

5.2.   Ground State Absorption Spectroscopy

5.2.1. Complexes 3, 8, 9, 10

The ground state absorption spectra of complexes 3, 8, 9 and 10 are displayed in figure 5.2, and the absorption maxima and extinction coefficients of the four complexes in both acetonitrile and water are given in table 5.1.
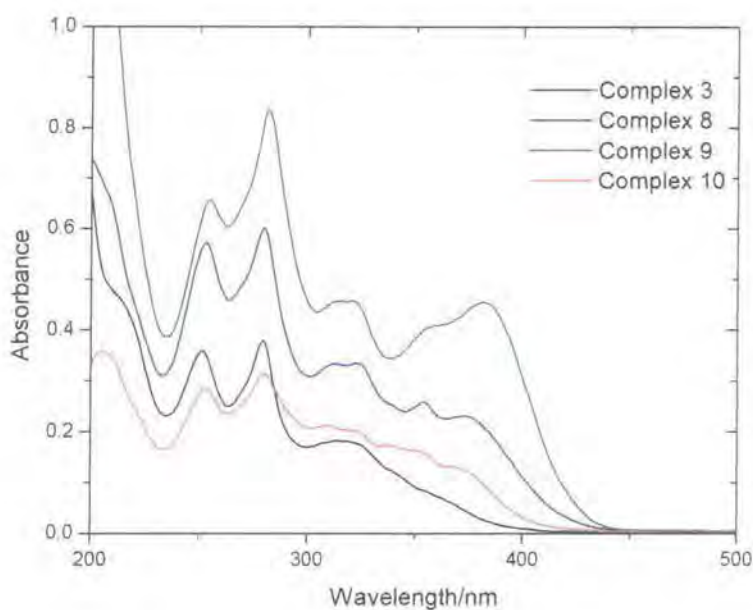
Figure 5.2 – *Absorption spectra of complexes 3, 8, 9 and 10 in water*

	Complex 3	Complex 8	Complex 9	Complex 10
		253 (40,700)	255 (70,900)	252 (43,200)
H$_2$O	251 (34,300)	280 (45,600)	282 (85,400)	279 (49,400)
λ_{max} (abs)/nm	280 (35,600)	317 (23,700)	321 (49,300)	316 (31,000)
ε (mol^{-1} dm^3 cm^{-1})	315 (16,800)	354 (18,000)	361 (41,700)	344 (25,500)
		375 (16,100)	381 (44,300)	367 (21,300)
		253 (42,700)	255 (78,200)	253 (68,300)
CH$_3$CN	250 (20,300)	280 (46,000)	282 (95,600)	280 (76,200)
λ_{max} (abs)/nm	280 (20,000)	317 (24,200)	318 (56,300)	316 (48,600)
ε (mol^{-1} dm^3 cm^{-1})	315 (10,200)	354 (19,100)	364 (50,200)	344 (39,700)
		375 (17,200)	380 (52,500)	367 (32,100)

Table 5.1 – *Absorption data for complexes 3, 8, 9 and 10*

All of the complexes are yellow or pale yellow, with strong absorption bands in the ultraviolet region tailing slightly into the visible. The large extinction coefficients of 10^4-10^5 M^{-1} cm^{-1} are consistent with predominantly ligand centred transitions. Complex 9 has the largest extinction coefficient, consistent with the fact that it has the largest number of aromatic rings and the most extended conjugation, whilst the values for complex 3 are significantly smaller, indicative of a less conjugated system (see below). The extent of conjugation also explains the energy onset, with that of the mesityl complex at highest energy, and complex 9 at marginally the lowest energy, compared to complexes 8 and 10.

The absorption tail on the low energy side of the spectra was noted previously in the work of Sauvage et al.,[1] on monoaryl-substituted complexes, and was assigned in principle to (i) contribution from low-energy metal to ligand charge transfer (^{1}MLCT) transitions, which are expected to correspond to absorption around 387 nm or below, calculated from Ir (III) / Ir (IV) oxidation potential and the tpy ligand reduction potential, (ii) formally forbidden transitions leading to direct population of triplet levels (S$_0$→T) due to the heavy atom effect, (iii) population of metal-centred (^{1}MC) levels, or (iv) conjugation effects due to the aryl group borne on the 4'-position of the tpy nucleus. Given that the low energy absorption tail was less pronounced for [Ir(tpy)$_2$]$^{3+}$ than the other complexes, which were substituted with an aryl ring at the 4'-position of the terpyridine nucleus, the fourth possibility seems the most convincing. In the present study, it is interesting that the tail is less pronounced for complex 3, where the pendent aryl group is not conjugated with the rest of the tpy ligand, due to the degree of twisting induced by the ortho-methyl substituents of the pendent mesityl group increasing the torsion angle between the pendent aryl group and the central pyridine ring. In fact, the spectrum is very similar to that of [Ir(tpy)$_2$]$^{3+}$ itself, strongly suggesting therefore that the low energy maxima and long wavelength tails in the other complexes are a direct consequence of additional conjugation at the 4'-position.

5.2.2. Complexes 4, 5 and 11

The ground state absorption spectra of complexes 4, 5 and 11 are shown in figure 5.3, with the extinction coefficient for each band given in table 5.2.
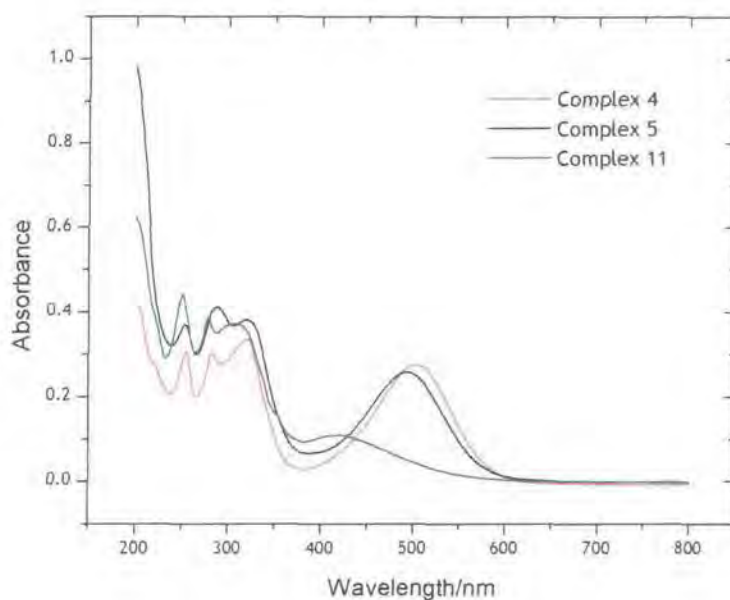
Figure 5.3 - *Absorption spectra of complexes 4, 5 and 11 in water*

	Complex 11	Complex 4	Complex 5
H₂O λ_{max} (abs), ε (mol⁻¹ dm³ cm⁻¹)	251 (35,000)	255 (25,700)	253 (39,200)
	278 (30,600)	283 (26,300)	287 (44,500)
	310 (29,800)	321 (27,600)	321 (40,900)
	420 (8,700)	510 (20,400)	494 (26,000)
CH₃CN λ_{max} (abs), ε (mol⁻¹ dm³ cm⁻¹)	251 (38,100)	255 (49,000)	253 (48,800)
	278 (29,600)	283 (48,000)	288 (54,800)
	322 (31,700)	321 (53,300)	321 (50,600)
	476 (9,400)	503 (44,800)	494 (35,100)

Table 5.2 - *Absorption data for complexes 4, 5 and 11*

The region of the spectrum between 250-350 nm is similar to that obtained for complexes 3, 8, 9 and 10, but a striking difference in complexes 4, 5 and 11 is the occurrence of a long wavelength band centred around 400-500nm. This is visibly apparent in the orange (complex 11) or deep red (complexes 4 and 5) colours of these complexes, compared to the pale yellow colours of complexes 3, 8, 9 and 10. This well-defined band in complexes 4, 5 and 11 is attributed to an intraligand charge transfer transition, in which the amino group of the pendent ring acts as an electron donor, and the metal bound terpyridyl moiety as an electron acceptor. The occurrence of such transitions in the free ligands has already been discussed in chapter 3, where it was suggested that the incorporation of the electron-donating amino group raises the energy of the π_{Ph} to a level higher than that of the π_{tpy}, resulting in an ICT transition (π_{Ph}-π_{tpy*}) rather than a LC transition (π_{tpy}-π_{tpy*}).[2] The free ligands display ILCT bands around 350 nm which, as described in chapter 3, are red-shifted upon complexation to zinc ions owing to the increased acceptor properties of the tpy π^* orbitals upon coordination to the positively-charged metal ion. A red-shift of similar or greater magnitude is to be expected upon binding to iridium (III) and, indeed, a similar low energy band has been reported in the iridium chloro complex [IrLCl$_3$] {L= 4'-(p-Bu$_2$N-C$_6$H$_4$-tpy)}.[5]

In the case of complex 11, further support for the ILCT assignment comes from the substantial red-shift (50 nm) of this band observed in acetonitrile compared to water (figure 5.4).
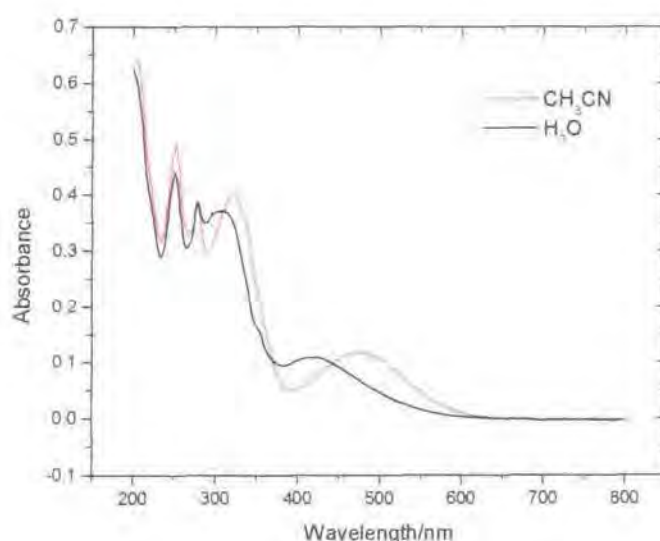
Figure 5.4 – *Red-shift observed in the ILCT band of complex 11 on changing solvent from H$_2$O (black) to CH$_3$CN (red).*

This negative solvatochromic behaviour is indicative of a polar ground state and a less polar excited state, and of a charge-transfer axis that lies colinear with the dipole axis.[6] On the other hand, for the homoleptic complexes 4 and 5, only a very weak, positive solvatochromism is observed in the corresponding absorption band. In these complexes, there is no permanent dipole moment in the ground state, and the formation of the ILCT excited state will be accompanied by, at most, a small increase in the polarity of the system.[6]

Upon acidification of complexes 4 and 11, the colour changes from orange/red to almost colourless, and the ILCT band disappears (figure 5.5). This is the result of protonation of the amino group preventing it acting as a donor in the ILCT process, and is in marked contrast to the behaviour of the free ligands, where a red-shift of the corresponding band was observed upon acidification, owing to protonation of the terpyridyl moiety. Clearly, in the complex, the terpyridyl nitrogens are not available for protonation leaving only the NMe_2 unit accessible. A pH titration in aqueous solution, obtained by monitoring the absorbance at 420 nm, gave an inflection point at 3.8 for complex 11, significantly lower than the pK_a of N, N-dimethylaniline (5.2) (which could be regarded as a simple organic model for comparison). This reduced basicity of the amine can be attributed to the presence of the electron withdrawing metal-terpyridyl fragment in direct conjugation with it, and the fact that protonation will be inhibited by the +3 charge on the complex; (related pyridyl-appended complexes display a comparable reduction in pK_a relative to pyridine).[3] The validity of the former argument is evident from the observation that complex 4, which has no interposed phenyl ring between the terpyridyl fragment and the dimethylaniline unit, is significantly less basic than complex 11 (by 1.3 units; see plots in figure 5.6)
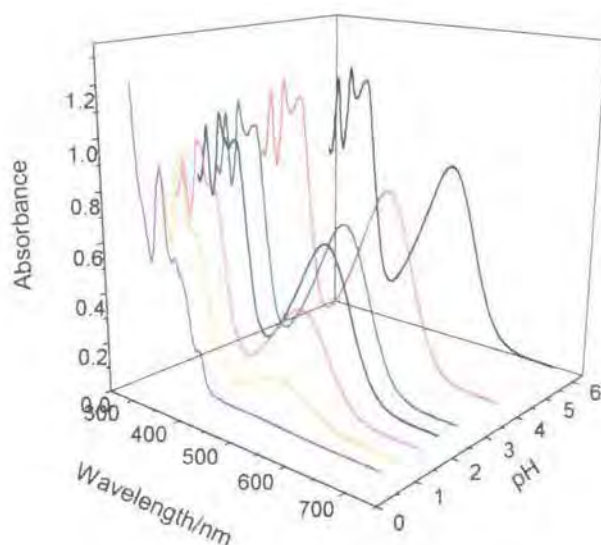
Figure 5.5 – *Effect of protonation on the ILCT band in the absorption spectrum of complex 11*
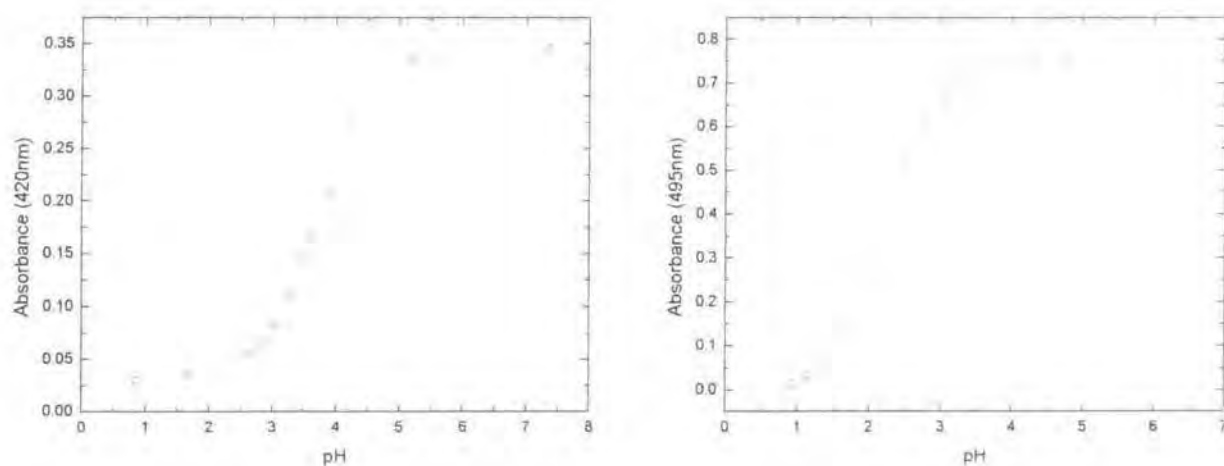
Figure 5.6 – *A pH titration profile obtained in aqueous solution for complex 11 (left) showing an inflection point of 3.8, and for complex 4 (right) with an inflection point of 2.5.*

Finally, the spectrum of complex 5 is unchanged upon acidification, as expected given the fact that triphenylamine is not basic ($pK_a\sim-5$), in contrast to dimethylaniline.

5.3. Emission Properties of Complexes 3, 8, 9 and 10

As discussed in section 5.1, previous investigations have assigned the emission from Ir (III) bis(terpyridine) complexes as predominantly ligand centred, with possibly some MLCT character.[1, 3, 4, 7, 8] These studies have reported highly structured emission from $[Ir(tpy)_2]^{3+}$ in solution at room temperature,[1, 7] whilst the introduction of aryl rings into the 4'-position of the ligands leads to a red-shift and a rather less structured spectrum, which has been interpreted in terms of the effect of enhanced conjugation on the ^3LC state.[1, 7] Table 5.3 summarises the photophysical properties of complexes 3, 8, 9 and 10.

	Complex 3	Complex 8	Complex 9	Complex 10
λ_{max} (em)/nm H₂O	457	571	587	553 584
λ_{max} (em)/nm CH₃CN	494	578	572	547 581
λ_{max} (em)/nm at 77K [b]	461, 494, 532	517, 546 (sh), 604 (sh)	524, 557, 607 (sh)	514, 546 (sh), 604 (sh)
φ (H₂O) [c]	0.0068	0.0051	0.0014	0.0035
φ (CH₃CN) [c]	0.0013	0.0011	0.0028	0.0015
τ (μs), in H₂O, degassed (aerated)	0.37 (0.32)	107 (3.6)	61(3.6)[d]	144 (3.7)
τ (μs), in CH₃CN, degassed (aerated)	0.40 (0.38)	6.0 (0.63)	17 (0.69)	6.2 (0.6)
τ (μs) at 77K [b]	9.5, 0.60	181	163 [d]	230

Table 5.3 – Photophysical data for complexes 3, 8, 9 and 10[a]

[a] *In solution at 295±3K unless otherwise stated.* [b] *In EtOH / MeOH (4:1 v/v), except for complex 1, for which an EPA glass was used (EPA = ethanol / isopentane / diethyl ether, 2:5:5 v/v)* (c) *In aerated solution, measured using an excitation wavelength of 368 nm, excitation and emission band-passes of 5.0 nm, and using $[Ir(ttpy)_2]^{3+}$ as the standard (ϕ=2.9x10⁻²)[1]; estimated uncertainty±15%.* [d] *A short-lived minor component to the emission was also observed; the quoted value is that of the major component obtained by fitting the data to biexponential decay kinetics.*

5.3.1. Emission Spectral Profiles

The room temperature luminescence spectra for solutions of complexes 3, 8, 9 and 10 in water are shown in figure 5.7.
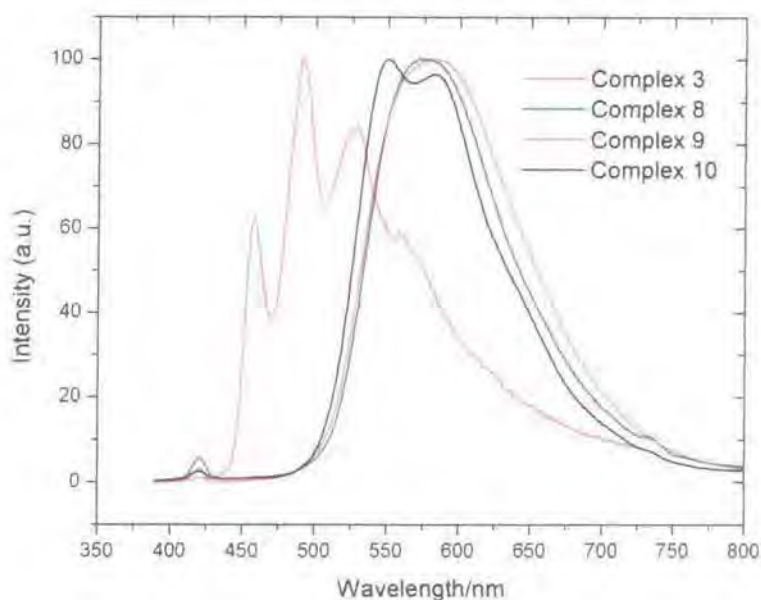
Figure 5.7 – *Corrected luminescence emission spectra of complexes 3, 8, 9 and 10 in water at room temperature, upon excitation at 368 nm*

It can be seen that the highest energy band maximum in the series is that for complex 3, where λ=457 nm, while for complexes 8, 9 and 10 λ=571, 587 and 553 / 584nm respectively. From the position of this highest energy (0-0) band, it is suggested that the luminescent level of complex 3 is higher in energy by about 2000 cm^{-1} compared to complexes 8, 9 and 10, in agreement with the conclusions made on the basis of the absorption data discussed previously. The different profile of the emission spectrum exhibited by complex 3 is also intriguing, since, despite possessing an aryl substituent at the 4'-position, the bis-mesityl substituted complex displays an emission spectral profile which is almost identical to that of the unsubstituted complex [Ir(tpy)$_2$]$^{3+}$,[1] and not at all like those of complexes 8, 9 and 10, or the previously reported aryl-substituted complexes, such as [Ir(ttpy)$_2$]$^{3+}$.[1] The difference in the energy and the shape of complex 3 and [Ir(tpy)$_2$]$^{3+}$ compared to the other complexes bearing 4'-aryl substituents, can be ascribed to the absence of additional conjugation in the former. In the case of [Ir(tpy)$_2$]$^{3+}$ the ligand centred excited state is restricted to the tpy frame, while complexes 8, 9 and 10 in this study, and the remaining complexes studied by Sauvage *et al.*[1] have a larger framework available. However, as discussed in Section 2.3, the *ortho*-methyl substituents on the pendent mesityl group in complex 3 cause twisting of the

pendent aryl ring such that the torsion angle between it and the central pyridine ring is 67.5°, compared to typical values of ~30°.[1, 9] This means that the aryl substituent is not in conjugation with the tpy fragment in complex 3, in contrast to complexes 8, 9 and 10, in effect restricting the ligand centred excited state to the tpy moiety, as for $[Ir(tpy)_2]^{3+}$. These combined results strongly suggest that it is the additional conjugation offered by the 4'-aryl group that is responsible for the different spectra exhibited by the aryl substituted systems compared to the parent complex.

A further reason for the difference in the spectral profile could be the spinning of the pendent aryl ring, resulting in a thermal distribution of conformers in solution, which might result in less resolved luminescence spectra for complexes 8, 9 and 10. In the case of complex 3, steric hindrance caused by the presence of the *ortho*-methyl groups could prevent such movement of the pendent ring.

It is also significant that the measured luminescence lifetime (eg. 400 ns in acetonitrile) is more comparable to that of $[Ir(tpy)_2]^{3+}$ ($\tau=1.2$ µs under the same conditions[1]) than to the longer values found for the aryl-substituted systems ($\tau>6$ µs[1]). Indeed, it is intriguing that the introduction of the mesityl group shortens the lifetime compared to the unsubstituted system, and since the quantum yield is similarly lowered, it implies that the mesityl complex is subject to enhanced non-radiative decay pathways. This could be associated simply with the increased availability of proximate C-C stretching vibrations able to facilitate the deactivation of the excited state, but it could also reflect the inductively electron-donating nature of the 2,4,6-trimethylphenyl substituent, which may serve to raise the energy of the higher-lying MLCT state, promoting it as a pathway of non-radiative decay.

5.3.2. Biphenyl-Substituted Complexes

Upon photoexcitation, the biphenyl, bis-biphenyl and cyano-biphenyl-substituted complexes 8, 9 and 10 display moderately intense yellow emission (with emission maxima in the range 550-600 nm) in degassed aqueous solution at room temperature. This represents a significant red-shift in the emission maxima relative to related complexes with just one aryl ring at the 4'-position (as opposed to a biphenyl unit), such as $[Ir(ttpy)_2]^{3+}$, although the quantum yields of luminescence in degassed solution are of similar magnitude (ca. 0.1). This red-shift in the emission energy of the complexes 8, 9

and 10 is attributed to the presence of the extra phenyl ring providing a higher degree of π-conjugation, which is expected to stabilise the ^{3}LC states.

On the other hand, since the increased conjugation offered by the additional phenyl ring lowers the ligand π* energy, not only will the LC states be stabilised, but also the MLCT excited states. Nevertheless, on the basis of the lifetime data, the emission from the complexes is again assigned to a ^{3}LC (π_{tpy}-π^*_{tpy}) emissive state, since the very long lifetimes (eg. 107 and 144 (±10) μs for complexes 8 and 10 respectively) are inconsistent with a significant charge-transfer contribution.

In agreement with the longer lifetimes and proposed greater triplet character, complexes 8, 9 and 10 also display higher sensitivity to oxygen. In air-equilibrated aqueous solution, lifetimes and quantum yields are reduced by a factor of around 20, compared to much smaller effects (ca. 4-fold) for [Ir(ttpy)$_2$]$^{3+}$,[1] with the result that the biphenyl complexes display significantly lower quantum yields than the monoaryl-substituted systems, under these conditions. The bimolecular rate constants of quenching by molecular oxygen are of the order 9 x 10^8 M^{-1} s^{-1}, about twice as large as the value of 4.3 x 10^8 M^{-1}s^{-1} for [Ir(ttpy)$_2$]$^{3+}$ in aqueous solution, and more in line with values typically observed for polypyridine transition metal complexes.[10]

In a frozen glass at 77K (in EtOH / MeOH, 4:1 by volume), complexes 8, 9 and 10 display a significant bathochromic shift of around 1500 cm^{-1} relative to the room temperature emission. Although such a change would be consistent with a small degree of ^{3}MLCT character, (since MLCT states normally blue-shift with decreasing temperature) behaviour of this kind could also arise if the luminescent excited state is coupled with nuclear rearrangements that are affected by the state of the solvent. It is anticipated that excitation of the biphenyl complexes will be accompanied by a torsional rearrangement between the planes of the terpyridyl fragment and the biphenyl moiety, and between the two constituent rings of the latter, since an approximately coplanar conformation of the three planes will be required to maximise the conjugation in the excited state compared to typical ground state dihedral angles in biphenyls of around 30°.[9] The necessary rearrangement to the more favourable conformation will be possible in fluid solution at room temperature, but not at 77K, accounting for the higher energy emission under the latter conditions. In line with this explanation is the

observation that the mesityl complex (3) shows almost no change in emission energy or spectral shape at 77K compared to room temperature. In this system, there is steric inhibition to attainment of the coplanar state, even at room temperature, and so immobilisation in a frozen glass is expected to have little effect.

Consideration of the quantum yield values given in table 5.3 reveals that complexes 8 and 10 are substantially less emissive in acetonitrile than in aqueous solution, even though the emission profiles in the two solvents are very similar (figures 5.7 and 5.8). After taking into account the effect of oxygen, the quantum yields in acetonitrile are estimated to be of the order of 18-25 times lower than in water.
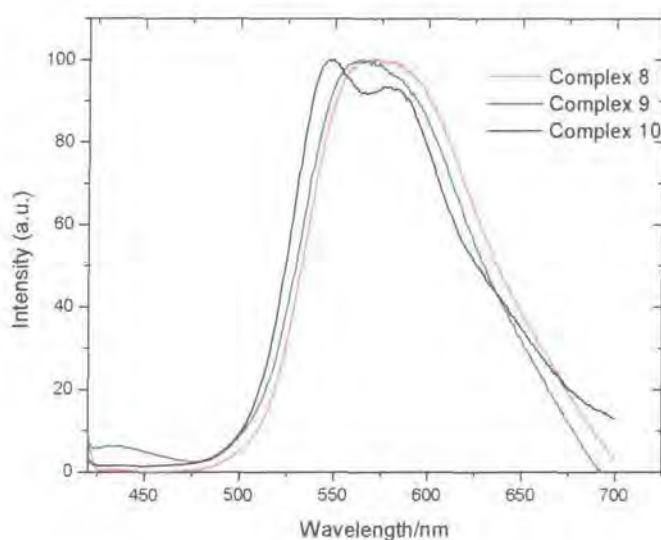
Figure 5.8 - *Corrected fluorescence emission spectra of complexes 8, 9 and 10 in acetonitrile upon excitation at 368 nm*

In addition to the weaker emission observed in air-equilibrated acetonitrile solutions, the lifetimes are also shortened, eg. for complex 8, $\tau = 6.0$ (± 0.5) μs in acetonitrile compared to 107 (± 10) μs in water (degassed solutions), an 18-fold decrease. That the quantum yields and lifetimes are reduced by comparable factors, (together with the similar forms of the spectra), suggests that the reduction is due to increased rates of non-radiative deactivation in acetonitrile, rather than to the radiative rate constant being substantially different in the two solvents (which might be expected if there were a switch to emission from a different type of excited state).

A similar trend to lower quantum yields and shorter lifetimes in acetonitrile has also been observed in the monoaryl series of complexes; however, the difference in that case

132

was less pronounced (a factor typically of about three). It is possible that the explanation for the more dramatic trend in the present instance could be the extent to which higher-lying ILCT states may influence the emission. As discussed earlier, complex 11 (bearing a dimethylamino substituent on the 4'-position of the pendent ring), revealed the presence of an ILCT state experimentally by a low energy band in the absorption spectrum. That this complex is scarcely emissive suggests that the charge-transfer state is subject to efficient non-radiative deactivation. Analogous ILCT states might be anticipated in complexes 8, 9 and 10, but owing to the more weakly electron-donating nature of the biphenyl and cyanobiphenyl pendents, such states would be expected at energies higher than those of the emitting $^3\pi\pi^*$ states. However, they may be stabilised in acetonitrile compared to water (as observed experimentally for the amino system, discussed earlier), and may therefore mix with the emissive $^3\pi\pi^*$ state to a greater extent in the former solvent, possibly providing a more efficient pathway of decay to the ground state. Configurational mixing of ^{1,3}ILCT excited states into emissive $^3\pi\pi^*$ and MLCT states has been reported by McMillin and co-workers in a series of 4'-aryl substituted [Pt(tpy)Cl]$^+$ complexes,[11] although in that case, it leads to an increase in lifetime and quantum yield over the parent, unsubstituted system which, itself, is almost non-emissive.

5.4. Emission Properties of Complexes 4 and 5

As discussed previously in section 5.2.2, complexes 4 and 5 are deep red in colour, owing to a broad, relatively intense absorption band centred around 500 nm, and attributed to an ILCT transition in which the NMe_2 / NPh_2 groups act as electron donors, and the metal bound terpyridine moiety acts as an electron acceptor. Excitation into this band using the second harmonic of a Nd:YAG laser (532 nm) led to weak emission in the near IR region, as shown in figures 5.9 to 5.11.
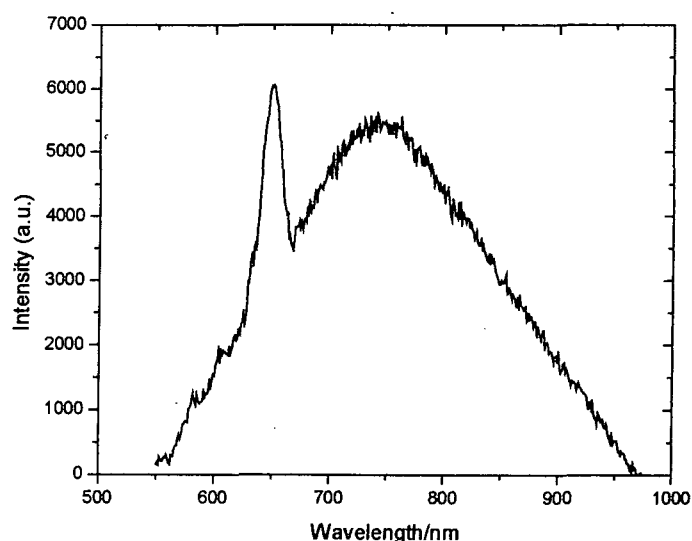
Figure 5.11 - *Emission spectrum of complex 5 in H_2O at room temperature $(\lambda_{ex}=532\ nm)$. (The Raman band of H_2O appears at 650 nm).*

Complex 4 displays an emission maximum of around 770 nm in acetonitrile but is scarcely emissive in water. Even with laser excitation, it was not possible to obtain a reliable spectrum in aqueous solution. On the other hand, complex 5 was found to emit with comparable intensities in both solvents (λ_{max}=750 nm in water and ~790 nm in CH_3CN). The emission is ascribed to a charge-transfer state, as discussed previously in chapter 3 for the zinc complexes of these ligands. In this instance, however, the emission is shifted further to the red, into the near IR region, possibly owing to the higher formal positive charge on Ir (III) compared to Zn (II).

Apart from this primarily electrostatic argument, however, the possibility of emission from a ^{3}ILCT (as opposed ^{1}ILCT) arises in the presence of iridium. In principle, a clue to this distinction could be obtained from the lifetimes of emission, but unfortunately the emission was too weak to obtain reliable estimates of the lifetimes using the available instrumentation. On the other hand, measurements in degassed and aerated solutions revealed a lack of sensitivity to the presence of oxygen, and this suggests very strongly that the lifetimes are short, probably less than 10 ns. A ^{1}ILCT assignment therefore seems more likely, and the weakness of the emission compared to the zinc complexes may simply reflect the typical trend of the "energy gap law" to more efficient non-radiative deactivation pathways as the energy gap between the excited and ground states decreases. The lack of emission of the NMe_2 complex (4) in water, but not the NPh_2 complex (5), is reminiscent of the poor emission of the NMe_2 ligand in

ethanol (whilst the NPh_2 ligand was quite strongly emissive), as discussed in chapter 3. The origin of the effects may be similar, namely that the formation of the CT state is accompanied by a twisting motion that is hindered in the NMe_2 case by hydrogen-bonding to water molecules (or to ethanol in the case of the ligand).

Although only weak emitters, it is noteworthy that complexes 4 and 5 are the only $[Ir(tpy)_2]^{3+}$ complexes (and possibly the only polypyridine complexes of this element) reported to date to emit in the near IR.

5.5.   References

[1]   J.-P. Collin, I. M. Dixon, J.-P. Sauvage, J. A. G. Williams, F. Barigelletti, and L. Flamigni, *J. Am. Chem. Soc*, 1999, **121**, 5009.

[2]   K. Araki, T. Mutai, J.-D. Cheon, and S. Arita, *J. Chem. Soc., Perkin Trans.2*, 2001, 1045.

[3]   M. Licini and J. A. G. Williams, *J. Chem. Soc., Chem. Commun*, 1999, 1943.

[4]   W. Goodall and J. A. G. Williams, *J. Chem. Soc., Dalton Trans.*, 2000, 2893.

[5]   D. Roberto, F. Tessore, R. Ugo, S. Bruni, A. Manfred, and S. Quici, *J. Chem. Soc., Chem. Commun*, 2002, 846.

[6]   S. D. Cummings and R. Eisenberg, *J. Am. Chem. Soc*, 1996, **118**, 1949.

[7]   N. P. Ayala, C. M. Flynn, Jr., L. Sacksteder, J. N. Demas, and B. A. Degraff, *J. Am. Chem. Soc*, 1990, **112**, 3837.

[8]   K. K.-W. Lo, C.-K. Chung, D. C.-M. Ng, and Zhu.N, *New J. Chem*, 2002, **26(1)**, 81.

[9]   Y. Kim and C. M. Lieber, *Inorg. Chem.*, 1989, **28**, 3990.

[10]   D. M. Roundhill, 'Photochemistry and photophysics of Metal Complexes', Plenum, New York, 1994.

[11]   J. F. Michalec, S. A. Bejune, D. G. Cuttel, G. C. Summerton, J. A. Gertenbach, J. S. Field, R. J. Haines, and D. R. Mcmillin, *Inorg. Chem.*, 2001, **40**, 2193.

6. Bimetallic complexes

6.1. Introduction

Application of the Suzuki cross-coupling reaction to the preparation of a range of terpyridine ligands bearing different functional groups substituted onto the 4'-pendent ring was discussed in chapter 2. Optimal yields were obtained through the coupling of 4'-bromoterpyridine with aryl boronates, using $Pd(PPh_3)_4$ as a catalyst and DME as the solvent. Subsequently, this type of coupling reaction was shown to be possible *whilst* the ligand was bound to an Ir (III) metal centre. In principle, therefore, it should be possible to make use of the coupling strategy to prepare dinuclear complexes, if a complex incorporating a boronic acid is used in place of the simple, organic aryl boronic acid. This chapter describes attempts to investigate this possibility, using complex 7 as the bromo partner, and complex 12 or 13 as the boronate substituted complex.
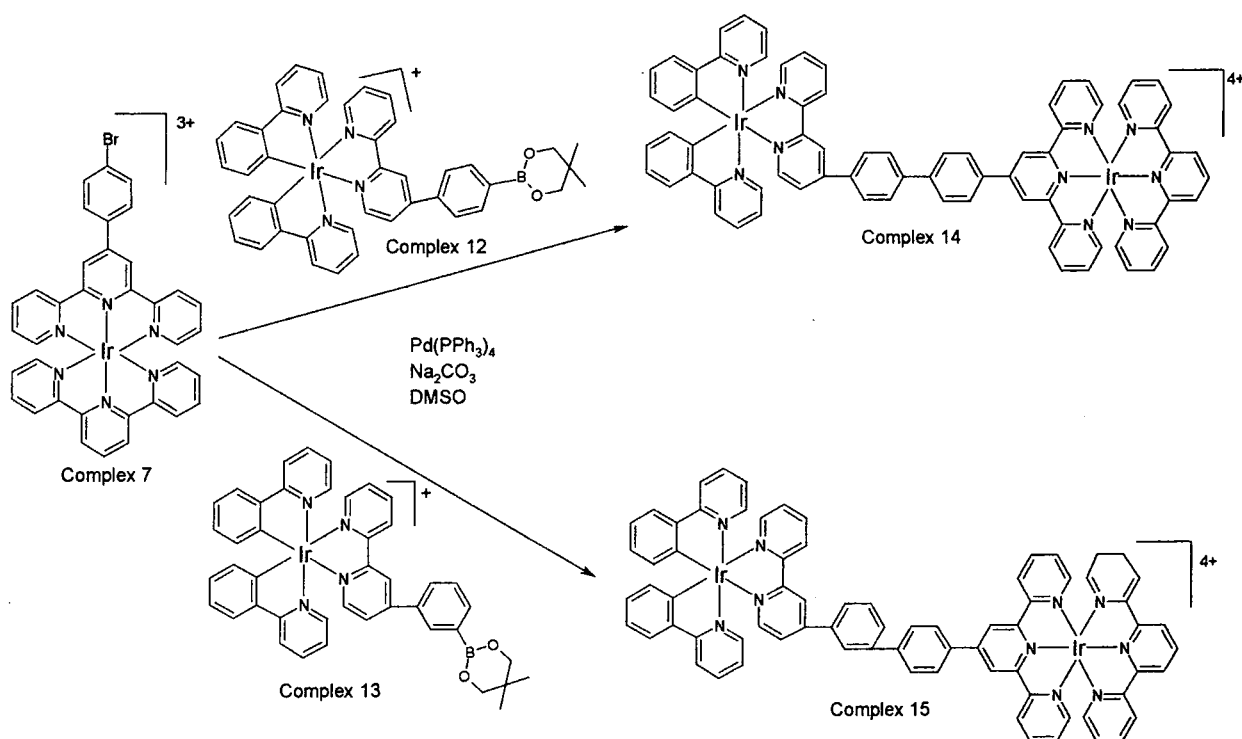
Figure 6.1 – *Preparation of bimetallic complexes via the Suzuki methodology*

138

6.2. Background to synthetic strategies for Polynuclear Complexes

Much work has been invested in the development of effective synthetic routes to multimetallic supramolecular systems through the assembly of their molecular components.[1-5]

Two common methodologies used for the synthesis of polynuclear systems are

- The "Complexes as Metals and Complexes as Ligands" strategy [3]
- Cross-Coupling Methodologies [1, 2, 4, 5]

6.2.1. The "Complexes as Metals and Complexes as Ligands" Strategy [3]

This procedure is based on the use of *complexes* in the place of both the metal (M) and the ligands (L) in the synthetic reaction

$$M + nL \rightarrow M(L)_n$$
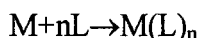
Mono- or polynuclear complexes that possess easily replaceable ligands can take the place of M, and the place of L can be taken by mono- or polynuclear complexes that contain free chelating sites.
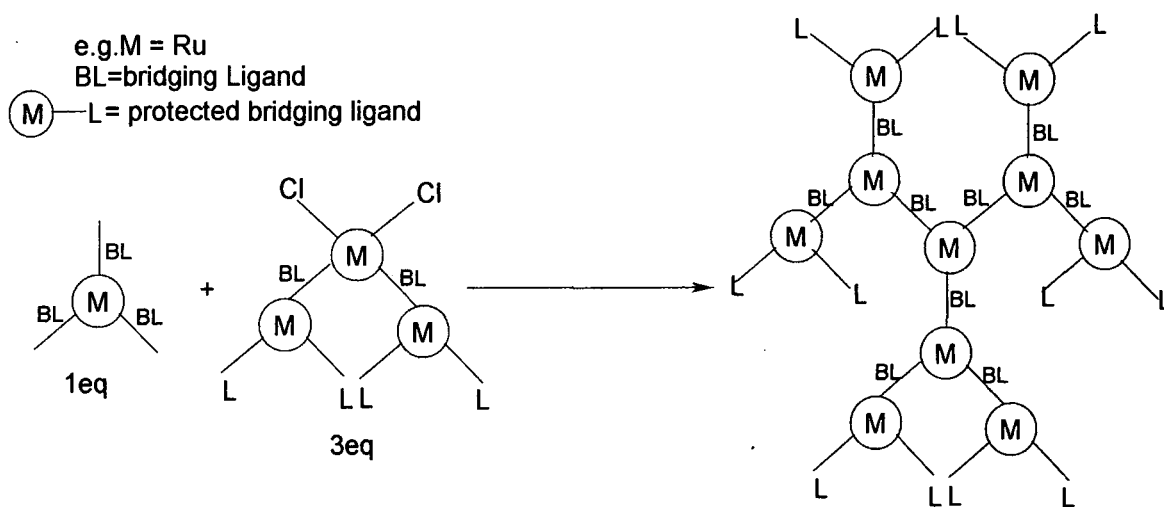
Figure 6.2 – *The "complexes as metals and complexes as ligands" strategy for the synthesis of polynuclear systems*[3]

This strategy was developed as a procedure to synthesise oligonuclear metal complexes of desired nuclearity and chemical structure. Unfortunately, it requires protection and deprotection steps to prevent the formation of other polynuclear metallic species formed as by-products, and these steps are costly of both time and materials.

6.2.2. Cross-Coupling Strategies [1, 2, 4, 5]

Cross-coupling reactions offer an alternative strategy for the synthesis of polynuclear complexes, which may overcome some of the problems mentioned above. However, it

is the Sonogashira-type coupling[2] that has received the most attention in this application, with the few examples of the Suzuki coupling limited to symmetrical, homometallic systems.[1, 4, 5]

Ziessel *et al.* prepared hybrid metal complexes containing ruthenium terpyridine and ruthenium bipyridine complexes as metallo terminals linked by a single ethynylene group, through iterative Sonogashira coupling reactions.[2] The group used conventional methodologies to prepare the relevant metallo synthon, which was coupled using Pd(PPh₃)₄ as the catalyst and acetonitrile as the solvent.
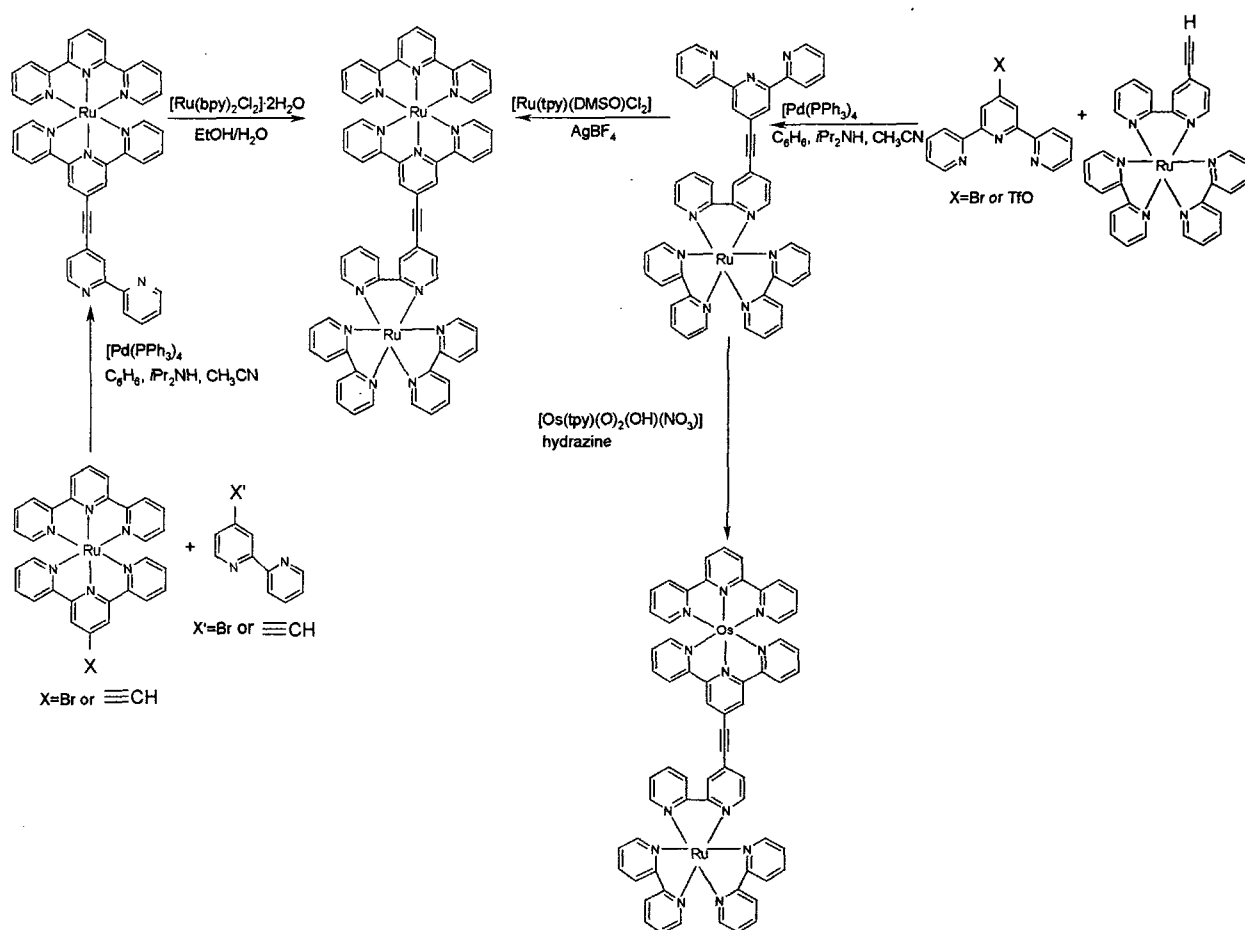
Figure 6.3 – *Polynuclear ruthenium complexes prepared by iterative Sonogashira reactions*[2]

Perhaps more elegant and more powerful is the work of Tor *et al.*, who coupled two preformed metal complexes possessing complementary functionalities.[6, 7]
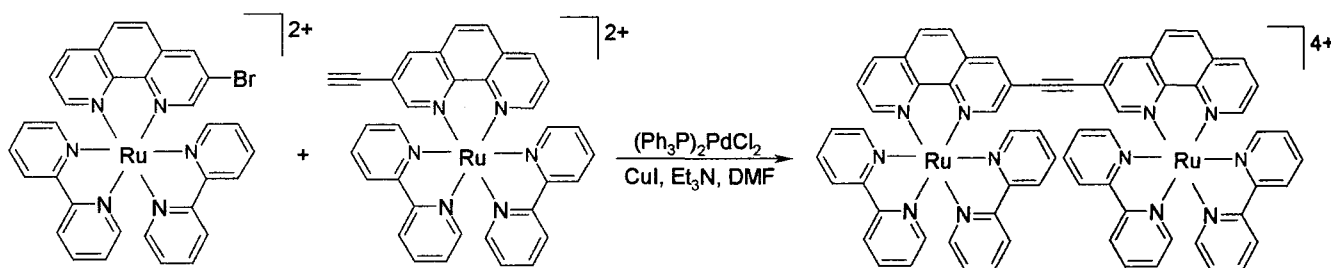
Figure 6.4 – *Use of enantiomerically pure coordination compounds as building blocks for polynuclear ruthenium systems*[6, 7]

Tor's approach represented a novel and versatile route to the efficient synthesis of diastereomerically-pure multi-Ru (II) arrays using enantiomerically-pure chiral coordination complexes as building blocks. Palladium mediated cross-coupling reactions between bromo- and ethynyl-functionalised octahedral Ru (II) complexes were used to prepare di-and trinuclear complexes with predetermined chirality at the metal centre.

One of the earliest examples utilising the Suzuki cross-coupling reaction was reported by Sauvage *et al.*[4] The group successfully applied the reaction to form symmetrical dimeric cyclometallated ruthenium complexes, in which the metal centres are linked by phenylene bridges of varying lengths, by using aryl diboronic esters.
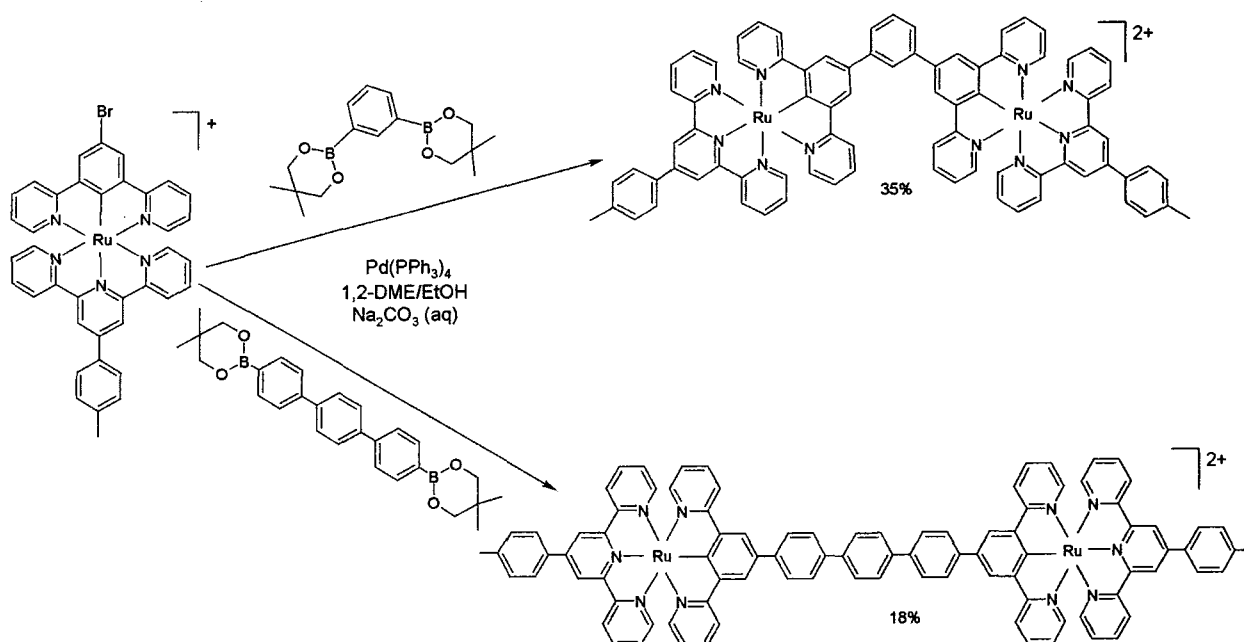
Figure 6.5 - *Symmetrical dimeric cyclometallated ruthenium complexes prepared via the Suzuki methodology*[4]

141

In 2001, Klemm *et al.* reported a novel conjugated polymer that contains a ruthenium (II) bipyridine complex similarly synthesised by a Suzuki coupling reaction, in which the ruthenium monomeric complexes were coupled to the diboronic derivative of the bridging phenyl group. [5]

Very recently (summer 2003), De Cola *et al.* have reported on the use of the same strategy to prepare binuclear iridium systems. [1]
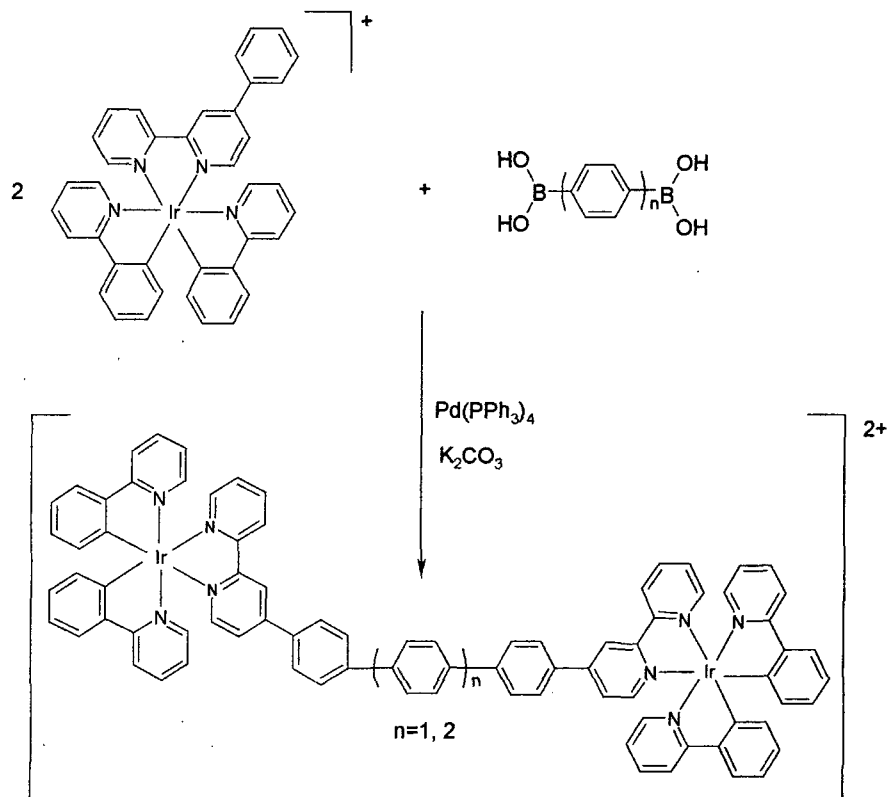
Figure 6.6 – *Binuclear Ir(III) complexes prepared via the Suzuki methodology* [1]

Apart from these few examples in the literature, the use of the Suzuki cross-coupling reaction for the preparation of polynuclear systems remains unexplored.

6.3. Application of the Suzuki Cross-Coupling Reaction for the Synthesis of Bimetallic Ir (III) Complexes

In order to investigate the possibility of employing the Suzuki reaction in the formation of non-symmetric dimeric metal complexes (as opposed to the dimerisation reactions of, for example figure 6.6), the coupling reactions represented earlier in figure 6.1 were attempted. Given the success in elaborating complex 7 *via* the Suzuki reaction (chapter 4) and the fact that the boronic acid substituted cyclometallated complex, complex 12 had been prepared in the group, this choice seemed appropriate. Moreover, the product of this reaction would incorporate a bis-cyclometallated iridium centre, which is a strong photo-reductant,[8-10] together with a bis-terpyridyl iridium moiety, which is strongly photo-oxidising.[11] Hence the target system could be an intriguing candidate for the study of photoinduced electron transfer between the two metal centres.

6.3.1. Synthesis of 4-(3-bromophenyl)-2, 2'-bipyridine[12, 13]

The Kröhnke methodology,[14] discussed previously for the synthesis of terpyridines, was utilised in this instance for the synthesis of 4-(3-bromophenyl)-2, 2'-bipyridine.[12, 13] As discussed previously, this methodology is a variation of the Hantzsch and Tschitschibabin syntheses of pyridine,[15, 16] involving the condensation of a pyridinium salt with an unsaturated ketone, to form a 1, 5-diketone. Ring cyclisation follows in the presence of ammonium acetate in glacial acetic acid.

This synthesis worked well for the preparation of 4-(3-bromophenyl)-2, 2'-bipyridine, with the reaction between the pyridinium salt and the α, β-unsaturated carbonyl compound shown in fig 6.7 leading to the isolation of the final product in 68 % yield. Ideally, *meta*-bromocinnamaldehyde would be used, to lead directly to the bipyridine. However, problems of self-condensation would make this difficult to prepare simply by an aldol reaction of *meta*-bromobenzaldehyde with acetaldehyde. Instead, the carboxylate derivative shown was used, drawing upon literature precedent in which the *para*-bromo isomer was prepared by initial base-catalysed condensation of the aryl aldehyde with sodium pyruvate.[12,13] This, of course, leads to the bipyridine 6'-carboxylate, but such compounds undergo facile thermal decarboxylation, and this was

duly achieved by rigorous heating under nitrogen, until effervescence of carbon dioxide ceased.
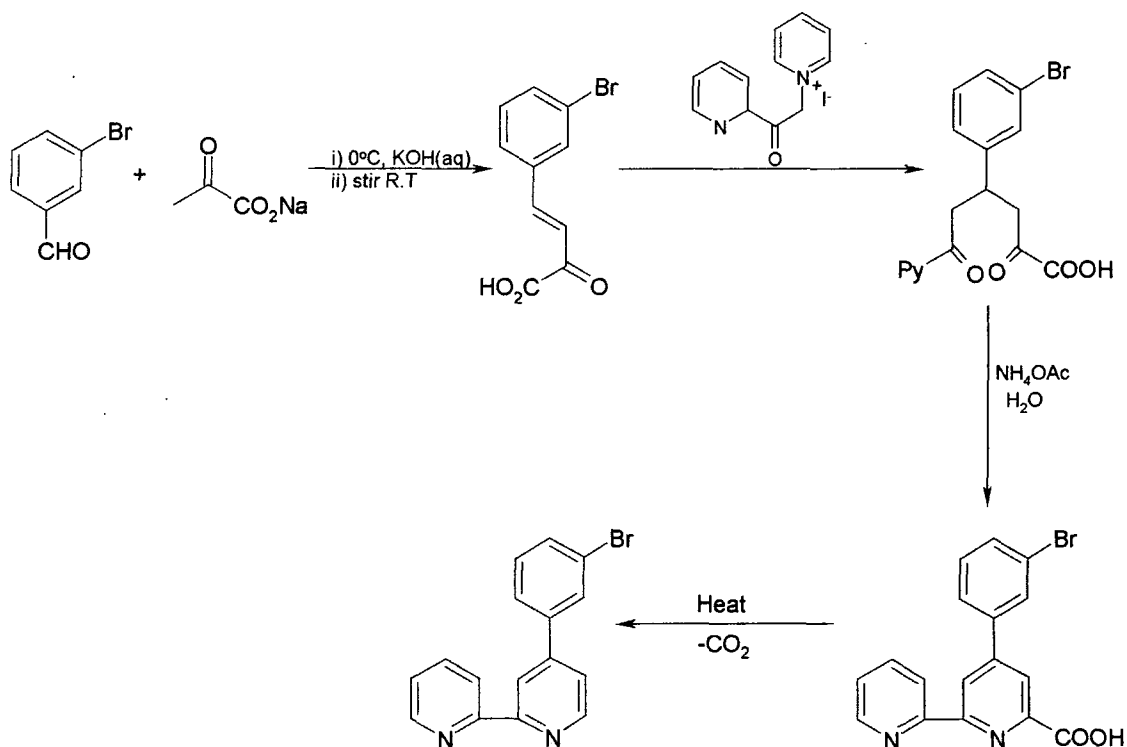
Figure 6.7 - *Synthesis of 4-(3-bromophenyl)-2, 2'-bipyridine via the Khrönke methodology*[12-14]

The preparation of the 1-(2-oxo-2(pyridin-2-yl)ethyl) pyridinium iodide was *via* the enolate of 2-acetyl pyridine, which generates α-iodoketone by a nucleophilic attack on iodine. Subsequent nucleophilic attack by pyridine displaces the iodine atom to produce the pyridinium salt, which is easily purified by crystallisation from ethanol and water. [12, 17]
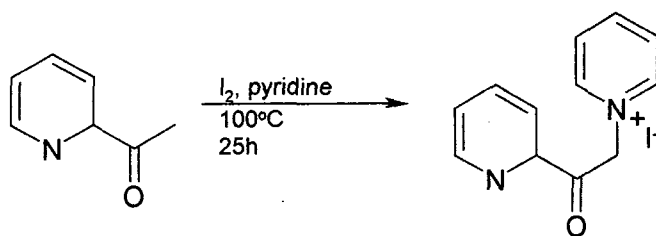
Figure 6.8 - *Preparation of the 1-(2-oxo-2(pyridin-2-yl)ethyl) pyridinium iodide*[12, 17]

6.3.2. Synthesis of 4-(3-(neopentylglycolatoboron)phenyl)-2, 2'-bipyridine

Having isolated 4-(3-bromophenyl)-2, 2'-bipyridine, the next stage was its conversion to the corresponding neopentyl boronate ester. This was achieved through the Miyaura cross-coupling reaction, under the conditions similar to those used previously for the synthesis of 4'-(neopentyl glycolatoboron)-2, 2': 6', 2"-terpyridine from 4'-bromo-2, 2': 6', 2"-terpyridine, namely Pd(dppf)Cl₂ as the catalyst, DMSO as the solvent in the presence of KOAc as a base.
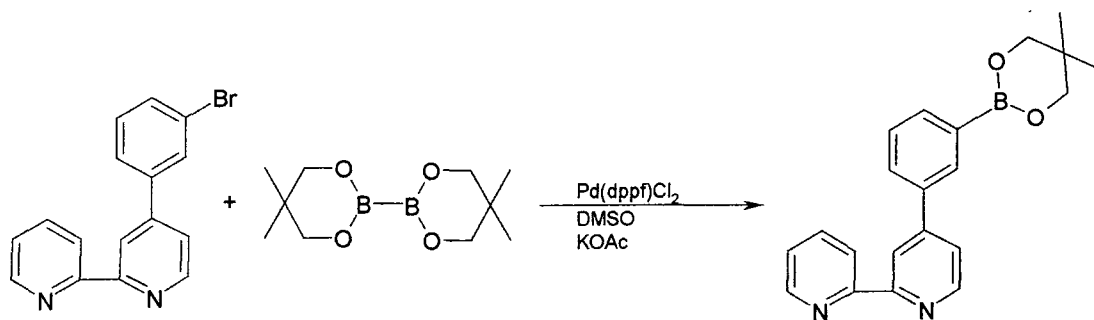
Figure 6.9 - *Synthesis of 4-(3-(neopentylglycolatoboron)phenyl)-2, 2'-bipyridine via the Miyaura methodology*[18]

Unfortunately, some unreacted 4-(3-bromophenyl)-2,2'-bipyridine as well as de-boronated material was present in the crude product. However, this was purified through exploiting the water solubility of the boronate anion formed upon addition of aqueous base in a similar procedure to that used for the analogous terpyridine system; i.e. through dissolution of the crude product into dichloromethane and extracting the product into basic water. The water was then carefully neutralised until a white precipitate appeared, which was then extracted back into dichloromethane. The product was finally isolated in 62 % yield.
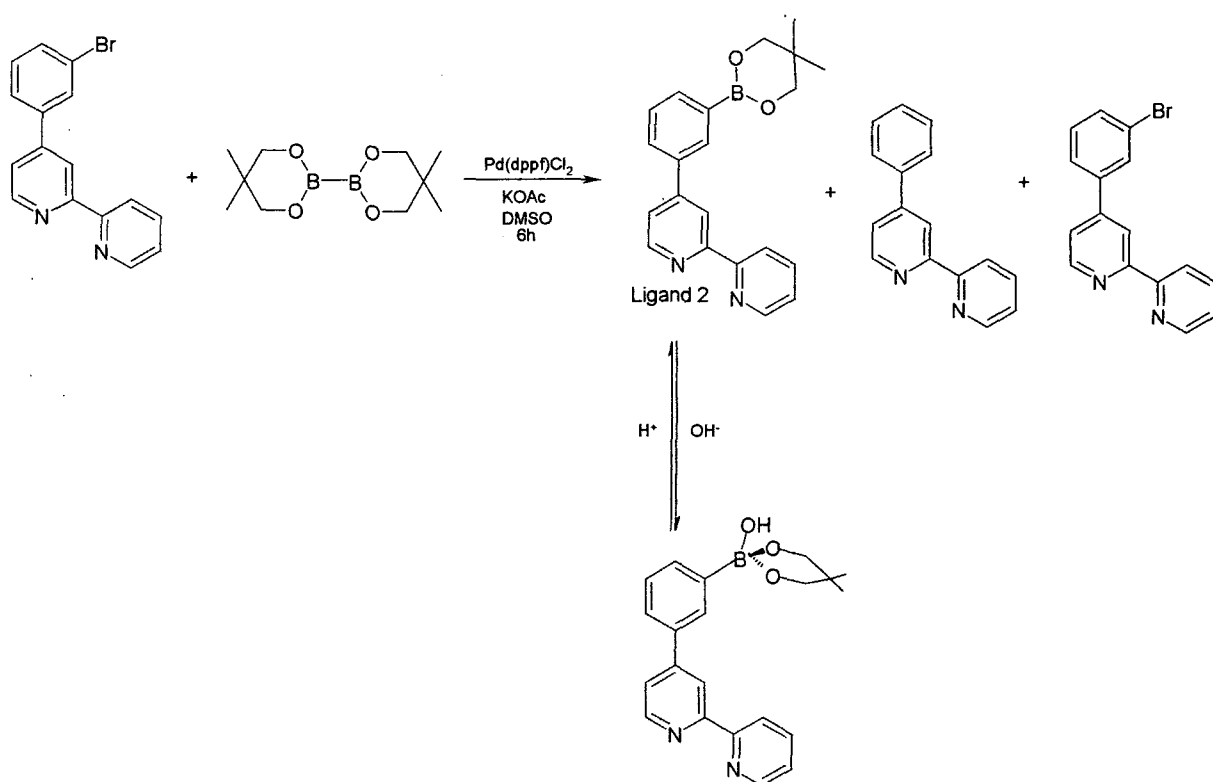
Figure 6.10 – *Purification via the water soluble boronate anion*

6.3.3. Synthesis of Iridium Complexes

Ir (III) complexes of the type [Ir(NC)₂(NN)]⁺, where NC is an *ortho*-metallating ligand and NN a neutral, bpy-like chelating ligand, are prepared by bridge-splitting reactions of the appropriate *ortho*-metallated dimer [Ir(NC)₂Cl]₂ with the chelating NN ligand.[19] This general procedure is adapted from a method used by Nonoyama, who generated rhodium complexes from a dimer containing benzo[H]quinoline ligands.[20] In this instance, the synthesis of complex 13 was achieved *via* tetrakis(2-phenylpyridine-C², N') (μ-dichloro)diiridium, shown in figure 6.11.
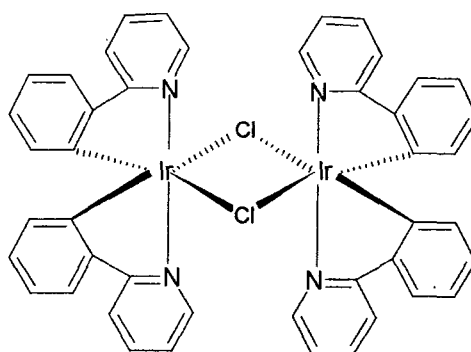
Figure 6.11 - *tetrakis(2-phenylpyridine-C^2, N') (μ-dichloro)diiridium, [Ir(ppy)$_2$Cl]$_2$*

The dimer was synthesised by the reaction of iridium trichloride with 2 equivalents of 2-phenylpyridine in 2-ethoxyethanol and water, in 85 % yield. [21] Since the Ir-Cl bridging bonds in the dimer are cleaved upon treatment with a ligand such as bipyridine, complex 13 was obtained by refluxing the dimer with 2 equivalents of 4-(3-(neopentylglycolatoboron)phenyl)-2, 2'-bipyridine (figure 6.12).
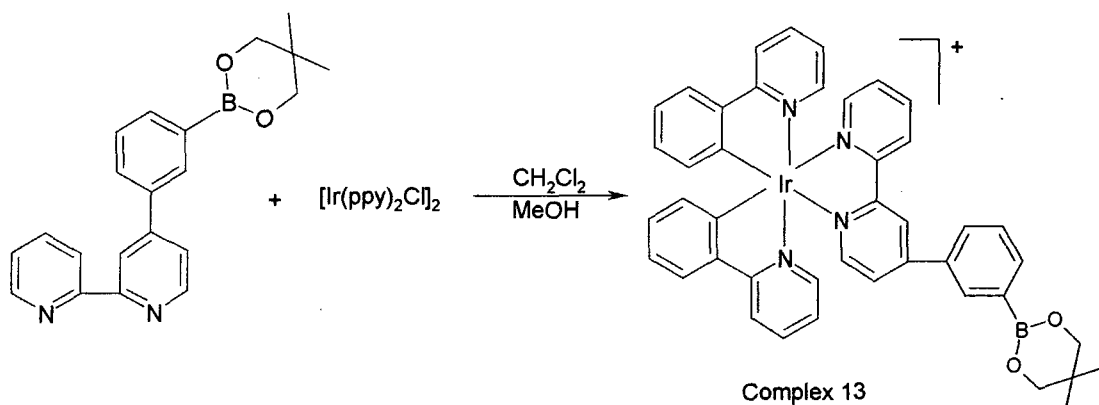
Figure 6.12 – *Synthesis of [Ir(ppy)$_2$(L^2)]*

Following the conditions reported by Neve *et al.* in which a mixture of CH$_2$Cl$_2$ and MeOH at reflux is used, [19] the complex was obtained in 55 % yield following ion exchange with ammonium hexafluorophosphate in methanol.

6.3.4. Application of Suzuki Cross-Coupling reactions to form bimetallic complexes

The coupling of the para-substituted boronic acid complex (complex 12) was attempted first (figure 6.1). The procedure employed was similar to that used previously for the cross-coupling of an aryl boronic acid to complex 7. In this instance, the reaction was heated for 24 h at 85°C. Unfortunately, analysis of the reaction mixture after this time using electrospray mass spectrometry revealed that the reaction had not been successful due to de-boronation of complex 12. The absence of any product whatsoever, together with the lack of consumption of complex 7 as evident from electrospray mass spectrometry and TLC, suggested that the starting material had deboronated completely before any of the complex had undergone the coupling reaction. [22]

It was thought that the influence of the positive charge on the iridium centre, in direct conjugation with the boron, may have promoted de-boronation in the complex. To test this hypothesis, the same cross-coupling reaction was repeated, this time using the *meta-* isomer complex 13, which should not be so predisposed towards deboronation, due to the absence of direct conjugation with the site of positive charge (figure 6.13).
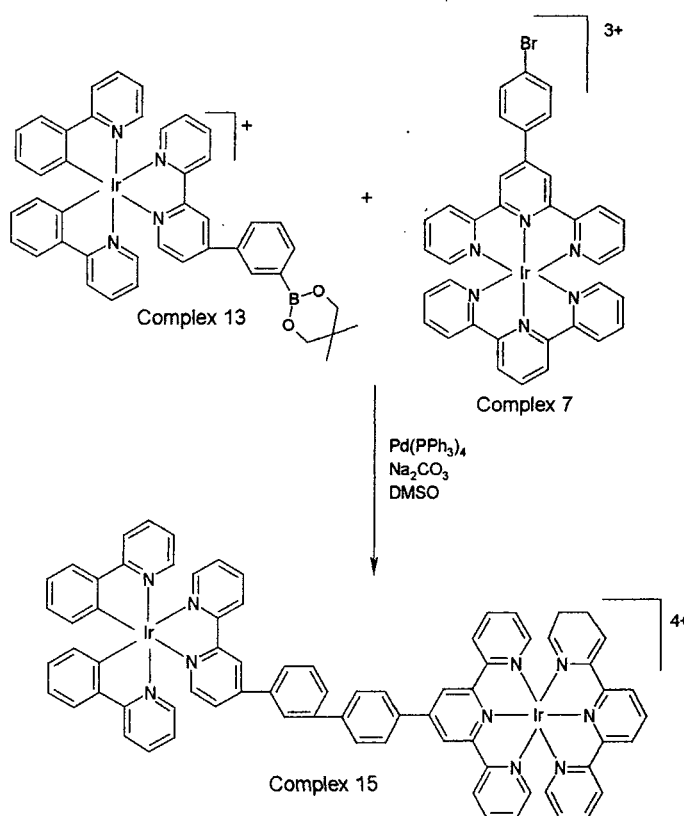
Figure 6.13 – *Synthesis of complex 15 via the Suzuki methodology*

Exactly the same procedure was carried out as in the previous example for the *para*-isomer, with the reaction monitored using thin-layer chromatography. Unfortunately, after three days heating at 85°C, with the addition of extra catalyst after 24 h and 48 h, TLC analysis repeatedly revealed the presence of starting material, and only a very small fluorescent yellow new spot emerged.

Indeed, purification of the reaction mixture by chromatography on silica led to the recovery of an almost quantitative mass of starting material. It should be noted however, that no de-boronated material was recovered, confirming the hypothesis that the use of the *meta*-isomer eliminated de-boronation as an undesirable side-reaction.

In this case, it is possible that the reaction had failed to proceed due to the strong coulombic interactions between the 3+ and 1+ complexes. It is noteworthy that there are no examples in the literature in which a triply-charged metal complex is coupled with another charged metallosynthon.

Having overcome the problems experienced through de-boronation by the use of the *meta-* isomer of the boronate complex, only to find the coupling of two charged synthons in this system problematic, the alternative approach discussed earlier was investigated, namely to introduce a second binding site by cross-coupling, and then complex the second metal. A Suzuki reaction was therefore attempted to couple the terpyridine complex to the 4-(3-neopentylglycolatoboron)phenyl-2, 2'-bipyridine in order to form complex 16 (figure 6.14).
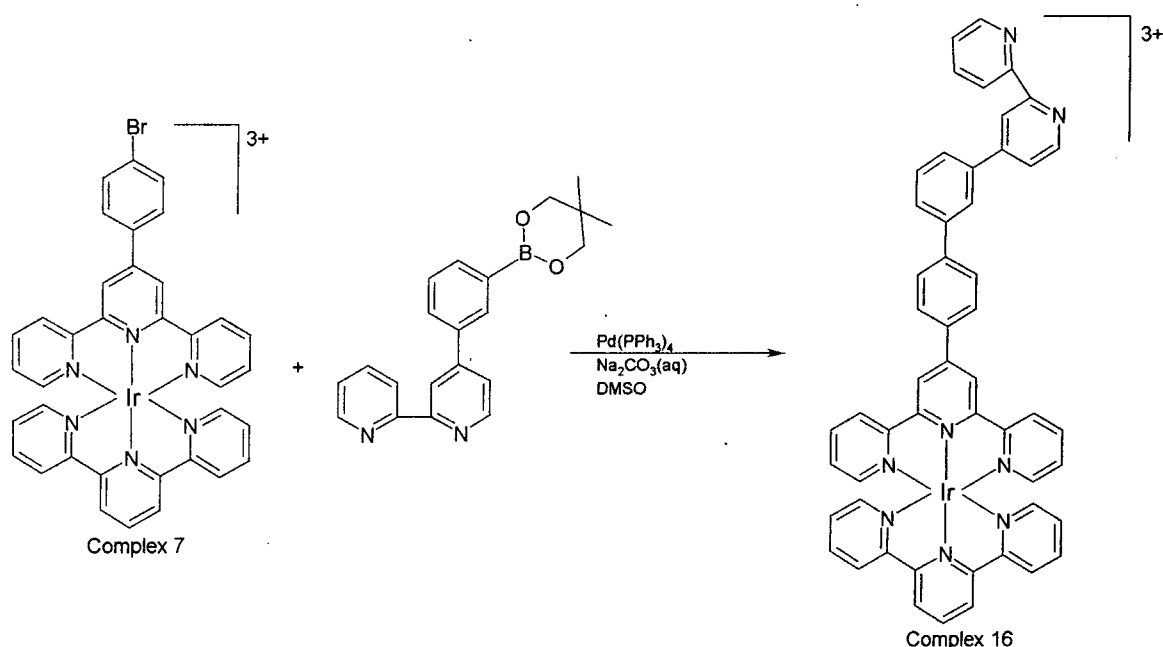
Figure 6.14 – *Synthesis of complex 6 via the Suzuki methodology*

It was anticipated that this reaction would be less problematic, and that the product would be able to react with the iridium dimer [Ir(ppy)₂Cl]₂ to form the desired product. Unfortunately however, attempts to synthesise complex 16 *via* the Suzuki cross-coupling reaction led only to recovery of starting material, even after prolonged heating and the addition of further catalyst.

6.4. References

1   E. A. Plummer, J. W. Hofstraat, and L. De Cola, *J. Chem. Soc. Dalton Trans.*, 2003, 2080.

2   A. Harriman, M. Hissler, A. Khatyr, and R. Ziessel, *Eur. J. Inorg. Chem*, 2003, 955.

3   G. Denti, S. Campagna, S. Serroni, M. Ciano, and V. Balzani, *J. Am. Chem. Soc*, 1992, **114**, 2944.

4   S. Chodrowski-Kimmes, M. Beley, J.-P. Collin, and J.-P. Sauvage, *Tetrahedron. Lett*, 1996, **37**, 2963.

5   W. Frank, T. Pautzsch, and E. Klemm, *Macromol.Chem.Phys*, 2001, **202**, 2535.

6   Y. Tor and D. Tzalis, *J. Am. Chem. Soc*, 1997, **119**, 852.

7   Y. Tor, *Synlett*, 2002, **No. 7**, 1043.

8   F. O. Garces, K. A. King, and R. J. Watts, *Inorg. Chem.*, 1988, **27**, 3464.

9   K. A. King and R. J. Watts, *J. Am. Chem. Soc*, 1987, **109**, 1589.

10 Y. Ohsawa, S. Sprouse, K. A. King, M. K. De Armond, K. W. Hanck, and R. J. Watts, *J. Phys. Chem*, 1987, **91**, 1047.

11 I. M. Dixon, J.-P. Collin, J.-P. Sauvage, L. Flamigni, S. Encinas, and F. Barigelletti, *Chem. Soc. Rev.*, 2000, **29**, 385.

12 R. A. Kipp, *J. Photochem. and Photobiol A*, 1999, **121**, 27.

13 M. Montalti, S. Wadhwa, W. Y. Kim, R. A. Kipp, and R. H. Schmehl, *Inorg. Chem.*, 2000, **39**, 76.

14 F. Krohnke, *Synthesis*, 1976, 1.

15 G. M. Loudon, 'Organic Chemistry', Benjamin Cummings, Redwood City, 1995.

16 A. E. Tschitschibabin, *J. Prakt. Chem*, 1924, **107**, 123.

17 S. M. Treffert-Ziemelis, J. Golus, D. P. Strommen, and J. R. Kincaid, *Inorg. Chem.*, 1993, **32**, 3890.

18 T. Ishiyama, M. Murata, and N. Miyaura, *J. Org. Chem.*, 1995, **60**, 7508.

19 F. Neve, A. Crispini, S. Campgna, and S. Serroni, *Inorg. Chem*, 1999, **38**, 2250.

20 M. Nonoyama, *J. Organomet. Chem*, 1974, **82**, 271.

21 S. Sprouse, K. A. King, P. J. Spellane, and R. J. Watts, *J. Am. Chem. Soc*, 1984, **106**, 6647.

22 H. G. Kuivila and K. V. Nahabedian, *J. Am. Chem. Soc*, 1961, **83**, 2167.

7. Summary

A family of 4'-aryl substituted terpyridines has been prepared via the palladium catalysed Suzuki cross-coupling reaction (chapter 2). The reaction proceeds under mild conditions and tolerates a wide range of functional groups, and therefore possesses some advantages over the traditional methods of terpyridine synthesis[1, 2] discussed in chapter 1. The cross-coupling of 4'-bromo terpyridine (or 4'-bromophenyl terpyridine) with arylboronic acids or esters, in the presence of $Pd(PPh_3)_4$ as the palladium catalyst and DME as the solvent, results in largely satisfactory yields, whilst conversions were poorer when 4'-triflate terpyridine was used in place of 4'-bromoterpyridine. The alternative coupling strategy involving the reaction of terpyridine-4-boronate (or terpyridine-4-phenylboronate) with the appropriate aryl halide was found to be less satisfactory owing, in part, to the difficulty in obtaining the former in high purity and good yield.

The luminescence properties of the terpyridine ligands prepared via the cross-coupling reaction have been studied in solution at room temperature (chapter 3). Most of the compounds emit in the near-UV region of the spectrum, with the biaryl-substituted compounds being slightly red-shifted compared to the monoaryl systems. Where measurements were possible, the fluorescence lifetimes lie in the range 1-5 ns. The emissive state of the ligands is assigned to a ^1LC (π_{tpy}-π_{tpy}*) excited state, however, the emission spectra of the amino-substituted compounds (tpy-$C_6H_4NR''_2$ and tpy-C_6H_4-$C_6H_4NR''_2$ where R''=CH_3 or Ph) display a large red-shift with increasing solvent polarity suggesting involvement of an intramolecular charge-transfer state (ICT). Coordination of zinc to the amino-substituted ligands led to the appearance of a new, long-wavelength band in the absorption spectrum, as well as red-shifted emission (by about 100 nm) attributed to the stabilisation of the ICT state by the coordinated metal ion. The relatively intense nature of this new red-shifted emission in the case of tpy-$C_6H_4NPh_2$ suggests potential application as a zinc sensor. The nature of the response of this ligand to Zn^{2+} is unique (with the single exception of Cd^{2+}) and lends itself to the technique of ratiometric fluorimetry, whilst excitation is possible at wavelengths suitable for intracellular studies. However, a water-soluble analogue would be required to allow use in genuine applications, including physiological studies. To this end, future work should focus on the functionalisation of the ligand to enhance solubility, while considering levels of toxicity if anticipating use in physiological studies. Strategies could include the substitution of poly(ethylene glycol) (PEG) or sodium dodecyl sulphate (SDS) chains onto the pendent pyridyl rings. Both routes offer the

advantages of enhancing solubility in aqueous solution and being inert to most chemical reactions.

The synthesis of iridium complexes of the terpyridine ligands prepared *via* the Suzuki reaction was attempted using conventional methodologies of complex formation, involving reaction of the ligands with $IrCl_3.3H_2O$.[3] The homoleptic complexes shown in figure 8.1 were prepared in this way (complexes 3, 4 and 5). However, the synthesis of heteroleptic complexes $[Ir(L^1)(L^2)]^{3+}$ *via* this route was difficult, since the harsh reaction conditions involved led to the formation of the homoleptic complexes $[Ir(L^1)_2]^{3+}$ and $[Ir(L^2)_2]^{3+}$ as side-products, which proved to be very difficult to separate from the desired product. However, following the success of the Suzuki cross-coupling reaction in derivatising terpyridine ligands at the 4'-position (chapter 2), the application of the cross-coupling methodology for the elaboration of terpyridine ligands, whilst they are already bound to an Ir (III) metal centre, was investigated as a new route to functionalised complexes of this type. The synthesis of complexes 8, 9, 10 and 11 shown in fig 7.1 was achieved through the reaction of $[Ir(tpy)(tpy-\phi-Br)]^{3+}$ with aryl boronic acids utilising a procedure similar to that used for the free ligands. In common with the ligand synthesis, $Pd(PPh_3)_4$ was employed as the catalyst, however in this instance DMSO was utilised as the solvent, as it provides complete dissolution of the reactants.
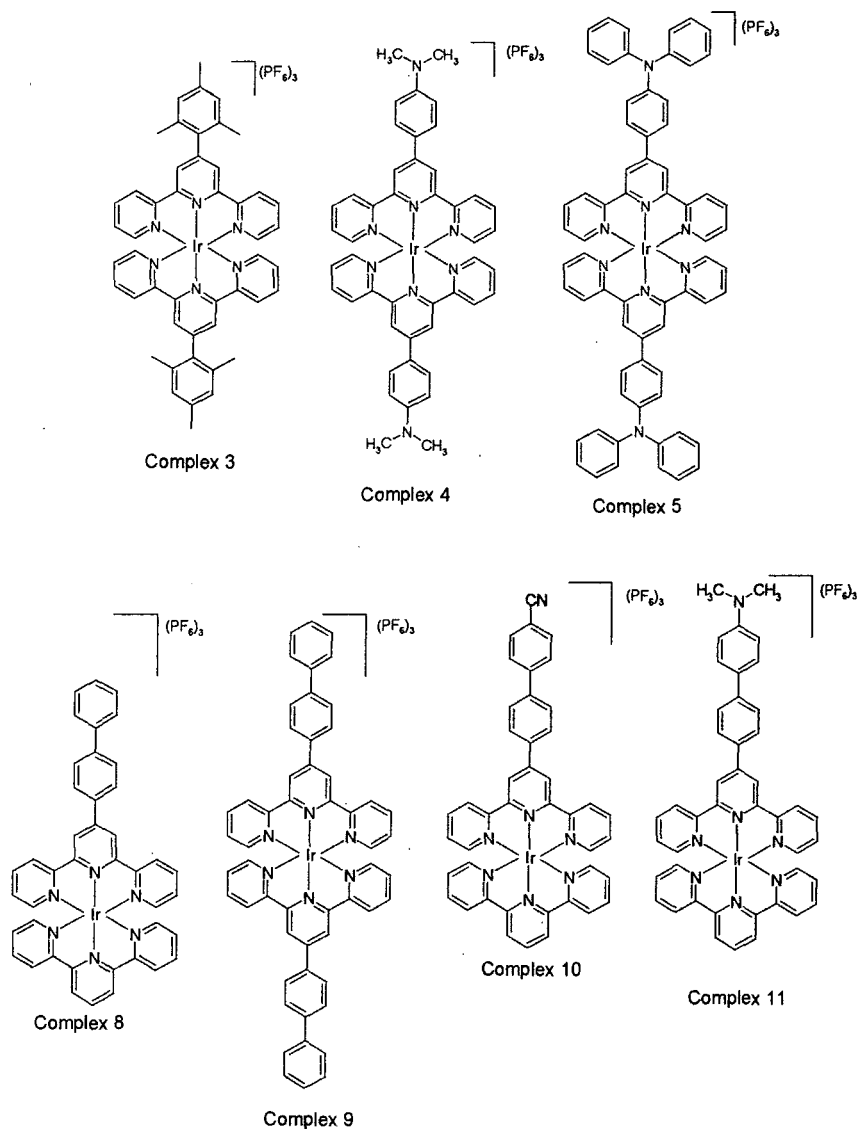
Figure 7.1 – *Ir (III) bis(terpyridine) complexes prepared during this work*

The biphenyl complexes 8, 9 and 10 displayed moderately intense yellow emission, which was slightly red-shifted compared to the analogous monoaryl complexes investigated previously.[3-6] This observation was attributed to increased conjugation in the biphenyl systems leading to stabilisation of the ^{3}LC (π_{tpy}-π_{tpy}*) emissive state. The observed lifetimes were substantially longer than those of [Ir(ttpy)$_2$]$^{3+}$ suggesting that any MLCT contribution to the excited state must now be small. In agreement with the longer lifetimes and proposed greater triplet character, complexes 8-10 also displayed higher sensitivity to oxygen.

Absorption and emission data of the mesityl-substituted complex 3, on the other hand, suggested a luminescent level higher in energy by about 2000 cm^{-1} compared to complexes 8, 9 and 10. Furthermore, the spectral profile of complex 3 was almost

identical to that of $[Ir(tpy)_2]^{3+}$, [7] and not at all like those of 4'-aryl substituted complexes. It is suggested that this is a result of the steric barrier to attainment of a coplanar conformation in the case of the mesityl system, effectively preventing the aryl group from augmenting the conjugation in the excited state, as it does in the other aryl substituted systems, leading to the distinctly different spectra.

Complexes 4 and 5 are deep red in colour, owing to a broad, relatively intense absorption band centred around 500 nm, attributed to an ILCT transition in which the NMe_2 / NPh_2 groups act as electron donors, and the metal bound terpyridine moiety acts as an electron acceptor. Excitation into the ILCT band leads to emission in the near infra-red region (λ_{max}=700-800 nm). The low energy of the excited state can be attributed to the effect of the iridium (III) centre in stabilising the charge-transfer state. Indeed, complexes 4 and 5 appear to be the only Ir (III) bis(terpyridine) complexes reported to date to emit in the near infra-red region of the spectrum.

Finally, attempts to make use of the *in situ* coupling strategy to couple together two metal complexes with complementary functionalities (a bromo-substituted complex and a boronate-substituted complex) have so far proved unsuccessful. Competitive deboronation of the boronate-substituted complex is problematic when the boron atom is in direct conjugation with the metal, whilst a lack of reactivity in the cross-coupling reaction may be due to the unfavourable nature of bringing together charged metal fragments at the transmetallation stage of the cycle.

7.1. References

[1] R.-A. Fallahpour, *Synthesis*, 2003, **No.2**, 155.

[2] A. M. W. Cargill Thompson, *Coord. Chem. Rev*, 1997, **160**, 1.

[3] J.-P. Collin, I. M. Dixon, J.-P. Sauvage, J. A. G. Williams, F. Barigelletti, and L. Flamigni, *J. Am. Chem. Soc*, 1999, **121**, 5009.

[4] K. K.-W. Lo, C.-K. Chung, D. C.-M. Ng, and Zhu.N, *New J. Chem*, 2002, **26(1)**, 81.

[5] M. Licini and J. A. G. Williams, *J. Chem. Soc., Chem. Commun*, 1999, 1943.

[6] W. Goodall and J. A. G. Williams, *J. Chem. Soc., Dalton Trans.*, 2000, 2893.

[7] N. P. Ayala, C. M. Flynn, Jr., L. Sacksteder, J. N. Demas, and B. A. Degraff, *J. Am. Chem. Soc*, 1990, **112**, 3837.

8. Synthetic Procedures and Characterisation

8.1. General Points

All solvents were Analar® quality and were used as supplied, with the exception of acetonitrile, which was HPLC grade. Water was purified using the Purite™ system. Thin layer chromatography was carried out using neutral aluminium oxide plates (Merck Art 5550) or silica plates (Merck Art 5554), both types being fluorescent on irradiation at 254 nm. Preparative column chromatography was carried out using neutral alumina (Aldrich Aluminium Oxide 90, activity I, 70-230 mesh), or using silica (Merck Silica Gel 60, 230-400 mesh).

^{1}H and ^{13}C NMR spectra were recorded on a Varian Mercury 200 (200 and 50.3 MHz respectively), Varian Unity-300 (300 and 75.5 MHz respectively), Varian-400 (400 and 100.6 MHz respectively) or Varian -500 (500 and 125.7 MHz respectively) spectrometer and were referenced to residual protio solvent resonances (^{1}H spectra) or to chloroform (^{13}C). All chemical shifts (δ) are quoted in ppm and coupling constants in Hz.

Electron ionisation (EI) and desorbed chemical ionisation (CI) mass spectra were measured using a Micromass Autospec instrument, with a VG 7070E spectrometer. Electrospray mass spectra were recorded using a VG platform spectrometer. High resolution spectra for accurate mass determinations were carried out by electrospray ionisation at the EPSRC National Mass Spectrometry Service Centre, Swansea.

8.2. Absorbance and Emission Spectra and Lifetimes

UV-Visible absorbance spectra were recorded using a Bio-Tek Instruments Uvikon-XS spectrometer using quartz cuvettes of 1 cm pathlength. Spectra were acquired with a bandwidth of 2 nm using a scan speed of 200 nm min^{-1} and a data interval of 1.0 nm. All spectra were run against a reference of pure solvent contained in a matched cell. Extinction coefficients were calculated using the Beer-Lambert Law: A = ε c l where A is the absorbance, c is the concentration (mol dm^{-3}) and l the path length (cm). The absorbance at a number of different solution concentrations was measured and the extinction coefficient obtained from the gradient of a plot of A against c. For none of

the ligands or complexes investigated was a significant deviation from the Beer-Lambert Law observed.

Steady-state emission spectra were recorded in 1 cm pathlength cuvettes, using an Instruments S.A. Fluromax equipped with a Hamamatsu R928 photomultiplier tube. Spectra were corrected for the wavelength dependence of the detector by multiplication of the data by a correction curve, obtained from the measured profile of a standard lamp. Band-passes of 2.5 or 5.0 nm were typically used, according to the emission intensity of the compound under study. Quantum yields of luminescence were measured using appropriate standards by the method of continuous dilution, which may be summarised as follows:

$$\phi = \frac{no.\ of\ photons\ emitted}{no.\ of\ photons\ absorbed} \propto \frac{E}{A}$$

where A is the area under the absorbance curve in the excitation band and E is the total area of the emission band.

Therefore $\dfrac{\phi_{sample}}{\phi_{std}} = \dfrac{E_{sample}\ /\ A_{sample}}{E_{std}\ /\ A_{std}}$

where "std" denotes values for the standard and "sample" for the compound under investigation. The investigated emission intensity of the standard and the sample were obtained under the same conditions, using minimum excitation slit widths (to minimise the spread of excitation wavelengths). Spectra were acquired for a number of solutions of different absorbance in the range 0.01-0.1 and the emission intensity was plotted against the absorbance. Under these conditions, the luminescence intensity should be directly proportional to the absorbance and a straight line is expected, the gradient of which gives E/A. The ratio of the gradients for sample and standard thus gives the relative quantum yield. Excitation wavelengths were chosen to correspond to reasonably "flat" portions of the absorbance spectra, thereby minimising the uncertainty in the absorbance.

Fluorescence lifetimes of the terpyridine ligands were measured using two techniques. Firstly, an Instruments S.A. Fluorolog τ-3 instrument allowed values to be obtained by global fitting of the demodulation and phase shift of the emission, following excitation with sinusoidally-modulated light over the frequency range 10-250 MHz. A suspension of Ludox® in water was used as the standard, which acts as a scattering sample of τ = 0.0 ns. Secondly, the technique of time-correlated single-photon counting was used to

determine the fluorescence lifetimes of the terpyridine ligands. The excitation source consisted of a pulsed 396 / 370 nm LED, providing output pulses of <1 ns at a repetition rate of 1 MHz. The fluorescence emission was collected at 90° to the excitation source, and the emission wavelength was selected using a monochromator. The fluorescence was detected using a photomultiplier tube linked to a time-to-amplitude converter and multichannel analyser. The instrument response function (IRF) of the apparatus was measured using a dilute suspension of milk powder in water as a scattering medium, giving an IRF with a duration of 1 ns full width at half maximum. The time per channel was typically ~50 ps, giving a full range of ~50 ns over the 1024 point data set. All fluorescence decays were recorded to a minimum of 10,000 counts in the peak channel of the pulse height analyser. The data were transferred to the computer and analysed using the standard method of iterative reconvolution and nonlinear least squares fitting in a Microsoft Excel spreadsheet.

Luminescence lifetimes of the Ir (III) bis(terpyridine) complexes were measured by excitation at 355 nm with the 3rd harmonic of a Q-switched Nd:YAG laser (Spectra Physics GCR-150-10). The energy of the laser was typically 1-2 mJ per pulse with a FWHM of approximately 6 ns. Stray light at 1064 nm (fundamental) and 532 nm (2nd harmonic) was removed by the use of optical filters. Luminescence was collected at 90° to the excitation beam and focused onto the entrance slits of a monochromator (Jobin Yvon Horiba, Triax 320) using a bandpass in the range of 0.1-2.0 nm. The intensity of light at a given wavelength was monitored by a photomultiplier tube (Hamamatsu R928). The transient decays were digitised and averaged by a digital storage oscilloscope (Tetronix TDS-340) over at least 64 laser pulses. The data were transferred to a PC for analysis by Microsoft Excel.

Low temperature spectra and lifetimes (at 77K) were obtained using a variable temperature liquid nitrogen cryostat, Oxford Instruments DN1704, controlled by an Oxford Instruments ITC temperature controller. The sample cell is loaded from the top and positioned at the bottom in a chamber which is pump-filled with dry helium prior to use. The sample is cooled by allowing a flow of liquid nitrogen from an insulated reservoir to the sample space heat exchanger through a capillary tube.

8.3. **Summary of Ligands**

Ligand 1 = 4'-phenyl-2, 2': 6', 2"-terpyridine

Ligand 2 = 4'-(3-aminophenyl)-2, 2': 6', 2"-terpyridine

Ligand 3 = 4'-(4-formyl phenyl)-2, 2': 6', 2"-terpyridine

Ligand 4 = 4'-(4-nitrophenyl)-2, 2': 6', 2"-terpyridine

Ligand 5 = 4'-(4-benzonitrile)-2, 2': 6', 2"-terpyridine

Ligand 6 = 4'-(4-N,N-dimethylaminophenyl)-2, 2': 6', 2"-terpyridine

Ligand 7 = 4'-(4-N,N-diphenylaminophenyl)-2, 2': 6', 2"-terpyridine

Ligand 8 = 4'-mesityl- 2, 2': 6', 2"-terpyridine

Ligand 9 = 4'-(biphen-4-yl)-2, 2': 6', 2"-terpyridine

Ligand 10 = 4'-(4'-cyanobiphen-4-yl)-2, 2': 6', 2"-terpyridine

Ligand 11 = 4'-(4-nitrophenyl)-4-phenyl-2, 2': 6', 2"-terpyridine

Ligand 12 = 4'-(4-N,N-dimethylaminophenyl)-4-phenyl-2, 2': 6', 2"-terpyridine

Ligand 13 = 4'-(4-N,N-diphenylaminophenyl)-4- phenyl-2, 2': 6', 2"-terpyridine

Ligand 14= 4'-(4-pyridyl)-2, 2': 6', 2"-terpyridine (*p*-qtpy)

Ligand 15 = 4'-(3-pyridyl)-2, 2': 6', 2"-terpyridine (*m*-qtpy)

Ligand 16 = "Back to back"-2, 2': 6', 2"-terpyridine

Ligand 17 = 2, 2': 6', 2"-terpyridine (tpy)

Ligand 18 = 4'-(4-tolyl)-2, 2': 6', 2"-terpyridine (ttpy)

Ligand 19 = 4'-bromo-2, 2': 6', 2"-terpyridine (tpy-Br)

Ligand 20 = 4'-(4-bromophenyl)-2, 2': 6', 2"-terpyridine (tpy-φ-Br)

Ligand 21 = 4'-methyl-2, 2': 6', 2"-terpyridine

8.4. Synthesis of Starting Materials and Catalysts

8.4.1. Ethyl 2-pyridine carboxylate[1,2]
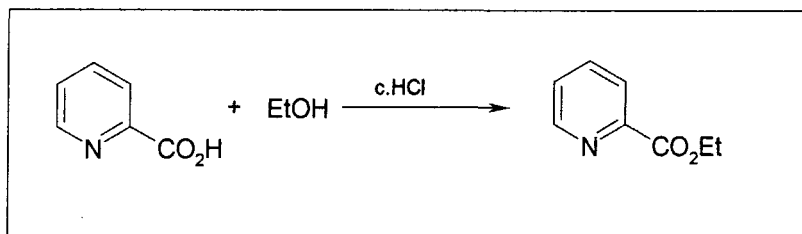
A solution of 2-picolinic acid (20 g) in EtOH (300 mL) to which HCl (37% aq, 18 mL) had been added, was refluxed for 18 h. The reaction was then neutralised with a saturated aqueous solution of Na_2CO_3. Removal of the EtOH and H_2O under reduced pressure left a white sticky solid, which was re-dissolved in the minimum of water. The product was extracted into DCM (3 x 20 mL), the organic layer dried over Na_2CO_3 and the solvent removed under reduced pressure to give the product as a colourless oil (15.2 g, 62%). δ_H (CDCl$_3$): 8.71 (1H, d, H^1, ^3J=4.0), 8.09 (1H, d, H^4, ^3J=7.0), 7.79 (1H, td, H^3, ^3J=6, ^3J=1.5), 7.43 (1H, ddd, H^2, signals too overlapping to resolve J), 4.43 (2H, q, H^{5}and H^6, ^3J=7.0), 1.40 (3H, t, H^7, H^8, H^9, ^3J=7.0).

8.4.2. 4'-Bromo-2, 2': 6', 2"-terpyridine: Ligand 19
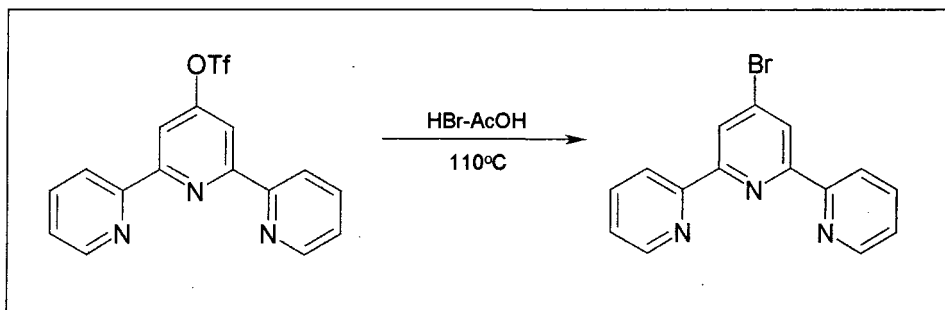
4'-Triflate-2, 2': 6', 2"-terpyridine (made via the procedure of Potts and Konwar)[1] (200 mg, 0.55 mmol) was dissolved in HBr-AcOH (4 mL) and the solution was heated with stirring to 110°C for 6h. The reaction mixture was then allowed to cool to ambient temperature and the solution was poured into ice (50 g). The aqueous solution was then made basic by the addition of KOH pellets, leading to the partial precipitation of the product. The basic aqueous solution was extracted with DCM (3 x 50 mL) and the combined organic fractions dried over K_2CO_3. Evaporation of the DCM led to isolation of the product as a white precipitate (180 mg, 100%). Spectroscopic analysis was

consistent with previously published data.[3] δ_H (CDCl$_3$): 8.70 (2H, d, H^6, ^{3}J=5.5), 8.65 (2H, s, H$^{3'}$), 8.58 (2H, d, H^3, ^{3}J=8), 7.86 (2H, td, H^4, ^{3}J=10, ^{3}J=1.5), 7.36 (2H, ddd, H^5).

8.4.3. Pd(dppf)Cl$_2$ [4]
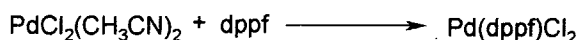
PdCl$_2$(CH$_3$CN)$_2$ (142 mg, 0.55 mmol) and dppf (303 mg, 0.55 mmol) were each placed in a small Schlenk tube fitted with a magnetic stirrer bar. The Schlenk tubes were evacuated and back-filled with nitrogen, before cannula addition of anhydrous, degassed toluene (10 mL to both schlenks). The solution of dppf was transferred via the cannula to the PdCl$_2$ (CH$_3$CN)$_2$ solution and the mixture stirred under nitrogen for 17 h. The toluene was decanted off under nitrogen via a cannula, and the orange solid residue was washed with degassed toluene (3 x 10 mL) and dried under vacuum. δ_H (DMSO): 7.85 (8H, m, phenyl (*ortho*)), 7.49 (12H, m, phenyl (*meta/para*)), 4.53 (4H, s, Cp), 4.23(4H, s, Cp). δ_p (DMSO): 35.4.

8.4.4. 4'-(neopentyl glycolatoboron)-2, 2': 6', 2''-terpyridine.[5]
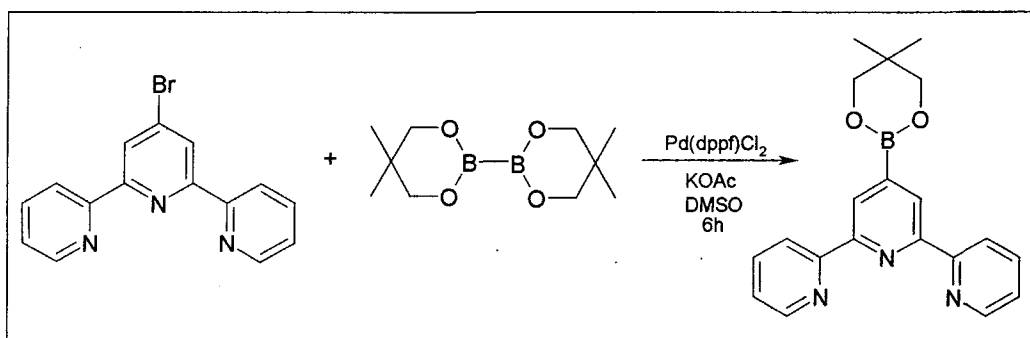
A Schlenk tube was charged with Pd(dppf)Cl$_2$ catalyst (31.3 mg, 0.039 mmol, 0.03 equiv), KOAc (378mg, 3.84 mmol, 3 equiv) and B$_2$neo$_2$ (302 mg, 1.34 mmol, 1.05 equiv), before being evacuated and back-filled with nitrogen. Anhydrous, degassed DMSO (10 mL) and 4'-bromoterpyridine(400 mg, 1.28 mmol, 1 equiv) were then added, and the reaction mixture was stirred under nitrogen at 80°C for 6.0 h. The reaction mixture was then diluted with toluene (100 mL), washed thoroughly with water (5 x 100 mL), and dried over MgSO$_4$. Evaporation of the solvent under reduced pressure

yielded a brown precipitate, which NMR revealed to be a mixture of the product contaminated with "back-to-back" homocoupled terpyridine. For purification, the crude product was dissolved in dichloromethane and extracted into KOH (0.2 M, aq, 3 x 10 mL). The water was then carefully neutralised by addition of HCl until a white precipitate appeared, which was then extracted back into dichloromethane. Evaporation of the solvent led to the desired product as a white solid that was pure by NMR. (236 mg, 54%). δ_H (CDCl$_3$):8.73 (1H, s, H$^{3'}$), 8.65 (1H, d, H^6, ^3J=4.2, ^4J=0.5), 8.54 (1H, d, H^3, ^3J=8.0), 7.78 (1H, td, H^4, ^3J=8.0, ^4J=2.0), 7.25 (1H, ddd, H^5, ^3J=5.0), 3.75 (2H, s, neopentyl CH$_2$), 0.97 (3H, s, neopentyl CH$_3$). m/z (EI): 345 (M$^+$), 330 (M$^+$-Me), 233 (terpy).

8.4.5. Pd(PPh$_3$)$_4$ [6]

$$2PdCl_2 + N_2H_4 + 4PPh_3 \xrightarrow{\text{dmso}} 2Pd(PPh_3)_4 + N_2 + 4HCl$$
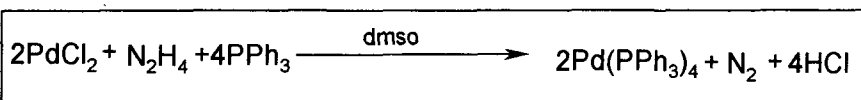
A mixture of palladium dichloride (270 mg, 1.53 mmol), triphenylphosphine (0.8 g, 3.06 mmol) and degassed dimethylsulfoxide (18 mL) was heated with stirring under nitrogen until complete dissolution occurred (ca.140°C). The solution was then cooled to 130°C and stirred rapidly for ca. 15 mins, followed by the addition of hydrazine hydrate (0.3 mL) which initiated a vigorous reaction with the evolution of N$_2$. The reaction mixture was then immediately cooled by immersion of the flask in a bath of boiling water until crystallisation began to occur, at which point the mixture was allowed to cool to ambient temperature without any additional external cooling. The solvent was decanted off via a cannula and the solid was washed under N$_2$ with 2 portions of EtOH (2 x 10 mL) and 2 portions of ether (2 x 10 mL), and then dried by passing a slow stream of N$_2$ over it. The resulting product was a yellow, crystalline, slightly air sensitive material.

8.4.6. 4'-(4-tolyl)-2, 2' : 6', 2''-terpyridine: ligand 18
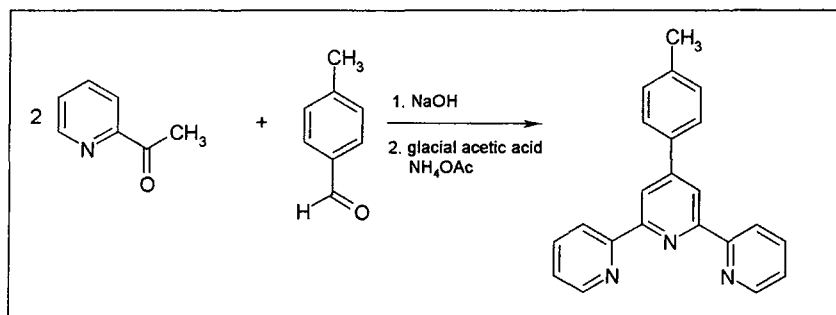
The procedure adopted provides a solvent free route to the immediate precursor of tolyl terpyridine, and is based on a recently described procedure for 4, 2': 6', 4''-terpyridines.[7] 2-Acetylpyridine (4.00 g, 33 mmol), 4-methylbenzaldehyde (1.98 g, 16.5 mmol) and NaOH pellets (1.32 g, 33 mmol) were crushed together with a pestle and mortar for 30 min until a pale yellow sticky gum was formed. The gum was dissolved in 30 mL of glacial acetic acid, with a minimum of DCM added to achieve complete solubilisation. Ammonium acetate (5.0 g) was added and the reaction mixture was refluxed for 2 h affording a dark green solution. After cooling, the mixture was neutralised with saturated potassium carbonate solution, extracted with DCM (3 x 30 mL) and the organic extracts dried over potassium carbonate. Solvent and other volatile material was removed under vacuum yielding a viscous dark green oil, which was purified using a very short column of alumina; gradient elution from 100% hexane to 90% hexane and 10% ethyl acetate (435 mg, 22%). NMR analysis was consistent with previously published data.[8] δ_H (CDCl$_3$): 8.67 (2H, s, H$^{3'}$), 8.66 (2H, d, H^6, ^3J=5.0), 8.61 (2H, d, H^3, ^3J=8.0), 7.83 (2H, td, H^4, ^3J=9.0, ^3J=2.0), 7.77 (2H, d, H^b, ^3J=8.0), 7.3 (2H, ddd, H^5, ^3J=7.5, ^3J=5.0), 7.25 (2H, d, H^a, ^3J=8.5), 2.37 (3H, s, CH$_3$).

8.5. Synthesis of Ligands (Chapter 2)

8.5.1. 4'-(phenyl)-2, 2': 6', 2''-terpyridine: ligand 1
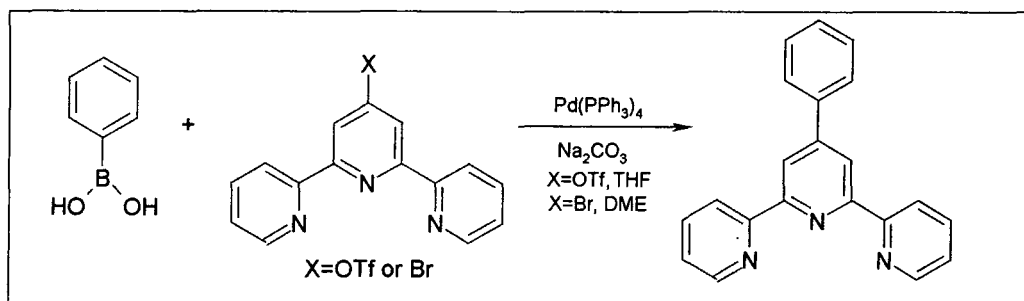
A solution of 4'-triflate terpyridine (250 mg, 0.69 mmol), phenylboronic acid (92 mg, 0.75 mmol) and Na_2CO_3 (182 mg, solubilised in the minimum of water) in THF (7 mL) was degassed via three freeze-pump-thaw cycles. $Pd(PPh_3)_4$ (40 mg, 0.034 mmol) was then added to the solution under a positive pressure of nitrogen, and the resulting mixture was stirred vigorously at room-temperature for 1 h, and then refluxed for 48 h under N_2, during which time the progress of the reaction was monitored using GCMS and TLC. The THF was removed under reduced pressure, and the residue taken up into a mixture of DCM and water. The organic layer was separated and washed with KOH (0.2 M, aq, 3 x 20 mL). After drying over $MgSO_4$ and removal of solvent, spectroscopic analysis of the product showed a mixture of the desired product, PPh_3 and unreacted triflate terpy, from which the product was obtained by recrystallisation from a minimum of ethanol with a few drops of ether added (20 mg, 9.5%). Spectroscopic data was consistent with that previously reported for this compound prepared by a different procedure.[9] δ_H (CDCl$_3$):8.76 (2H, s, $H^{3'}$), 8.74 (2H, d, H^6, ^3J=6.5), 8.68 (2H, d, H^3, ^3J=8.0), 7.92 (2H, d, H^b, ^3J=7.0), 7.90 (2H, td, H^4, ^3J=7.5), 7.52 (2H, t, H^a, ^3J=7.5), 7.46 (1H, t, H^c, ^3J=7.0), 7.37 (2H, ddd, H^5, ^3J=7.5, 5.0). δ_C (CDCl$_3$): 149.0 (C^6), 137 (C^4), 129.0 ($C^{c,b}$), 128.9 (C^a), 127.4 (C^b), 123.9 (C^5), 121.4 (C^3), 119.0 ($C^{3'}$), 156.1, 155.8, 150.4, 138.4 (quaternaries). (Interpretation of proton NMR was carried out with the aid of the NOESY spectrum, and carbon NMR with the aid of HETCOR analysis). m/z (EI$^+$): 309 (M$^+$), 231 (M$^+$-py), 78 (ph). The experiment was later repeated following the same procedure, but starting from 4'-bromoterpyridine in place of 4'-triflate terpyridine, and using DME rather than THF as the solvent. These changes led to a greatly improved yield (80%) and the reaction proceeded much more cleanly with less triphenylphosphine produced as a side product, and complete reaction of all the 4'-bromoterpyridine present.

8.5.2. 4'-(3-aminophenyl)-2, 2': 6', 2''-terpyridine: ligand 2

Method 1
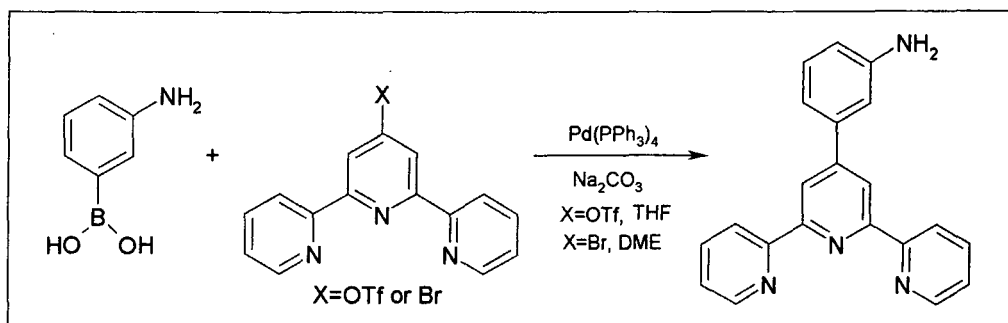
This compound was prepared by the same procedure as that described above for ligand 1, starting from 3-aminophenyl boronic acid (188 mg, 1.21 mmol), in place of phenyl boronic acid, together with 4'-triflate terpyridine (400 mg, 1.1 mmol), Pd(PPh$_3$)$_4$ (65 mg, 0.055 mmol), Na$_2$CO$_3$ (292 mg in 0.8 mL H$_2$O, 2.75 mmol). As before, the mixture was first stirred for 1 h at room temperature, but in this case was then heated under reflux for 3 days, until TLC analysis showed complete consumption of the product. Initial work-up as described above gave a yellow oil, NMR analysis of which showed it to be a mixture of the desired product and triphenylphosphine oxide. The product was dissolved in HCl (1M, 6 mL), and the solution washed with DCM to remove PPh$_3$. The aqueous layer was then made basic by addition of KOH pellets, and the product was extracted into DCM. Evaporation of the solvent gave the pure product (50 mg, 14 %), mp = 235-236°C. δ_H (CDCl$_3$): 8.73 (2H, d, H^6, ^3J=6.0), 8.70 (2H, s, H$^{3'}$), 8.67 (2H, d, H^3, ^3J=10.0), 7.87 (2H, td, H^4, ^3J=9.5, 1.5), 7.34 (2H, dd, H^5, ^3J=9.5, 6.0), 7.29 (1H, m, H^b), 7.28 (1H, m, H^a), 7.22 (1H, s, H^d), 6.77 (1H, dt, H^c,^3J=9.0, 2.5). δ_C (CDCl$_3$): 149.1 (C^6), 136.9 (C^4), 129.8 (C^b), 123.7 (C^5), 121.4 (C^3), 118.9 (C$^{3'}$), 117.7 (C^a), 115.7 (C^c), 113.8 (C^d), 156.3, 155.8, 150.5, 146.9 and 139.5 (Quaternaries). (Interpretation of proton NMR was carried out with the aid of the NOESY spectrum, and carbon NMR with the aid of HETCOR analysis). m/z (EI$^+$): 324 (M$^+$), 246 (M$^+$-py). HRMS(EI): 324.1374 (M$^+$); calc. for C$_{21}$H$_{16}$N$_4$, M: 324.1375.

Method 2

The procedure given in Method 1 was followed, using 4'-bromo terpyridine rather than 4'-triflate terpyridine, and DME rather than THF as the solvent. Once again, the reaction was stirred for 1h at room temperature and then heated at 80°C, this time for

proceeded much more cleanly with less triphenyl phosphine produced as a side product, and complete reaction of all the 4'-bromo terpyridine present.

8.5.4. 4-nitrobenzene-pinacolboronic ester
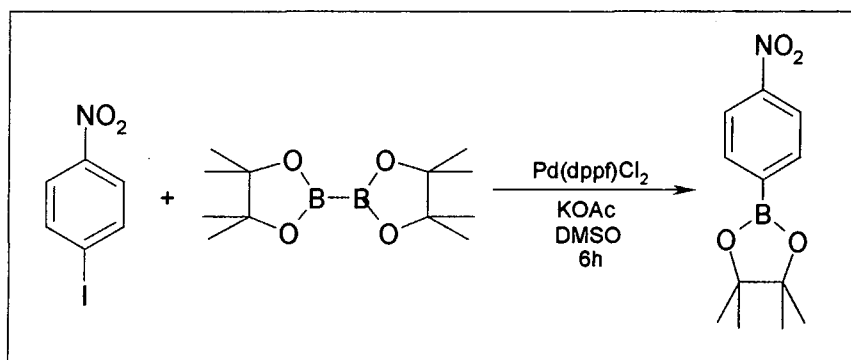
The procedure followed was similar to that described previously for the synthesis of terpyridine neopentyl boronic ester (section 8.3.5) starting from B_2pin_2 (429 mg, 1.69 mmol, 1.05 equiv), 4-iodonitrobenzene (400 mg, 1.61 mmol, 1 equiv), $Pd(dppf)Cl_2$ catalyst (39 mg, 0.05 mmol, 0.03 equiv), KOAc (474 mg, 4.83 mmol, 3 equiv). The reaction mixture was diluted with toluene (50mL), and washed with a small volume of HCl (1M, aq, 2 x 50mL), and dried over $MgSO_4$. Evaporation of the solvent under reduced pressure yielded the crude product, NMR and mass spectral analysis of which confirmed the presence of two compounds, namely the desired product and 4, 4'-dinitrobiphenyl i.e. the product formed from homocoupling of the 4-iodo-nitrobenzene starting material. Purification was achieved by dissolving the product in the minimum volume of DCM, followed by extraction of the product into KOH (0.2M, aq, 3 x 10 mL). Acidification of the aqueous solution led to precipitation of the product, which was isolated via re-extraction into DCM followed by evaporation of the solvent yielding the product as a white solid (165mg, 57%). δ_H (CDCl$_3$): 1.29 (12H, s, CH$_3$), 7.89 (2H, d, Ar, ^3J=8.4), 8.12 (2H, d, Ar, ^3J=8.4). m/z (ES$^+$): 272 (sodium salt of nitrobenzene boronic ester). Analysis of the impurity obtained from the dichloromethane extraction from the acidic water confirmed its identity as 4, 4'-dinitrobiphenyl. δ_H (CDCl$_3$): 8.31 (4H, d, H^1, ^3J=8.5), 7.73 (4H, d, H^2, ^3J=9.0).

The reaction was found to be successful also for 4-bromonitrobenzene, however the yield was slightly lower (due to the formation of more 4, 4'-dinitrobiphenyl than was

formed in the previous reaction), and the reaction time longer (stirring under N_2 at 80°C for 18 h). (250mgs, 34%).

8.5.5. 4-Nitrobenzene neopentyl boronic ester
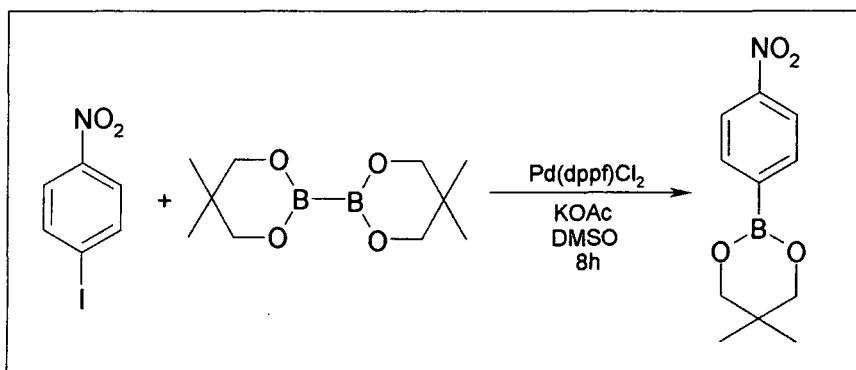
This was prepared in the same way as the pinacol ester above, using B_2neo_2 (1.0 g, 4.42 mmol, 1.05 equivs), 4-iodonitrobenzene (1.04 g, 4.2 mmol, 1 equiv), Pd(dppf)Cl$_2$ (102 mg, 0.13 mmol, 0.03 equivs), KOAc (1.24 g, 12.63 mmol, 3 equivs) and DMSO (~25 mL). The reaction mixture was stirred under nitrogen at 80-85°C for 8 h, after which time it was diluted with toluene, washed twice with HCl (1 M, aq, 2 x 60 mL), and the toluene layer dried over anhydrous magnesium sulphate. Removal of the toluene led to the isolation of the product (628 mg, 64%). NMR analysis revealed no significant competing formation of the homo-coupled product that had occurred during the preparation of the corresponding pinacol ester. δ_H (CDCl$_3$): 8.17 (2H, d, Ar ^{3}J=6.0), 7.94 (2H, d, Ar, ^{3}J=6.0), 3.79 (4H, s, H^b), 1.03 (6H, s, H^a).

8.5.6. 4'-(4-nitrophenyl)-2, 2': 6', 2''-terpyridine: ligand 4

Method 1
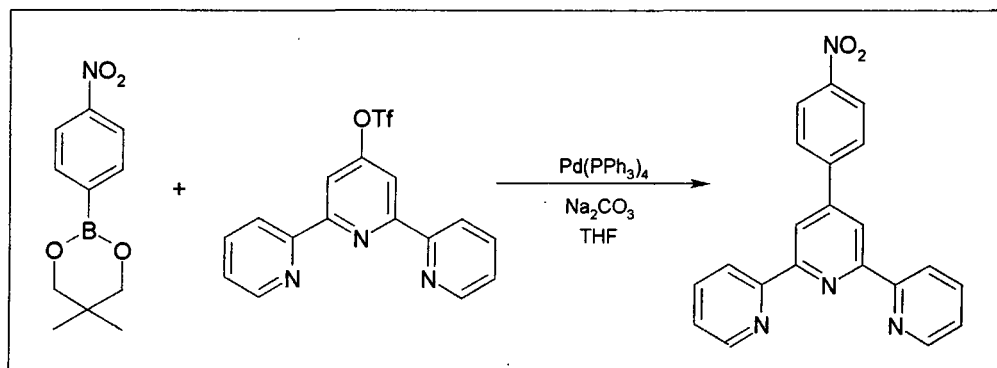
A similar procedure given for the synthesis of ligand 1 was used, starting from triflate terpy (493 mg, 1.35 mmol), 4-nitro benzene pinacol boronic ester (370 mg, 1.49 mmol), Na_2CO_3 (358 mg, dissolved in 1ml water, 3.38 mmol), $Pd(Ph_3P)_4$ (80.0 mg, 0.07 mmol). The reaction was stirred for 1h at room temperature and then refluxed under N_2 for 3h. The solvent was removed to yield a yellow solid that was dissolved in DCM, washed with KOH (0.2 M, aq, 3 x 30 mL), followed by removal of the solvent to isolate the product contaminated with Ph_3P. Recrystallisation from EtOH led to isolation of a small amount of pure product, however the yield was very poor.

The experiment was repeated, this time using the 4-nitro benzene neopentyl boronic ester, and refluxing for 15h rather than 3h. The reactants used in this case were 4-nitrobenzene neopentyl boronic ester (628 mg, 2.67 mmol), triflate terpy (883 mg, 2.42 mmol), $Pd(Ph_3P)_4$ (120mgs, 0.102mmol), Na_2CO_3 (641 mg dissolved in 1.76 mL water, 6.05 mmol). As before, the solvent was removed to yield a yellow solid that was dissolved in DCM, washed with KOH (0.2 M, aq, 3 x 30 mL), followed by removal of the solvent to isolate the product. NMR analysis of the crude product this time showed it to be contaminated with Ph_3P as before, as well as unreacted triflate terpy. The crude product was then dissolved in DCM and washed first with 1M HCl (3 x 15 mL) followed by KOH (0.3 M, aq, 3 x 15 mL). The precipitate from the acidic water wash was collected, dissolved in KOH (0.2 M, aq, 20 mL) and extracted into DCM to yield a yellow/brown solid that contained the product, contaminated with PPh_3. (NMR data as in method 2).

Method 2
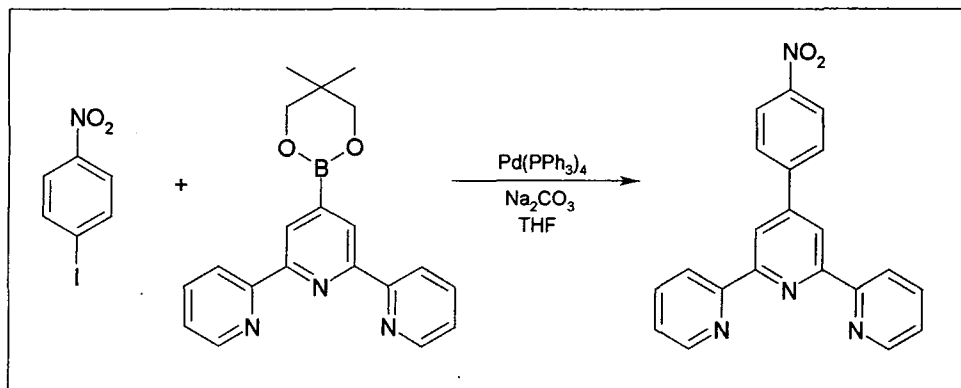
In the second method, the terpyridine boronic ester was coupled with the haloaromatic using Pd(PPh₃)₄ as the catalyst, by a procedure comparable to that of the earlier couplings of terpyridine triflate. The reactants were as follows: terpyridine neopentyl ester (560 mg, 1.62 mmol), 4-iodonitrobenzene (367 mg, 1.47 mmol), Pd(PPh₃)₄ (86 mg, 0.07 mmol), Na₂CO₃ (390 mg, 3.68 mmol). In this case the reaction was stirred for 1.5 h at room temperature and then refluxed for 22 h, with the progress of the reaction monitored by TLC. On completion of the reaction, the THF was removed and the solid was dissolved in DCM. The DCM was then washed with a small quantity of KOH (0.2 M, aq, 3 x 20 mL), and evaporation of the solvent gave a brown solid. NMR analysis showed the solid to contain the desired product as well as some 4-iodonitrobenzene starting material, triphenyl phosphine and homocoupled terpy formed through homocoupling. The crude product was partially dissolved in EtOH with heating to remove the iodonitrobenzene which was found to be much more soluble than the other products. A grey solid was then collected from the ethanol solution after cooling and recrystallised once again from ethanol. However, the product obtained in this way was still slightly contaminated with the homocoupled terpy side product. m/z (ES): 354 (M⁺), 377 (M⁺+Na), 324 (M⁺-NO), 308 (M⁺-NO₂), 465 (bis terpy), 487 (bis terpy +Na), 842 (bis terpy(Na)M⁺). δ_H (CDCl₃): 8.74 (2H, s, H³'), 8.73 (2H, d, H⁶, ³J=4.5), 8.67 (2H, d, H³, ³J=7.5), 8.36 (2H, d, Hᵃ, ³J=8.0), 8.04 (2H, d, Hᵇ, ³J=8.0), 7.90 (2H, td, H⁴, ³J=7.5, 2), 7.32 (2H, ddd, H⁵, ³J=7.5, 4.5, 1.0). δ_C (CDCl₃): 149.2 (C⁶), 137.0 (C⁴), 128.3 (Cᵇ), 124.2 (Cᵃ), 124.2 (C⁵), 121.4(C³), 118.9(C³'), 156.3, 155.6, 147.8, 144.9 and 148.1 (quaternaries). (Interpretation of proton NMR was carried out with the aid of the NOESY spectrum, and carbon NMR with the aid of HETCOR analysis).

8.5.7. 4'-(4-benzophenyl)-2, 2': 6', 2''-terpyridine: ligand 5

Method 1
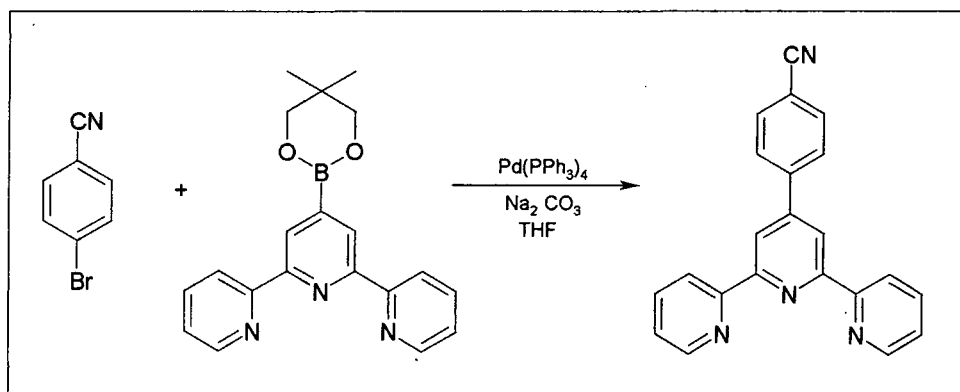
A procedure similar to that described for ligand 4 (method 2) was employed, starting from terpyridine neopentyl boronic ester (530 mg, 1.53 mmol), 4-bromobenzonitrile (253 mg, 1.39 mmol), Na_2CO_3 (368 mg, 3.47 mmol) and $Pd(Ph_3P)_4$ (81 mg, 0.07 mmol). The reaction was stirred for 1.5 h at room temperature followed by refluxing for 16 h. TLC analysis showed that the reaction had progressed rapidly in the first 2 hours of heating, after which the reaction rate slowed dramatically. After 16 h TLC analysis indicated that there remained some starting material, however the reaction was not progressing any further. The solvent was then removed from the reaction mixture, and the solid obtained was dissolved in dichloromethane. The organic layer was washed with KOH (0.2 M, aq, 3 x 20 mL) and evaporation of the solvent led to a green residue. NMR analysis identified the presence of the desired product as well as 4-bromobenzonitrile and "back-to-back" homocoupled terpyridine. Recrystallisation from ethanol followed by purification on a silica column with gradient elution from 100% DCM to 4% MeOH/96% DCM gave the most pure sample of the final product, although NMR analysis revealed still a trace of the "back-to-back" homocoupled terpyridine product (176 mg, 34 %). δ_H (CDCl$_3$): 8.74 (2H, s, H$^{3'}$), 8.73 (2H, d, H^6, ^3J=5.0), 8.69 (2H, d, H^3, ^3J=8.0), 8.00 (2H, d, H^b, ^3J=8.5), 7.90 (2H, td, H^4, ^3J=7.5, 2.0), 7.82 (2H, d, H^a, ^3J=10.0), 7.32 (2H, ddd, H^5, ^3J=6.0, 5.0, 1.5). δ_C (CDCl$_3$): 148.3 (C^6), 137.0 (C^4), 132.7 (C^a), 128.0 (C^b), 124.1 (C^5), 121.3 (C^3), 118.6 (C$^{3'}$), 112.6 (CN), 156.3, 155.7, 143.1 and 118.7(quaternaries). m/z (EI): 334 (M$^+$), 256 (M$^+$-py). HRMS(EI): 334.1211 (M$^+$); calc. for C$_{22}$H$_{14}$N$_4$, M: 334.1218. (Interpretation of proton NMR was carried out with the aid of the NOESY spectrum, and carbon NMR with the aid of HETCOR analysis).

Method 2
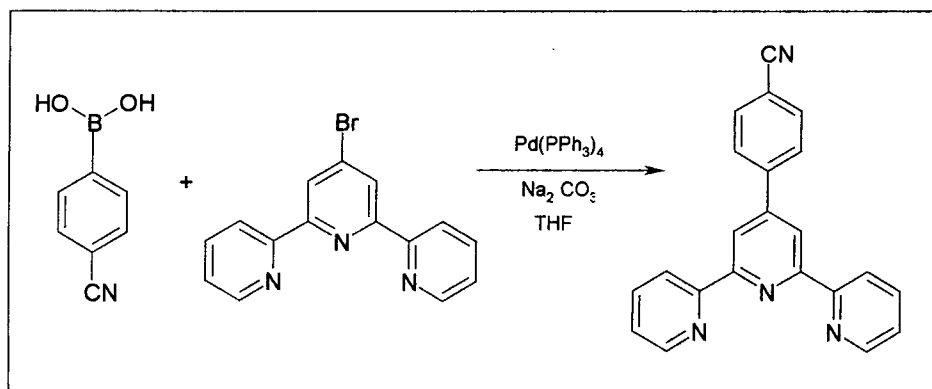
A similar procedure was adopted, but using 4'-bromo terpyridine (583 mg, 1.87 mmol) in place of the terpyridine boronate, and 4-benzonitrile boronic acid (302 mg, 2.06 mmol) in place of 4-bromobenzonitrile, together with $Pd(PPh_3)_4$ (110 mg, 0.09 mmol), and Na_2CO_3 (496 mg, 4.68mmol) in THF (20 mL). The reaction was stirred at room temperature for 1.5 h, and then refluxed under nitrogen for 48 h, with the progress of the reaction monitored by TLC. The procedure for the work-up was the same as that given in method 1, except this time the product was easily purified by recrystallisation from ethanol, without the need for a column. (497 mg, 80%), mp = 202-203°C. (See above NMR and mass spectral data).

8.5.8. 4'-(di-methylamino phenyl)-2, 2': 6', 2''-terpyridine: ligand 6
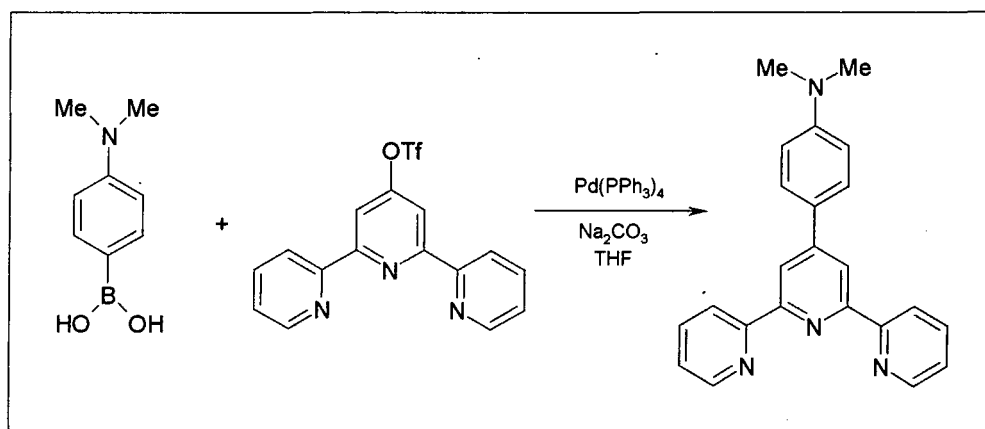
A similar procedure to that described for ligand 1 was employed, starting from: 4'-triflate terpyridine (700 mg, 1.92 mmol), N, N-dimethyl-amino-benzene boronic acid (348 mg, 2.11 mmol), Pd(PPh$_3$)$_4$ (113 mg, 0.096 mmol), and Na$_2$CO$_3$ (509 mg dissolved in 1.6 mL water, 4.8 mmol), in THF (14 mL). The reaction mixture was stirred at room temperature for 1 h, and refluxed under N$_2$ for 15 h. Upon completion of the reaction, the THF was removed under reduced pressure and the residue was dissolved in DCM and washed with KOH (0.2 M, aq, 3 x 20 mL). The yellow solid obtained upon removal of the DCM was shown by NMR analysis to be the desired product contaminated with a small amount of PPh$_3$. Purification was achieved by dissolving the product in HCl (1M, 6 mL) and washing with DCM, followed by addition of NaOH pellets to the acidic layer (pH 11), and re-extraction of the product into DCM. Evaporation of the solvent led to isolation of the pure product (479 mg, 65%), mp = 206-207°C. δ_H (CDCl$_3$): 8.75 (2H, d, H^6, ^3J=5.0), 8.74 (2H, s, H$^{3'}$), 8.68 (2H, d, H^3, ^3J=8.0), 7.90 (2H, d, H^b, ^3J=9.0), 7.88 (2H, td, H^4, ^3J=7.5), 7.36 (2H, ddd, H^5, ^3J=7.5, 5.0, 1.0), and 6.83 (2H, d, H^a, ^3J=9.0), 3.05 (6H, s, CH$_3$). δ_C (CDCl$_3$): 150.1 (C^6), 137.2 (C^4), 128.1 (C^b), 123.7 (C^5), 121.5 (C^3), 117.7 (C$^{3'}$), 112.4 (C^a), 156.3, 155.3, 151.1, 148.8, 125.0 (quaternaries), 40.4 (CH$_3$). (Interpretation of proton NMR was carried out with the aid of the NOESY spectrum, and carbon NMR with the aid of HETCOR analysis). m/z (EI$^+$):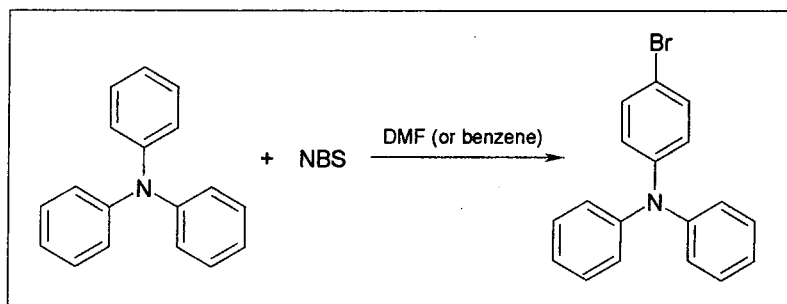 352 (M$^+$), 308 (M$^+$-NMe$_2$). HRMS(EI): 352.1686 (M$^+$); calc. for C$_{23}$H$_{20}$N$_4$, M: 352.1688. Found C, 76.71, H, 5.58, N, 16.32; calc. for C$_{23}$H$_{20}$N$_4$·0.5H$_2$0: C, 76.43, H, 5.86, N, 15.5.

8.5.9. 4-bromo-N, N-diphenylaniline

Method 1.[10, 11]

A solution of NBS (1.45 g, 0.01 moles) in dry DMF (40 mL) was added to a solution of triphenylamine (2 g, 0.01 moles) in dry DMF (40 mL) and stirred at room temperature for 24h. The mixture was then poured into water (200 mL) and extracted with DCM. The extract was washed well with water, dried ($MgSO_4$) and evaporated under pressure to yield the crude product. GCMS analysis showed the presence of the desired product contaminated with starting material and the di-brominated product. Repeating the experiment in benzene rather than DMF as the solvent failed to improve the selectivity of the bromination, yielding a mixture of starting material, the desired product and di-brominated product as before.

8.5.10. 4-bromo-N, N-diphenylaniline

Method 2[12]
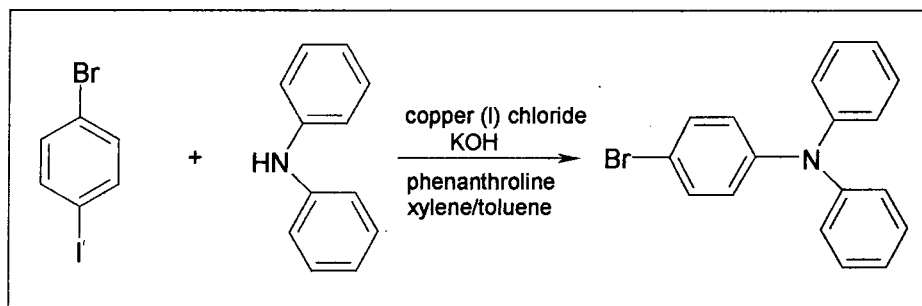
To a 100 mL round-bottomed flask equipped with a mechanical stirrer, a nitrogen gas purge, a small Dean-Stark trap under a reflux condenser and containing xylene (10 mL), the following reactants were added in the order given while maintaining good stirring; diphenylamine (1.86 g, 0.01 moles), 1-bromo-4-iodobenzene (3.11 g, 0.01 moles), 1,10-

phenanthroline (72mg, 0.4 mmol), cuprous chloride (40mg, 0.4mmol) and potassium hydroxide flakes (4.83g, 0.09moles). The reaction was rapidly heated over the course of 30 mins to reflux, however difficulties were experienced in obtaining sufficient reflux of the xylene in order to collect water in the Dean-Stark trap, so a small volume of toluene (5 mL) was added to lower the boiling point. After refluxing for 48 h the reaction mixture was cooled to 75°C and partitioned between toluene (50 mL) and water (50 mL). After washing with an additional amount of water (100 mL), the organic phase was decolourised by refluxing in the presence of Al_2O_3 (4 g), the adsorbents were then removed by hot filtration, and the solvent removed under pressure. The product was subject to further purification by column chromatography on silica with gradient elution from 100% hexane to 74% hexane/26% toluene; the product was observed on the column as a bright purple band under long wave UV light. The purity of the final product was checked using GCMS where a single peak was observed m/z: (325). (1.48g, 41%). Spectroscopic data were consistent with those previously reported for this compound prepared by bromination of triphenylamine.[10]

8.5.11. 4-(neopentylglycolatoboron)-N, N-diphenylaniline
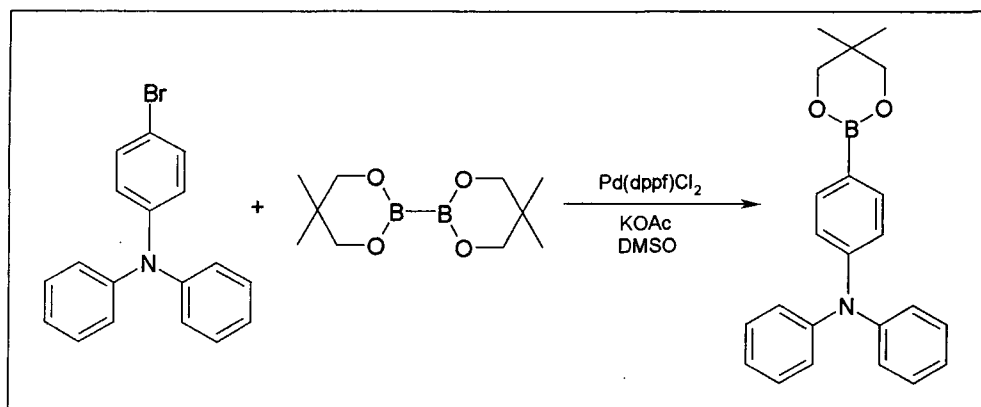
The procedure followed was similar to that described previously for the synthesis of terpyridine neopentyl boronic ester starting from 4-bromo-N,N-diphenylaniline (500mg, 1.54 mmol, 1equiv), B_2neo_2 (366 mg, 1.62mmol, 1.05 equiv), KOAc (454 mg, 4.62mmol, 3 equiv), Pd(dppf)Cl$_2$ (39 mg, 0.05mmol, 0.03 equiv). Purification was achieved by the same method as that employed for the terpyridine neopentyl boronic ester (500mg, 93%). m/z (ES+): 358 (100%, M+H$^+$). δ_H (CDCl$_3$): 7.69 (2H, d, H *ortho* to B, ^3J=6.5), 7.27 (4H, t, *meta* H of pendent Ph, ^3J=7.5), 7.13 (4H, d, *ortho* H of

pendent Ph, ^3J=7.5), 7.06 (2H, d, H *meta* to B, ^3J=6.5), 7.04 (2H, t, *para* H of pendent Ph, ^3J=5.0), 3.77 (4H, s, CH_2), 1.04 (6H, s, CH_3).

8.5.12. 4'-(4-N, N-diphenylaminophenyl)-2, 2': 6', 2''-terpyridine: ligand 7
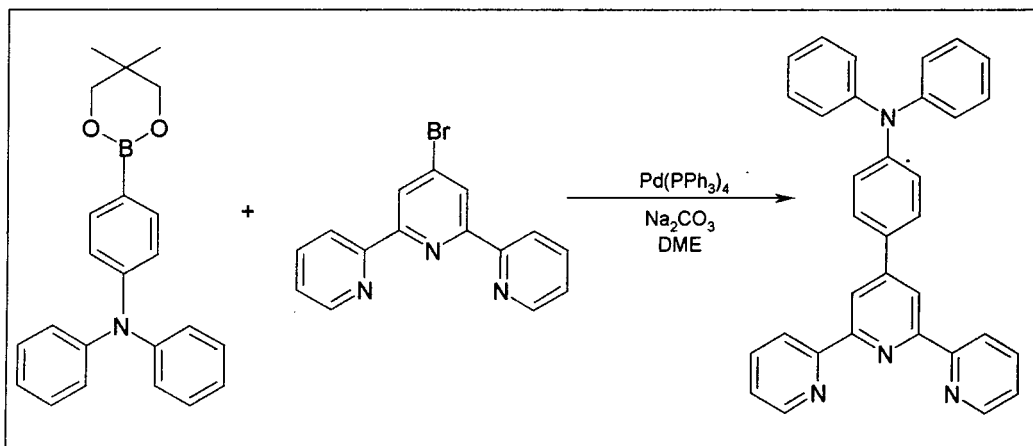
The procedure followed was similar to that described previously for the synthesis of ligand 1 starting from 4-(neopentylglycolatoboron)-N, N-diphenylaniline (512.3 mg, 1.43 mmol), tpy-Br (405.6 mg, 1.3 mmol), Pd(PPh₃)₄ (76.4 mg, 0.065 mmol), and Na₂CO₃ (344.5 mg, 3.25 mmol, dissolved in 1.5 mL of water). For this experiment, DME was used as a solvent rather than THF, and the reaction was stirred for 1 h at room temperature before heating at 80°C for 24 h. The product obtained after the work-up was slightly contaminated with PPh₃, which was removed by recrystallisation from EtOH. (400mg, 59%), mp = 213-214°C. δ_H (CDCl₃): 8.72 (2H, d, H^6, ^3J=4.0), 8.71 (2H, s, $H^{3'}$), 8.67 (2H, d, H^3, ^3J=7.5), 7.87 (2H, td, H^4, ^3J=8.0, 2.0), 7.79 (2H, d, H^b, ^3J=8.5), 7.35 (2H, ddd, H^5, ^3J=7.5, 5.0, 1.0), 7.30 (4H, t, (o-Ph), ^3J=7.5), 7.17 (2H, d, H^a, ^3J=8.0), 7.17 (4H, dd, (m-Ph), ^3J=8.0, 5.0), 7.07 (2H, t, (p-Ph), ^3J=7.5). δ_C (CDCl₃): 148.7 (C^6), 136.8 (C^4), 129.4 (C^a), 128 (C^b), 124.8 (m-Ph), 123.8 (C^5), 123.3 (o-Ph), 123.1 (p-Ph), 121.4 (C^3), 118.3 ($C^{3'}$), 156.3, 155.8, 149.7, 149.2, 147.4 and 131.8 (quaternaries). (Interpretation of proton NMR was carried out with the aid of the NOESY spectrum, and carbon NMR with the aid of HETCOR analysis). m/z (CI): 477 (M+H⁺).

8.5.13. 4'-(4-N, N-diphenylaminophenyl)-4-phenyl-2, 2': 6', 2''-terpyridine: ligand 13
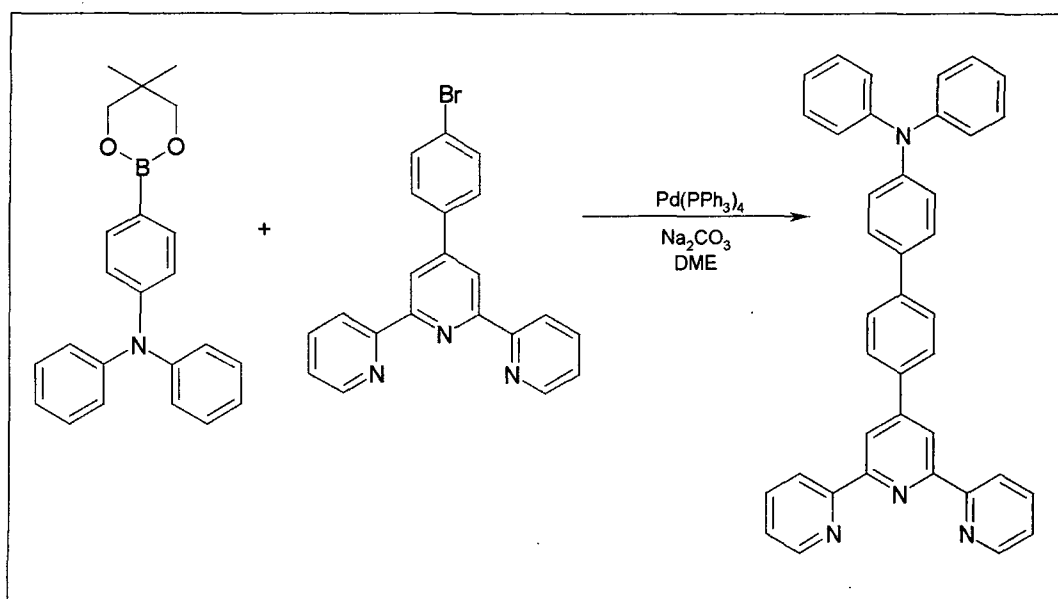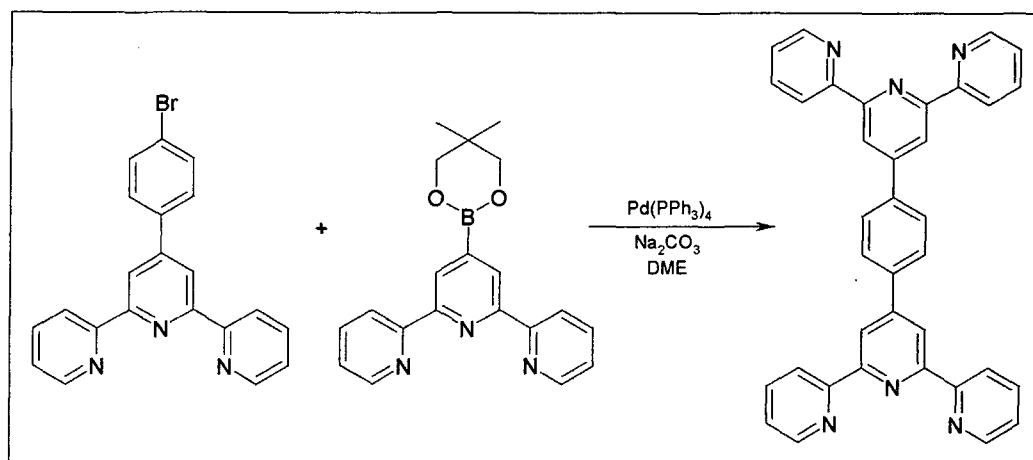

The procedure followed was similar to that described previously for the synthesis of ligand 1 starting from 4-(neopentylglycolatoboron)-N, N-diphenylaniline (90 mg, 0.25 mmol), bromophenylterpy (88 mg, 0.23 mmol), Pd(PPh₃)₄ (14 mg, 0.01 mmol), Na₂CO₃ (64 mg, 0.6 mmol). After completion of the work-up procedure, NMR analysis revealed the presence of the desired compound in the crude product. Purification was achieved by recrystallisation from ethanol, followed by column chromatography on alumina with DCM/MeOH as the eluting solvent. (85 mg, 67%).

δ_H (CDCl₃): 8.79 (2H, s, $H^{3'}$), 8.74 (2H, d, H^6, $^3J=4.0$), 8.69 (2H, d, H^3, $^3J=8.0$), 7.99 (2H, d, H^b, $^3J=8.0$), 7.89 (2H, td, H^4, $^3J=8.0$, 2.0), 7.72 (2H, d, H^a, $^3J=8.5$), 7.56 (2H, d, $H^{b'}$, $^3J=8.5$), 7.36 (2H, ddd, H^5, $^3J=7.5$, 5.0, 1.0), 7.29 (4H, t, (m-Ph), 8.5), 7.17 (2H, d, $H^{a'}$, $^3J=7.5$), 7.17 (4H, d, (o-Ph), 7.0), 7.05 (2H, t, (p-Ph), 7.0). δ_C (CDCl₃): 149.8 (C^5), 149.1 (C^6), 136.9 (C^4), 129.3 (m-Ph), 127.5 (C^b), 127.0 (C^a), 126.7 ($C^{b'}$), 124.5 ($C^{a'}$), 123.8 (o-Ph), 123.0 (p-Ph), 121.4 (C^3), 118.6 ($C^{3'}$), 156.3, 155.9, 149.8, 147.5, 141.3, 136.9, 136.7 and 134.1 (quaternaries). (Interpretation of proton NMR was carried out with the aid of the NOESY spectrum, and carbon NMR with the aid of HETCOR analysis). m/z (CI): 553 (M+H⁺).

8.5.14. "Back to back"-2, 2': 6', 2''-terpyridine: ligand 16

The procedure followed was similar to that described previously for the synthesis of ligand II starting from terpyridine neopentyl boronic ester (260 mg, 0.75 mmol), 4'-bromo phenyl terpyridine (264 mg, 0.68 mmol), Pd(PPh₃)₄ (40 mg, 0.034 mmol), and Na₂CO₃ (183 mg, 1.73 mmol, dissolved in the minimum volume of water), in DME (6 mL). The reaction was stirred under nitrogen at room temperature for 45 mins before heating at 85°C for ca. 40 h. After the reaction had cooled to room temperature, the solvent was removed and the remaining white solid was dissolved in DCM and washed with KOH (0.2 M, aq, 3 x 20 mL). Unfortunately, evaporation of the organic layer resulted only in a brown solid that did not contain the desired product. However the aqueous layer contained some white solid/emulsion, which extracted into DCM after careful neutralisation of the water through the addition of 1M HCl, to reveal the pure product as a white solid upon evaporation of the DCM. (255 mg, 69%). δ_H (CDCl₃): 8.78 (4H, s, H$^{3'}$), 8.74 (4H, d, H^6, ^{3}J=5), 8.67 (4H, d, H^3, ^{3}J=8), 8.05 (4H, s, arom), 7.88 (4H, td, H^4, ^{3}J=7), 7.35 (4H, dd, H^5).

8.6. Synthesis of Complexes (Chapter 6)

8.6.1. Ir(Ligand(18))Cl₃: Intermediate 1[13]
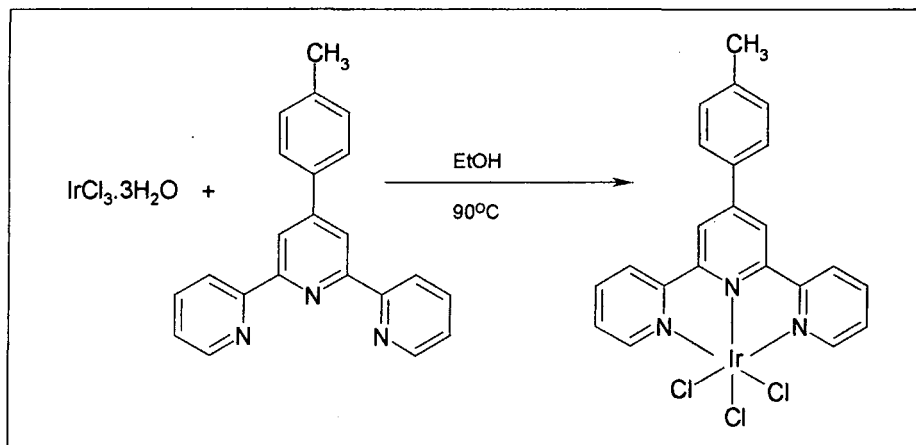
$IrCl_3 \cdot 3H_2O$ (356 mg, 1.01 mmol) was added to a solution of 4'-(4-tolyl)-terpyridine (326 mg, 1.01 mmol) dissolved in EtOH (23 mL). The solution was refluxed for 3 h and then allowed to cool. The brown solid that precipitated out was washed with toluene followed by EtOH and finally Et_2O, and dried under vacuum (380 mgs, 61 %). v_{max} (KBr): 3064m (Ar-H), 2950 (aliphatic C-H), 1617m (CN), 1597s (aromatic ring), 1470-1430w (CH_3). Due to the insoluble nature of the solid, the crude material was used in subsequent reactions without further purification.

181

8.6.2. Ir(Ligand(21)Cl₃: Intermediate 2
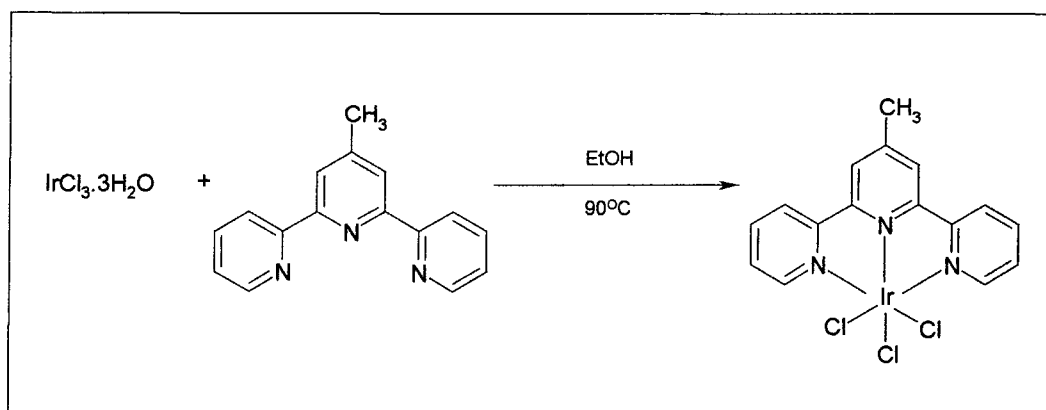
Intermediate 2 was prepared using a similar procedure, from: 4'-(4-methyl)-2, 2': 6', 2"-terpyridine (300 mg, 1.21 mmol) and $IrCl_3·3H_2O$ (427 mg, 1.21 mmol) in ethanol. In this case the mixture was refluxed for 4 h. Due to the insoluble nature of the solid, the crude material was used in the subsequent stage without further purification. (500 mg, 75%).

8.6.3. Ir(Ligand 17)Cl₃: Intermediate 3[13]
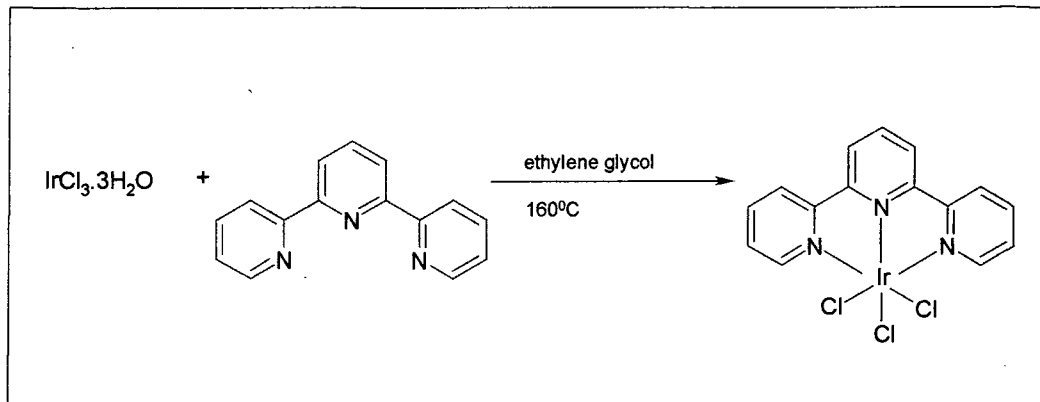
2, 2': 6', 2"-terpyridine (219 mg, 0.94 mmol) and $IrCl_3·3H_2O$ (333 mg, 0.94 mmol) were heated at 160°C in anhydrous ethylene glycol (12 mL), under nitrogen and in the dark for 15 mins, during which time a red precipitate formed. Upon cooling to ambient temperature, the precipitate was collected and washed with EtOH, H_2O and Et_2O to yield pure Ir(tpy)Cl₃. (221 mg, 44%). δ_H (CD₃CN): 9.23 (2H, dd, H^6, ^3J=5.0, ^4J=0.7), 8.78 (2H, d, H^3, ^3J=8.2), 8.74 (2H, d, $H^{3'}$, ^3J=8.0), 8.34-8.20 (3H, m, H^4 and $H^{4'}$), 7.98 (2H, ddd, H^5, ^3J=6.0, ^4J=0.5).

8.6.4. Ir(Ligand 19)Cl₃: Intermediate 4
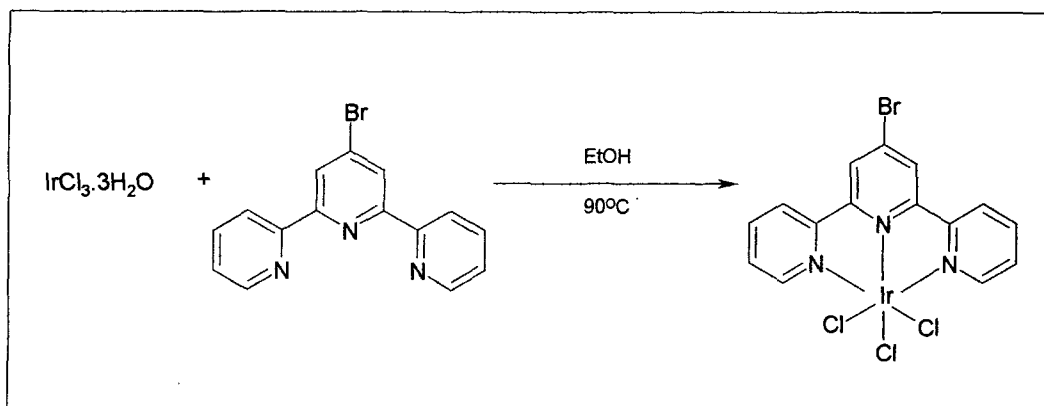
Intermediate 4 was prepared similarly from 4'-(4-bromo)-2, 2': 6', 2"-terpyridine (300 mg, 0.96 mmol) and IrCl₃·3H₂O (339 mg, 0.96 mmol). Due to the insoluble nature of the solid, the crude material was subsequently used without further purification. (400 mg, 68%).

8.6.5. [Ir(Ligand 18)(CF₃SO₃)₃]: Intermediate 5[14]
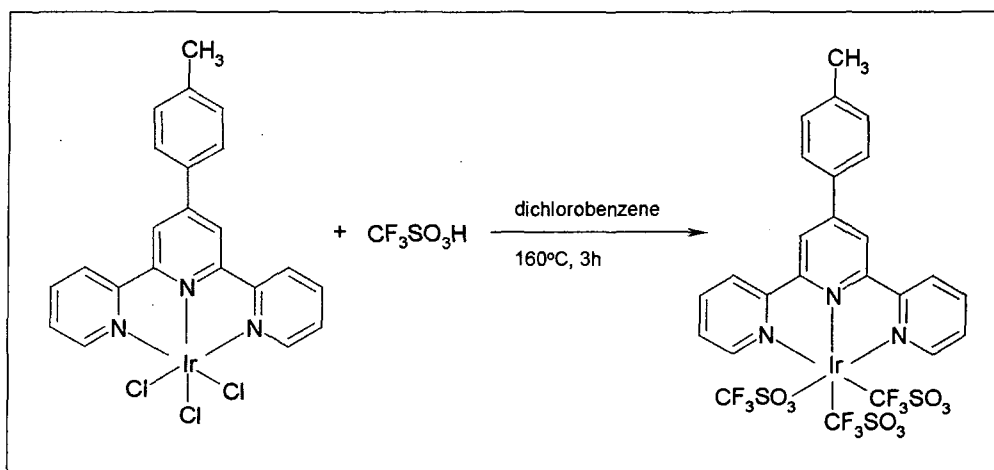
A mixture of Ir(ttpy)Cl₃ (Intermediate 1) (212 mg, 0.34 mmol) and trifluoromethanesulphonic acid (1.5 mL, 17 mmol) was heated in dichlorobenzene (25 mL) at 160°C for 3h. The reaction was then allowed to cool to room temperature, the solvent and excess acid were carefully removed by decantation, and the remaining yellow semi-solid was washed with copious amounts of petroleum ether followed by dichloromethane. The pure product was then obtained from the remaining solid by recrystallisation from a mixture of acetone and petroleum ether. Spectroscopic data was

consistent with that previously published. (135 mg, 41%). δ_H (acetone): 9.33 (2H, dd, H^6, ^3J=5.5, 1.0), 9.23 (2H, s, $H^{3'}$), 9.06 (2H, d, H^3, ^3J=7.5), 8.56 (2H, td, H^4, ^3J=6.0, 1.5), 8.29 (2H, ddd, H^5, ^3J=7.5, 6.0, 1.5), 8.20 (2H, d, H^a, ^3J=-8.0), 7.56 (2H, d, H^b, ^3J=8.0), 2.54 (3H, s, CH_3).

8.6.6. [Ir(Ligand 8)$_2$]$^{3+}$: Complex 3.
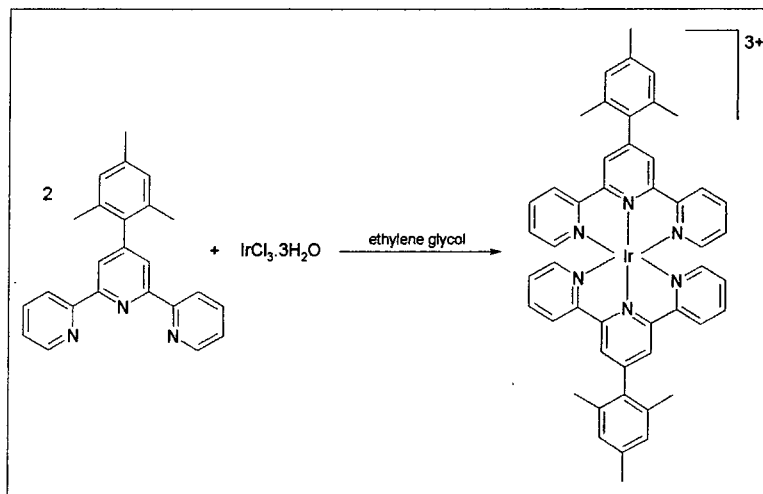
$IrCl_3.3H_2O$ (102 mg, 0.29 mmol) and 4'-(mesityl)- 2, 2': 6', 2"-terpyridine (200 mg, 0.57 mmol) were dissolved in ethylene glycol (25 mL) and heated with stirring under N_2 at 100°C for 2.5 h, followed by a further 1.5 h at 190°C. After allowing the solution to cool to ambient temperature, it was added to a saturated aqueous solution of KPF_6 to precipitate the crude product as an orange solid. Recrystallisation from acetone and toluene yielded the pure product as a pale yellow solid. (150 mg, 38%). The complex was observed as a single yellow spot with R_f = 0.80 upon TLC analysis on silica plates, using 70% CH_3CN / 26% H_2O / 4% KNO_3 as the solvent. δ_H (d_6-acetone): 9.16 (2H, s, $H^{3'}$), 9.02 (2H, d, H^3, ^3J=8), 8.39 (2H, td, H^4, ^3J=8), 8.21 (2H, d, H^6, ^3J=4.0), 7.66 (2H, ddd, H^5, ^3J=8.0), 7.19 (2H, s, H^a), 2.36 (6H, s, CH_3), 2.42 (3H, s, CH_3). δ_C (d_6-acetone): 143 (C^4), 130 (C^5), 129 (C^a), 128 ($C^{3'}$), 128 (C^6). m/z (ES^+): 894 (M^+), 520 (M^++PF_6)/2. HRMS(ES^+): 1185.2384 (M+2PF_6)$^+$; calc. for ($C_{48}H_{42}N_6Ir$)(PF_6)$_2$, (M+2PF_6)$^+$: 1185.2384.

8.6.8.   [Ir(Ligand 7)₂]³⁺ : complex 5
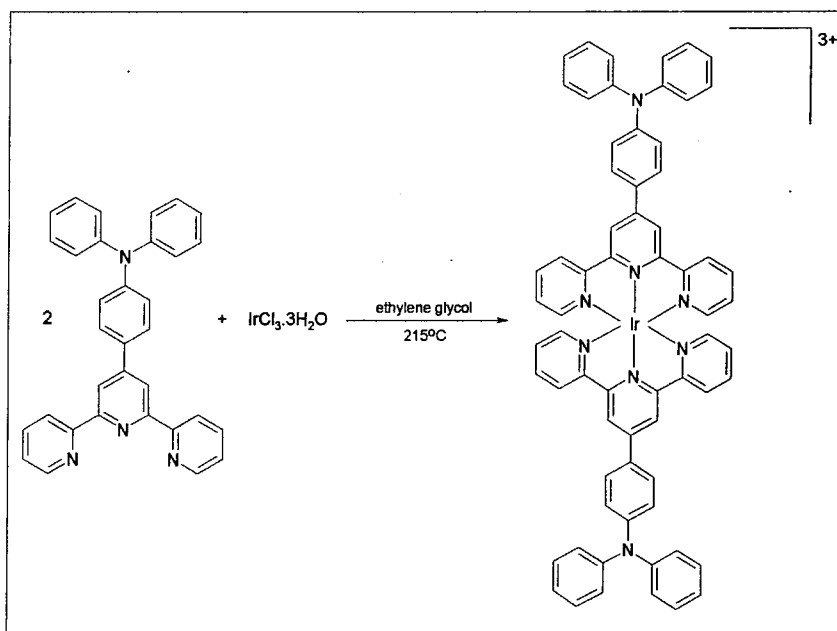
4'-(4-N, N-diphenylaminophenyl)-2, 2': 6', 2"-terpyridine (200 mg, 0.42 mmol, 2 equiv) and IrCl₃.3H₂O (74.1 mg, 0.21 mmol, 1 equiv) were dissolved in ethylene glycol (15 mL) and heated with stirring at 90°C for 2 h, followed by a further 2.5 h at 165°C. The solution was then added to a saturated aqueous solution of KPF₆ to precipitate the crude product as the hexafluorophosphate salt. However, NMR analysis showed that the reaction had stopped after coordination of the first ligand to form the intermediate. The intermediate was then re-dissolved in ethylene glycol, further ligand (100 mg) was added and the solution was heated for 6 h with stirring at 215°C. Once again the solution was added to KPF₆ (aq) to precipitate the crude product, NMR analysis of which suggested that it contained a mixture of the desired complex and unreacted ligand. The majority of the ligand was removed by washing the solid with toluene, and the remainder by column chromatography on silica using a gradient elution from 100% CH₃CN to 91.6 % CH₃CN / 8% H₂O / 0.4 % KNO₃. After ion-exchange using KPF₆ (aq, sat), a second column on alumina was required to remove a fluorescent yellow impurity, gradient elution from 100% CH₃CN to 93.4% CH₃CN / 6% H₂O / 0.6% KNO₃. Another ion exchange was carried out to obtain the product as the PF₆⁻ salt. (55 mg, 17%). δ_H (acetone): 9.42 (2H, s, H³'), 9.10 (2H, d, H³, ³J=8.0), 8.33 (2H, td, H⁴, ³J=5.0, 1.0), 8.24 (2H, d, Hᵇ or Hᵃ, ³J=9.0), 8.21 (2H, d, H⁶, ³J=6.0), 7.60 (2H, td, H⁵, ³J=5.0), 7.45 (4H, overlapping t and d, (p-ph) and Hᵃ or Hᵇ), 7.26 (8H, overlapping t and d, o-/m-ph). m/z (ES⁺): 1144 (M⁺), 572 (M²⁺), 645 (M⁺+PF₆)/2.

8.6.9. [Ir(Ligand 12)₂]³⁺ : complex 6
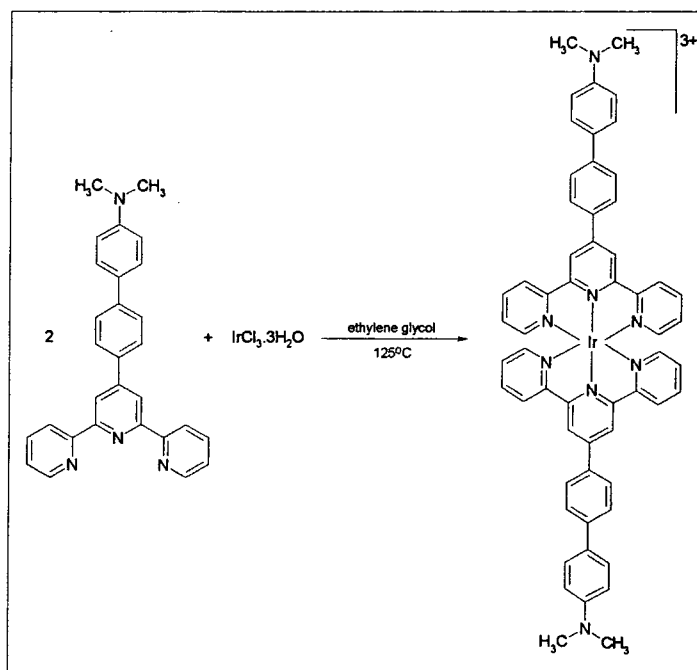
4'-(4-N,N-dimethylaminophenyl)-4-phenyl-2, 2': 6', 2"-terpyridine (51 mg, 0.12 mmol) and IrCl₃.3H₂O (21 mg, 0.06 mmol) were dissolved in ethylene glycol (6 mL) and heated with stirring at 215°C for 30 mins. Once cooled to ambient temperature, the clear red solution was added to water, upon which a small amount of solid precipitated, which was separated using a centrifuge. The remaining clear solution was then added to a saturated KPF₆ solution to precipitate the crude product as a red solid, which was washed with water. Purification of the product was achieved through column chromatography on silica using a gradient elution from 100% CH₃CN to 83.5 % CH₃CN / 15% H₂O / 1.5 % KNO₃, followed by ion exchange using KPF₆ (aq, sat) of the fractions that contained the product. A second column on alumina with gradient dilution from 100% CH₃CN to 91.5% CH₃CN / 8% H₂O / 0.5% KNO₃ resulted in isolation of the pure product which was ion exchanged using KPF₆ (aq, sat) as before. (4 mg, 5%). δ_H (CD₃CN): 9.22 (4H, s, H³'), 8.85 (4H, d, H³, ³J=8.0), 8.38 (4H, d, Hᵃ, ³J=8.0), 8.34 (4H, t, H⁴, ³J=7.5), 8.15 (4H, d, Hᵇ, ³J=8.0), 7.87 (4H, d, Hᵇ', ³J=8.0), 7.81 (4H, d, H⁶), 7.60 (4H, t, H⁵, ³J=7.0), 7.02 (4H, d, Hᵃ', ³J=8.5). m/z (ES⁺): 524 (M²⁺), 597 (M⁺+PF₆)/2.

8.6.10. [Ir(L^{17})(L^{20})]$^{3+}$: Complex 7.
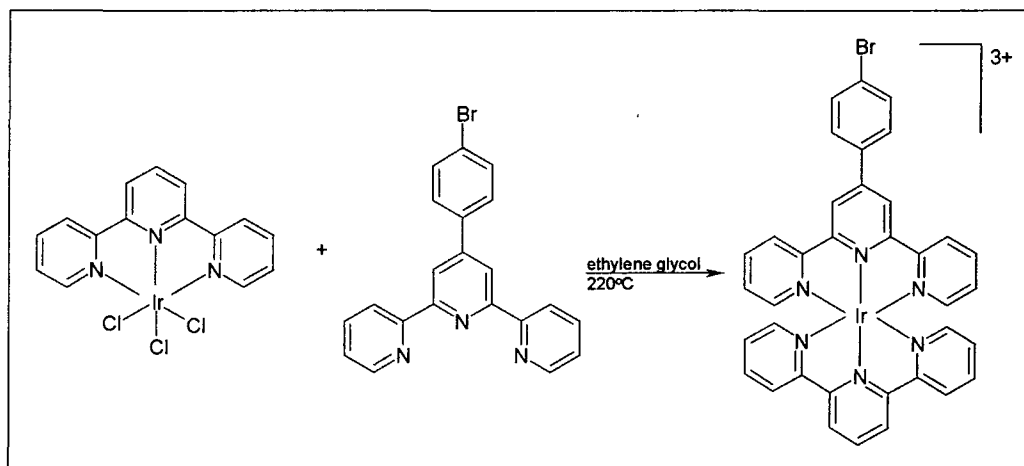
A mixture of Ir(tpy)Cl$_3$ (220 mg, 0.41 mmol) and 4'-bromophenylterpyridine (159 mg, 0.41 mmol) in ethylene glycol (12 mL) was heated at 220°C until a clear red solution was obtained (15 mins). After cooling to ambient temperature, the solution was diluted with water (40 mL), and the small amount of red precipitate obtained (unreacted Ir(tpy)Cl$_3$) was separated off by centrifugation. The remaining solution was then treated with saturated aqueous KPF$_6$ (10 mL), precipitating the crude product as the hexafluorophosphate salt, which was collected and washed with water. Purification was achieved by column chromatography on silica, gradient elution from CH$_3$CN to 53% CH$_3$CN / 45% H$_2$O / 2% KNO$_3$ (satd, aq). Fractions containing the product were concentrated under reduced pressure and subject to a second metathesis with KPF$_6$, leading to the required complex. (200 mg, 60%). δ_H (CD$_3$CN): 9.05 (2H, s, H$^{3'}$on Brphtpy), 8.86 (2H, d, H$^{3'}$on tpy, $^3J=8.5$), 8.77 (1H, t, H$^{4'}$, $^3J=8.5$), 8.70 (2H, d, H^3 on Brphtpy, $^3J=8.0$), 8.59 (2H, d, H^3 on tpy, $^3J=8.0$), 8.21 (4H, 2 overlapping td, H^4 on tpy and Brphtpy, $^3J=13$, 10.5), 8.12 (2H, d, H^b, $^3J=8.5$), 7.98 (2H, d, H^a, $^3J=8.5$), 7.68 (2H, d, H^6, $^3J=5.5$), 7.59 (2H, d, H^6, $^3J=5.5$), 7.48 (4H, m, H^5 from tpy and Brphtpy). HRMS(ES$^+$): 813.0939 (M$^+$), 271.0331 (M^{3+}); calc. for C$_{36}$H$_{25}$BrN$_6$Ir, M$^+$: 813.0953, M^{3+}: 271.0318. m/z (ES$^+$): 813 (M$^+$), 407 (M^{2+}), 479 (M$^+$+PF$_6$)/2.

8.6.11. [Ir(L^17)(L^9)]^3+: Complex 8.
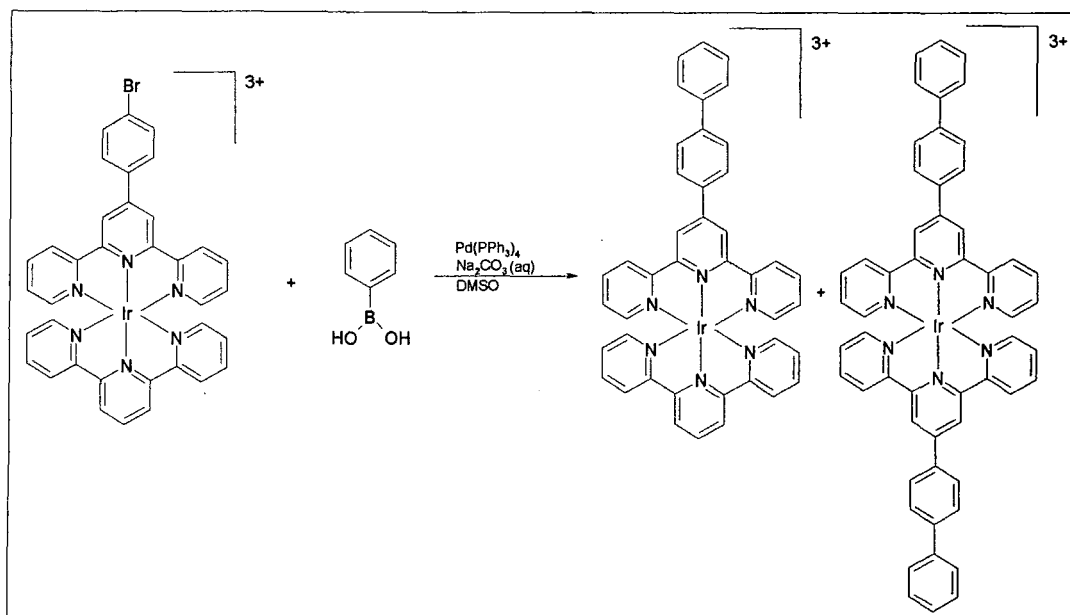
A procedure similar to that described above was followed, in this case using complex 7 (84 mg, 0.07 mmol), phenylboronic acid (17 mg, 0.14 mmol), Na$_2$CO$_3$ (22 mg, 0.2 mmol, dissolved in a minimum volume of water), Pd(PPh$_3$)$_4$ (5 mg, 4.2 μmol, 0.06equiv), DMSO (6 mL). The mixture was heated at 85°C for 4h, after which time, TLC indicated complete consumption of the starting material. A small amount of free ligand 9 was suspected to be present in the crude mixture, (based on comparison of the TLC with that for a previously prepared sample of the ligand); this was readily removed by diluting the reaction mixture with water and washing with dichloromethane. Treatment of the aqueous solution with KPF$_6$ led to a precipitate, the NMR and ESMS of which revealed it to be a mixture of the desired product and a smaller amount of the homoleptic complex [Ir(L^9)$_2$]$^{3+}$. Separation was achieved using column chromatography on alumina; gradient elution from CH$_3$CN to 86.5% CH$_3$CN / 12.0% H$_2$O / 1.5% KNO$_3$ (sat, aq), eluting [Ir(L^9)$_2$]$^{3+}$, and subsequently to 77% CH$_3$CN / 20% H$_2$O / 3.0% KNO$_2$ (sat, aq) for elution of [Ir(L^{17})(L^9)]$^{3+}$. Treatment with KPF$_6$ led to the complexes as their hexafluorophosphate salts: [Ir(L^{17})(L^9)]$^{3+}$ (10 mg, 18%) and [Ir(L^9)$_2$]$^{3+}$ (6 mg, 9%).

Data for [Ir(L^{17})(L^9)]$^{3+}$: δ$_H$ (CD$_3$CN): 9.13 (2H, s, H$^{3'}$(Ph$_2$tpy)), 8.86 (2H, d, H$^{3'}$(tpy), ^{3}J=8), 8.78 (1H, t, H$^{4'}$(tpy), ^{3}J=8), 8.73 (2H, d, H^3(Ph$_2$tpy), ^{3}J=8.0), 8.59 (2H, d, H^3(tpy), ^{3}J=8.0), 8.33 (2H, d, H^b, ^{3}J=8.0), 8.22 (4H, td (overlapping), H^4(both ligands)), 8.10 (2H, d, H^a, ^{3}J=8.5), 7.87 (2H, d, H$^{b'}$, ^{3}J=7.5), 7.70 (2H, d, H^6(Ph$_2$tpy), ^{3}J=5.5), 7.59 (4H, H^6 (tpy) and H$^{a'}$), 7.49 (5H, H^5 (both ligands) and p-Ph, m). HRMS(ES$^+$): 270.4152

(M^{3+}); calc. for $C_{42}H_{30}N_6Ir$, M^{3+}: 270.4055. m/z (ES^+): 270 (M^{3+}), 478 ($M^+ + PF_6$)/2. The complex was observed as a single yellow spot with $R_f = 0.36$ upon TLC analysis on silica plates, using 70% CH_3CN / 26% H_2O / 4% KNO_3 as the solvent.

Data for $[Ir(L^9)_2]^{3+}$: δ_H (CD_3CN): 9.14 (2H, s, $H^{3'}$), 8.75 (2H, d, H^3, $^3J=8$), 8.34 (2H, d, H^b, $^3J=8.5$), 8.25 (2H, td, H^4, $^3J=8$), 8.10 (2H, d, H^a, $^3J=8$), 7.87 (2H, d, $H^{b'}$, $^3J=7$), 7.73 (2H, d, H^6, $^3J=5$), 7.59 (2H, t, $H^{a'}$, $^3J=7.5$), 7.51 (3H, m, H^5 and p-Ph). m/z (ES^+): 321 (M^{3+}), 962 (M^+).

8.6.12. $[Ir(L^{17})(L^{10})]^{3+}$: Complex 10

Method 1.
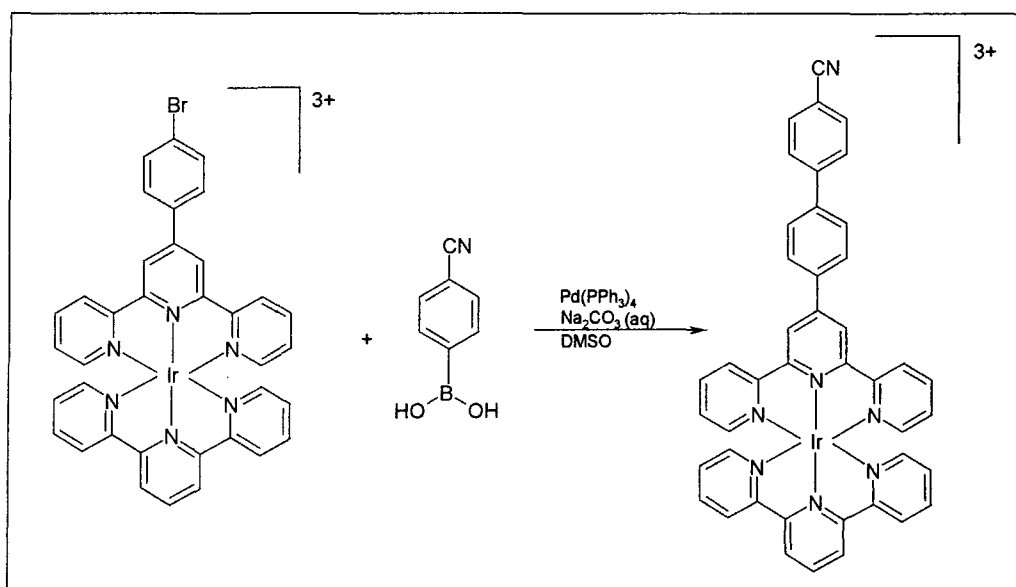
The procedure was similar to that described above, in this case using complex 7 (40 mg, 0.03 mmol), 4-cyanobenzene boronic acid (8.8 mg, 0.06 mmol), Na_2CO_3 (9.5 mg, 0.09 mmol), $Pd(PPh_3)_4$ (2 mg, 1.8 μmol, 0.06 equiv), DMSO (5 mL). After 2 h at 80°C, TLC indicated complete consumption of the starting material. Following anion exchange upon treatment with KPF_6 (sat, aq), analysis of the crude product by ^1H NMR indicated that the desired complex was contaminated with the free ligand 10, as well as a trace of $[Ir(L^{17})_2]^{3+}$. The former was removed by passage through a small column of alumina (Brockman I), initially eluting with hexane / ethyl acetate to remove ligand 10, and then switching to acetonitrile / water, to elute the mixture of complexes. These two complexes were subsequently separated by chromatography on alumina (Brockman II-III); gradient elution from acetonitrile to 87% acetonitrile / 12% water / 1% potassium

nitrate (sat, aq). After treatment with KPF_6 (sat, aq), the desired complex was obtained as the hexafluorophosphate salt. (9 mg, 36%).

δ_H (CH$_3$CN): 9.13 (2H, s, H$^{3'}$(CNPh$_2$tpy)), 8.86 (2H, d, H$^{3'}$ (tpy), ^3J=8), 8.78 (1H, t, H$^{4'}$(tpy), ^3J=7), 8.73 (2H, d, H^3(CNPh$_2$tpy), ^3J=8), 8.59 (2H, d, H^3(tpy), 3J=8), 8.35 (2H, d, H^b(CNPh$_2$tpy), ^3J=8.5), 8.23 (4H, two overlapping td, H^4(both ligands)), 8.14 (2H, d, H^a(CNPh$_2$tpy), ^3J=8.5), 8.02 (2H, d, H$^{b'}$(CNPh$_2$tpy), ^3J=8.5), 7.95 (2H, d, H$^{a'}$(CNPh$_2$tpy), ^3J=8.5), 7.69 (2H, d, H^6(CNPh$_2$tpy or tpy), ^3J=6), 7.59 (2H, d, H^6(CNPh$_2$tpy or tpy), ^3J=4.5), 7.49 (4H, m, H^5(both ligands)). m/z (ES$^+$): 278 (M^{3+}), 835 (M$^+$), 490 (M$^+$+PF$_6$)/2. HRMS(ES$^+$): 278.6572 (M^{3+}); calc. for C$_{43}$H$_{29}$N$_7$Ir, M^{3+}: 278.7371.

Method 2.

A mixture of Ligand 10 (55 mg, 0.13 mmol) and Ir(tpy)Cl$_3$ (74 mg, 0.14 mmol) in ethylene glycol (6 mL) was heated with stirring at 215°C for 20 mins. After cooling to ambient temperature, the clear red solution was diluted with water, and treated with KPF$_6$ (aq, sat), to precipitate the crude product as a yellow solid, which was collected and washed with water. Purification was achieved using chromatography on silica, gradient elution from CH$_3$CN to 68% CH$_3$CN / 30% H$_2$O / 2% KNO$_3$ (aq); product-containing fractions were treated with KPF$_6$ (aq, sat), leading to the desired complex (76 mg, 43%). ^{1}HNMR and ESMS data were consistent with those given above. The complex was observed as a single yellow/orange spot with R$_f$ = 0.30 upon TLC analysis on silica plates, using 70% CH$_3$CN / 26% H$_2$O / 4% KNO$_3$ as the solvent.

8.6.13. [Ir(L^{17})(L^{12})]$^{3+}$: Complex 11.
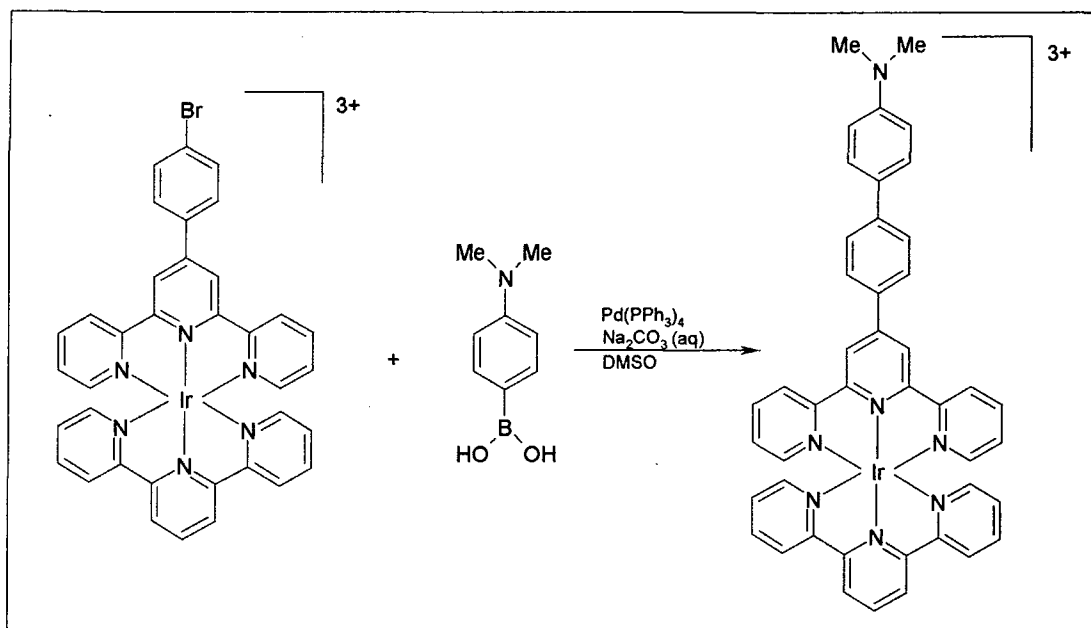
A Schlenk tube was charged with complex 7 (100 mg, 0.08 mmol), 4-(dimethylamino) benzeneboronic acid, (26 mg, 0.16 mmol), Na$_2$CO$_3$ (25 mg, 0.24 mmol, dissolved in the minimum volume of H$_2$O) and DMSO (12 mL), and the system was degassed via 3 freeze-pump-thaw cycles. Pd(PPh$_3$)$_4$ (5.4 mg, 4.8 μmol, 0.06 eq) was then added under a positive pressure of N$_2$ and the mixture heated at 85°C for 12 hours, the progress of the reaction being monitored by TLC. After anion exchange with potassium hexafluorophosphate, the crude product was found to contain the desired compound, together with small amounts of the two homoleptic complexes [Ir(L^{17})$_2$]$^{3+}$ and [Ir(L^{12})$_2$]$^{3+}$. The latter was readily removed by chromatography on alumina, gradient elution from CH$_3$CN to 95% CH$_3$CN / 5% H$_2$O; however, a further column was required to separate all traces of [Ir(L^{17})$_2$]$^{3+}$, together with an unidentified, bright yellow fluorescent impurity; gradient elution from 50% CH$_3$CN / 50% (CH$_3$)$_2$CO to 41%CH$_3$CN / 41% (CH$_3$)$_2$CO / 16% H$_2$O / 2.0% KNO$_3$. The fractions containing the product were concentrated and treated with KPF$_6$(aq), leading to the desired complex as the hexafluorophosphate salt. (17 mg, 26%). δ$_H$ (CD$_3$CN): 9.11 (2H, s, H$^{3'}$(Me$_2$Ntpy)), 8.86 (2H, d, H$^{3'}$ on tpy, ^3J=8), 8.77 (1H, t, H$^{4'}$(tpy), ^3J=7.5), 8.73 (2H, d, H^3(Me$_2$Ntpy), ^3J=8), 8.59 (2H, d, H^3(tpy), ^3J=8), 8.27 (2H, d, H^b, ^3J=8.5), 8.21 (4H, overlapping td, H^4(both ligands)), 8.04 (2H, d, H^a, ^3J=8.5), 7.76 (2H, d, H$^{b'}$, ^3J=8.5), 7.70 (2H, d, H^6(tpy or Me$_2$Ntpy), ^3J=5.5), 7.59 (2H, d, H^6(tpy or Me$_2$Ntpy), ^3J=5.5), 7.48 (4h, overlapping dd, H^5(both ligands), 6.91 (2H, d, H$^{a'}$, ^3J=8.5), 3.06(6H, s, CH$_3$). m/z (ES$^+$): 853 (M^{3+}), 427 (M^{2+}), 499 (M$^+$+PF$_6$)/2.

8.7. Synthesis of bimetallic complexes (Chapter 6)

8.7.1. 3-bromo-(3-carboxyl-3-oxoprop-1-enyl)benzene.
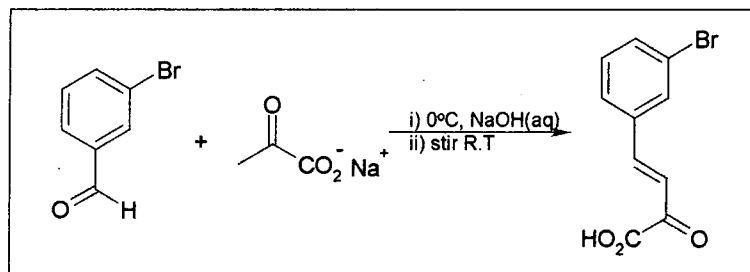
The method employed was based on that described by Kipp for the 4-bromo isomer.[15] A solution of 3-bromobenzaldehyde (7.77g, 0.042 mol) in ethanol (45 mL) was added to a rapidly stirred and cooled solution of sodium pyruvate (7.00g, 0.063 mol) in water (100 mL) contained in a beaker immersed in an ice bath. The resulting pale yellow suspension was stirred vigorously for 2 min, after which 10 mL of 10% sodium hydroxide solution was added, which resulted in the solution turning clear after 3-5 min. The reaction was allowed to warm to room temperature and stirring was continued for a further 45 min, leading to a yellow precipitate. The solution was then acidified to pH 3-4 using 5M HCL (aq) and stirred for a further 5 min. The precipitate was filtered and washed with a small amount of water and ethanol, before drying under vacuum. (10g, 93%). δ_H (CDCl$_3$): 7.89 (1H, s, H^a), 7.67 (1H, d, H^d, ^3J=8.0), 7.59 (1H, d, H^b, ^3J=8), 7.38 (2H, overlapping doublet and triplet, H^c and vinyl proton, ^3J=8.0 and ^3J=16.0 respectively), 6.86 (1H, d, vinyl proton, ^3J=16).

8.7.2. 1-(2-pyridinylcarbonyl) pyridinium iodide.[15]
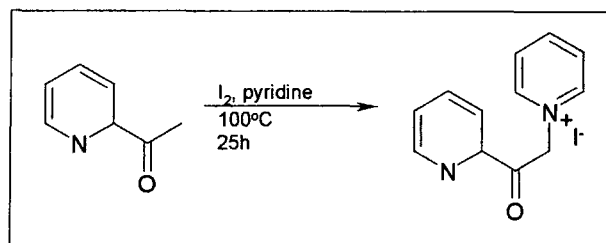
A solution of iodine (20.4 g, 0.074 mol) dissolved in pyridine (60 mL) was added to a solution of 2-acetylpyridine (8.28 mL, 0.074 mol) in pyridine (20 mL), and the mixture was refluxed at 120°C for 2.5 hours. The solution was then allowed to stand for 12 hours, resulting in the formation of a dark precipitate, which was collected and re-dissolved in water/ethanol (80/20). Charcoal was used to decolourise the solution, before reducing the volume to induce the product to crystallise. (11.7g, 49%). δ_H (DMSO): 9.01 (2H, d, H^8 and H^{12}, ^3J=6), 8.88 (1H, d, H^4, ^3J=4), 8.73 (1H, t, H^{10}, ^3J=6.5), 8.28 (2H, t, H^{11} and H^9, ^3J=6.5), 8.14 (1H, t, H^2), 8.08 (1H, d, H^1, ^3J=7.5), 7.84 (1H, ddd, H^3), 6.51 (2H, s, H^6 and H^7). δ_C (DMSO): 150.5 (C^4), 146.4 (C^8 and C^{12}), 146.4 (C^{10}), 138.2 (C^2), 129.2 (C^3), 127.7 (C^{11} and C^9), 122.1 (C^1), 66.7 (C^6 and C^7).

8.7.3. 4-(3-bromophenyl)-2, 2'-bipyridine.
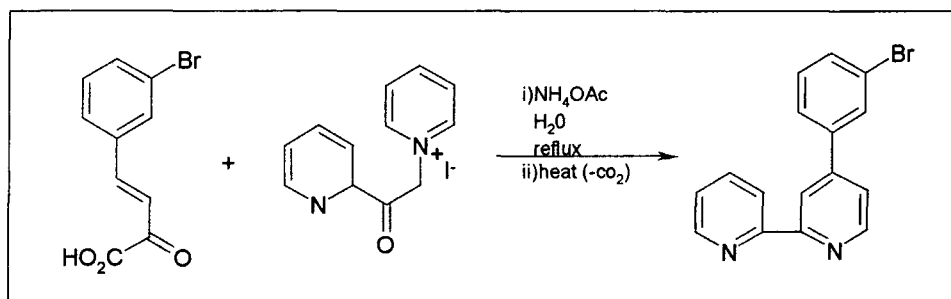
The method employed was similar to that published for the 4-bromo isomer.[15]
1-(2-pyridinylcarbonyl) pyridinium iodide (7.18 g, 0.02 mol), 3-bromo-(3-carboxyl-3-oxoprop-1-enyl)benzene (5.09 g, 0.02 mol), NH$_4$OAc (13.5 g, 0.18 mol) and water (150 mL) were heated to reflux with stirring for 6h, during which time a yellow precipitate formed. Once the solution had cooled, the precipitate was collected via filtration, washed with acetone before drying under vacuum, and then transferred to a clean, dry Schlenk tube which was evacuated and back-filled with nitrogen. The precipitate was

then heated under an atmosphere of nitrogen until it liquefied and effervesced, indicating decarboxylation. After allowing the sample to cool, NMR analysis revealed that the decarboxylation was complete. (4.2g, 68%). δ_H (CDCl$_3$): 8.71 (1H, d, H^6, ^{3}J=5.0), 8.69 (1H, dd, H$^{6'}$, ^{3}J=4, 1.0), 8.61 (1H, d, H^3, ^{3}J=1.5), 8.43 (1H, d, H$^{3'}$, ^{3}J=8.0), 7.88 (1H, t, H^a, ^{3}J=2), 7.83 (1H, td, H$^{4'}$, ^{3}J=8.0, 2.0), 7.66 (1H, dd, H^b, ^{3}J=7.6, 0.8), 7.55 (1H, dd, H^d, ^{3}J=8.0, 1.0), 7.48 (1H, dd, H^5, ^{3}J=5.0, 1.5), 7.33 (2H, overlapping ddd and t, H$^{5'}$ and H^c). δ_C (CDCl$_3$): 156.7 (q), 155.7 (q), 149.7 (C^6), 149.1 (C$^{6'}$), 147.6 (q), 140.2 (q), 136.9 (C$^{4'}$), 131.9 (C^d), 130.5 (C^c/C^5), 130.0 (C^a), 125.7 (C^b), 123.9 (C^c/C$^{5'}$), 123.1 (q), 121.4 (C^5), 121.2 (C$^{3'}$), 118.8 (C^3).

8.7.4. 4-(3-(neopentylglycolatoboron)phenyl)-2, 2'-bipyridine
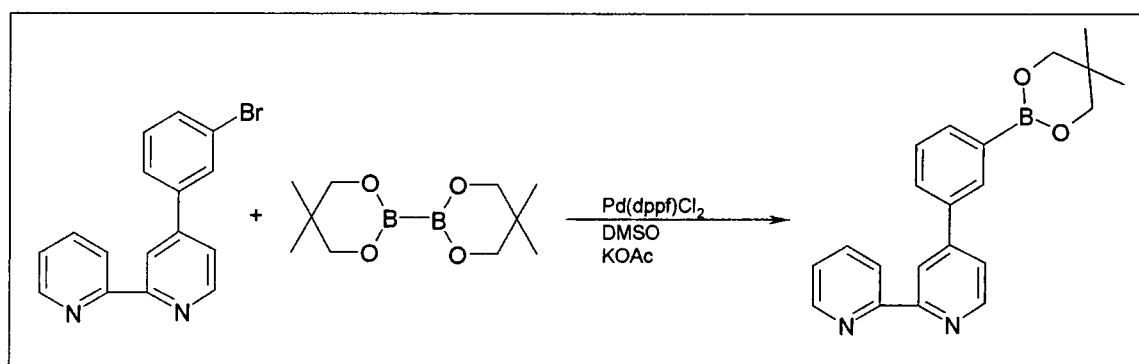
A Schlenk tube was charged with 4-(3-bromophenyl)-2, 2'-bipyridine (500 mg, 1.61 mmol, 1 equiv), B$_2$neo$_2$ (382 mg, 1.69 mmol, 1.05 equiv), KOAc (473 mg, 4.83 mmol, 3 equiv) and DMSO; the system was then degassed via 3 freeze-pump-thaw cycles. Pd(dppf)Cl$_2$ (39 mg, 0.048 mmol, 0.03 equiv) was then added under a positive pressure of nitrogen, and the reaction was stirred under nitrogen at 80°C for 5.5 h. After cooling to room temperature, the reaction mixture was diluted with dichloromethane and the organic layer was washed with copious amounts of water, dried and finally the solvent evaporated under vacuum to yield a mixture of the product contaminated with de-boronated material (4-phenyl bipy). For purification, the crude product was dissolved in dichloromethane and extracted into KOH (0.2 M, aq). The water was then carefully neutralised until a white precipitate appeared, which was then extracted back into dichloromethane. Evaporation of the solvent this time led to a white solid, analysis of which revealed it to be the product. (343 mg, 62%). m/z (EI): 344 (M$^+$), 232 (M$^+$-B$_2$neo$_2$). δ_H (CDCl$_3$): 8.71 (2H, m, H^{6}and H$^{6'}$), 8.69 (1H, s, H^3), 8.45 (1H, d, H$^{3'}$, ^{3}J=8),

8.21 (1H, s, H^a), 7.88 (1H, d, H^b, ^3J=7.5), 7.84 (2H, m, H^d and H^4), 7.59 (1H, dd, H^5, ^3J=5.0, 1.5), 7.49 (1H, t, H^c, ^3J=8.0), 7.33 (1H, ddd, H$^{5'}$).

8.7.5. [Ir(phenylpyridine)$_2$(4-(3-(neopentylglycolatoboron)phenyl-2, 2'-bipyridine))]PF$_6$: Complex 13
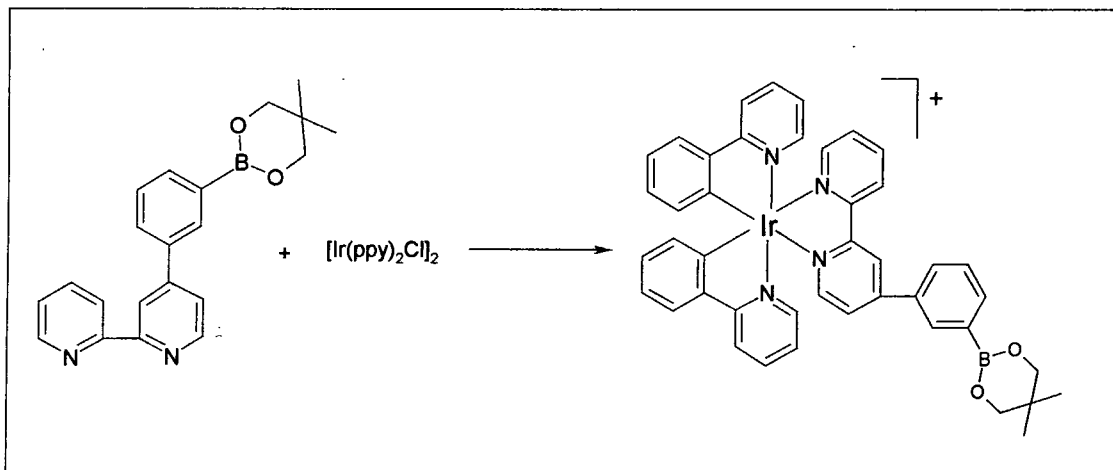
A solution of 4-(3-(neopentylglycolatoboron)phenyl)-2, 2'-bipyridine (120, mg, 0.35 mmol) in dichloromethane (10 mL) was added to a stirred suspension of [Ir(ppy)$_2$Cl]$_2$[16] (187 mg, 0.18 mmol) in MeOH (15 mL) and the reaction was heated to reflux for 4.5 h. (Previous reports of this reaction suggested a clear orange solution would be formed; however, an orange solution with a yellow precipitate was obtained. Analysis of the precipitate, after it had been removed from the reaction after cooling to room temperature to leave an orange solution, revealed it to be a mixture of un-reacted [Ir(ppy)$_2$Cl]$_2$ and other impurities). A saturated solution of ammonium hexafluorophosphate in MeOH (5 mL) was added to the remaining clear orange solution and stirred for a few hours. Partial evaporation of the solvent volume caused an orange solid to precipitate, which was collected using a centrifuge, washed thoroughly with MeOH and dried under vacuum to yield the product. (150 mg, 55%). m/z (ES$^+$): 791 ([HOBOMe]$^+$ adduct). Signals in NMR too overlapping for interpretation.

8.7.6. Complex 14.
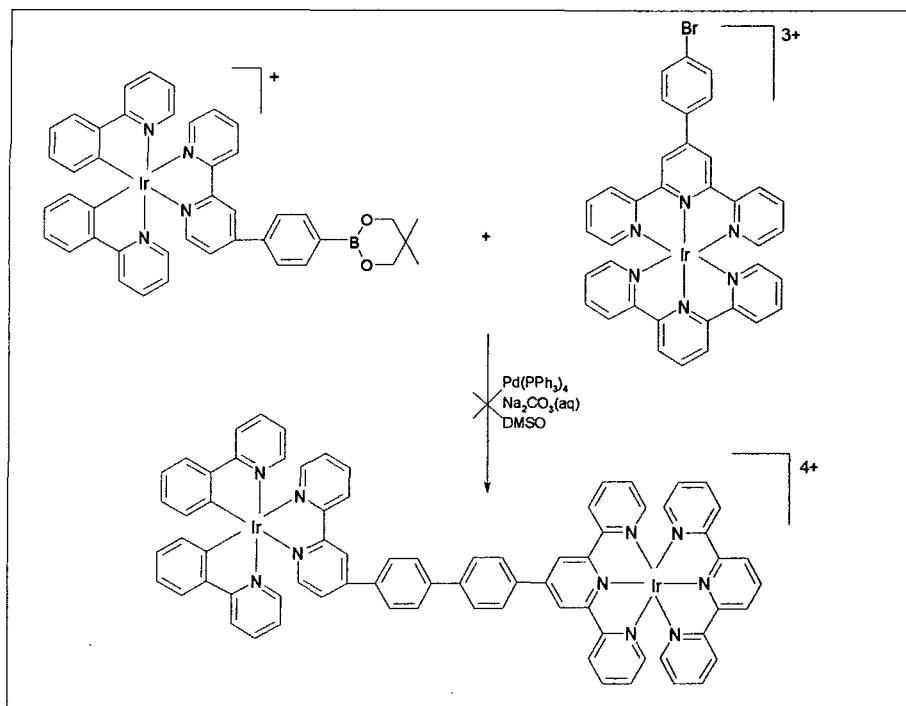
A Schlenk tube was charged with complex 7 (63 mg, 0.05 mmol, 1 equiv), complex 12 (57 mg, 0.05 mmol, 1 equiv), Na$_2$CO$_3$ (16 mg, 0.15 mmol, 3 equiv, dissolved in the minimum volume of water) and DMSO (5 mL). The system was then degassed via three freeze-pump-thaw cycles, before adding Pd(PPh$_3$)$_4$ (13 mgs, 3.6x10^{-3} mol, 0.06 equiv) under a positive pressure of nitrogen. The reaction was stirred at room temperature for 1 hour before heating under nitrogen at 85°C for 24 h. Unfortunately, electrospray mass spectroscopy revealed that the reaction had not been successful due to complete de-boronation of the complex 12 before the complex had undergone the coupling reaction.

8.7.7. Complex 15.
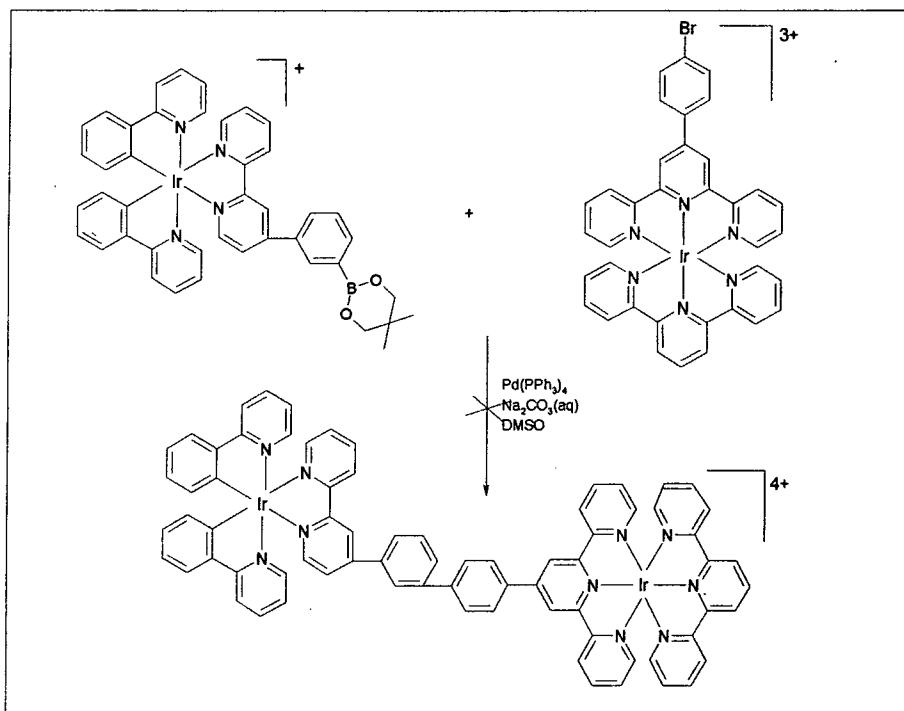
The same procedure was used for the synthesis of complex 15 as given previously for complex 14, using complex 7 (74 mg, 0.06 mmol, 1 equiv), complex 13 (47 mg, 0.06 mmol, 1 equiv), Na_2CO_3 (19 mg, 0.18 mmol, 3 equiv, dissolved in the minimum volume of water) and $Pd(PPh_3)_4$ (10 mgs, 3.6×10^{-3} mol, 0.06 equiv) in DMSO (5 mL). In this case the reaction was heated to 85°C immediately. The reaction was continued for 3 days at 85°C, with the addition of further catalyst during this time. However, TLC analysis repeatedly revealed the presence of starting material in the reaction mixture, and only a small new spot emerged. Attempts to separate this new spot from the starting material using a silica column with $CH_3CN/H_2O/KNO_3$ as the eluting solvent led only to the recovery of the starting materials, and a small quantity of a compound whose structure could not be elucidated.

8.8. References

1   K. T. Potts and D. Konwar, *J. Org. Chem.*, 1991, **56**, 4815.

2   E. C. Constable and M. D. Ward, *J. Chem. Soc., Dalton Trans.*, 1990, 1405.

3   J. Sauer, D. K. Heldmann, and G. R. Pabst, *Eur. J. org. Chem*, 1999, 313.

4   T. Hayashi, M. Konishi, and M. Kumada, *Tetrahedron. Lett*, 1979, 1871.

5   C. J. Aspley and J. A. G. Williams, *New J. Chem*, 2001, **25**, 1136.

6   L. S. Hegedus, *Inorg. Synth*, 1972, **13**, 121.

7   G. W. V. Cave and C. L. Raston, *Chem. com.*, 2000, 2199.

8   J.-P. Collin, *et al.*, *Inorg. Chem.*, 1991, **30**, 4230.

9   G. W. V. Cave and C. L. Raston, *J. Chem. Soc., Perkin Trans. 1*, 2001, 3258.

10 S. C. Suh, M. C. Suh, and S. C. Shim, *Macromol.Chem.Phys*, 1999, **200**, 1991.

11 M. Nicolas, *Electroanal Chem*, 2000, **482**, 211.

12 H. B. Goodbrand and N.-X. Hu, *J. Org. Chem*, 1999, **64**, 670.

13 J.-P. Collin, *et al.*, *J. Am. Chem. Soc*, 1999, **121**, 5009.

14 K. K.-W. Lo, *et al.*, *New J. Chem*, 2002, **26(1)**, 81.

15 R. A. Kipp, *J. Photochem. and Photobiol A*, 1999, **121**, 27.

16 S. Sprouse, *et al.*, *J. Am. Chem. Soc*, 1984, **106**, 6647.

Appendix 1 – Crystallography Data for 4'-mesityl-2, 2': 6', 2"-terpyridine[†]

Crystal data and structure refinement for 01srv124.

Identification code	01srv124
Empirical formula	$C_{24} H_{21} N_3$
Formula weight	351.44
Temperature	120(2) K
Wavelength	0.71073 Å
Crystal system	Orthorhombic
Space group	Pbcn
Unit cell dimensions	a = 8.217(1) Å α= 90°.
	b = 13.359(1) Å β= 90°.
	c = 17.167(1) Å γ = 90°.
Volume	1884.4(3) Å^3
Z	4
Density (calculated)	1.239 Mg/m^3
Absorption coefficient	0.074 mm^{-1}
F(000)	744
Crystal size	0.45 x 0.30 x 0.16 mm^3
Theta range for data collection	2.37 to 27.50°.
Index ranges	-10<=h<=10, -17<=k<=17, -22<=l<=22
Reflections collected	19602
Independent reflections	2177 [R(int) = 0.0496]
Completeness to theta = 27.50°	100.0 %
Absorption correction	None
Refinement method	Full-matrix least-squares on F^2
Data / restraints / parameters	2177 / 0 / 173
Goodness-of-fit on F^2	1.078
Final R indices [I>2sigma(I)]	R1 = 0.0457, wR2 = 0.1101
R indices (all data)	R1 = 0.0603, wR2 = 0.1193
Extinction coefficient	0
Largest diff. peak and hole	0.342 and -0.263 e.Å^{-3}

[†] Crystals of 4'-mesityl-2, 2': 6', 2"-terpyridine grown by Kerstin Wild.

Table 1.   Atomic coordinates   (x 10^4) and equivalent   isotropic displacement parameters (Å^2x 10^3)

for 01srv124.   U(eq) is defined as one third of the trace of the orthogonalized U^{ij} tensor.

	x	y	z	U(eq)
N(1)	5000	2497(1)	2500	22(1)
C(2)	5743(2)	3023(1)	1931(1)	22(1)
C(3)	5753(2)	4067(1)	1909(1)	22(1)
C(4)	5000	4609(1)	2500	22(1)
C(5)	5000	5733(1)	2500	22(1)
C(6)	4136(2)	6260(1)	1924(1)	24(1)
C(7)	4146(2)	7305(1)	1938(1)	28(1)
C(8)	5000	7839(1)	2500	29(1)
C(9)	3180(2)	5732(1)	1293(1)	32(1)
C(10)	5000	8971(2)	2500	41(1)
N(11)	7485(2)	2975(1)	803(1)	28(1)
C(12)	6576(2)	2437(1)	1306(1)	23(1)
C(13)	6395(2)	1400(1)	1245(1)	28(1)
C(14)	7151(2)	905(1)	630(1)	33(1)
C(15)	8103(2)	1447(1)	121(1)	37(1)
C(16)	8250(2)	2470(1)	234(1)	35(1)

Table 2.   Bond lengths [Å] and angles [°] for 01srv124.

N(1)-N(1)#1	0.000(3)
N(1)-C(2)#1	1.3491(15)
N(1)-C(2)	1.3491(15)
C(2)-N(1)#1	1.3491(15)
C(2)-C(3)	1.3950(18)
C(2)-C(12)	1.4943(18)
C(3)-C(4)	1.3921(16)
C(3)-H(3)	0.936(16)
C(4)-C(3)#1	1.3921(16)
C(4)-C(5)	1.502(2)
C(5)-C(6)#1	1.4065(16)
C(5)-C(6)	1.4065(16)
C(6)-C(7)	1.3955(19)
C(6)-C(9)	1.512(2)
C(7)-C(8)	1.3904(17)
C(7)-H(7)	0.970(18)
C(8)-C(7)#1	1.3904(17)
C(8)-C(10)	1.512(3)
C(9)-H(91)	0.99(2)
C(9)-H(92)	1.02(2)
C(9)-H(93)	0.98(2)
C(10)-H(101)	0.94(3)
C(10)-H(102)	1.04(4)
C(10)-H(103)	1.10(4)
N(11)-C(16)	1.3432(18)
N(11)-C(12)	1.3488(17)
C(12)-C(13)	1.3972(19)
C(13)-C(14)	1.392(2)
C(13)-H(13)	0.957(18)
C(14)-C(15)	1.379(2)
C(14)-H(14)	0.981(18)
C(15)-C(16)	1.386(2)
C(15)-H(15)	0.980(19)
C(16)-H(16)	0.998(18)
N(1)#1-N(1)-C(2)#1	0(10)
N(1)#1-N(1)-C(2)	0(10)
C(2)#1-N(1)-C(2)	117.21(15)

N(1)#1-C(2)-N(1)	0.00(11)
N(1)#1-C(2)-C(3)	122.91(12)
N(1)-C(2)-C(3)	122.91(12)
N(1)#1-C(2)-C(12)	117.03(12)
N(1)-C(2)-C(12)	117.03(12)
C(3)-C(2)-C(12)	120.06(12)
C(4)-C(3)-C(2)	119.84(13)
C(4)-C(3)-H(3)	121.1(9)
C(2)-C(3)-H(3)	119.1(9)
C(3)-C(4)-C(3)#1	117.27(16)
C(3)-C(4)-C(5)	121.36(8)
C(3)#1-C(4)-C(5)	121.36(8)
C(6)#1-C(5)-C(6)	119.96(17)
C(6)#1-C(5)-C(4)	120.02(8)
C(6)-C(5)-C(4)	120.02(8)
C(7)-C(6)-C(5)	119.01(13)
C(7)-C(6)-C(9)	118.83(13)
C(5)-C(6)-C(9)	122.16(13)
C(8)-C(7)-C(6)	121.90(14)
C(8)-C(7)-H(7)	118.6(10)
C(6)-C(7)-H(7)	119.5(10)
C(7)-C(8)-C(7)#1	118.23(18)
C(7)-C(8)-C(10)	120.89(9)
C(7)#1-C(8)-C(10)	120.89(9)
C(6)-C(9)-H(91)	111.5(12)
C(6)-C(9)-H(92)	112.4(11)
H(91)-C(9)-H(92)	108.8(16)
C(6)-C(9)-H(93)	109.8(13)
H(91)-C(9)-H(93)	105.9(17)
H(92)-C(9)-H(93)	108.2(18)
C(8)-C(10)-H(101)	111.4(18)
C(8)-C(10)-H(102)	114(2)
H(101)-C(10)-H(102)	49(2)
C(8)-C(10)-H(103)	107.2(19)
H(101)-C(10)-H(103)	62(2)
H(102)-C(10)-H(103)	108(3)
C(16)-N(11)-C(12)	117.26(13)
N(11)-C(12)-C(13)	122.59(12)
N(11)-C(12)-C(2)	115.78(11)
C(13)-C(12)-C(2)	121.62(12)

C(14)-C(13)-C(12)	118.75(14)
C(14)-C(13)-H(13)	122.6(10)
C(12)-C(13)-H(13)	118.6(10)
C(15)-C(14)-C(13)	118.97(14)
C(15)-C(14)-H(14)	122.5(10)
C(13)-C(14)-H(14)	118.6(10)
C(14)-C(15)-C(16)	118.58(14)
C(14)-C(15)-H(15)	122.8(11)
C(16)-C(15)-H(15)	118.6(11)
N(11)-C(16)-C(15)	123.78(15)
N(11)-C(16)-H(16)	114.4(10)
C(15)-C(16)-H(16)	121.8(10)

Symmetry transformations used to generate equivalent atoms:

#1 -x+1,y,-z+1/2

Table 3. Anisotropic displacement parameters $(\text{Å}^2\text{x } 10^3)$ for 01srv124. The anisotropic

displacement factor exponent takes the form: $-2\pi^2[\text{ } h^2 \text{ a*}^2 U^{11} + ... + 2 \text{ h k a* b* } U^{12}]$

	U^{11}	U^{22}	U^{33}	U^{23}	U^{13}	U^{12}
N(1)	22(1)	22(1)	22(1)	0	-3(1)	0
C(2)	20(1)	24(1)	22(1)	-1(1)	-3(1)	1(1)
C(3)	22(1)	23(1)	22(1)	2(1)	1(1)	0(1)
C(4)	21(1)	21(1)	24(1)	0	-2(1)	0
C(5)	22(1)	20(1)	24(1)	0	4(1)	0
C(6)	23(1)	24(1)	26(1)	2(1)	3(1)	0(1)
C(7)	24(1)	25(1)	34(1)	6(1)	3(1)	3(1)
C(8)	24(1)	20(1)	42(1)	0	8(1)	0
C(9)	34(1)	30(1)	32(1)	2(1)	-7(1)	-1(1)
C(10)	32(1)	20(1)	72(2)	0	2(1)	0
N(11)	33(1)	29(1)	23(1)	1(1)	4(1)	6(1)
C(12)	24(1)	24(1)	21(1)	0(1)	-4(1)	4(1)
C(13)	34(1)	24(1)	25(1)	0(1)	-5(1)	4(1)
C(14)	44(1)	26(1)	30(1)	-5(1)	-10(1)	12(1)
C(15)	49(1)	38(1)	23(1)	-3(1)	0(1)	19(1)
C(16)	43(1)	38(1)	23(1)	1(1)	6(1)	11(1)

Table 4. Hydrogen coordinates (x 10^4) and isotropic displacement parameters ($Å^2$x 10 ^{3}) for 01srv124.

	x	y	z	U(eq)
H(3)	6272(18)	4391(11)	1494(9)	25(4)
H(7)	3550(20)	7673(13)	1545(10)	38(4)
H(91)	3820(30)	5661(14)	811(13)	62(6)
H(92)	2790(20)	5043(17)	1463(12)	61(6)
H(93)	2220(30)	6134(17)	1151(13)	73(7)
H(101)	5950(40)	9230(20)	2730(20)	19(7)
H(102)	6040(50)	9280(30)	2260(30)	41(10)
H(103)	4930(60)	9210(30)	3110(20)	51(11)
H(13)	5730(20)	1062(12)	1618(10)	35(4)
H(14)	6970(20)	182(14)	572(10)	40(5)
H(15)	8690(20)	1138(13)	-314(11)	44(5)
H(16)	8940(20)	2895(13)	-111(11)	43(5)

207
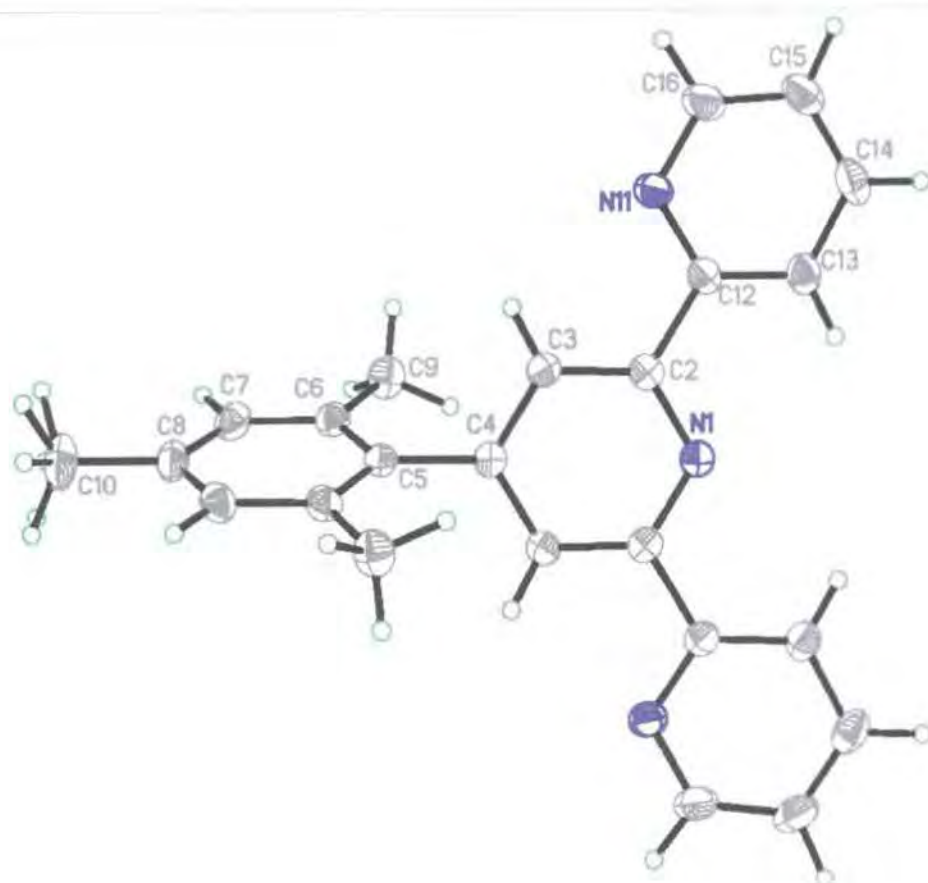
Appendix 2 – Crystallography Data for 4'-(4-N,N-dimethylaminophenyl)-2, 2': 6', 2''-terpyridine

Table 1. Crystal data and structure refinement for 02srv018.

Identification code	02srv018
Empirical formula	C23 H20 N4
Formula weight	352.43
Temperature	120(2) K
Wavelength	0.71073 Å
Crystal system	Monoclinic
Space group	P2(1)/c
Unit cell dimensions	a = 15.2264(4) Å $\alpha = 90°$.
	b = 7.6465(2) Å $\beta = 106.0450(10)°$.
	c = 16.0808(5) Å $\gamma = 90°$.
Volume	1799.33(9) Å^3
Z	4
Density (calculated)	1.301 Mg/m^3
Absorption coefficient	0.079 mm^{-1}
F(000)	744
Crystal size	0.66 x 0.24 x 0.06 mm^3
Theta range for data collection	1.39 to 27.47°.
Index ranges	-19<=h<=19, -9<=k<=9, -20<=l<=20
Reflections collected	17151
Independent reflections	4109 [R(int) = 0.0342]
Completeness to theta = 27.47°	99.8 %
Absorption correction	Semi-empirical from equivalents
Max. and min. transmission	0.995 and 0.949
Refinement method	Full-matrix least-squares on F^2
Data / restraints / parameters	4109 / 0 / 324
Goodness-of-fit on F^2	1.012
Final R indices [I>2sigma(I)]	R1 = 0.0400, wR2 = 0.0953
R indices (all data)	R1 = 0.0594, wR2 = 0.1069
Extinction coefficient	.
Largest diff. peak and hole	0.290 and -0.225 e.Å^{-3}

Table 1. Atomic coordinates (x 10^4) and equivalent isotropic displacement parameters ($Å^2$x 10^3)

for 02srv018. U(eq) is defined as one third of the trace of the orthogonalized U^{ij} tensor.

	x	y	z	U(eq)
N(1)	-202(1)	3220(2)	3941(1)	30(1)
C(1)	78(1)	2520(2)	4809(1)	30(1)
C(2)	-1117(1)	3882(2)	3600(1)	29(1)
C(11)	405(1)	3289(2)	3449(1)	23(1)
C(12)	1289(1)	2579(2)	3749(1)	24(1)
C(13)	1879(1)	2563(2)	3234(1)	24(1)
C(14)	1637(1)	3291(2)	2403(1)	21(1)
C(15)	774(1)	4065(2)	2120(1)	24(1)
C(16)	166(1)	4064(2)	2618(1)	25(1)
N(2)	3425(1)	2829(2)	755(1)	22(1)
C(21)	2256(1)	3170(2)	1839(1)	21(1)
C(22)	2831(1)	1728(2)	1892(1)	22(1)
C(23)	3393(1)	1602(2)	1347(1)	22(1)
C(24)	2864(1)	4213(2)	695(1)	22(1)
C(25)	2278(1)	4434(2)	1218(1)	23(1)
N(3)	3821(1)	-1326(2)	1857(1)	27(1)
C(31)	3997(1)	38(2)	1399(1)	22(1)
C(32)	4709(1)	27(2)	1012(1)	27(1)
C(33)	5270(1)	-1434(2)	1114(1)	31(1)
C(34)	5094(1)	-2842(2)	1578(1)	30(1)
C(35)	4362(1)	-2733(2)	1932(1)	29(1)
N(4)	2175(1)	6651(2)	-204(1)	34(1)
C(41)	2880(1)	5528(2)	11(1)	24(1)
C(42)	3576(1)	5530(2)	-395(1)	26(1)
C(43)	3538(1)	6722(2)	-1054(1)	31(1)
C(44)	2813(1)	7873(2)	-1282(1)	37(1)
C(45)	2159(1)	7796(2)	-840(1)	41(1)

Table 2. Bond lengths [Å] and angles [°] for 02srv018.

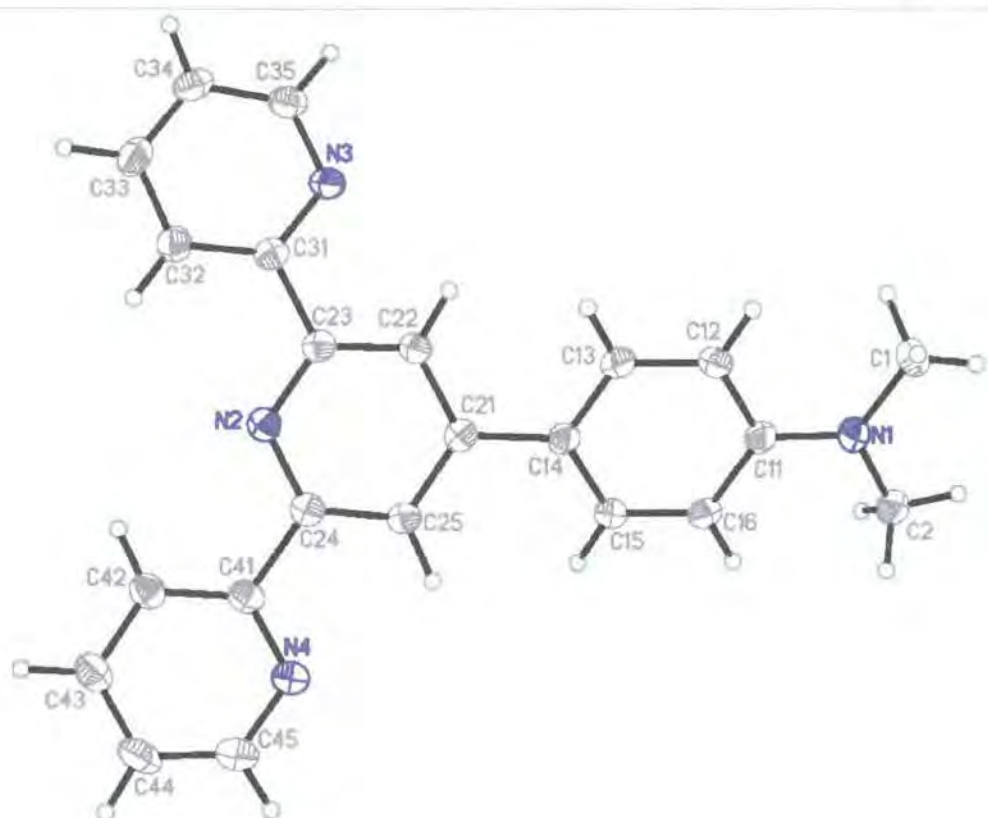|			
N(1)-C(11)	1.3745(17)	C(34)-H(34)	0.943(19)
N(1)-C(2)	1.4410(18)	C(35)-H(35)	1.007(17)
N(1)-C(1)	1.4441(18)	N(4)-C(45)	1.342(2)
C(1)-H(1C)	1.003(19)	N(4)-C(41)	1.3430(18)
C(1)-H(1B)	0.985(18)	C(41)-C(42)	1.3904(19)
C(1)-H(1A)	1.009(19)	C(42)-C(43)	1.387(2)
C(2)-H(2C)	0.997(17)	C(42)-H(42)	0.966(17)
C(2)-H(2B)	0.979(17)	C(43)-C(44)	1.380(2)
C(2)-H(2A)	0.982(17)	C(43)-H(43)	1.004(17)
C(11)-C(12)	1.4064(19)	C(44)-C(45)	1.377(2)
C(11)-C(16)	1.4142(19)	C(44)-H(44)	0.951(19)
C(12)-C(13)	1.3815(19)	C(45)-H(45)	0.97(2)
C(12)-H(12)	0.948(16)		
C(13)-C(14)	1.3985(19)	C(11)-N(1)-C(2)	120.05(12)
C(13)-H(13)	0.968(15)	C(11)-N(1)-C(1)	120.32(12)
C(14)-C(15)	1.3982(18)	C(2)-N(1)-C(1)	119.62(12)
C(14)-C(21)	1.4806(18)	N(1)-C(1)-H(1C)	110.6(10)
C(15)-C(16)	1.3813(19)	N(1)-C(1)-H(1B)	109.0(10)
C(15)-H(15)	0.966(15)	H(1C)-C(1)-H(1B)	107.9(14)
C(16)-H(16)	0.962(15)	N(1)-C(1)-H(1A)	112.2(10)
N(2)-C(23)	1.3459(17)	H(1C)-C(1)-H(1A)	106.0(14)
N(2)-C(24)	1.3466(17)	H(1B)-C(1)-H(1A)	111.0(15)
C(21)-C(22)	1.3951(19)	N(1)-C(2)-H(2C)	111.6(9)
C(21)-C(25)	1.3974(19)	N(1)-C(2)-H(2B)	109.3(10)
C(22)-C(23)	1.3883(18)	H(2C)-C(2)-H(2B)	109.9(13)
C(22)-H(22)	0.953(16)	N(1)-C(2)-H(2A)	111.2(9)
C(23)-C(31)	1.4959(18)	H(2C)-C(2)-H(2A)	105.5(13)
C(24)-C(25)	1.3960(18)	H(2B)-C(2)-H(2A)	109.2(13)
C(24)-C(41)	1.4946(19)	N(1)-C(11)-C(12)	121.24(12)
C(25)-H(25)	0.968(15)	N(1)-C(11)-C(16)	121.47(12)
N(3)-C(35)	1.3395(18)	C(12)-C(11)-C(16)	117.29(12)
N(3)-C(31)	1.3455(17)	C(13)-C(12)-C(11)	121.07(12)
C(31)-C(32)	1.3909(19)	C(13)-C(12)-H(12)	119.3(9)
C(32)-C(33)	1.388(2)	C(11)-C(12)-H(12)	119.7(9)
C(32)-H(32)	0.973(18)	C(12)-C(13)-C(14)	121.78(12)
C(33)-C(34)	1.378(2)	C(12)-C(13)-H(13)	118.3(9)
C(33)-H(33)	0.998(17)	C(14)-C(13)-H(13)	119.8(9)
C(34)-C(35)	1.386(2)	C(15)-C(14)-C(13)	117.08(12)

C(15)-C(14)-C(21)	121.80(12)	C(45)-N(4)-C(41)	117.30(13)
C(13)-C(14)-C(21)	121.06(12)	N(4)-C(41)-C(42)	122.51(13)
C(16)-C(15)-C(14)	122.06(12)	N(4)-C(41)-C(24)	116.44(12)
C(16)-C(15)-H(15)	117.7(8)	C(42)-C(41)-C(24)	121.02(12)
C(14)-C(15)-H(15)	120.1(8)	C(43)-C(42)-C(41)	118.91(14)
C(15)-C(16)-C(11)	120.62(12)	C(43)-C(42)-H(42)	121.8(10)
C(15)-C(16)-H(16)	120.1(9)	C(41)-C(42)-H(42)	119.2(10)
C(11)-C(16)-H(16)	119.2(9)	C(44)-C(43)-C(42)	118.93(14)
C(23)-N(2)-C(24)	116.99(11)	C(44)-C(43)-H(43)	122.1(10)
C(22)-C(21)-C(25)	116.85(12)	C(42)-C(43)-H(43)	118.9(10)
C(22)-C(21)-C(14)	120.45(12)	C(45)-C(44)-C(43)	118.39(14)
C(25)-C(21)-C(14)	122.66(12)	C(45)-C(44)-H(44)	120.5(11)
C(23)-C(22)-C(21)	120.19(12)	C(43)-C(44)-H(44)	121.1(11)
C(23)-C(22)-H(22)	118.2(9)	N(4)-C(45)-C(44)	123.94(15)
C(21)-C(22)-H(22)	121.5(9)	N(4)-C(45)-H(45)	115.2(12)
N(2)-C(23)-C(22)	123.11(12)	C(44)-C(45)-H(45)	120.8(12)
N(2)-C(23)-C(31)	117.12(11)		
C(22)-C(23)-C(31)	119.77(12)		
N(2)-C(24)-C(25)	123.33(12)		
N(2)-C(24)-C(41)	116.33(11)		
C(25)-C(24)-C(41)	120.32(12)		
C(24)-C(25)-C(21)	119.52(12)		
C(24)-C(25)-H(25)	120.1(9)		
C(21)-C(25)-H(25)	120.3(9)		
C(35)-N(3)-C(31)	117.47(12)		
N(3)-C(31)-C(32)	122.48(13)		
N(3)-C(31)-C(23)	116.03(11)		
C(32)-C(31)-C(23)	121.47(12)		
C(33)-C(32)-C(31)	118.86(14)		
C(33)-C(32)-H(32)	120.5(10)		
C(31)-C(32)-H(32)	120.6(10)		
C(34)-C(33)-C(32)	119.14(14)		
C(34)-C(33)-H(33)	121.1(10)		
C(32)-C(33)-H(33)	119.7(10)		
C(33)-C(34)-C(35)	118.29(14)		
C(33)-C(34)-H(34)	121.7(11)		
C(35)-C(34)-H(34)	120.0(11)		
N(3)-C(35)-C(34)	123.75(14)		
N(3)-C(35)-H(35)	115.9(9)		
C(34)-C(35)-H(35)	120.3(9)		

Table 3. Anisotropic displacement parameters ($\text{Å}^2 \times 10^3$) for 02srv018. The anisotropic displacement factor exponent takes the form: $-2\pi^2[\, h^2\, a^{*2}U^{11} + ... + 2\, h\, k\, a^*\, b^*\, U^{12}\,]$
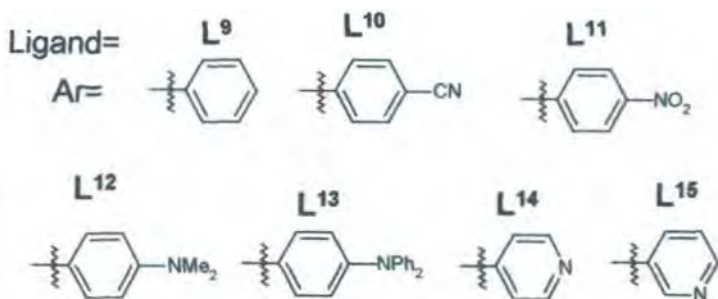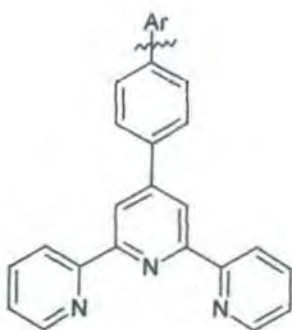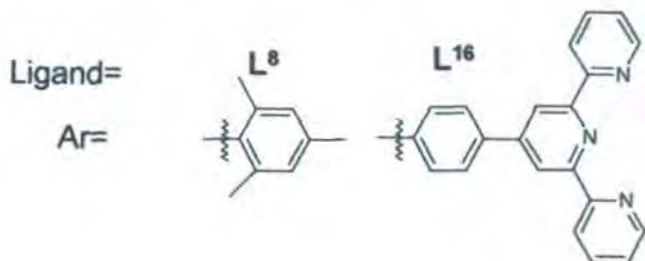
	U^{11}	U^{22}	U^{33}	U^{23}	U^{13}	U^{12}
N(1)	28(1)	35(1)	30(1)	8(1)	14(1)	9(1)
C(1)	34(1)	32(1)	29(1)	4(1)	14(1)	0(1)
C(2)	27(1)	28(1)	35(1)	4(1)	13(1)	3(1)
C(11)	25(1)	18(1)	26(1)	-1(1)	9(1)	1(1)
C(12)	27(1)	23(1)	22(1)	4(1)	6(1)	2(1)
C(13)	22(1)	22(1)	27(1)	2(1)	5(1)	4(1)
C(14)	23(1)	18(1)	24(1)	-1(1)	7(1)	0(1)
C(15)	25(1)	22(1)	24(1)	4(1)	6(1)	3(1)
C(16)	23(1)	23(1)	28(1)	4(1)	7(1)	5(1)
N(2)	22(1)	22(1)	22(1)	0(1)	5(1)	-2(1)
C(21)	20(1)	21(1)	22(1)	-1(1)	5(1)	-1(1)
C(22)	21(1)	21(1)	22(1)	2(1)	4(1)	-1(1)
C(23)	19(1)	21(1)	23(1)	-1(1)	3(1)	-1(1)
C(24)	22(1)	21(1)	22(1)	-2(1)	4(1)	-3(1)
C(25)	23(1)	19(1)	25(1)	0(1)	5(1)	1(1)
N(3)	30(1)	25(1)	26(1)	4(1)	8(1)	5(1)
C(31)	22(1)	23(1)	19(1)	-2(1)	2(1)	1(1)
C(32)	26(1)	30(1)	26(1)	1(1)	8(1)	1(1)
C(33)	27(1)	39(1)	29(1)	-3(1)	9(1)	7(1)
C(34)	32(1)	32(1)	23(1)	-2(1)	2(1)	12(1)
C(35)	35(1)	27(1)	24(1)	3(1)	6(1)	6(1)
N(4)	36(1)	29(1)	38(1)	10(1)	15(1)	7(1)
C(41)	28(1)	20(1)	23(1)	-2(1)	5(1)	-3(1)
C(42)	31(1)	21(1)	26(1)	-2(1)	9(1)	-3(1)
C(43)	44(1)	25(1)	29(1)	-2(1)	17(1)	-6(1)
C(44)	53(1)	27(1)	32(1)	9(1)	14(1)	-2(1)
C(45)	46(1)	33(1)	45(1)	15(1)	16(1)	11(1)

Table 4.   Hydrogen coordinates (x 10^4) and isotropic displacement parameters ($Å^2$x
10 ^{3})
for 02srv018.

	x	y	z	U(eq)
H(1C)	318(11)	1300(20)	4806(11)	39(5)
H(1B)	-457(12)	2470(20)	5040(11)	40(5)
H(1A)	590(13)	3220(20)	5201(12)	43(5)
H(2C)	-1440(11)	3290(20)	3047(11)	33(4)
H(2B)	-1458(11)	3710(20)	4028(11)	36(4)
H(2A)	-1113(10)	5130(20)	3460(10)	30(4)
H(12)	1490(10)	2130(20)	4320(11)	27(4)
H(13)	2483(10)	2080(20)	3469(10)	26(4)
H(15)	568(10)	4550(20)	1543(10)	23(4)
H(16)	-437(10)	4540(20)	2391(10)	25(4)
H(22)	2825(10)	780(20)	2276(10)	23(4)
H(25)	1880(10)	5440(20)	1141(9)	25(4)
H(32)	4815(11)	1030(20)	680(11)	35(4)
H(33)	5797(11)	-1440(20)	859(11)	36(4)
H(34)	5463(12)	-3850(20)	1668(11)	41(5)
H(35)	4197(11)	-3760(20)	2251(11)	36(4)
H(42)	4072(11)	4700(20)	-211(11)	33(4)
H(43)	4038(11)	6720(20)	-1351(11)	35(4)
H(44)	2761(12)	8690(20)	-1738(12)	44(5)
H(45)	1628(14)	8550(30)	-997(13)	57(6)

Summary of Ligands

Ligand=	L¹	L²	L³	L⁴

Ar= phenyl; 3-aminophenyl (NH₂); 4-CHO-phenyl; 4-NO₂-phenyl

Ligand=	L⁵	L⁶	L⁷

Ar= 4-CN-phenyl; 4-NMe₂-phenyl; 4-NPh₂-phenyl

Ligand=	L⁸	L¹⁶

Ar= 2,4,6-trimethylphenyl; 4-(terpyridyl)phenyl

Ligand=	L⁹	L¹⁰	L¹¹

Ar= phenyl; 4-CN-phenyl; 4-NO₂-phenyl

L¹²	L¹³	L¹⁴	L¹⁵

4-NMe₂-phenyl; 4-NPh₂-phenyl; 4-pyridyl; 3-pyridyl
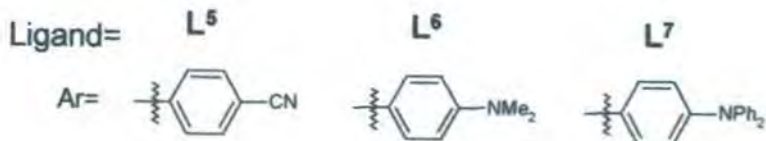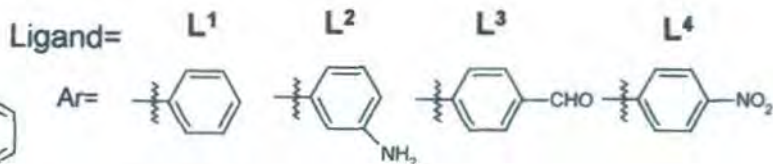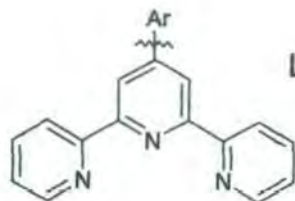
*Ligands L⁶, L¹⁰, L¹¹, L¹² prepared by Kirstin Wild
and Ligands L¹⁴ and L¹⁵ prepared by Kathryn Arm

Summary of Complexes
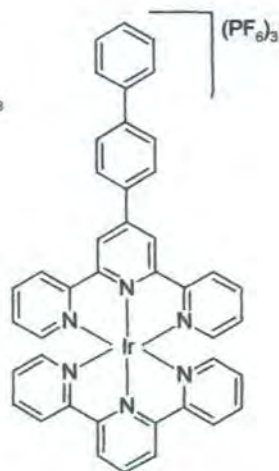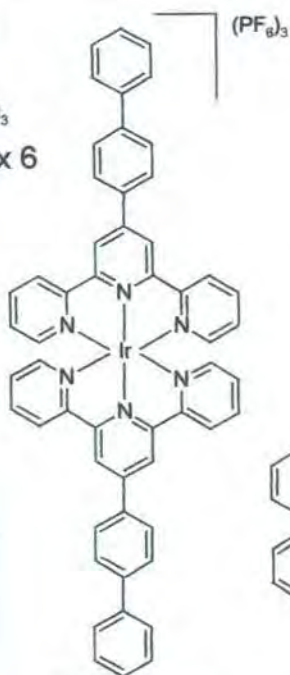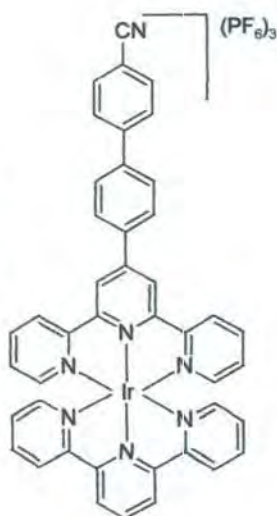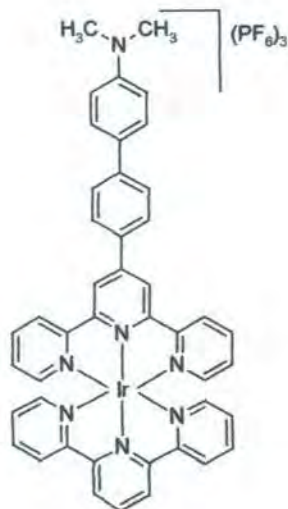

Complex 1
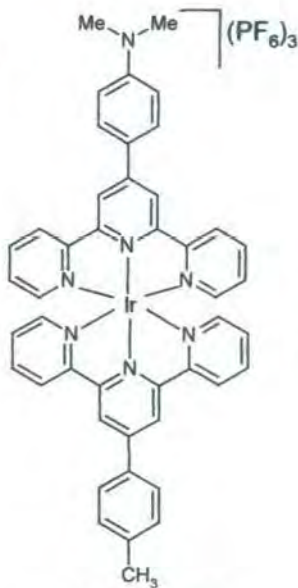
Complex 2
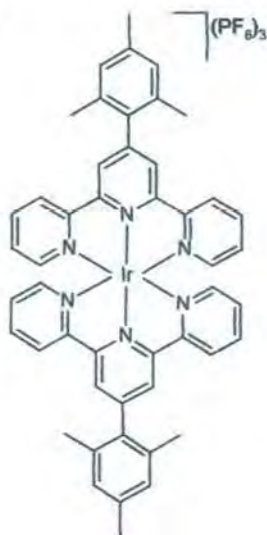
Complex 3
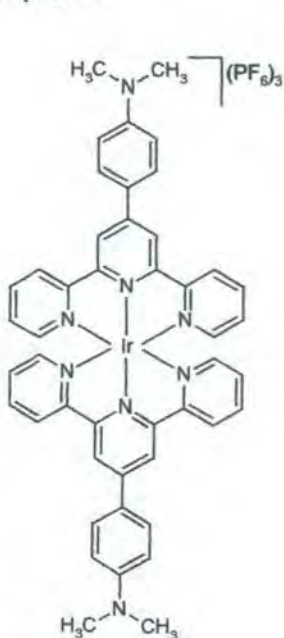
Complex 4
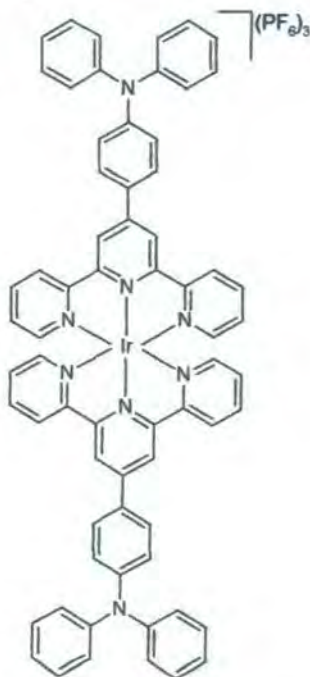
Complex 5

pto.
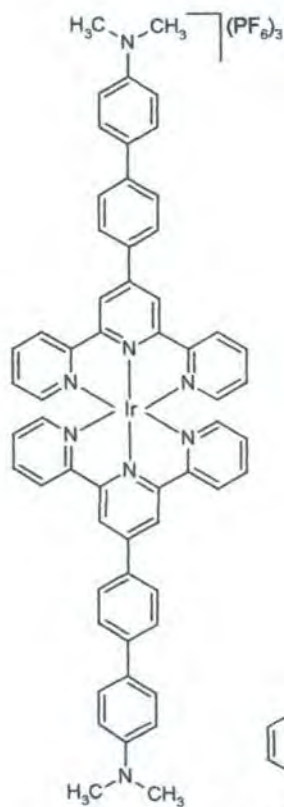
Complex 6
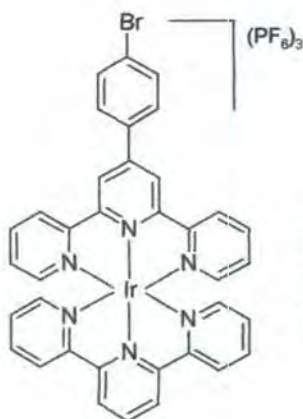
Complex 7

Complex 8

Complex 9

Complex 10

Complex 11